Vibration Characteristics of Steel-deck Composite Floor Systems under Human Excitation

Sandun S. De Silva
BSc Eng (Hons) MSc (Struct)

**A THESIS SUBMITTED
IN PARTIALFULFILMENT OF THE REQUIREMENTS OF
THE DEGREE OF DOCTOR OF PHILOSOPHY**

School of Urban Development
Faculty of Build Environment and Engineering

October 2007

In memory of my father

ABSTRACT

Steel-deck composite floor systems are being increasingly used in high-rise building construction, especially in Australia, as they are economical and easy to construct. These composite floor systems use high strength materials to achieve longer spans and are thus slender. As a result, they are vulnerable to vibration induced under service loads. These floors are normally designed using static methods which will not reveal the true behaviour and miss the dynamic amplifications resulting in inappropriate designs, which ultimately cause vibration and discomfort to occupants. At present there is no adequate design guidance to address the vibration in these composite floors, due to a lack of research information, resulting in wasteful post event retrofits.

To address this gap in knowledge, a comprehensive research project is presented in this thesis, which investigated the dynamic performance of composite floors under various human induced loads. A popular type of composite floor system was selected for this investigation and subjected to load models representing different human activities. These load models have variable parameters such as load intensity, activity type (contact ratio), activity frequency and damping and are applied as pattern loads to capture the maximum responses in terms of deflections and accelerations. Computer models calibrated against experimental results are used in the analysis to generate the required information. The dynamic responses of deflections and accelerations are compared with the serviceability deflection limits and human comfort levels (of accelerations) to assess these floor types.

This thesis also treats the use of visco-elastic (VE) dampers to mitigate excessive vibrations in steel-deck composite floors. VE damper properties have been presented and their performances in reducing the excessive vibrations have been assessed this thesis.

The results identified possible occupancies under different loading conditions that can be used in planning, design and evaluation. The findings can also be used to plan retrofitting measures in problematic floor systems.

KEYWORDS

Floor vibration, human perceptibility, finite element modelling, composite floors, human-induced loads, pattern loading, damping, dynamic amplifications, accelerations, visco-elastic dampers

PUBLICATIONS

De Silva, P.S.S., Thambiratnam, D.P., 2005, Dynamic Characteristics of Composite Floors, Tenth International Conference on Civil, Structural and Environmental Engineering Computing, 2005, Rome, Italy

De Silva, P.S.S., Thambiratnam, D.P., 2005, An investigation in to the Dynamic Amplifications in the Response of Composite Floors, Smart Systems 2005 Postgraduate Research Conference, QUT, Brisbane, Australia.

De Silva, P.S.S., Thambiratnam, D.P., 2006, Effect of Damping in Vibration of Composite Floors, Infrastructure 2006 Postgraduate Research Conference, QUT, Brisbane, Australia.

De Silva, P.S.S., Thambiratnam, D.P., 2007, Dynamic response of steel deck composite floors subjected to human induced loads, SWAC 2007, India.

De Silva, P.S.S., Thambiratnam, D.P, 2007, Dynamic Characteristics of Multi Panel Composite Floor Slabs, Journal of Computers & Structures (Under preparation)

ACKNOWLEDGEMENT

My deepest gratitude to my supervisor, Professor David Thambiratnam, for his scholarly guidance, endless encouragements and continuous support given throughout my research. He has been more than an academic overseer. He is a mentor. I thank him for steering me towards the goals of this research project and for helping me to overcome the difficulties encountered during the candidature. Our days of discussion will be deeply sealed in my heart. The successes of this project are shared with Professor Thambiratnam; the failures are my own. Also, I wish to thank Dr. A. Nasir, for kindly being my associate supervisor. I extend by sincere thanks to Adjunct Prof. Nimal Perera for his professional guidance.

I gratefully acknowledge financial support from the Faculty of Built Environment and Engineering (BEE) of QUT, for providing Postgraduate Research Scholarship to carry out my research. Further, I wish to pay my gratitude to Robert Bird and Partners for their great support on this project and specially, Mr. Jason Langer, Senior Engineer and Mr. Jared Stubbs, Engineer, both at Robert Birds and Partners. Also I wish to acknowledge the material support from Ready Mix concrete, Australia and Blue Scope Steel.

I extend my sincere appreciation for the support, discussion and friendship to the staff in the School of Urban Development (formerly School of Civil Engineering) and especially to those at the Structures Laboratory of BEE and High Performance Computing Facility of QUT. Many thanks also go to Dr. Adriana Bonarova for her comments in correcting the text.

Finally, I wish to thank all my friends at QUT for their encouragements and sharing the times.

TABLE OF CONTENT

LIST OF FIGURES

LIST OF TABLES

LIST OF NOTATIONS

a	Stiffness proportional damping coefficient
A	Shear area of the VE material (mm^2)
a_o	Limiting value of acceleration (g)
A_o, A_1, … A_n	Acceleration (g)
b	Mass proportional damping coefficient
b	Width (mm)
C_d	Damping parameter of the VE damper (Ns/m)
D_{Max}	Maximum static mid span deflection for SLS (mm)
d	Diameter (mm)
E	Modulus of elasticity
F	Force (kN)
f, f_0, f_s, f_p	Step frequency or load frequency or activity frequency (Hz)
f_1	Fundamental or first natural frequency (Hz)
f_2	Second natural frequency (Hz)
f_{cm}	Mean value of concrete compressive strength (MPa)
G	Dead load on the structure (kPa)
g	Acceleration due to gravity (m/s^2)
G'	Shear storage modulus of VE material
G''	Shear loss modulus of VE material
h	Height (mm)
I	Second moment of area (mm^4)
k	Stiffness of the structure (kN/m)
k_d	Stiffness parameter of the VE damper (N/m)
L	Length / span (mm)
l_s	Stride length (m)
m	Mass (kg or tons)
Q	Live load on the structure (kPa)
R	Response factor
t	Thickness (mm) / time (s)
w	Uniformly distributed load (kN/m)
w_p	Effective weight of participants per unit area (kg/m^2)

w_t	Effective weight of the floor including the participants (kg/m^2)
$[K]$	Stiffness matrix
$[M]$	Mass matrix
$\{F\}$	Applied force vector
$\{x\}$	Displacement vector
$\{\dot{x}\}$	Velocity vector
$\{\ddot{x}\}$	Acceleration vector
α	Contact ratio
γ	Shear strain
Δ	Mid span deflection of a simply supported beam (mm)
Δ_{max}	Maximum allowable serviceability deflection (mm)
Δ_{static}	Serviceability deflection (mm)
ζ	Structural damping
ν	Poisson's ratio
ρ	Density (kg/m^3)

ABBREVIATIONS

AP	Activity Panel(s)
AS	Australian Standards
AISC	American Institute of Steel Construction
ASCE	American Society of Civil Engineers
COV	Coefficient of Variation
DAF	Dynamic Amplification Factor
EBM	Equivalent Beam Method
FE	Finite Element
FEA	Finite Element Analysis
FEM	Finite Element Method
LVDT	Linear Variation Displacement Transducers
NAP	Non Activity Panel(s)
NRC	National Research Council of Canada
PL1-1	Pattern Loading 1 of Structural Configuration 1
PL1-2	Pattern Loading 1 of Structural Configuration 2
PL2-1	Pattern Loading 2 of Structural Configuration 1
PL2-2	Pattern Loading 2 of Structural Configuration 2
PL3-1	Pattern Loading 3 of Structural Configuration 1
PL4-1	Pattern Loading 4 of Structural Configuration 1
PTMD	Pendulum Tuned Mass Damper
SDOF	Single Degree of Freedom
SLS	Serviceability Limit State
TMD	Tuned Mass Damper
VE	Visco-elastic

STATEMENT OF ORIGINAL AUTHORSHIP

The work contained in this thesis has not been previously submitted to meet requirements for an award at this or any other higher education institution. To the best of my knowledge and belief, the thesis contains no material previously published or written by another person except where due reference is made.

Sandun De Silva
Signature:

Date:

Chapter 1 - Introduction

1.1 Background

Today's structures built to cater to the expectations of the community are aesthetically pleasing and use high strength materials and new construction technology. These structures are thus slender and therefore, unfortunately exhibit vibration problems under various service loads, causing discomfort to the occupants and raising questions on their use for the intended propose. At times, these vibrations have also been the cause of structural failure.

One such case of structural failure that caused many lives was the collapse of Hyatt Regency Hotel walkway in Kansas City, US, which happened during a weekend "tea dance" in 1981 (McGrath and Foote 1981), refer to Figure 1-1.

Figure 1-1: After Hyatt Regency Hotel walkway collapse in Kansas City in 1981

In the absence of appropriate theories and necessary information at that time, no one really understood the cause of this devastation. Some argued that the walkway buckled from the "harmonic" vibrations set up by people swaying or dancing, resulting in wavelike motion that caused it to collapse, while others argued that the walkways were overwhelmed by the weight of the large numbers of people unable to hold them (McGrath and Foote 1981). Either-way, the dynamic effect of crowd of people performing the dance-type activity, or exerting similar loads from other

human activities has played a significant role to cause this devastation. Such dynamic events not only cause loads much greater than the static loads to which the structure could have been designed, but also excite modes of vibration due to higher harmonics of the forcing frequencies, ultimately forcing them to collapse.

Another recent and well-known case of vibration problem in a structure was the Millennium Bridge in London, England (refer Figure 1-2). Two days after opening in year 2000 the bridge had to be closed to the public, due to the excessive sideway movements otherwise called synchronous lateral excitation (SLE), which happened when large groups of people crossed the bridge (Dallard, Fitzpatrick A.J. et al. 2001). This caused the occupants to adhere to the rails while walking, and some felt uncomfortable. Though this SLE did not cause any structural damage, probably because the bridge was closed to human traffic upon the realisation of large lateral vibration, this phenomenon certainly raised serviceability concerns.

Figure 1-2: Millennium bridge, London

Similar concerns in vibration hazards have been also reported in human assembly structures such as stadiums, grandstands and auditoriums (Ellis and Littler 2004; Sim, Blakeborough et al. 2006). Some examples are the Cardiff Millennium Stadium (Rogers 2000), Liverpool's Anfield Stadium and Old Trafford Stadium (Sim 2006).

The structures mentioned above are all slender with natural frequencies that fall within the frequency of human-induced loads, which consequently produced

vibrations. As a result, they caused human discomfort, crowd panic or in the extreme case, collapse of the structures (Dallard, Fitzpatrick A.J. et al. 2001).

Steel-deck composite floor structures are another example of slender of structures used in multi-storey buildings and have been known to experience vibration problems under human activity. There are a number of different configurations of these floors slabs, but they are all slender as they use high strength materials to achieve longer spans and hence reduced sections. They are being increasingly used in high-rise buildings, especially in Australia, as they are economical and easy to construct. These composite floor slabs are normally designed using static methods which will not reveal the true behaviour under human-induced dynamic loads resulting in the vibration problems. Their one-way spaning behaviour makes them even more vulnerable to vibration problems, in contrast to the conventional two-way spaning reinforced concrete floor slabs (Davison 2003). Figure 1-3 depicts a popular steel-deck composite floor system (dovetailed profile) used in Melbourne, Australia for a commercial and residential building while Figure 1-4 depicts a similar steel-deck composite floor system for a commercial application in Brisbane, Australia. These and similar floor slabs in other parts of Australia had experienced service load induced vibration problems. The design consultants who were involved in these projects wished to address this matter and initiated the research project described in this thesis. This research will therefore focus on this particular (dovetailed profile) type of steel-deck composite floor slabs, though the findings will be applicable to other types.

The vibration problems in a different type of composite floor system has been initially identified by Chien and Richie (1984), which later resulted in other researchers to investigate the behaviour under dynamic loads on floors. Bachmann et al. (1987), Allen and Murray (1993), Williams and Waldron (1994) presented experimental investigations and da Silva et al. (2003), Hicks (2004) and Ebrahimpour et al. (2005) used FE method of analysis to contribute research information under various human-induced loads on composite floor systems. The current methods of designing composite floor systems against vibration are based on this information and are found in the Steel Design Guide Series 11 (Murray, Allen et al. 1997) and Design Guide on the Vibration of Floors (Wyatt 1989). The guidelines

given in these standards however are approximate as they model the composite floor as a single degree of freedom system. Such a simplified model cannot predict the multi-modal vibrations in multi panel steel-deck composite floors, especially under pattern loading. The present research project will address this gap in the knowledge.

Figure 1-3: Composite floor in construction for a high rise office and residential complex in Melbourne

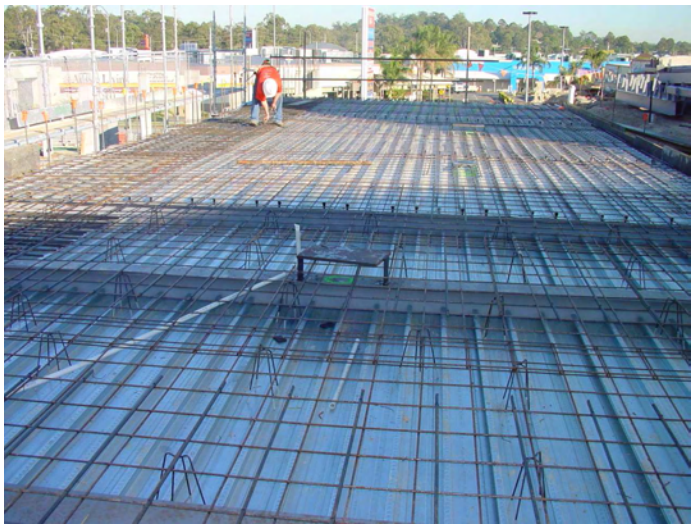

Figure 1-4: Composite floor construction in a shopping mall, Logan City Hyper-dome, Brisbane

Pattern loading occurs in multiple panel floor systems when different panels are loaded. In modern buildings these multiple panel floors are planned for mixed occupancies. Office only areas, commercial areas and residential areas may thus be combined with exercise halls, dance halls and even aerobics classes, which contribute to exert different human-induced loads within the same floor structure. These mixed occupancies generate pattern loading, and thus for adequate

serviceability, a proper evaluation of the floor structure based on its dynamic response is needed. With this in mind, a comprehensive research project was undertaken to study the vibration characteristics of multi panel steel-deck composite floors using dynamic computer simulations supported by limited experimental testing. This research information is used to evaluate the response of the composite floors under different types of human-induced pattern loads and to assess their compliance against the current requirements of serviceability and comfort and hence the suitability of the floor to the different types of occupancies.

1.2 Aim and scope of present study

The main aim of this project is to generate fundamental research knowledge on the vibration characteristics of slender steel-deck (with dovetailed profile) composite floor structures subjected to human-induced loads in order to evaluate their compliance against the serviceability and comfort requirements in the current design standards. Additional aims are:

- To develop comprehensive finite element (FE) models to carry out dynamics computer simulations and to study the influence of parameters, such as structural damping, activity type, load intensity, load frequency and location of activity (pattern loading).
- To establish Dynamic amplification factors (DAFs) in deflection and acceleration responses and evaluating them against serviceability limits for structural control and human comfort.
- To recommend suitable occupancies of the floor slabs and their operating conditions that would not cause discomfort to the occupants of adjacent floor panels.
- To investigate the use of passive visco-elastic (VE) dampers to mitigate the large amplitude vibration.

This investigation treats single panel initially and then multiple panel steel-deck composite floor systems subjected to different human-induced loading at different damping levels. The present research considers only one type of profiled steel deck composite floor slab and only human induced loading of “dance-type”. The load

parameters will be the activity type, frequency, density and location of the activity. The type of activity will be defined in terms of contact time of the feet with the floor. The study of human sensitivity or equipment sensitivity to vibration is not covered in this thesis as the acceptable vibration magnitudes will be governed by the posture of the individuals and the different types of the equipment.

1.3 Research methodology

In order to achieve the research aims, a slender steel-deck composite floor system with a dovetailed profile was selected for the experimental and analytical investigation. This type of composite floor consists of concrete floor elements cast in-situ on top of the dovetailed profiled steel-deck sheet. This is the most frequently used type of floor structure in modern Australian residential and commercial building construction.

This research was carried out using dynamic computer simulations based on FE techniques. Limited experimental testing was carried out to calibrate FE models and to obtain experimental dynamic characteristics of the investigated composite floor. The experimental investigation consisted of:

- static tests,
- heel-drop tests, and
- forced vibration tests.

FE models were developed using PATRAN 2004 (used as the pre and post processor) and analysed using ABAQUS solver (Hibbitt Karlsson & Sorensen Inc. 2000). The FE model was calibrated against the experimental results.

After calibration, seven single panel floors of different sizes were modelled and analysed under different human-induced loads and frequencies at different damping levels. The results were used to establish the dynamic response under human-induced loading conditions.

The multiple panel floor models were analysed for different pattern loading cases. Two FE models of four and nine panels constituted the study of multiple panel

behaviour. Pattern loading cases were identified for each model and analysed under different human-induced “dance-type” loads at different damping levels. The results were used to establish dynamic response and the findings were analysed and discussed.

Finally, visco-elastic dampers were employed in a multiple panel floor model to mitigate the excessive responses. The reductions in both displacement and acceleration responses were obtained, analysed and discussed.

1.4 Layout of the thesis

The research reported in this thesis is organised in to nine chapters. Their content is as follows:

Chapter 1: An introduction and background to the research topic, aims and scope, outlining the method of investigation used in this research have all been described in this chapter.

Chapter 2: This chapter highlights a review of previous literature published on the dynamic performance of floor structure systems under human-induced loading. It describes the current design methods and previous experimental and numerical investigations and identified the gaps in the knowledge.

Chapter 3: The experimental investigation and the testing procedure for a single panel floor are described here. The results are used to determine the dynamic characteristics of the investigated floor system as well as used in the calibration and validation of FE models, which is described in the next chapter.

Chapter 4: The development of single panel FE models and their calibration and validation are described in this chapter. It also includes the development of the multiple panel floor models that are studied under pattern loading.

Chapter 5: This chapter describes the dynamic analyses and their results of single panel models. The dynamic responses (DAFs and acceleration responses) under human-induced dynamic activities are discussed.

Chapter 6: This chapter investigates the dynamic behaviour of a four panel floor system subjected to pattern loading under human-induced activities of “dance-type” at different levels of structural damping to establish occupancies that comply with the current acceptance levels.

Chapter 7: The dynamic behaviour of nine panel floor system subjected to pattern loading is described here. Similar to the previous chapter it includes an investigation under various operating conditions and establishes suitable occupancy conditions.

Chapter 8: This chapter investigates the possible use of VE dampers in mitigating excessive dynamic responses in the multiple panel floor system.

Chapter 9: This final chapter highlights the main contributions of this research and points some recommendations for further research.

Chapter 2 - Literature Review

In civil engineering dynamics, human-induced vibrations are becoming increasingly vital serviceability and safety issues. Numerous researchers examined these issues and their findings of the effect of dynamic loads on structures are reviewed in this chapter. Investigations carried out on human induced loads, particularly on floor structures are subsequently reviewed. Then the current state of knowledge in the floor design addressing the performance of human-induced dynamic loads, is examined. The important design parameters, such as activity/forcing frequencies, fundamental frequencies and damping and their evaluations, are also observed. A review of predicting the fundamental frequency and damping is also included. The use of passive damping methods applied in mitigating the vibration problems in floor structures is reviewed further. An introduction to finite element methods and to composite floor construction is included in the last part of the literature review. Finally, this chapter summarises the present state of knowledge, identifying the gaps in knowledge and the contribution of this research to the current research in the area of floor vibration due to human activity.

2.1 Dynamic loads on structures

Dynamic loads, in general have been the cause of severe failures in structures. The most recent events and well known incidents were the Tsunami wave attack in Asia, September 11- World Trade Centre collapse, swaying of the Millennium Bridge in London (Dallard, Fitzpatrick et al. 2001a), (2001b), Cardiff Stadium vibration during a rock concert and Brisbane GABBA Stadium vibration during a football match, extensive damage to transportation facilities due to Hyogo-ken Nanbu earthquake in Japan (Japan Society of Civil Engineers 1996) just to mention a few. All the above-mentioned events occurred due to dynamic loads of varied origins initiated various sources. By considering the origins, dynamic loads can generally be categorized as wind-induced, earthquake-induced, traffic-induced and human-induced loads.

Wind-induced, earthquake-induced and traffic-induced vibrations in buildings are classified as externally generated, while human-induced vibrations are classified as internally induced vibrations.

Wind is the most common source of naturally occurring dynamic load on structures. Wind excited dynamic loads are necessary to consider in design of bridges and tall structures. Earthquake induced dynamic loads are another type of naturally occurring dynamic load sometimes which can be violent. They originate from an earthquake eruption, where a shock wave is propagated through the earth material causing the structure to vibrate. Traffic loads, on the other hand, arise from moving vehicles, where bridge structures and parking floors are the most vulnerable structures (Xia, Zhang et al. 2005). Traffic loads generate waves, which propagate through the layer of soil reaching the neighbouring buildings, causing them to vibrate (Hunadidi 2000).

Human-induced dynamic loads originate from various human actions. Although, it had not been significant problem in past, a number of serviceability problems were reported due to properties of today's structures, which have longer spans, are lighter and have a reduced damping. Floor and bridge type structures are the most vulnerable to human-induced dynamic loads, which cause them to vibrate. These include foot-bridges, gymnasiums, sports halls, dance halls, concert halls and grandstands. The vibrations were reported after construction, while servicing. To avoid such problems, it is desirable that a proper understanding of this behaviour is considered in design.

2.1.1 History

Human related structural vibrations have been reported since about 100 years ago. The first documented incident happened in a case of bridge, where the bridge collapsed when a team of solders was marching on. Due to the lack of knowledge, the mechanism of failure of the bridge structure was unexplainable at that time. Later research revealed that this was due to the resonance, which occurred when marching frequency came close to the natural frequency of the bridge.

One of the first research oriented work emphasizing human perceptibility to vibration originated from H.R.A. Mallock in 1901. Prompted by numerous complains of the Hyde Park residents, in UK, Mallock investigated the effects of vibration response

from passing trains (Steffens 1965). Mullock concluded that accelerations of 0.05 g were perceived by the occupants as acceptable. However, working on a similar problem, Hyde and Lintern (1929) dismissed Mallock's equipment and developed their own. After using their equipment they concluded that "a persistent vibration of this nature would be decidedly uncomfortable to the persons in buildings". This bought the awareness of importance of "exposure durations" on human response. However, acceleration limit is highly dependent on the person as per their personal level of sensitivity.

After, Hyde and Lintern's work in 1930, various papers relating various aspects of human vibration were published, some of the first works examined influence based on the vibrations induced by traffic (Hunaidi 2000).

2.1.2 Mathematical classification

Dynamic loads can mathematically classify as harmonic, periodic, transient or impulsive. Harmonic loads have been represented by sine functions. These loads are caused by people walking, dancing or performing aerobics. Furthermore, machines with synchronously rotating masses, which are slightly out of balance, or machines with intentional out-of-balance forces can also cause harmonic loads. Periodic loads repeat at regular intervals. In this case, the load time function within a period is arbitrary and the repetition allows it to be decomposed into series of harmonic loads. The cause of periodic loads may be due to human motion, machines having oscillating parts, unbalanced masses and periodically impacting parts or they can be caused by the wind. Transient loads do not exhibit any period in time and are arbitrary. The cause of the transient loads may be the wind, earthquakes, water waves or ground motion due to road traffic and construction works. The nature of the impulsive load is the same as that of transient loads, however impulsive load duration is shorter and its structural response is quite different. The structural response may occur from blast waves, impacts such as a moving object hitting on a structure or a sudden collapse of a bearing member, just to mention a few.

2.1.3 Resonance

The above-described dynamic forces cause resonance vibration in structures. Resonance vibration occurs when the natural frequency of a structure is at or near the

activity frequency. In each frequency of the forcing dynamic load, energy is fed into the structure causing the structure to vibrate. These vibrations attain their peaks at resonance, in both, acceleration and displacement. These peaks are dependent on the amount of damping in the structural system. Lower the damping in the structure higher the response resulting discomfort to the occupants (refer to Figure 2-1).

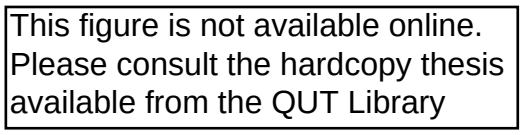

Figure 2-1: Floor acceleration due to a cyclic forcing frequency (Allen and Pernica 1998)

During any human activity, people apply repeated forces on the floor which are known as step frequency. Resonance occurs when the forcing frequency of human activity coincides with the natural frequency of the structure. Furthermore resonance can occur not only at the forcing load frequency but also at the multiples of harmonics of this frequency (Bachmann and Ammann 1987), (Pavic and Reynolds 1999) (Dougill, Blakeborough et al. 2001). For example, if a human activity such as jumping, running, aerobics, is being done to a step frequency of 2.0 Hz, it will produce harmonic vibrations at multiples of 2.0 Hz, i.e. at 2.0 Hz (first harmonic), at 4.0 Hz (second harmonic), at 6.0 Hz (third harmonic) etc. Second, third or fourth harmonics loading vibration are more likely to occur since the natural frequencies of floors are usually more than 3 Hz. The lower the harmonic, the larger the vibration produced. On the other hand, Ellis et al. (2000) has observed that this phenomena happened on a number of floors that had fundamental natural frequencies above 8 Hz with low damping. Similarly, Ji (1994) provided evidence of possible resonance

harmonics in the components of the load function, resulting in resonance in relatively stiff floors. Therefore, it can be stated that discomfort due to vibration can occur on a wide range of natural frequencies of a floor structure. Floors with long spans and inadequate stiffness are essentially the ones with problems due to vibrations causing human discomfort. Innovative composite floor systems have smaller thickness (less stiff), longer spans which achieved using high strength materials such as high strength steel and concrete makes the floor structures vibrate (Elnimeiri and Iyengar 1989) (da Silva, da S Vellasco et al. 2003). Consequently it is necessary to explore the vibration response of floor structures. The structural response of a floor structure depends on the dynamic properties of the structure, as well as the load applied to it. A composite floor system had been selected for the current research, due to its reduced slab thickness and longer span (refer Section 2.8.2 for properties of the composite floor system). As stated earlier, such floor system is slender and vibration sensitive to human-induced loads. Further, the frequency content in the dynamic load, the mode shapes of the floor structure and the properties of the floor system influence the response.

2.2 Human-induced dynamic loads on floors

Resonance vibration problems can occur in many types of structures such as bridge structures or floor structures. The most problematic response is due to the human-induced vibration reported in office building floors, shopping mall floors, aerobic dance floors, gymnasiums and parking floors (Hanagan 2003), (Ngo, Gad et al. 2006). Laboratory floor structures which use sensitive laboratory equipment are among those, vibrations of which caused by footfall are problematic (Ungar and White 1979), (Yazdanniyaz, Carison et al. 2003). The following Figure 2-2 depicts an aerobics which pronounce vibration on floors class and becomes a source of human discomfort.

All movements by people result in a fluctuating reaction force on floors. For example, the simplest walking causes a modest cyclic change in the height of the body mass above the floor, and the product of the mass with the respective accelerations equates to a cyclic force. Similarly, human actions including jumping,

running and performing aerobics on floors causes these cyclic forces, which create vibration problems.

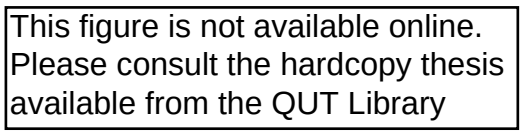

Figure 2-2: Doing aerobics on floors (Wajon 1996)

Periodic or harmonic load functions have been used to describe the human actions and the respective forces. The periodic or harmonic dynamic loads are repeated are time and nature of human induced dynamic loads depends on many factors, such as pacing rate, floor type or surface condition, person's weight, type of footwear and person's gender. Willford, (2001) showed that the dynamic loads induced by crowd jumping depends on the factors describing how energetic their dancing is and the quality of their coordination. Thus, it is clear that there are several factors, which contribute to vibration of slender floors in response to human actions.

A lot of research had been done to obtain graphical and mathematical formulae to understand human-induced loads. These graphical and mathematical expressions are important and were used in the research reported in this thesis in order to understand the structural response of steel-deck composite floors. Galambos et al. (1970), Wheeler (1982), Bachman et al. (1987), Maguire et al. (1999), Ginty et al. (2001) and Smith (2002) made research contributions to express the human-induced dynamic loads in terms of different human actions.

2.2.1 Walking

The human motion of walking gives rise to considerable dynamic loading which causes vibrations in slender floor structures (Ellis 2001b). The first known work dealing with the forces caused by walking excitation was from Haper (1962) as referenced in Pavic and Reynolds (2002). Afterwards, Galambos et al. (1970),

Wheeler (1982) and Eriksson (1994) published their work related to walking excitation forces acting on various structures.

Galambos et al.'s (1970) involvement in developing an intruder detection system based on earth micro-tremors, found that the loading fluctuation due to walking has its own periods and speeds and gave typical forcing patterns described in Figure 2-3. Similar loading pattern for running was also found by Galambos et al. (1970).

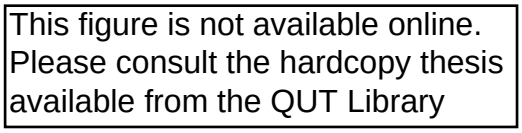

Figure 2-3: Typical forcing patterns for running and walking (Galambos and Barton 1970)

From the above Figure 2-3, it can be observed that human actions such as walking and running make observable differences in force magnitudes. The forces produced in walking are relatively smaller than the forces produced in running and each leg overlaps the periods of walking. Thus, a continuous ground contact in walking and a flying time in running events can be clearly seen.

Wheeler (1982) gave a reasonably good graphical representation for walking excitation caused by six different modes of human actions as seen in Figure 2-4.

The terms "Pacing Rate", "Forward Speed" and the "Stride Lengths" have been used to describe the human actions for walking and running events. The pacing rate f_s in walking or running are the number of footfalls per second (FF/s) which causes the dynamic load. At most times, the pacing rate has expressed in Hz due to the nature of the loading. The forward speed or pedestrian propagation v_s, is the actual frontal speed of walking measured in m/s while stride length l_s is the distance between ground contacts on two successive foot falls.

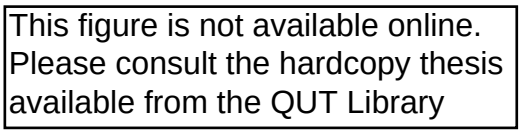

Figure 2-4: Time history patterns for various modes of walking and jumping / running excitation (Wheeler 1982)

The pacing rate of individual event is the most important phenomenon to understand, since the walking induced dynamic loads applied to the floor structures are being in phase with the pacing rate. Wheeler (1982) derived relationships for pacing rates, forward speeds and stride lengths by averaging test results for various walking speeds. The following Table 2-1 describes the pacing rates, forward speeds and stride lengths of walking action measured by Wheeler (1982). Table 2-2 presents pacing rates for different events such as walking, jogging or sprinting.

Table 2-1: Pacing rate, pedestrian propagation and stride length for walking

Event	Pacing rate, f_s (Hz)	Pedestrian propagation, v_s (m/s)	Stride length, l_s (m)
Slow walk	~ 1.7	1.1	0.60
Normal walk	~ 2.0	1.5	0.75
Fast walk	~ 2.3	2.2	1.00

Table 2-2: Pacing rates for different events

Event	Pacing rate (Hz)
Normal walk on horizontal surface	1.5~2.5
Normal jogging	2.4~2.7
Sprinting	About 5.0

Load-Time Function

The load-time function describes the vertical or the horizontal load exerted on a structure. This load-time function depends upon the pacing rate, floor type or surface condition, person's weight, type of footwear and / or person's gender.

For mathematical representation of walking, a general Fourier series expression was produced by Ji et al. (1994) and Bachmann et al. (1987) as outlined in Equation 2-1:

$$F_P(t) = G + \Delta G_1 \sin(2\pi f_s t) + \Delta G_2 \sin(2\pi f_s t - \varphi_2) + \Delta G_3 \sin(2\pi f_s t - \varphi_3), \quad \textbf{Equation 2-1}$$

where $F_p(t)$ is the dynamic load induced from walking, G is the weight of the person (static load of the person), ΔG_1, ΔG_2, ΔG_3 is the first, second, third harmonic of the load component respectively, f_s is the pacing rate and φ_2 , φ_3 are the phase angle of the second harmonic relative to the first harmonic and phase angle of the third harmonic relative to the second harmonic respectively.

The static load of an individual person G is considered to be 800 N, while the first harmonic load component ΔG_1 has been taken as 0.4 for pacing rates of 2.0 Hz and 0.5 for pacing rates of 2.4 Hz. The second and third harmonic load components (ΔG_2 and ΔG_3) are equal to 0.1 for pacing rates of 2.0 Hz. The relative phase angles do not play an important role, since human walking phenomenon is governed by one single harmonic. However, it should be stressed that when it comes to floor type structures, the resonance can occur due to the second harmonic or higher harmonics of the loading frequency.

It has been found that the horizontal loading due to walking is much lower than that of the vertical loading and thus can be considered negligible. However, Darallard et al. (2001a) after investigating the lateral swaying of London Millennium Bridge

provided an evidence of the importance of understanding the horizontal loading component. Horizontal loading is important in instances where the lateral stiffness of the floor structure is considerably low, which is not a common occurrence in floor structures.

2.2.2 Running / Jumping

Running is another human action, which cause floor structures to vibrate. The graphical representation of jumping is the one which is the most similar to running, for details refer Figure 2-3 and Figure 2-4. The load produced by running / jumping can be several times higher than the load resulting from standing still. The normal frequency of pacing in running / jumping varies from 1.8 to 3.4 Hz. The pacing rates, forward speeds and stride lengths for running / jumping were proposed by Wheeler (1982) and are described in the following Table 2-3.

Table 2-3: Pacing rate, pedestrian propagation and stride length for running events (Wheeler. J.E. 1982)

Event	Pacing rate, f_s (Hz)	Pedestrian propagation, v_s (m/s)	Stride length, l_s (m)
Slow running (jogging)	~ 2.5	3.3	1.30
Fast Running (sprinting)	> 3.2	5.5	1.75

Load-Time Function

The mathematical representation for the running / jumping events has been simplified as discontinuous half sine wave described in Equation 2-2 (Smith 2002) and Figure 2-5.

$$F_p(t) = \begin{matrix} k_p G \sin\left(\pi \, t/t_p\right) \longrightarrow t < t_p \\ 0 \longrightarrow t_p < t \le T_P \end{matrix}, \qquad k_p = \frac{F_{p,\max}}{G} \qquad \text{Equation 2-2}$$

where k_p is the dynamic impact factor, $F_{p,max}$ is the peak dynamic load, G is the weight of the person, t_p is contact duration which can vary from 0 to T_p and T_p is the pace period or step period derived from f_s as $1/f_s$.

The dynamic impact factor, k_p was obtained from Figure 2-5b and pace period T_p is taken from Table 2-3.

To reduce complexity in describing the running / jumping formulation the half sine time-function described above was transformed into Equation 2-3.

$$F_p(t) = G + \sum_{n=0}^{\infty} \Delta G_n \cos\left[2\pi n f_s\left(t - \frac{t_p}{2n}\right)\right], \qquad \textbf{Equation 2-3}$$

where G is the weight of the person, ΔG_n is the load component of the n^{th} harmonic, n is the number of harmonics, f_s is the pacing rate and t_p is the contact duration.

This figure is not available online.
Please consult the hardcopy thesis
available from the QUT Library

Figure 2-5: Idealized load-time function for running and jumping (a) half-sine model (b) impact factor depending on contact duration ratio (Bachmann. H. and Ammann. W. 1987)

2.2.3 Dancing / Aerobics

Dancing and performing aerobics result in dynamic forces similar to those of jumping (Ebrahimpour and Sack 1988) (Ebrahimpour and Sack 1989). However, unlike jumping, the frequency of these dynamic forces varies from 1.5 Hz to 3.4 Hz. Research by Wyatt (1985) and Ginty et al. (2001) showed that the frequencies of dancing can vary from 1.2 Hz ~ 2.8 Hz for individual jumping, 1.5 Hz ~ 2.5 for small groups and 1.8 Hz ~ 2.5 Hz for large groups.

Load-Time Function

An early research done by Allen (1990a) investigated the vibrational behaviour of a 20 m span non-composite joist floor and recommended a loading function, $F_p(t)$ using a periodic function containing three sinusoidal harmonic components, to represent loads induced by aerobics activity, as noted in Equation 2-4.

$$F_p(t) = \sum_{i=1}^{3} \alpha_i w_p \sin 2\pi i f t \,, \qquad \textbf{Equation 2-4}$$

where α are the dynamic load factors $\alpha_1 = 1.5, \alpha_2 = 0.6, \alpha_3 = 0.1$ for the third harmonics respectively, w_p is the maximum weight of participants over the loaded area, f is the maximum jumping frequency, t *is* the time. For various excitation frequencies induced by the groups of people jumping or dancing together, similar dynamic load factors were presented by Willford (2001) through a parametric study, giving the confidence level for use in the design of gymnasium floors and dance floors as seen in Figure 2-6. The dynamic load factors were 1.5 for excitation frequencies 1.5 ~ 3.0 Hz, 0.6 for excitation frequencies 3.0 ~ 6.0 Hz, 0.1 for excitation frequencies 6.0 ~ 9.0 Hz.

This figure is not available online.
Please consult the hardcopy thesis
available from the QUT Library

Figure 2-6: Dynamic load factors for different excitation frequencies (Willford 2001)

A theoretical research done by Ji et al. (1994) investigated floor response produced by dancing and aerobics and provided possible resonance at higher harmonics. It suggested an equation to calculate the number of Fourier terms or harmonics needed

to be considered in the analysis (refer to Equation 2-5). The number of Fourier terms needed to be considered was determined as follows:

$$I = Interger\left(\frac{1}{\beta_i}\right), \qquad \textbf{Equation 2-5}$$

where I is the number of Fourier terms, β_i is the ratio of excitation frequency to the considered and i^{th} natural frequency of the system.

Although this equation had not been thoroughly verified by experimental measurements, the numerical analysis was explained through an example by which author suggested that possible resonance can occur on a relatively stiff dance floor.

2.3 Design criteria against floor vibrations

Design criteria against floors vibrations are based on the acceleration responses from which human response scales were developed as primary design tools against floor vibration problems. Attempts to achieve and quantify an accurate acceleration response in floor motions have been tried for many years and still are being reviewed in modern floor construction, which are being designed with a view of addressing future complaints of annoying vibrations (Hewitt and Murray 2004a).

Allen and Pernica (1998) quoted from a paper by Tredold published in 1828:

> *"girders should always be made as deep as they can to avoid the inconvenience of not being able to move on the floor without shaking everything in the room."* (Allen and Pernica 1998)

This statement describes that the early problems associated with floor vibration problems were addressed for example by increasing the thickness of the slab / floor.

The Australian standards for design of concrete structures provide the following clause against the effects of floor vibration.

Vibration of slabs, AS 3600 (2001), Clause 9.5 states:

"Vibration in slabs shall be considered and appropriate action taken, where necessary, to ensure that vibrations induced by machinery or vehicular and pedestrian traffic will not adversely affect the serviceability of the structure".

In contrast, the design criteria of floors against the effects of vibration can be found in subsidiary publications, AISC Steel Design Guide Series 11 (Murray, Allen et al. 1997) and Design Guide on the Vibration of Floors (Wyatt 1989). In this context, different scales were developed, such as acceleration limits and response factor method, to design floor structures against human-induced vibrations. British Standards have give acceleration limits by considering the human comfort under vibrations (BS 6472 1984).

2.3.1 Acceleration limits

Acceleration limits provide a floor vibration assessment considering the occupancy of the building. Bachmann et al. (1987), Allen et al. (1990a), (1998), Naeim (1991), Benidickson Y.V. (1993), Commentary A (1995) by National Research Council (NRC Canada), Murray et al. (1997), Maurenbrecher et al. (1997), presented design acceleration limits for floors and design charts for buildings. These design limits and charts provide peak acceleration limits formulated from frequencies and damping ratios of the floor structure, in different human action scenarios.

2.3.1.1 Acceleration limits for walking excitation

One of the first well-known and widely recognised criterion for acceleration limits for walking was developed by Reiher and Meister in 1930's. Their research involved a group of standing people subjected to steady-state vibration of frequencies 3 ~ 100 Hz and amplitudes of 0.01016 to 10.16 mm (Murray 1990a). The subjective reactions by standing people, yielded a scale "slightly perceptible", "distinctly perceptible", "strongly perceptible", "disturbing", and "very disturbing" to describe the vibrations. However, several investigations by Lenszen in 1960's on joist-concrete floor systems, gave a modified Reiher-Meister scale (refer to Figure 2-7). The original scale was applicable only if it was scaled down by a factor of 10 for floor systems with less then 5 % critical damping (Naeim 1991).

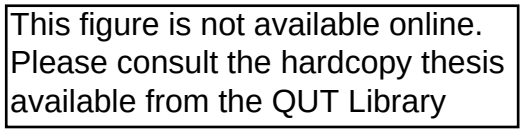

Figure 2-7: Modified Reiher-Meister scale (Naeim 1991)

Although the modified Reiher-Meister scale is the basic and frequently used criterion, it has been used with another additional method to pass on the judgement of perceptibility. This is due to the lack of reflecting on the damping in this method. Murray in 1970's showed that this scale can result in complaints from the occupants living in steel-beam concrete floors with damping from 4% to 10% (Naeim 1991). Consequently, Murray et al. (1989) have been involved in further development and after considering the occupancy of the floor they presented the following inequality to be used with modified Reiher-Meister scale to address the presence of damping (Murray 1990b).

$$D > 1.38 A_o f_1 + 2.5, \qquad \textbf{Equation 2-6}$$

where D is the percentage of damping, A_o is the initial amplitude of the heel impact test in mm and f_1 is the first natural frequency.

The required damping percentages are described in the Section 2.5.1. The assessment also needs heel drop amplitude A_o, which can be obtained from experimental analysis of the floor. The natural frequency, f_1 can be calculated using finite element method for more accuracy however, the simplified approaches described in the Section 2.4 are adequate for the above criterion.

In contrast, more recent publication by Murry et al. opposes the use of the modified Reiher-Meister scale. The reason being that the developed criterion was calibrated against 1960's and 1970's floor systems (Hewitt and Murray 2004a). Thus, the need

for an improved criterion to be used for modern day slender floor systems has been identified.

For cases of walking excitation, acceleration response criterion was published by Steel Design Series 11 (Murray, Allen et al. 1997). In this context, an acceleration response function due to walking excitation was presented by Murray, Allen et al. (1997) as follows:

$$\frac{a}{g} = \frac{R\alpha_i P}{\zeta W}\cos(2\pi i f_{step} t), \qquad \textbf{Equation 2-7}$$

where *a/g* is the ratio of the floor acceleration response to the acceleration of gravity, *R* is the reduction factor (0.7 for footbridges and 0.5 for floor structures), α_i is the dynamic coefficient of the i^{th} harmonic force component, *P* is the persons weight, ζ is the modal damping ratio, *W* is the effective weight of the floor and f_{step} is the step frequency. For design purposes, the Equation 2-7 was further simplified by approximating the step relationship between the dynamic coefficient α_i and frequency *f* by $\alpha = 0.83\exp(-0.35 f)$ as seen in Equation 2-8:

$$\frac{a_p}{g} = \frac{P_o \exp(-0.35 f_n)}{\zeta W}, \qquad \textbf{Equation 2-8}$$

where a_p / g is the estimated acceleration response in a fraction of gravity, f_n is the natural frequency of the floor structure, P_o is the constant force (0.29 kN for floors and 0.41 kN for footbridges), ζ is the modal damping ratio and *W* is the effective weight of the floor. The peak acceleration due to walking excitation is then compared with the appropriate limits described in Figure 2-8.

Brand (1999) used Equation 2-8 in long-span joist floors, which in turn gave affirmative results. By considering the above formulae presented by Murray et al. (1997), Hanagan et al. (2001) made an effort to develop a simple design criteria for a slab/deck profiled floor system. However, this simple design criterion was limited to a single class of floors using grade 50 steel and thus needs to be expanded.

This figure is not available online.
Please consult the hardcopy thesis
available from the QUT Library

Figure 2-8: Recommended peak acceleration limits design chart (Murray, Allen et al. 1997)

Another approach was presented by Canadian Steelwork Association (CSA), which provided a threshold for the peak acceleration due walking (refer to Figure 2-9). This is similar to the criterion provided by the AISC Steel Design Guide Series 11, except for the acceleration response, which was measured by heel impact excitations done on the floor system (Wyatt 1989). The "continuous vibration" line in the Figure 2-9 is used to assess the response due to average peak acceleration due to walking, while "walking vibration" curves asses the response by the peak acceleration due to a heel impact excitation.

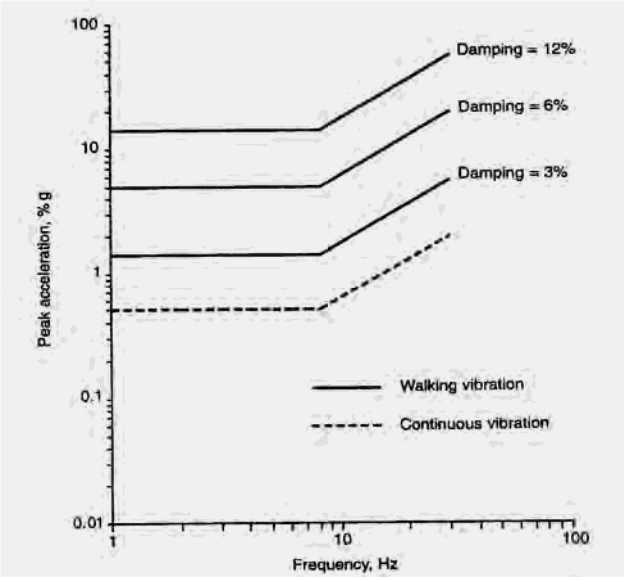

Figure 2-9: Canadian floor vibration perceptibility scale

After verity of field tests done by Williams and Waldrom (1994) in assessing the applicability of the Concrete Society Method (CSA) of assessing the floor vibrations, these gave unsatisfactory results. This was due to the heel drop tests used in the criterion, the excitation force of which is unknown at most times.

2.3.1.2 Acceleration limits for rhythmic excitation

In the case of acceleration limits for rhythmic excitation on floors during performance of aerobics, dancing and audience participation Ellingwood and Tallin (1984), presented acceleration limit criterion using available literature. An equation (refer to Equation 2-9) to calculate the maximum mid span acceleration of a floor a_o due to rhythmic activity of frequency f was developed and the limits were presented in a tabular format as seen in Table 2-4.

$$a_o = (2\pi f)^2 \left(\frac{\alpha F_s}{k}\right) \frac{1}{\left|1-\left(\frac{f}{f_1}\right)^2\right|}, \qquad \textbf{Equation 2-9}$$

where αF_s is the sinusoidal dynamic force, f_1 is the fundamental frequency, k is the static stiffness.

This table is not available online.
Please consult the hardcopy thesis
available from the QUT Library

Table 2-4: Suggested acceleration limits by occupancy (Ellingwood and Tallin 1984)

Due to lack of indication of the damping coefficient in the Equation 2-9, Allen (1990a), presented an incorporated acceleration response with damping ratio for rhythmic excitation. This approach has been the basis for design against vibration due rhythmic excitation used in current design approaches such as Steel Design Series 11 for design of the floor structure. Thus Murray, Allen et al (1997) provided a criterion detailed in Equation 2-10 to incorporate this approach in the design of floor against rhythmic excitation:

$$\frac{a_p}{g} = \frac{1.3\alpha_i \, w_p / w_t}{\sqrt{\left[\frac{f_n}{f} - 1\right]^2 + \left[\frac{2\zeta f_n}{f}\right]^2}}, \qquad \textbf{Equation 2-10}$$

where a_p/g is the peak acceleration ratio in a fraction of gravity, α_i dynamic amplification factor for i^{th} harmonic, w_p is the effective weight per unit area of participants distributed over the floor panel, w_t is the effective distributed weight per unit area of floor panel, including occupants, f_n is the natural frequency of the floor, f is the forcing frequency (in terms of the step frequency) and ζ is the damping ratio. The dynamic coefficient α_i , weight of participants, w_p and excitation frequencies are presented in the Table 2-5.

This table is not available online.
Please consult the hardcopy thesis
available from the QUT Library

Table 2-5: Estimated loading during rhythmic events (Murray, Allen et al. 1997)

2.3.2 Response factor method

In an approach to design floors against the adverse effects of vibration, the use of a response factor was recommended by Wyatt, (1989) and Murray et al. (1998). This factor is then compared with a limit depending upon the occupancy. The calculation of the response factor depends upon whether the fundamental natural frequency of the floor exceeds 7 Hz. In this context, two equations were developed to represent each case when the fundamental natural frequency exceeds 7 Hz and when it does not.

If the fundamental natural frequency exceeds 7 Hz, in which case floors are of high natural frequency the response factor R is given by (Wyatt. T.A. 1989):

$$R = \frac{30000}{mb_e L}, \qquad \textbf{Equation 2-11}$$

where m is the floor mass in kg/m^2, b_e is the minimum of either the floor beam spacing b (m) or 40 times the average slab thickness, and L is the floor beam span.

If the fundamental frequency is less than 7 Hz, referred to as floors of low natural frequency the response factor R is given by:

$$R = \frac{68000 C_f}{mSL_{eff}\zeta}, \qquad \textbf{Equation 2-12}$$

where m is the floor mass in kg/m^2, S is the floor effective width, L_{eff} is the floor beam effective span, ζ is the structural damping (critical damping ratio) and C_f is the Fourier component factor.

The critical damping ratio ζ was considered to be 0.03 for normal, open plan and furnished floors, 0.015 for an unfurnished floor of composite deck construction and 0.045 for a floor with partitions.

The value of the Fourier component factor C_f was found as a function of the floor frequency f_o of which when:

$$3Hz \le f_o < 4Hz \qquad C_f = 0.4,$$

$4Hz \leq f_o < 4.8Hz$ $C_f = 1.4\text{-}0.25f_o$,

$f_o \geq 4.8Hz$ $C_f = 0.2$.

The criteria for the response factor *R* for office floors are described in Table 2-6.

Table 2-6: Response factor R for offices (Wyatt 1989)

Type of Office	Response Factor, R
General Office	8
Special Office	4
Busy Office	12

For large public circulation areas such as pedestrian and shopping malls, lobbies and assembly halls a response factor of four was proposed and this value should not increase in case of residential floors.

2.3.3 Assessment of vibration design criteria

Many researchers using both experimental and analytical work assessed the floor systems using the design criteria presented in Section 2.3.1 and 2.3.2. Number of case studies has been done in this respect.

Osborne et al., (1990) analysed a long-span lightweight composite slab of 16 m span and a thickness of 120 mm supported on 1.2 mm gauge steel deck. Using various available methods they checked the acceptability of vibration characteristics both experimentally and numerically. Their results provide clearly agreed with the AISC Design Guide 11's acceleration limits. Later, Williams et al. (1994) tried to assess the floor vibration dynamic characteristics, as reflected by fundamental frequency and design methods using a set of full-scale vibration tests. As a part of the design approach, they recommended the use of a high-power computational method, such as finite-element analysis for more accurate results. Murray et al. (1998) evaluated the differences between the procedures of the acceleration limits and the response factor method in terms of a typical office floor and found them to be the same evaluation in both cases. Similar work was carried out by Baglin, Cox et al. (2005a), (2005b).

Various researchers tried to understand the floor response due to human actions and as described above, the acceleration response has been used as a design tool for floor vibration in most design guidelines (Wyatt 1989; Murray, Allen et al. 1997). The frequencies considered in these design tools, such as the first mode of natural frequencies obtained from simplified equations, do not provide sufficient evidence of higher order mode shapes. In today's modern, long span floor constructions with lower damping, the applicability of these design tools remains unsolved.

All these design guidelines provide responses of floor vibration due to human activities where the activity has originated within the floor panel. However, there is no clue in the design procedure as to the acceleration response due to pattern loading. None of the design guidance has looked at the vibration measurements in either, the adjacent floor panel or the behaviour of the entire floor due to pattern loads. This is particularly important, when a continuous floor is being used for different human-activities with little or no permanent partition.

2.4 Determination of natural frequency

Every structure has its own natural frequency. Particularly with floor structures, there are various methods published in literature to determine the natural frequency. Some are simple methods and others are more sophisticated. To assess the floor response to dynamic loads, an accurate calculation of the first natural frequency is important to use in the design criteria against floor vibrations (refer to Section 2.3.1 and 2.3.2 for design criteria). Research done by Wyatt (1989), Williams et al. (1994), Bachmann and Pretlove (1995), Brand and Murray (1999) yielded the following methods to estimate natural frequencies of floors:

1. Equivalent beam method.

2. Component frequency approach.

3. Concrete society method.

4. Self-weight deflection approach.

5. Finite element method of analysis.

These methods can be classified as general approaches and sophisticated approaches and it must be noted that the natural frequencies of a floor depend upon numerous factors including material property, structural type, slab thickness and boundary conditions just to mention a few.

2.4.1 General approaches

Equivalent beam method, component frequency approach, concrete society method and self weight-deflection approached can be classified as general approaches. Most of these scenarios in these approaches are to predict the natural frequency of a floor structure based on 1-way spaning approximation. The equivalent beam method (EBM) outlined in Equation 2-13 and concrete society method approximate the behaviour of floor to an equivalent simply supported beam to obtain the first natural frequency (Williams and Waldron 1994):

$$f = \frac{\pi}{2}\sqrt{\frac{EI}{ml^4}}, \qquad \textbf{Equation 2-13}$$

where E and I are the modulus of elasticity and second moment of area respectively, m is the mass per unit length and l is the span. Although EBM is a simple method, Williams et al. (1994) provided an evidence of its non-applicability on concrete floors.

A similar approach to EBM is the one proposed by Murray, Allen et al. (1997) for a beam or joist and girder panel to calculate fundamental natural frequency f_n (Hz) as stated here:

$$f_n = \frac{\pi}{2}\left(\frac{gE_sI_t}{wL^4}\right)^{1/2}, \qquad \textbf{Equation 2-14}$$

where g is the acceleration of gravity, E_s is the modulus of elasticity of steel, I_t is the transformed moment of inertia, w is the uniformly distributed load per unit length and L is the span. This equation was further simplified using the mid span deflection equation of a simply supported beam;

$$f_n = 0.18\sqrt{\frac{g}{\Delta}}, \qquad \textbf{Equation 2-15}$$

where Δ is the mid span deflection of a simply supported beam member and can be derived from $\Delta = 5wL^4 / 384E_s I_t$.

When a floor system has a significant interaction with the main beam deflection, a change in fundamental mode shape and thus the natural frequency results. Therefore, a modification factor C_B was recommended to use with the above EBM in Equation 2-13 to calculate the natural frequencies. Wyatt (1989) presents the values for C_B for a single span, for both end pined to be 1.57, for one end pinned and the other fixed to be 2.45, for both end fixed to be 3.56 and for cantilever to be 0.56. Furthermore for continuous spans, Wyatt (1989) recommended to use the following Figure 2-10. This is known as the component frequency approach.

Figure 2-10: Frequency factor, C_B for continuous spans (Wyatt. T.A. 1989)

Concrete Society method also uses the 1-way spaning approximation of equivalent beam approach. In addition, it introduces modification factors to incorporate the increased stiffness of 2-way spaning floors, yielding two independent natural frequencies for the two perpendicular span directions.

In another publication by Wyatt (1989), the self weight deflection approach uses the Equation 2-16 to determine the natural fundamental frequency f (Hz) of an un-damped structural system:

$$f = \frac{1}{2\pi}\sqrt{\frac{k}{m}}, \qquad \textbf{Equation 2-16}$$

where k and m are the stiffness (kN/m) and the mass (tonnes) respectively. Considering that in many plate and beam problems, weighted average of the defection y_w is taken at about ¾ of the maximum value of the self-weight deflection y_o (in mm), and using the basic equation of motion, $F = k\Delta$, where $mg = k(y_w)$, the fundamental Equation 2-16 was rewritten for first natural frequency of a floor system as:

$$f = \frac{18}{\sqrt{y_o}}. \qquad \textbf{Equation 2-17}$$

This has been used as a basic approach in many designs approaches for floor systems. However, due to the fact that in joist floor systems resistance to floor vibration is not only due to the slab itself but also due to the beams on girders supported by columns, Maurenbrecher et al. (1997), Brand and Murray (1999) used the following Equation 2-18 to take this into account:

$$f = \frac{18}{\sqrt{y_j + y_g + y_c}}, \qquad \textbf{Equation 2-18}$$

where y_j, y_g and y_c are the static deflections under weight, supported due to bending and shear for the beam or joist, for girder and for column for axial strain respectively.

A similar approach to EBM was developed by Murray et al. (1997), to determine the fundamental frequency of a floor consisting of a concrete slab or deck, supported on steel beams or joists which were on steel girders or walls. In this context, the natural frequencies of beam or joist and girder panel are calculated from the fundamental natural frequency equation, and Dunkerley's relationship is used to estimate the combined mode or system frequency.

Dunkerley's Relationship

As floor systems usually comprises of three identifiable components such as floor slab, floor beams and main beams, in determining a natural frequency of a complete floor system it is important to take account of the behaviour of these components individually. This was done by considering each component separately using approximate methods. The component frequencies are combined using the

Dunkerly's method in Equation 2-19 for the total evaluation of the natural frequency f_o for the floor system (Bachmann, Pretlove et al. 1995), (Wyatt 1989) (Brand and Murray 1999):

$$\frac{1}{f_o^2} = \frac{1}{f_{c1}^2} + \frac{1}{f_{c2}^2} + \frac{1}{f_{c3}^2}, \qquad \textbf{Equation 2-19}$$

where f_{c1}, f_{c2} and f_{c3} are the component frequencies for each component of floor slab, floor beams and main beams of the floor system

2.4.2 Sophisticated approach

The general approaches described in Section 2.4.1 yielded many erroneous results. Consequently, the Institution of Structural Engineer's interim guidance report in 2001 concluded:

> *"Shortcut methods for determination of natural frequency based on the deflected shape under static loading or on rules of thumbs may not be adequate and can be very misleading"* (Dougill, Blakeborough et al. 2001)

The most sophisticated and superior method to determine the natural frequency of a structure is by finite element modelling (El-Dardiry, Wahyuni et al. 2002). Commercially available softwares such as ABAQUS, ALGOR and SAP 2000 can be used for this purpose. The use of this approach not only provides greater accuracy but it also speeds up calculations for more complex structures. However, it should be noted that the use of FEM for obtaining the first natural frequency output, directly depends on the input of structural properties.

The general methods described earlier use the conventional equation of dynamics or its derivatives and have been idealised to a single degree of freedom system (SDOF) which generate the first mode fundamental frequency. Williams et al. (1994) after investigating above general methods with field exercises, advises to use a computational method such as finite element method. Pavic et al. (2002) provide evidence that the currently popular in-situ cast concrete floors, modelled using SDOF systems based on fundamental mode, is likely to produce erroneous results. With multi-degrees of freedom structures in modern construction, the general approaches are not effective. Hence, the ideal solution to determine the natural frequencies of a

floor system is to use FEMs. Thus the FEMs have been used in the research reported in this thesis.

2.5 Evaluation of damping

2.5.1 Damping coefficients

Damping refers to the dissipation of vibrational energy. All physical systems have some inherent damping, but the level of damping can be improved by increasing energy dissipation. In this way, the response of a structure driven at a resonant frequency can greatly decrease. Not only the components of the structural system but also the non-structural components play a major role in damping, such as non-structural elements, finishes, partitions, standing objects (Chen 1999). Furthermore, the resistance provided by air can cause a certain amount of damping although it is not significant. The damping can be either external or internal. The material or contact areas within structures such as bearings and joints, are classified as internal damping materials while external contacts such as non-structural elements are classified as external damping materials (Mahrenholtz and Bachmann 1995). The amount of damping in a structure is provided by a damping ratio or damping factors.

Research done by Elnimeiri (1989), on composite floors recommended a damping coefficient of 3.0% for open floors and 4.5%-6% damping for finished floors with partitions. Murray et al., (1989) presented critical damping percentage requirements for different floor design situations, where the critical damping for a typical office floor system with hung ceiling and minimal mechanical duct work was estimated to be at 3.0%. Furthermore, Murray et al., (1989) states that if the required damping is between 3.5% ~ 4.2 % it is important to consider the configuration of the office and its intended use. Osborne et al. (1990) commented that measured damping of a floor was considerably lower than the values generally assumed, verifying the difficulty of estimating the damping. The damping of a floor also depends upon the usage or occupancy. Thus, Maurenbrecher et al. (1997) after considering occupancy of structures provided the following damping factors: damping of 1% for footbridges, 2% for shopping centres and 2%-5% for offices and residences. The partitions and other non-structural components on a lightweight floor provide higher damping than those in heavy floors (Kullaa and Talja 1999). Thus, to observe the damping

properties of lightweight floors with the effect of non-structural components, Murray et al. (2004), in a recent publication presented a damping criteria which provided damping ratio of 2% ~ 2.5% for an electronic office with limited number of cabinets and without full-height partitions. For an open office space with cubicles with no full height partitions, they proposed a damping factor of 2.5% ~ 3.0% while for an office library with full-height bookcases a damping factor of 2% ~ 4%.

In general, the damping coefficient appears to be in a rage of 2.0% ~ 6.0%. The human presence on the floor area was neglected in the above mentioned research. A research done by Brownjohn (2001), proved that in the presence of humans on a floor system, damping could increase up to 10%. Further, his full-scale experiments performed on a function hall showed that the harmonic resonance was fully damped out by seated humans. The review of the literature demonstrates that depending on the dynamic properties of the empty structure has however the ability to increase damping in the structure (Sachse 2002). This damping effect, however has not been endorsed by the authorities that sets the standards and hence needs further investigation on lightweight floors.

Findings of the above studies reveal that damping in the floor structure is difficult to determine and only approximate values can be provided for inherent damping in floor systems.

2.5.2 Measurement of damping

The measurement of damping was obtained by a decay of vibration response method of estimation. The following Figure 2-11 depicts decay in acceleration response due to heel impact excitation.

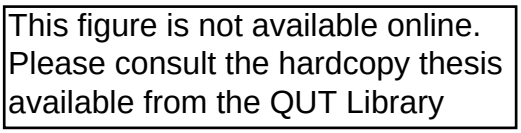

Figure 2-11: Decay of vibration response (Ellis 2001a)

For a vibration decay described in Figure 2-11, the damping coefficient can be determined using Equation 2-20 (Ellis 2001a).

$$\xi = \frac{1}{2n\pi}\log_e \frac{A_o}{A_n}, \qquad \textbf{Equation 2-20}$$

where A_o and A_n are the acceleration amplitudes between n consecutive cycles.

The decay of vibration response method is the simplest method and it is best suited for better approximation of damping.

2.6 Dynamic tests on floors

Dynamic floor tests provide considerable research evidence on finding the dynamic response, natural frequency and damping coefficients of floors. Several dynamic tests can be done on floor structures. It must be noted that these dynamic tests need sophisticated equipment to excite and measure the responses. Ellis (2001a) presented five different testing procedures described below to obtain the dynamic characteristics of floors.

1. Ambient test.
2. Heel impact test.
3. Sand bag test.
4. Impact hammer test.
5. Forced vibration test

Table 2-7 gives a summary of dynamic characteristics that can be obtained from each of these tests.

Table 2-7: Types of dynamic tests on floors

Test	Natural Frequency	Damping	Stiffness	Mode Shape
Ambient	Yes	-	-	-
Heel impact	Yes	Yes	-	-
Sand bag	Yes	Yes	-	-
Impact hammer	Yes	Yes	Yes	-
Forced vibration	Yes	Yes	Yes	Yes

In additon there are methods like micro-seismic blast loading, free vibration tests etc, for determing the natural frequency.

2.6.1 Ambient test

In ambient test, the structure is set to vibrate on its natural existence and the responses obtained from accelerometer readings are amplified using sophisticated equipment to obtain the result spectrum (Ellis 2001a). Although this method can be used in any system, its main disadvantage is the length of time it takes to gain a better spectrum response.

2.6.2 Heel impact test

Heel impact test is the most widely used test on floors (Bachmann, Ammann et al. 1995). A person is asked to sit in the centre span of the structure, they are requested to raise their feet on toes and make a sudden drop on to the heels. This creates a sudden impact force on the floor. The floor response is recorded to calculate the natural frequency and the damping coefficient. The main drawback of this test is that the floor vibration characteristics vary from person to person. Nevertheless, design evaluations of serviceability of floor structures have been based on this test.

2.6.3 Sand bag test

The sand bag test has the same characteristics as that of the heel impact test (Bachmann, Ammann et al. 1995). The main difference from the heel impact test is the use of a 1 kg sand bag, which is dropped on to the centre of the floor structure.

2.6.4 Impact hammer

The testing procedure in impact hammer test is to excite the floor by means of a damper impulse, then measure the response, including the impact force (Bachmann, Ammann et al. 1995). The main advantage of this test is that it can be undertaken at a short period of time.

2.6.5 Forced vibration testing

Forced vibration test is the most comprehensive test used to measure the stiffness and mode shape of a mode of vibration (Bachmann, Ammann et al. 1995). This is the proposed test for the research project in this thesis. It involves the use of vibration generator to vibrate the floor in a controlled manner. The vibration generator needs to be attached to the test rig and activated to provide sinusoidal excitation forces. The transducers or acceleration meters are attached to the floor system to monitor the motion and the response. The frequency of the excitation forces needs to be incremented through a selected variety of values to observe a wide range of the response spectrum. Peaks of the response spectrum identify the natural frequencies of the structure. The mode shapes for each mode are obtained by measuring the transducer responses at various positions on the structure when the structure is subjected to steady-state excitation at its natural frequency. The measurement of damping is obtained from resulting decay of oscillation after suddenly stopping the excitation at the natural frequency.

2.7 Remedial measures against floor vibration

Several methods have been described in literature to rectify the vibration problems causing human discomfort. It must be noted that such problems are often reported only after construction and huge amount of money needs to be used for retrofitting. Thus, it is critical to have a better understanding of the vibration response at a design

phase prior to construction, making the environment safer and diminishing future human discomfort problems. The following procedures and methodologies had been reported as remedial measures.

1. Frequency tuning.

2. Relocation of activities.

3. Stiffening.

4. Damping devices.

5. Isolation.

Generally, retrofitting can be done in two ways as active or passive (Hanagan, Rottmann et al. 1996a). Active methodology used an active control system while servicing the structure for occupants. Normally, an active control system is present physically, on a venerable floor system, which comprises of electromagnetic proof-mass actuator, an amplifier, a velocity sensor and electromagnetic feedback controller (Hanagan and Murray 1997). This active control system reduces the floor vibrations by adding forces and damping to counteract the resonant motion of the floor (Lichtenstein 2004). These forces are generated from the proof-mass actuator. The excessive motion of the floor is detected by the velocity sensor. The sensor takes signals to the electromagnetic feedback controller and then to the actuator to generate forces to counteract the resonant motions.

2.7.1 Frequency tuning

Frequency tuning is adjusting or changing the natural frequency of a structure to avoid the range of loading frequencies, which in turn helps to avoid the resonance. The fundamental structural frequency, natural frequency f_1 can be either increased high tuning or reduced low tuning to the relevant loading frequency f_0 (refer to Figure 2-14). The success of tuning is closely related to damping and frequency separation. The use of tuned mass dampers (TMDs) used in frequency tuning is briefly discussed in section 2.8.

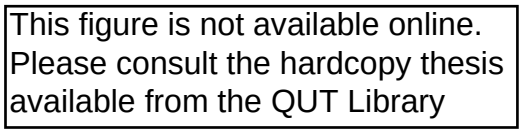

Figure 2-12: Frequency response curve of an SDOF system under constant load excitation (Bachmann. H. and Ammann. W. 1987)

Table 2-8 describes the natural frequency tuning thresholds for different structures recommended by Bachmann et al. (1987) (1988; Zivanovic, Pavic et al. 2005).

2.7.2 Relocation of activities

The relocation of the source of vibration or sensitive occupancy may be an option to remedy the problems of vibration. For example, aerobics exercises may be relocated from the top floor of a building to floors below, or complains of a floor vibration can be dealt with by positioning the source near to the column.

2.7.3 Stiffening

Increasing the stiffness of the structural element can reduce the vibration caused by walking or rhythmic activities. For example, introducing a new column from affected floor to the foundations will increase the stiffness of the floor.

Table 2-8: Recommended fundamental structural frequencies (natural frequencies) of structures with man-induced vibrations (Bachmann. H. and Ammann. W. 1987)

2.7.4 Damping devices

The added damper devices such as damper posts, tuned mass dampers or viscous dampers, may be effective in reducing the resonance vibration. Hanagan, Rottmann et al. (1996a) reported the difficulty in improving the damping of a floor system with dampers, due to the presence of multiple complex modes shapes and closely spaced natural frequencies of the floor system.

2.7.5 Isolation

Isolation as a remedial measure against floor vibration means to isolate the excitation paraphernalia from the structure. For example isolation of vibration machinery from the floor by placing them it springs may be effective. This separates machine and the floor structure reducing the vibration transmitted from the machinery to the floor (Gordon 2005).

2.8 Damping devices for vibration control

One of the common methods used to mitigate the excessive vibration is by adding damping devices to the structural system. These damping devices can be classified as passive, semi-active and active (Hanagan, Rottmann et al. 1996b) (Mackriell, Kwok et al. 1997).

Passive damping — This approach consists of incorporating "passive" devices to the structure. These passive devices may be visco-elastic dampers, friction dampers, TMDs (Setareh, Ritchey et al. 2006) etc. This is the most common approach in vibration control techniques.

Active damping — This approach involves the use of actuators to produce a counteract force to reduce the resonant vibration. The method uses actuators, sensors and controllers, both analog and digital to generate the counteract oscillation.

Semi-active damping — This approach is combination of both active and passive damping, also known as adaptive-passive damping. It uses a self adjustable passive control scheme, where the response of damping is adjusted to the oscillation of the structural system.

2.8.1 The use of passive damping devices

The most commonly used vibration control techniques are based on the use of passive damping devices. These devices are capable of absorbing part of the energy

induced by the structure, while reducing the energy dissipation through the other structural elements. As a result, the deflections and accelerations are controlled. The power needed to counteract the vibrational effects is provided by the relative motion between the two ends of the attachment, which is the damping device. This relative motion determines the amplitude and the direction of the counteract force. An active control system on the other hand, requires actuators, sensors, controllers and computer technology and as a result the installation is more complex and costly. For this reason, active damping devices are not generally used in the floor systems subjected to human-induced loads.

Ebrahimpour and Sack (2005) retrofitted a laboratory-constructed floor to perform at acceptable vibration levels, by laminates of carbon fibre reinforced polymer (CFRP) and layers of visco-elastic material. In controlling the vibrations produced, the CFRP and VE material act as VE passive damping system. Using a mass-drop test which is similar to heel-drop test, the vibration response was observed. 400% increase in the damping ratio, from 2.4% to 11.7% was found and as a result, 70% deflection reduction was achieved. This type of VE damping system in floor system is yet to be studied comprehensively, especially in composite floors.

TMDs are another passive damping devices that have been tested on controlling floor vibration (Hanagan, Rottmann et al. 1996b). Webster et al. (Webster and Vaicaitis 2003) Setareh, Ritchey et al. (2006) presented cases studies of using TMDs to control excessive floor vibrations. The TMDs consist of massive elements elastically connected to the structure. This connection allows relative motion between the mass and the structure, so that a large inertia force is produced. To gain such a large inertia force, the natural frequency of the structure needs to be close to the fundamental frequency of the structure. This mechanism of TMDs is most effective in controlling the first mode of vibration. Setareh et al. (Setareh, Ritchey et al. 2006) presented an analytical and experimental study of pendulum tuned mass damper to control excessive floor vibrations due to human movements. Although it resulted in significant reductions in the excessive vibrations caused by humans, due to the off-tuning caused by variations in the floor live loads, the TMD did not perform effectively. Consequently, TMDs were found to be the most effective in addressing only the first mode of vibration. The floor systems subjected to multi-modal

vibrations did not produce such favourable results. Thus, the current study did not use the TMDs as a retrofitting tool in floor system subjected to multi-mode vibration. VE dampers were proposed instead as a more suitable retrofitting tool in controlling vibration in composite floors. A conceptual study on using VE dampers in controlling human-induced floor vibrations is presented and discussed in Chapter 8 of this thesis.

2.8.2 VE Dampers

Passive VE damper system is the most promising energy dissipation system that can be used in floor structures although its technology is relatively new (Keel and Mahmoodi 1986). VE dampers were first used in the USA in 1969, in the building of the World Trade Centre twin towers. Later in 1980, these dampers were used in Columbia Sea First and Two Union Square buildings in Seattle and in 1994 in Chien-Tan Railroad Station, Taipai (Cho 1998). On most occasions, these VE dampers were used either to control the seismic response or to reduce wind induced vibrations. Only a limited research has been conducted on using VE dampers in floor structures to control human-induced vibrations.

A typical VE damper is illustrated in Figure 2-13. These shear type VE damper, presented in Figure 2-15 consists of two VE layers of uniform thickness confined by three steel pates. These three steel plates move with respect to each other in the axial direction. In a dynamic event, the plates undergo a relative motion causing the VE material to deform, with a certain amount of energy being lost due to shear force. Thus, the mount of energy dissipated in a dynamic event is purely based on the properties of the VE material. As the name implies, visco-elastic material has combined features of elastic solid and viscous liquid, when undergoing deformation. These features are defined by shear storage modulus G' and shear loss modulus G''. The expressions for these moduli were presented by Abbas et al. (1993) and are expresses here in Equation 2-21 and Equation 2-22. These moduli exhibit sensitivity to frequency, temperature and strain amplitude.

$$G' = 16.0 f^{0.51} \gamma^{-0.23} e^{(72.46/temp)}, \qquad \textbf{Equation 2-21}$$

$$G' = 18.5 f^{0.51} \gamma^{-0.20} e^{(73.89/temp)}, \qquad \textbf{Equation 2-22}$$

where γ is the shear strain and *f* is the frequency.

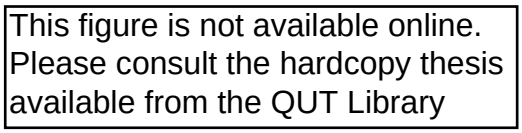

Figure 2-13: Typical shear type visco-elastic damper (Cho 1998)

In FE modelling, a VE damper linear spring elements and dashpot elements known as Kelvin Model can be used in parallel. The spring represents the stiffness and the dashpot represents the damping. According to Abbas et al. (1993), for a given dimension of the damper and the VE material property given by G' and G'', the stiffness k_d and damping coefficients C_d of the Kelvin model can be expressed:

$$k_d = \frac{G'A}{t}, \qquad \textbf{Equation 2-23}$$

$$C_d = \frac{G''A}{ft}, \qquad \textbf{Equation 2-24}$$

where A is the shear area of the VE material, t is the thickness of the VE material, f is the loading frequency of the VE damper, G' is the shear storage modulus and G'' the shear loss modulus. These parameters are used in this thesis to determine the contribution of knowledge in using VE dampers to mitigate floor vibrations.

2.9 Introduction to composite floor construction

Composite floors denote the composite actions of steel beams and concrete or composite slabs that form a structural floor. Composite slabs comprise of steel down-stand beams called girders, profiled steel decking or sheeting as the permanent formwork, lightweight or normal weight concrete slabs and anti-crack steel mesh (Widjaya 1997).

The first design rules, covered in design of steel decking and composite slabs were incorporated into British Standard in 1982 (BS 5950 : Part 4. 1994). Since then the design guidelines have been improved. However, the knowledge of vibration responses of steel-deck composite floors in published work is minimal and needs to be explored. This section presents an introduction to the steel deck composite floors and continues with a description of the selected composite floor system used for the research presented in this thesis.

2.9.1 Construction materials – steel sheet

One type of the construction material that has been used for composite floor are profiled steel sheets (Wright, Evans et al. 1987). According to their profile, profiled steel deck are categorised in to two types, dovetailed deck profiles as seen in Figure 2-14 and trapezoidal deck profiles as seen in Figure 2-15.

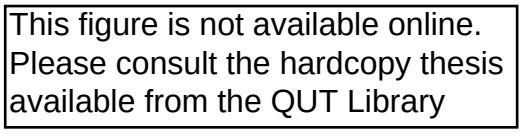

Figure 2-14: Dovetailed deck profiles (Mullett 1998)

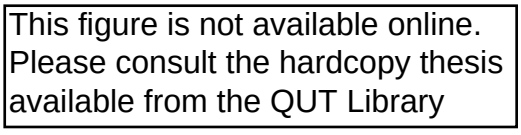

Figure 2-15: Trapezoidal deck profiles (Mullett 1998)

The use of profiled steel decking has many advantages and benefits as within certain limits (Luger 2006):

1. It provides safe working platform.
2. It acts as formwork for wet concrete and helps resist imposed load after hardening.
3. It supports working loads during construction.

The typical thickness of the steel deck sheets varies form 0.9 - 1.5 mm, however, thicker profiled steel sheets are being used in modern construction. The nominal deck profiles are in the range of 45-80 mm. The nominal steel grade of 280 N/mm^2 is being used in most cases, however, higher yield strength grades are being used for longer spans (Davison 2003).

2.9.2 Construction materials – concrete

Another construction material that is used in composite construction is concrete. Normal weight concrete (NWC) or light weight concrete (LWC) are used and the concrete grade generally varies from 30 – 40 N/mm^2.

2.9.3 Construction methodology

The normal construction procedure of casting a composite floor, is to first place the steel deck and then to pour concrete. Props are used to support the load of the wet concrete. The props can be removed after hardening of the concrete at pre-described dates. Further, the concrete should be cured regularly until its nominal strength is acquired. A steel mesh is layered prior to placing of the concrete. This is to reduce the shrinkage cracks, which may develop in the hardening process.

It is necessary to make sure that the surface of the steel deck is free from foreign matter. Otherwise the bonding between the concrete and steel will loosen, which can create de-bonging, causing lateral splitting.

In most instances, the composite deck systems come with the manufacture's specifications. Therefore, it is advisable to follow the guidance given by the manufacturer.

2.10 Finite element method of analysis

Finite element method (FEM) is known to have been developed during early 1950s. It is a mathematical modelling technique used to determine the response of real structures to external loads, sometimes also to internal loads. Used in solving most of the phenomena, the FEM of analysis has become one of the main computing tools for engineers and scientists. Due to its cost and time-efficiency compared with physical experiments, it plays an important role in engineering practice. Furthermore, it can be employed to model and analyse simple structures as well as complex irregular structures, which are more difficult to model using traditional analytical techniques. However, one must understand that the accuracy of the result obtained from finite element analysis (FEA) depends upon the quality of the input data. Thus, a limited experimental calibration is needed to guarantee acceptable results.

The basic methodology behind the finite element approach is to split a complex problem into simplified solvable ones (Clough and Penzien 1993). For example, an odd-shaped wing of an aircraft is represented using a large assemblage of small triangular / rectangular shapes or elements. Taking advantage of the high computational power of modern computers and some advanced techniques of matrix mathematics, these large numbers of elements can be used to solve intractable problems.

It has become more simple and user-friendly to make use of FEM, with the use of finite element (FE) software. There are many commercially available FE software such as ALGOR, ABAQUS, MSC PATRAN, SAP, LS DYNA, MFEAP. Every software analysis process involves the following three major phases.

1. Pre-processing

The pre-processing involves defining an appropriate finite element mesh, assigning suitable material properties and applying boundary conditions (restraint or constraints) and loads. In general, pre-processing is used to build an input file.

2. Solution

The solution phase performs the execution of the input data file to from the output, results file. In this phase, the input data are assembled into matrix format and solved numerically. The assembly process depends upon the user's requirements i.e. static or dynamic and model element types and properties, material properties, boundary conditions and loads. The assembly process of a multi-degree of freedom system is governed according to Equation 2-25:

$$[M]\{\ddot{x}\}+[C]\{\dot{x}\}+[K]\{x\}=\{F(t)\}, \qquad \textbf{Equation 2-25}$$

where: $\dot{x}(t) = dx(t)/dt$

$$\ddot{x}(t) = d^2x(t)/dt^2$$

where $[M]$ is the mass matrix, $[C]$ is the structural damping matrix, $[K]$ is the stiffness matrix, $\ddot{x}(t)$ is the acceleration vector, $\dot{x}(t)$ is the velocity vector, $\{x(t)\}$ is the displacement vector and $F(t)$ is the applied load vector.

The mass matrix $[M]$, structural damping matrix $[C]$ and stiffness matrix $[K]$ are defined upon the element type and material properties, whilst acceleration vector $\ddot{x}(t)$, velocity vector $\dot{x}(t)$ and displacement vector $x(t)$ are developed based upon the boundary conditions. The applied load vector $F(t)$ is developed using the applied external loads on the system. In the solution phase, the above equation is solved for displacement and stretches to obtain internal / external loads or stresses. This method is called displacement method or stiffness method.

3. Post-processing

The post-processing involves presenting the solved system to the end-user graphically or numerically. In addition, it provides information on errors occurred in the solution. Most advanced finite element software provides a log file, which gives information on erroneous results and a quantitative measure of integrity.

In this research project, MSC PATRAN 2004 version is being used as the pre-processor and post-processor, while ABAQUS/Standard version 6.4 is being used as the solver.

2.10.1 Finite elements

The ABAQUS code contains a large number of finite elements, which can be used to build complex structures. Most commonly used finite elements are described in Figure 2-16.

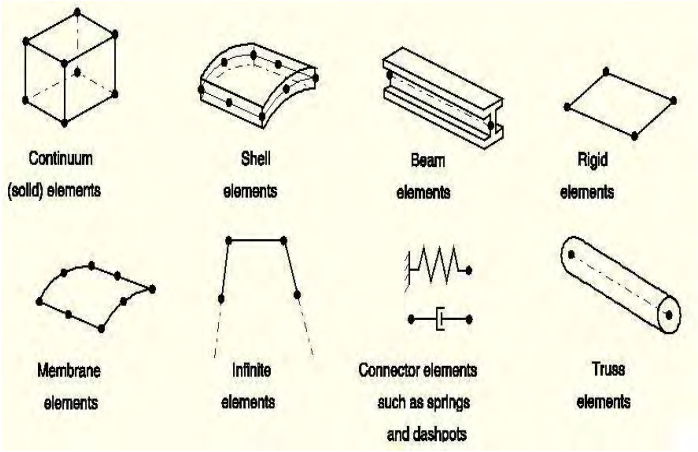

Figure 2-16: Finite elements used by ABAQUS

2.10.2 Analysis techniques

This section describes in detail the finite element solving techniques used in this thesis's research approach.

2.10.2.1 Linear static analysis

Most engineering design and practice rules are based on linear behaviour of material and static load. In such approach it is expected that, if a given loading is doubled, the resulting deflections are doubled. Furthermore, it is assumed that all deformations are recovered when the load is removed. However, it has been concluded that linear analysis approximates the true behaviour of the structural system used for basic design methods, and it is not adequate for research purposes (Hibbitt Karlsson & Sorensen Inc. 2001).

Linear static analysis is used in a case, where time independent loads are not applied to the structural system. The Equation 2-25 can be modified to describe the linear static analysis of structural systems by omitting the mass matrix [*M*] and structural damping matrix [*C*] as depicted in Equation 2-26.

Thus,

$$[K]\{x\} = \{F\}, \qquad \textbf{Equation 2-26}$$

2.10.2.2 Non-linear static analyses

Non-linear static analyses are complex analyses which occur when the force-displacement relationship of the system is non-linear. Thus, the force vector, and the stiffness matrix [*K*] are formulated on nodal displacements. This is mainly due to the fact that real structures have a certain degree of non-linearity as a result of material non-linearity, geometric non-linearity and boundary non-linearity (Abacus Analysis User's Manual 2003).

Material non-linearity

Structural materials like steel exhibit non-linearity in their behaviour and hence it is desirable to add non linearity in modelling the material. Thus, the stress-strain relationship of the material must be fed into the FE program. Usually, this has been done by feeding an approximated stress-strain curve either bi-linearly or multi-linearly.

Geometric non-linearity

This type of non-linearity occurs when the system's internal forces are dependent upon the final deformation. Thus, the original stiffness matrix is no longer valid and needs to be adjusted accordingly. This can be illustrated by considering a wire hanging on its own weight and loaded centrally. The system is said to be materially linear as the wire relocates to its original shape when the load is removed, provided that the wire does not exceed the elastic limit. However, it is geometrically non-linear since its ability carry to the load depends upon the final deformation of "V" shape.

Two methods have been suggested to rectify the problem. First one being an approximate method, which assumes the size of the individual element representing the system is constant, and reorientates the element stiffness matrix due to the elemental deformation. Second method then recalculates the stiffness matrix with the calculated displacements according to the preceding nodal coordinates.

Boundary Non-linearity

Boundary non-linearity occurs when the boundary conditions change during analysis. Non-linear elastic springs, multi-point constraints are examples of sources of boundary non-linearity (Abacus Analysis User's Manual 2003).

2.10.2.3 Dynamic analysis

In dynamic analysis, the forces and the displacements experienced by the structure are dependent upon the time history of the forcing function. Equation 2-25 has been used to formulate dynamic analysis incorporating a time-dependent function. However, when the structural system is materially or geometrically non-linear, time-consuming step-by-step integration of the dynamic equation is required. ABAQUS / Standard offers a variety of dynamic analysis processes, which are briefly described below.

Natural frequency analysis

A premier to a full dynamic analysis is the analysis of free vibration. This is to observe the structures' natural frequency and mode shapes. From an engineer's point of view, it is important to understand the natural frequencies and the mode shape as the structure could resonate at such frequencies with externally applied dynamic loads, causing excessive vibrations. Free vibration analysis depends on the structures mass and stiffness and can be derived from Equation 2-25 by making force vector $\{F(t)\}$ and damping matrix $[C]$ equals to null vector and matrix respectively.

Thus it can be re-written:

$$[M]\{\ddot{x}\}+[K]\{x\}=0\,. \qquad \textbf{Equation 2-27}$$

Since free vibration is harmonic and therefore assuming:

$$x = A\sin(\omega t + \phi)$$

Thus,

$$\ddot{x} = -A\omega^2 \sin(\omega t + \phi)\,.$$

By substituting for *x and* $\ddot{x}$ in Equation 2-27, Equation 2-28 was derived. Herein, ω represents the natural frequency of a structure. The number of natural frequencies present in the structure is equal to the number of degree of freedom.

$$(-\omega^2[M] + [K])\{A\} = 0\,. \qquad \textbf{Equation 2-28}$$

Direct-integration dynamic analysis

The direct-integration dynamic analysis provides response due to harmonic excitation. This analysis assembles the mass, stiffness and damping matrices and solves the equations of dynamic equilibrium detailed in Equation 2-21 at each point in time. The ABAQUS uses the physical number of degrees of freedom of a model directly, to calculate the steady-state response of a system. From this analysis, the structural response due to human excitation can be extracted since all the human actions are mathematically modelled using harmonic functions.

2.11 Summary and contribution to the current research

2.11.1 Summary

The literature review presented in this chapter covered the effect of dynamic loads on floor structures particularly human-induced loads and the current state of knowledge in designing floor systems against human induced vibration. Following this literature review, the conclusions and arguments made are listed below:

- Dynamic effects of floor structures are an important design consideration especially at or near resonance. Most design approaches use the first mode of natural frequency calculated using simplified approaches.
- Human-induced loads, such as walking or performing aerobics or other dance-type loads can create resonant vibration in floor systems.

- Dynamic responses of floors on which the dynamic load has been initiated have been calculated. This does not provide the dynamic responses under pattern loading in multiple panel floor construction.
- All structures have some inherent damping, which depends on the construction type, including cladding and partitions, and is being assumed in design.
- Vibration effects can be mitigated by altering the structure's natural frequency, or periods of vibration, by adding mass, or by increasing damping through passive damping techniques using artificial damping or tuned mass dampers and VE dampers.

2.11.2 Contribution

The research contribution of this thesis extends the current knowledge on vibration of floor structures, particularly in multiple panel composite floor construction. The current design criteria for dynamic responses pertain to the floors from which activity originated. This does not help to establish the dynamic responses that occur during pattern loading, when different portion of the floor are being used for different human activities. Thus, multiple panel floor construction with modern day floor layout / fit-outs can inhabit several occupancies. Consequently, the research in this thesis is carried out to investigate the performance to steel-deck composite floors subjected to pattern loading. It aims to carry out comprehensive investigation with different panel number configurations at various operating conditions. These operating conditions include human-densities, load frequency, damping levels and location of activity. Finally, it addresses the use of a passive damping technique that renders the vibration problem. The results from this research are presented in the following chapters.

Chapter 3 - Experimental Investigation

3.1 Introduction

This chapter presents the experimental study carried out on a single panel steel-deck composite floor system in a laboratory controlled environment. It contains the descriptions of test methodology, equipment used and test results. In addition, this chapter describes the process of determination of mechanical properties of concrete and steel, using the cylinder compressive tests and tensile tests.

The experimental study on floor panels covers tests from static to dynamic, with an objective to generate fundamental research data to calibrate and validate FE models, and to understand the response of floor panels under dynamic loads. Static tests, force vibration tests and heel drop tests were the main tests carried out. Using these test results static as well as dynamic characteristics, such as stiffness, Dynamic Amplification Factors (DAFs), fundamental frequency and damping of the floor system were determined.

A steel-deck floor system was chosen from many commercially available composite floors used in Australia. It has a dovetailed deck profile and is the most popular and widely-used steel-deck composite floor system in Australian building construction. Herein, the steel sheets or otherwise called steel deck were used as permanent shuttering capable of supporting the wet concrete and construction loads. Subsequently, these profiled steel sheets structurally bond with the hardened concrete and replace all or part of the tensile reinforcement in the finished floor. Thus, this steel-deck floor was used for laboratory tests, which were carried out on six full-scale floor panels. These six panels comprised of three panels with top reinforcement mesh and three without top reinforcement mesh. This was done deliberately to explore variations in dynamic characteristics due to top reinforcement in steel-deck composite floors. This was a secondary objective that arose from the industry partners sponsoring the experiments.

Finally, conclusions were drawn from the experimental study and data for calibration of FE model were gathered.

3.2 Test samples

As the dynamic response of steel-deck floors varies with span and thickness, test specimens were prepared for a selected span with minimum slab thickness. Such test samples would produce adequate results with available resources for calibration of computer models and then experimental dynamic responses will be obtained. Usually, the product manufacturers offer design charts or design software for the design and construction of steel-deck composite floors for the user. Using this information, steel-deck floor panels sized 3.4 m x 1.8 m x 100 mm thick were selected for the tests.

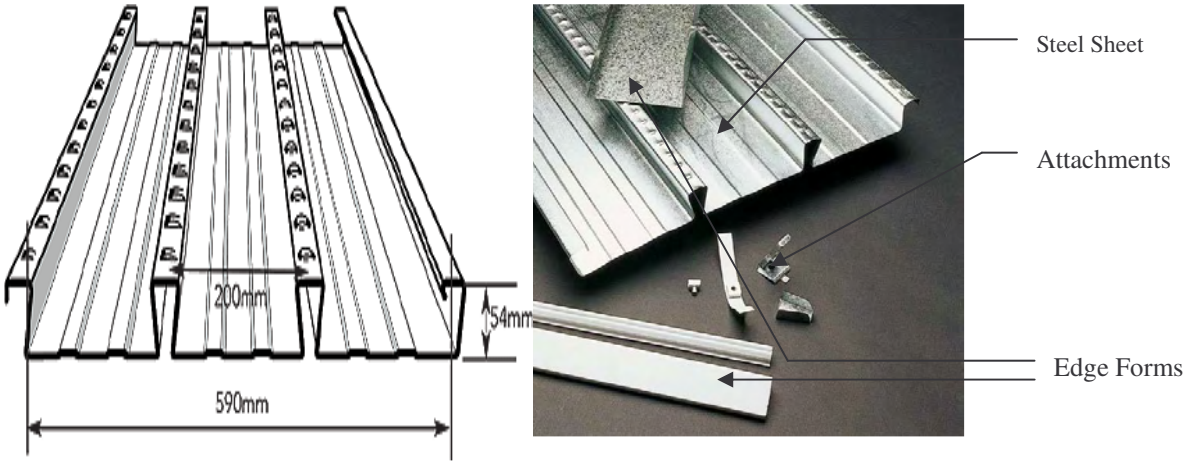

Figure 3-1: Components of steel-deck floor system (BlueScope Lysaght)

The components of the steel-deck are shown in the above Figure 3-1. The steel sheet is used as permanent formwork in a floor system and the edge forms are used at the ends or sides of a particular span. The attachments are mostly used in post-construction situations where objects such as suspended ceilings, air ducts are attached. Coated in Zinc, deck-sheets are generally manufactured in three thicknesses, - 0.65, 0.75 and 1.0 mm, using high strength steel of 550 MPa. The typical size and basic dimensions of the steel-deck section are shown in Figure 3-2. After considering the most common thicknesses used in the construction practice a thickness of 1.0 mm was chosen for the current project.

The steel-deck composite floor system consists of a dovetailed profiled steel-deck along with concrete poured over the top of it in-situ. A typical cross section

dimension of a single panel, including both steel-deck and concrete, used for the current research, are presented in Figure 3-3.

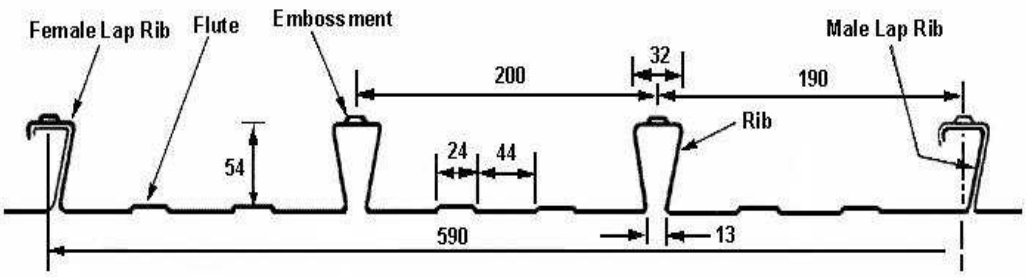

Not to Scale
Dimensions are in millimetres

Figure 3-2: Steel deck profile used in the experiments

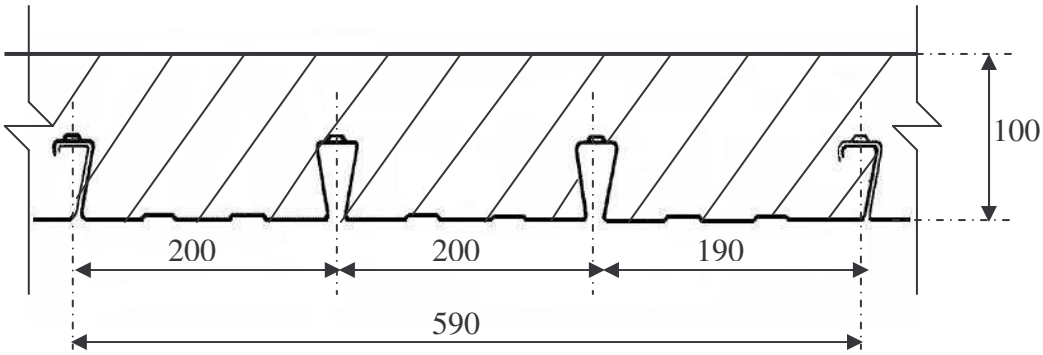

Not to Scale
Dimensions are in millimetres

Figure 3-3: Section of slab panel

Since, one of the objectives of the experimental research presented in this thesis is to determine the dynamic characteristics of these steel-deck composite floors with and without top reinforcement, to account for the variability, three panels were cast without top reinforcement and three with top reinforcement. The top reinforcements are laid over the entire size of the panel. The top reinforcement used in this case is 6 mm in diameter, 200 x 200 mm welded mesh similar to that used as in construction practice. The procedure used for making, casting and testing the panel specimens is described in the following sections.

3.2.1 Preparation of testing panels

All the preparation of the tests panels was conducted in the Structures Laboratory of the School of Urban Development, formerly School of Civil Engineering at QUT.

The fabrication of the composite floor panels was carried out according to the design and construction guide provided by the manufacturer.

The floor panels were cast on a raised by temporary beam platform. Three rows of 100 x 50 mm pine timber beams were used as a pre-described platform, allowing easier handling. The bearings of the three supports were kept at 100 mm. A single sheet was 0.6 m wide between the ribs. The selected width of the sample was 1.8 m. Thus, three sheets had to be interlocked to form the desired width. The deck system provides a self interlocking system against the movement of each sheet. The design manual describes the following two methods to interlock overlapping sheets as outlined in Figure 3-4 and Figure 3-5.

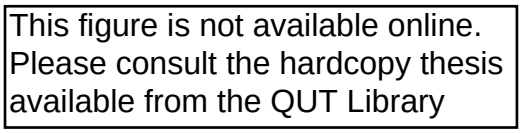

Figure 3-4: Interlocking by applying pressure - Method 1 (BlueScope Steel 2003)

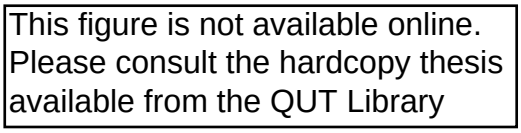

Figure 3-5: Interlocking by lowering sheet by arc - Method 2 (BlueScope Steel 2003)

The first method as seen in Figure 3-4, is to lay female lap rib overlapping the male lap rib of the adjacent sheets and apply foot pressure on to the female lap rib. The second method is to keep a new sheet's female lap rib at an angle on a previously laid sheet's male lap rib and lower it down as seen in Figure 3-5. Although the steel-deck for the current panels were interlocked using method 1, neither of the above methods provide adequate interlocking due to the damage or distortion caused by handling. Therefore, to have an absolute certainty against movement between

adjacent steel-sheets, a separate fastening method was needed. Thus, hexagonal headed self-drilling screws of 10-24 x 16 mm at 200 mm spacing were selected and used (refer to Figure 3-6).

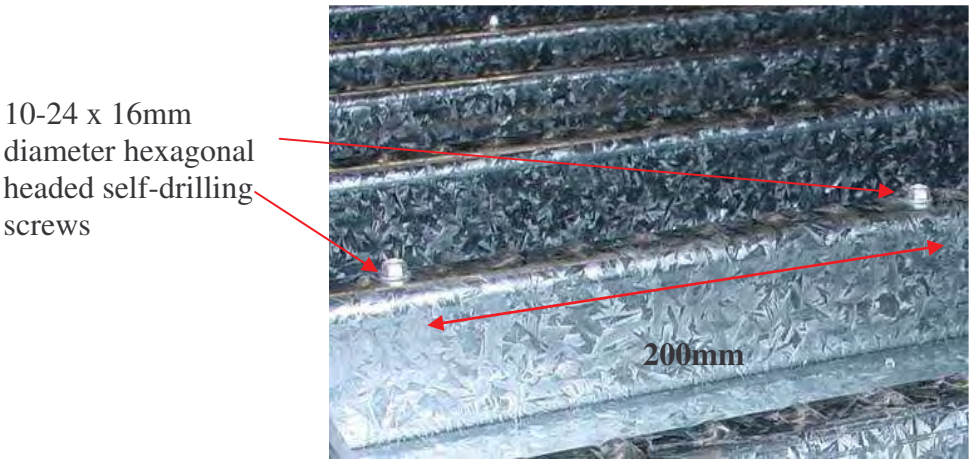

Figure 3-6: Interlocking adjacent steel sheets with screws

To obtain a 100 mm thickness of the slab, edge forms ready-made with steel were fastened on the four sides of the panel. The edge forms were fixed to the assembled steel-sheets using 10-24 x 16 mm self driving screws at 400 mm spacing as seen in Figure 3-7. In composite floor panels these edge forms provide side formwork to the system.

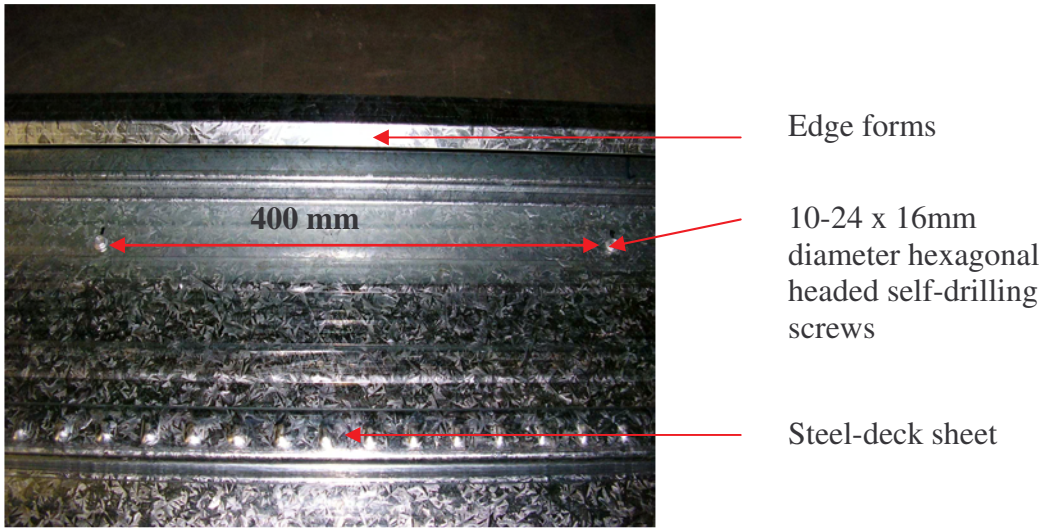

Figure 3-7: Fastening of edge forms

Figure 3-8 describes the fully prepared, ready to concrete steel-deck panels.

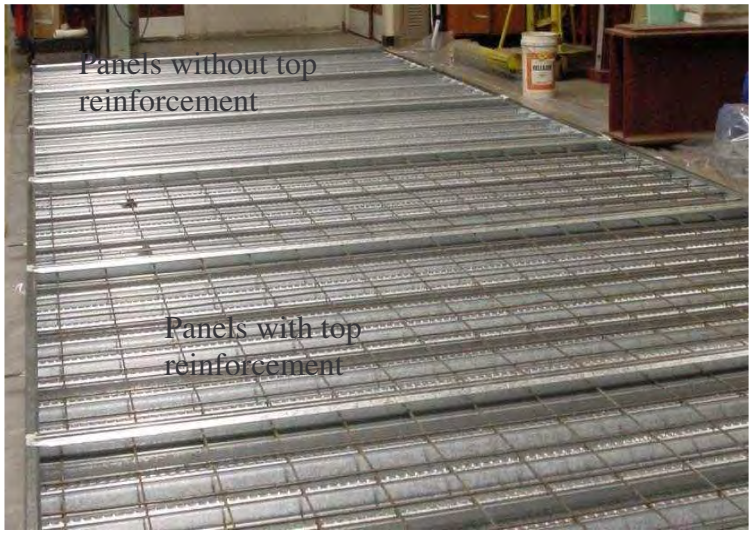

Figure 3-8: Ready to concrete steel-deck panels

Wire-mesh of 200 x 200 mm produced by MetalCorp steel, Australia was used as reinforcement for the panels with top reinforcement. The mesh was placed using 75 mm high plastic spacers in order to avoid contact with the steel deck and to perform as the top reinforcement as depicted in Figure 3-9.

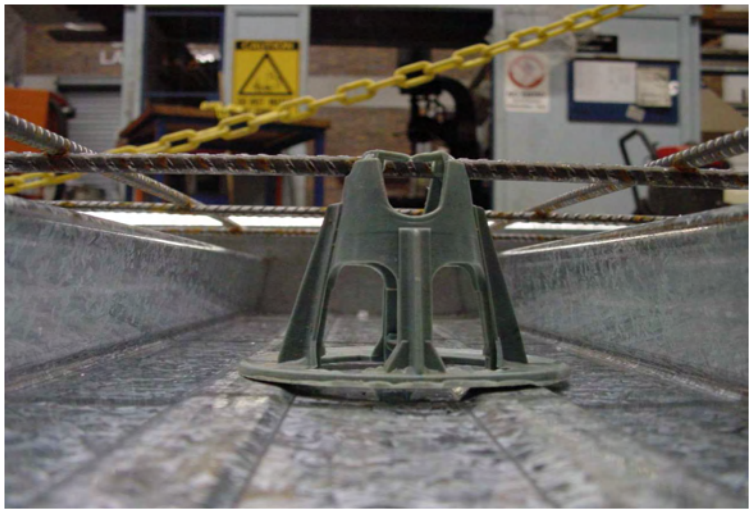

Figure 3-9: Plastic separators for avoiding contact with steel-deck

3.2.2 Lifting lugs

In order to transport the cast panels to the test rig using the laboratory ganty crane, four lifting lugs were cast in the panels. These were pre-fabricated using 16 mm threaded bars welded on to 150 x 150 x 5 mm thick steel plates. Lifting lugs were placed before the pouring of concrete, at pre-designed locations detailed in Figure

3-10 that caused minimum deflection and behaviour within the elastic range during the transport.

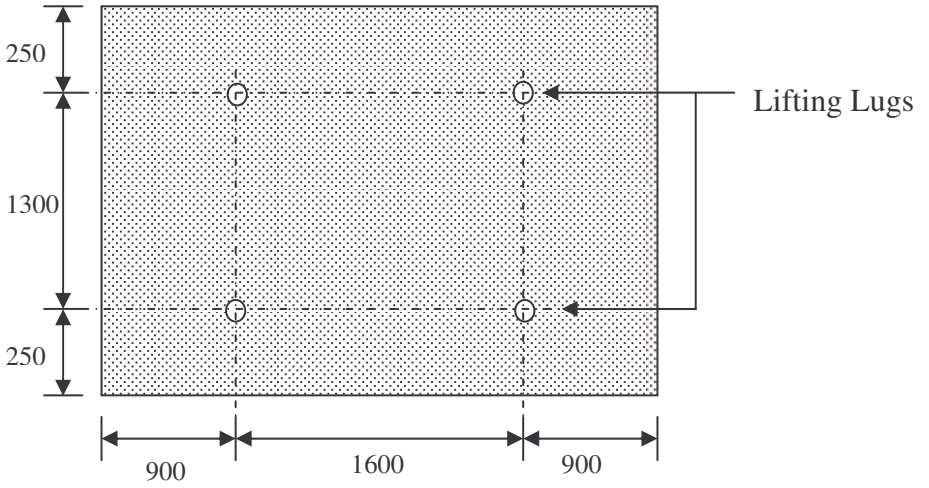

Dimensions are in millimetres
Not to scale

Figure 3-10: Lifting lug positions

3.2.3 Casting of panels

The six prepared panel decks were cast in-situ, using ready-mix concrete on Thursday the 2nd of September 2004. The slump of 70 mm was measured and six cylinders were cast for 7-days and 28-days cylinder compressive tests. Proper compaction of the panels was achieved by employing two poker vibrators. The top surface of the panels was smoothed using a trimmer bar to achieve an even surface as seen in Figure 3-11.

Figure 3-11: Casting, trimming and spreading concrete

3.2.4 Curing

After the six panels had been cast, they were covered with polythene sheets and allowed to cure for 30 days.

3.2.5 Support conditions for test rig

Two supports, allowing translations along the span and rotations about the span, were fabricated specially for the research work presented in this thesis. Solid, high strength steel circular rods of diameter 100 mm were welded on to the top flange of 700 x 255 x 25 mm "I" section to fabricate the supports, as shown in Figure 3-12 and Figure 3-13. The "I" beam was given extra strength by welding mid and end stiffeners. Moreover, another 25 mm thick stiffener was welded on the inside, mid length of the support, since the load from the slab is not transferred vertically through the "I" beam.

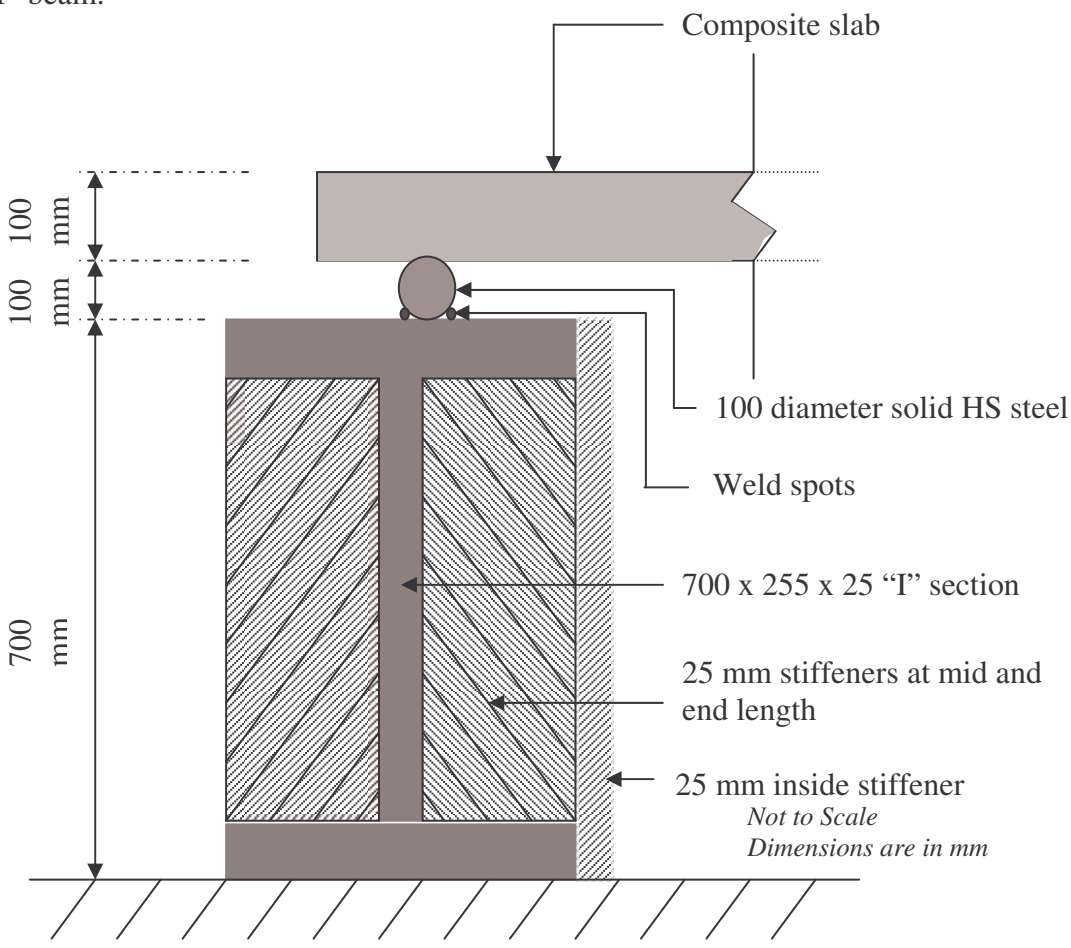

Figure 3-12: Sectional view of support condition

After the supports were fabricated, they were positioned to give a span of 3200 mm. Steel bars were cross-welded onto the rig posts to avoid any changes in their position

during the experiments. The rig posts used were further stiffened by using cross beams to another set of rig posts. This support provided high stiffness of the test rig in total, specially during the force vibration tests.

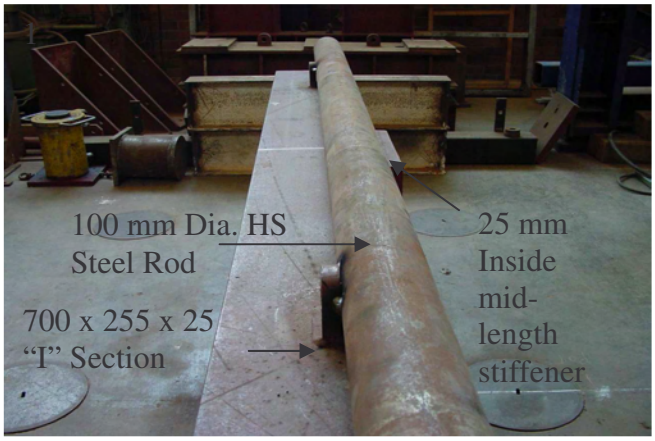

Figure 3-13: Support conditions on one end, same as those on the other end

3.2.6 Loading Frame

The loading frame of the test rig consisted of a hydraulic jack system, a spreader beam and timber logs to achieve an evenly spread load across the whole panel. The load was applied via a hydraulic jack system, attached to the test-rig spreader beam, using 20mm diameter fastener bolt. The hydraulic jack system consisted of a displacement transducer, an actuator and a load cell. The hydraulic system was then attached to the spreader beam via 20 mm diameter fastener bolt, from which the load was transferred onto the timber packing and then to the slab. The spreader beam was an "I" beam of 460 x 185 x 20 mm, stiffened at mid and end length. The main objective of timber packing used, was to spread the load evenly over the surface of the slab. This timber packing produced a distributed line load over a width of 200 mm, across the full width of the panel.

Figure 3-14 and Figure 3-15 show an isometric view and a sectional view of the loading frame setup respectively. This loading frame was used in both static and forced vibration tests. The methodology of using this loading frame in each test is described in test methodology and procedure in Section 3.3.

A load cell attached to the Moog actuator gave the load values applied hydraulically to the system. The weight of the timer packing logs were weighed separately and

their weight was added to the weight of the "I" beam spreader, to obtain the value of the total load applied by the loading frame.

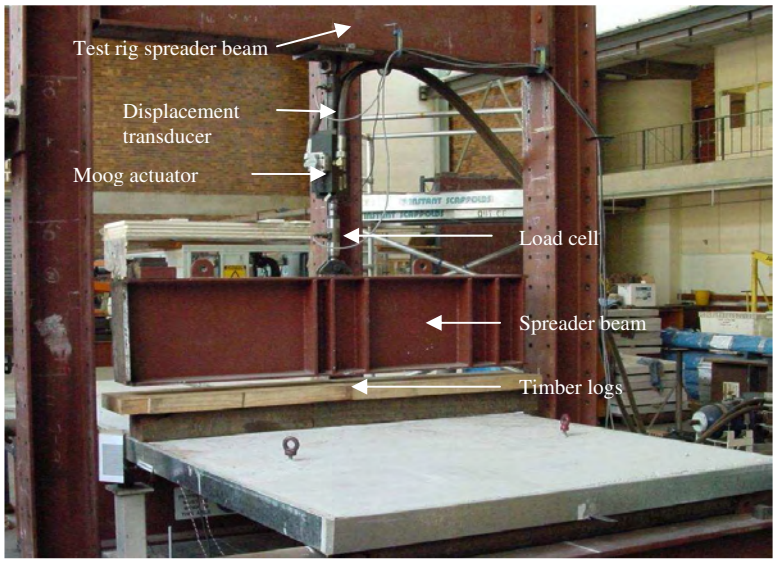

Figure 3-14: Isometric view of the loading frame

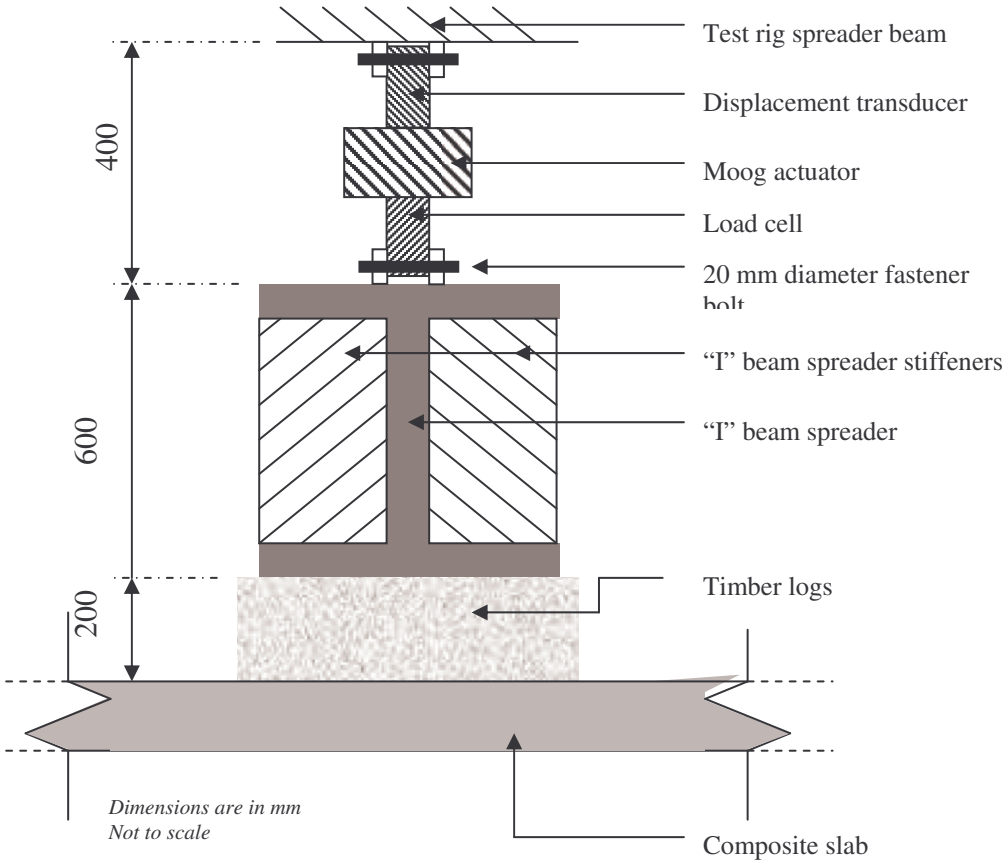

Figure 3-15: Sectional view of the loading frame

3.2.7 Instrumentation

For each test panel, linear-variation-displacement-transducers (LVDTs), strain gauges and accelerometers were attached prior to the test at the locations described in Figure 3-16. West and east LVDTs as seen in Figure 3-17a and Figure 3-17b, were used to measure the mid span vertical deflections.

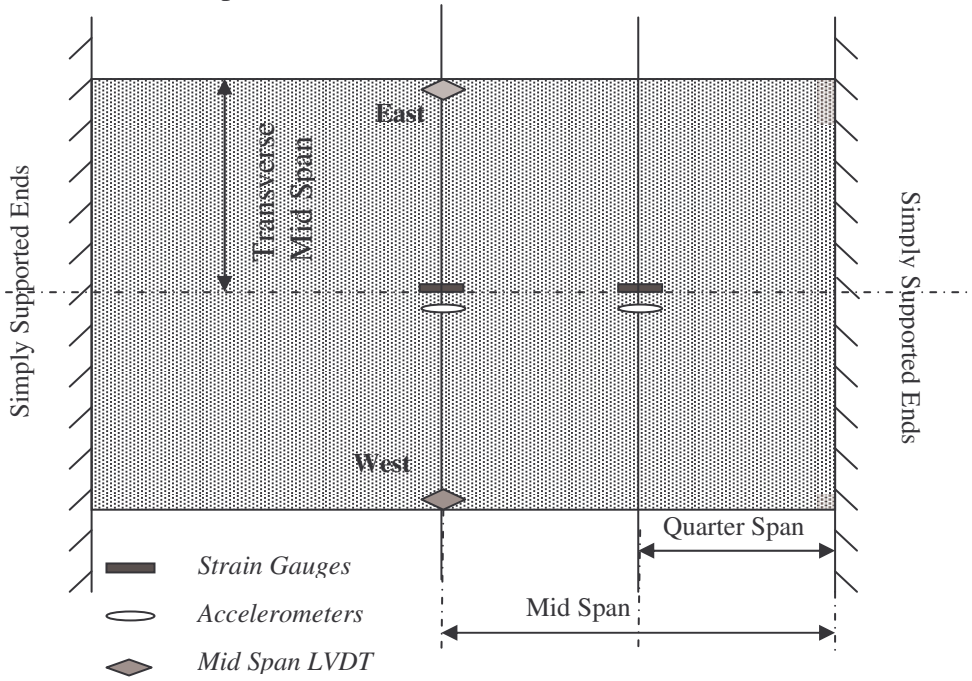

Figure 3-16: Locations of LVDT's, strain gauges and accelerometers

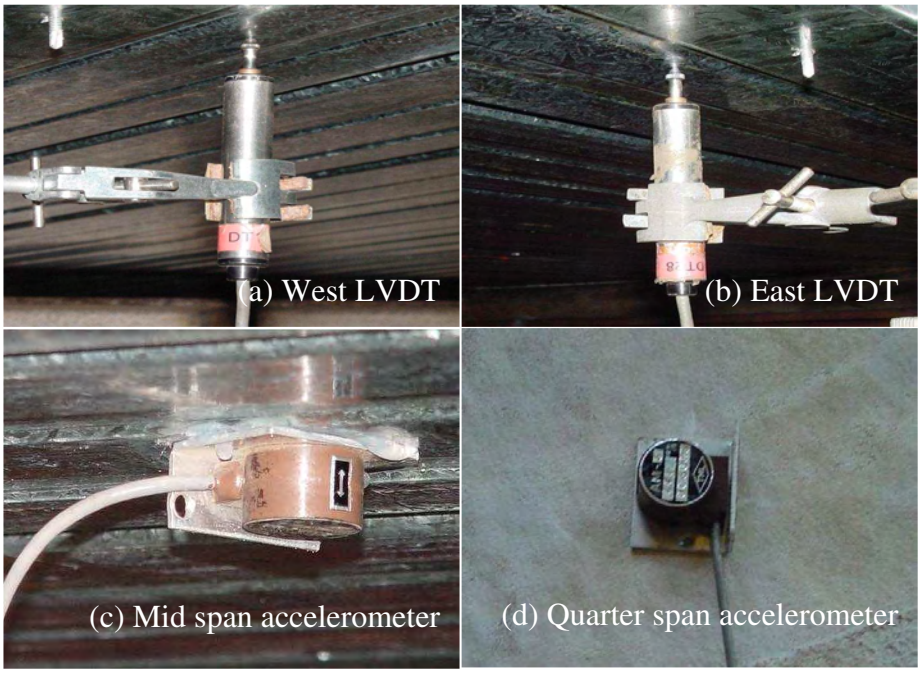

Figure 3-17: LVDT and accelerometer set-up locations

Under the static conditions, preliminary finite element model analysis, gave a maximum 10 mm mid span deflection to a maximum load of 50 kN. This was used to select a suitable LVDT size for both, static and forced vibration tests. The floor subjected to forced vibration could invoke higher defections than that subjected to static deflections. Thus the use of 10 mm LVDTs was considered not adequate and therefore, 20 mm LVDTs were used at mid span both west and east. Accelerometers with a capacity of measuring up to 5 g were used to measure the vibration response in both, forced vibration and the heel impact tests. The mid span accelerometer in Figure 3-17c was fixed onto the bottom steel-deck, due to the obstruction by the loading frame at the top. The quarter span accelerometer in Figure 3-17d was fixed onto the top of the floor panel. To obtain strain readings for the static test, the two strain gauges, one at mid span and the other at quarter span were attached to the bottom longitudinal direction of the test panel.

3.2.8 Data acquisition system

The data acquired from all of the above attachments, including the data from the load cell of the loading frame, were connected to a separate data acquisition system. The data acquisition system consisted of a Pentium I computer running on Microsoft Windows 2000 operating system, with a data logger. LABTECH NOTEBOOK version 1 software was used for all of the data acquisitions in all the tests performed. The maximum capacity of the data acquisition system is 1000 samples per second. For faster and more accurate data acquisition, specially in the forced vibration test, the number of data acquisition channels were reduced to five. Similarly, the number of channels for the heel impact test was limited to four, giving high precision in measuring the response.

3.3 Test methodology

All static tests, forced vibration tests and heel impact tests were carried out at the structures laboratory, School of Urban Development, formerly School of Civil Engineering at QUT, after 30 days of curing. The static test was performed in order to obtain the load deflection curve, which facilitated the calibration of finite element model. The forced vibration tests were performed at various loads on average starting from 5 kN to 45 kN in 5 kN steps and at sinusoidal frequencies, starting from 1 Hz to

9 Hz in steps of 0.5 Hz. Heel impact tests were performed in order to measure the experimental fundamental natural frequency and the damping coefficient of the floor system. The following sections describe the procedures and the methodology adopted for each test.

3.3.1 Static tests

Firstly the test panels were positioned on the fabricated supports to achieve a span of 3200 mm. West LVDT, east LVDT, strain gauges at mid span and quarter span were placed in a correct position for the static test. After all the data channels were fixed and tested, the panels were loaded at the mid span line load via displacement / position controlled moog actuator controller. The displacement / position controlled moog actuator permitted the increase of the load manually and incrementally. Starting from zero, the loads were applied to a maximum of 50 kN. Mid span deflections at two edges, east and west and strain gauge readings at mid span and quarter span, together with load cell data readings, were acquired using above described data acquisition system at each 2 kN increment of the load. This static test was done on each of the six panels and the above-described data were acquired.

3.3.2 Forced vibration tests

The forced vibration tests were performed on each of the panels after the completion of the static tests. A comprehensive test setup was established to vibrate the cast floor panel in a controlled manner under sinusoidal excitation. A hydraulic system with a Moog actuator, frequency generator and oscilloscope were set up to generate sinusoidal forced vibration excitation. Figure 3-18 depicts the equipment set up for the forced vibration tests.

The forced vibration frequency was generated by the Tektronix CFG 280 Frequency generator (Tektronix Inc. 1991). The generator sends signals giving the frequency to the HP oscilloscope (Hewlett Packard Inc. 1992) for processing and viewing, whilst sending a command to the moog actuator controller as depicted in Figure 3-19. The oscilloscope then generates a sinusoidal wave signal of the desired frequency and sends out commands to the moog actuator, providing information on the magnitude of the sine function. The moog actuator controller processes the information and

sends it to the actuator attached to the test rig, which generates the required force and frequency.

Figure 3-18: Frequency generator, oscilloscope, actuator controller, pump controller and data acquisition computer

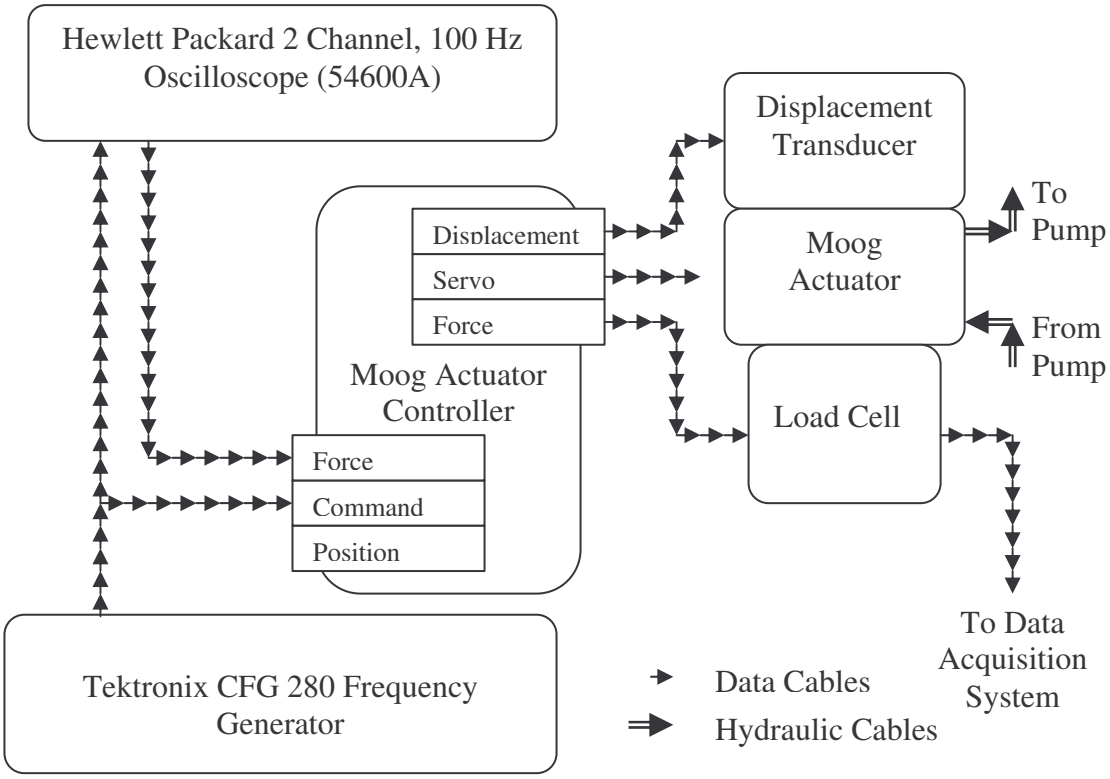

Figure 3-19: Experimental setup for forced vibration tests

The required sets of frequencies were obtained using Tektronix Frequency Generator's frequency change knob while the necessary load was obtained by changing the voltage output in the Hewlett Packard oscilloscope. Herein, 10 Volts

gave 50 kN of load and the oscilloscope sinusoidal voltage output was changed starting from 1 V, peak to peak, up to 10 Volts in steps of 1 V to provide sinusoidal forces starting from 5 kN in 5 kN steps. The frequency of the force was incremented starting from 1 Hz to 9 Hz, with various load increments on average starting from 5kN to 45 kN. Figure 3-20 shows typical sinusoidal load excitations at 1.0 Hz, 2.0 Hz, 3.0 Hz, 4.0 Hz, 5.0 Hz, 6.0 Hz, 7.0 Hz and 8.0 Hz, applied to the system at average load of 10 kN. It is important to note that Figure 3-20 shows a part of the dynamic loads that were applied due to space limitations, rather than the loads that were applied on 0.5 Hz increments. Since the load cell was brought to zero at the beginning of each test, the total load was calculated by adding the load cell records to the load applied from the spreader beam and the timber packing, which was 2.7 kN.

This test procedure was conducted on all six panels and altogether about 500 forced vibration tests were performed.

The maximum capacity of the data acquisition system of 1000 rpm was used to obtain data from the forced vibration test. Thus, a limited number of channels, including the key readings, were used to obtain data. Five channels consisting of displacement LVDTs at east and west positions and two accelerometer readings at mid span and quarter span, along with the load cell readings were used. A sampling rate of 200 samples per second was used and the data were acquired for 2 seconds for each load at each frequency. Also, each data set was acquired after 30 seconds, when system was assumed to reach the steady state condition.

Due to the system limitations the acquisition of data at higher loads and at higher frequencies was restricted. However, the responses at lower loads such as 5 kN, 10 kN, 15 kN were obtained using entire frequency range from 1 Hz ~ 9 Hz.

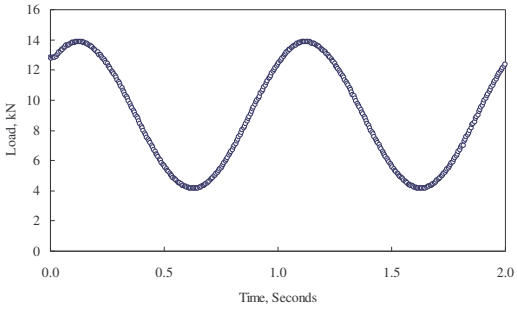

(a) Sinusoidal load 10 kN at 1 Hz

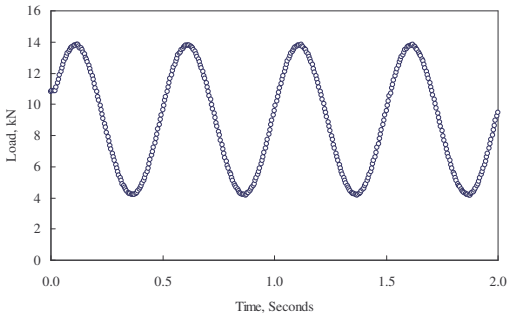

(b) Sinusoidal load 10 kN at 2 Hz

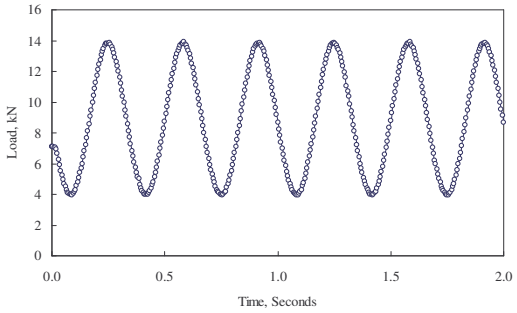

(d) Sinusoidal load 10 kN at 3 Hz

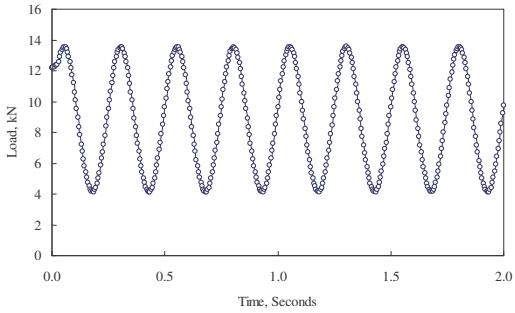

(c) Sinusoidal load 10 kN at 4 Hz

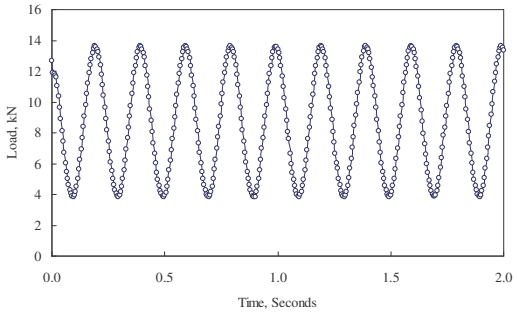

(f) Sinusoidal load 10 kN at 5 Hz

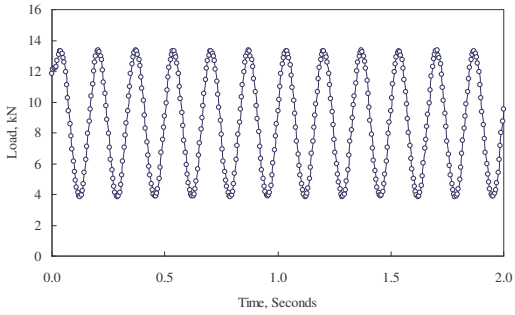

(e) Sinusoidal load 10 kN at 6 Hz

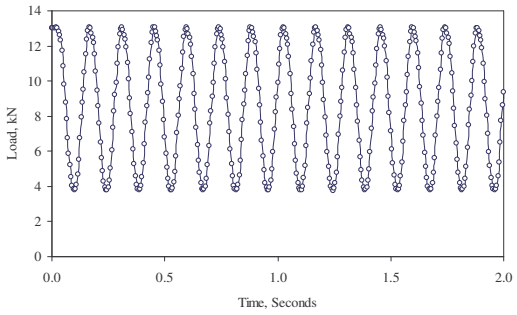

(h) Sinusoidal load 10 kN at 7 Hz

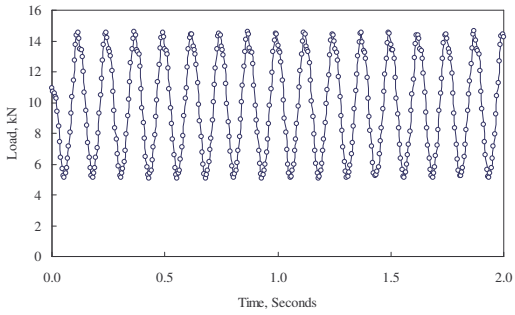

(g) Sinusoidal load 10 kN at 8 Hz

Figure 3-20: Typical sinusoidal loads at 1 Hz, 2 Hz, 3 Hz, 4 Hz, 5 Hz, 6 Hz, 7 Hz and 8 Hz applied on the panels

3.3.3 Heel impact tests

Heel impact tests were performed on every panel. As these tests have many drawbacks (Blakeborough and Williams 2003), three heel impact tests were done for each panel to achieve greater accuracy. The procedure for the heel impact tests is to perform a heel drop excitation on a floor. An average person was asked to sit-up at the mid span of test floor, raise their heel to about 50 mm and produce a sudden impact on the floor (refer to Figure 3-21). The resulting responses of deflection and accelerations were obtained. Since the deflections at mid spans were small, 5 mm LVDT's were attached on west and east spans for grater accuracy. Accelerometers of 5 g, at mid span and at quarter span were used to acquire the vibration response. To gain a maximum yield, the data was acquired for 5 seconds at a rate of 1000 samples per second.

Figure 3-21: Heel impact excitation

3.4 Cylinder compressive strength tests

To obtain characteristic compressive strength of concrete, concrete cylinders were cast on the 2nd of September 2004. The results of this test were also used in the finite element model described in Chapter 4. Six cylinders were cast to obtain a mean value. They were tested on the 7th of September 2004 for the 7-day test and on the 30th of September 2004 for the 28-day test at the Concrete Testing Facility at QUT. These tests were carried out in accordance with Australian Standards, AS 1012.8.1 (AS 1012.8.1 Standards Australia 2000) and AS 1012.9 (AS 1012.9 Standards Australia 1999). The following procedure was adopted in preparation and in testing of the six test specimens:

- The specimens were taken out from the curing basin, cleaned using pressurized air to remove all loose particles, and numbered in a recognizable manner for identification as seen in Figure 3-22a and Figure 3-23a.
- Each specimen was weighed using an electronic balance. The weight values were recorded in Table 3-1 and Table 3-2.
- A layer of capping material of fly ash mixed with sulphur was used to smooth the surface (refer to Figure 3-22b and Figure 3-23b). A release agent WD 40 was used to ease the removal of the capping material from the capping mould. It was ensured that after capping, the surface was free from irregularities.

Figure 3-22: Concrete cylinders for 7 day test

Figure 3-23: Concrete cylinders for 28 day test

- Two diameters, d_1 and d_2 at two right angle positions and the height h of each specimen as seen in Figure 3-24 were measured and recorded in Table 3-1 and Table 3-2.

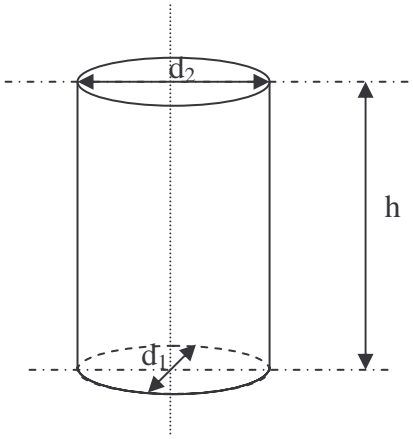

Figure 3-24: Recorded dimensions of the cylinder

- Each specimen was placed in the Pro-Lab Concrete Compressive Strength Testing machine and load was applied to the capped surface until failure as seen in Figure 3-25a and Figure 3-25b.

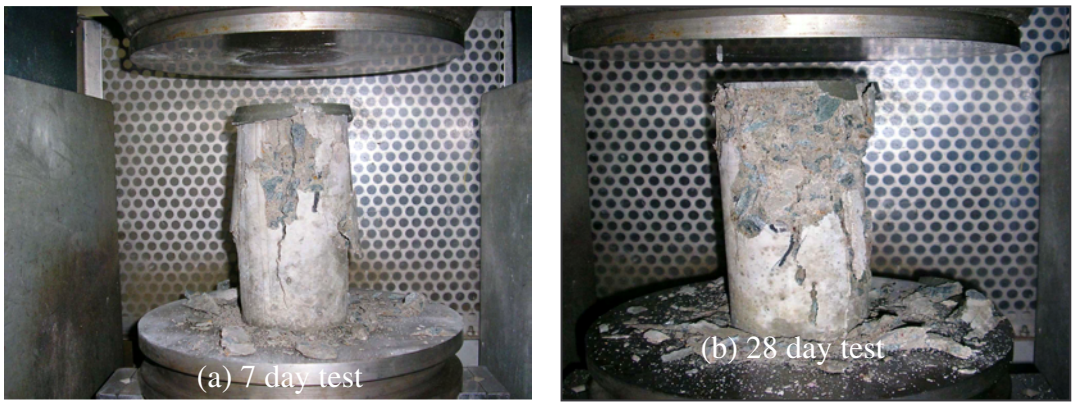

Figure 3-25: Typical failure pattern of the concrete compressive strength

- Finally, load at the point of failure was recorded and the compressive strength was calculated.

The data collected from the 7 day and 28 day cylinder compressive strength test are described in Table 3-1 and 3-2 respectively. The average 7-day compressive strength of the concrete was 28.5 MPa while the average 28-day compressive strength of concrete was 37.1 MPa. The calculated density of the concrete was 2428 kg/m^3.

Table 3-1: Readings of the 7-day concrete compressive test

Specimen No	Weight (g)	Diameter d_1 (mm)	Diameter d_2 (mm)	Height h (mm)	Ultimate load (kN)	Compressive strength (MPa)	Calculated density (kg/m^3)
1	3870	100.2	100.2	204	233.1	29.6	2405.8
2	3870	100.0	100.0	204	220.3	28.0	2415.4
3	3890	100.4	100.4	203	224.4	28.3	2420.4

Average 7-day compressive strength of concrete: 28.5 MPa

Table 3-2: Readings of the 28-day concrete compressive test

Specimen No	Weight (g)	Diameter d_1 (mm)	Diameter d_2 (mm)	Height h (mm)	Ultimate load (kN)	Compressive strength (MPa)	Calculated density (kg/m^3)
4	3910	100.2	100.2	203.4	259.0	32.8	2439.0
5	3877	100.0	100.0	203.0	297.4	37.8	2432.9
6	3941	100.4	100.4	203.0	323.0	40.8	2453.4

Average 28-day compressive strength of concrete: 37.1 MPa

Average density of concrete: 2428 kg/m^3

3.5 Tensile tests for steel

Tensile tests were done on three specimens obtained from the sheet decking, to calculate the tensile capacities and elastic modulus of steel. The specimens were prepared as per the sketch (in Figure 3-26) in accordance with AS 1391 (AS 1391 Standards Australia 1991). The width, the thickness and the thickness of the Zn coating were measured, at three locations along the gauge length. The values were recorded in Table 3-3.

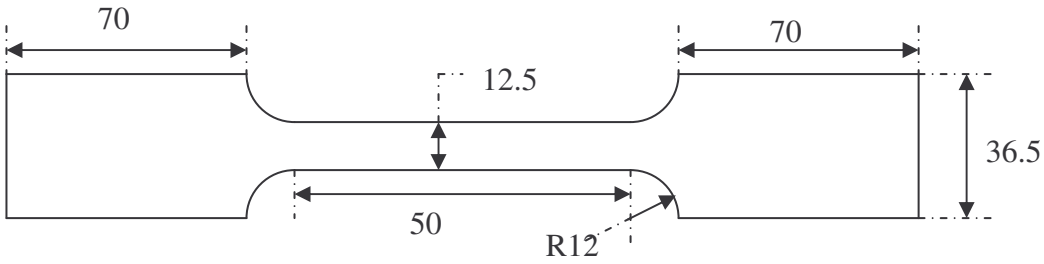

Dimensions are in millimetres
Not to scale

Figure 3-26: Dimensions of the tensile test specimens

The physical testing was carried out using the Tinius Olsen and Honsfield tensile testing machine at QUT testing facility, on the 19th of November 2004, using the standard procedures recommended by AS 1391 (AS 1391 Standards Australia 1991). A special jaw system was attached to the test machine cross heads, to eliminate the specimen twisting that usually occurs when the grips are tightened. After the tensile specimen was aligned and the grip in the test machine was secured, a 50 mm extensometer was attached to the gauge length portion of the specimen (refer to Figure 3-27). Then the specimen was loaded until failure. The load and the extensometer readings were recorded via a data acquisition system attached to the testing machine.

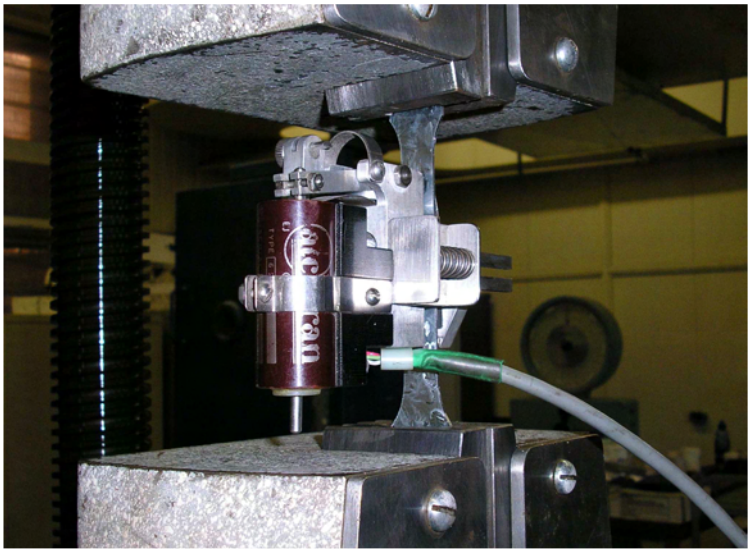

Figure 3-27: Tensile test set-up

Table 3-3 shows the specimen dimensions, ultimate load and the ultimate strength of the test specimens.

Table 3-3: Section properties of the steel specimens for the tensile test

	Width *b* (mm)	Thickness *t* (mm)	Zinc coating thickness (mm)	Ultimate load (kN)	Ultimate strength (kN/m^2)
Specimen 1	12.42	1.06	0.06	7.9377	639.3
	12.40	1.06	0.06		
	12.43	1.06	0.06		
Specimen 2	12.36	1.06	0.06	7.7984	629.7
	12.40	1.06	0.06		
	12.39	1.06	0.06		
Specimen 3	12.42	1.06	0.06	7.8855	634.0
	12.44	1.06	0.06		
	12.45	1.06	0.06		

The tensile test yielded the stress-strain relationships shown in Figure 3-28, from which the modulus of elasticity of slab deck's material was calculated. Since equipment did not have the capability of measuring the strain at more than 4% strain, the ultimate strength was calculated from the measured ultimate load.

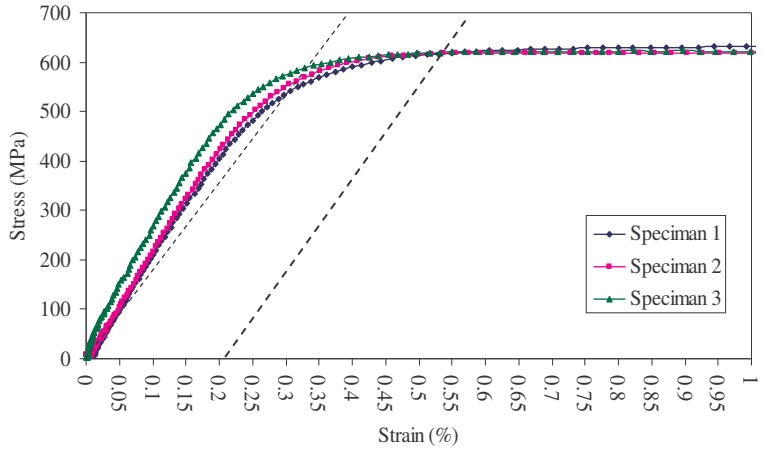

Figure 3-28: Stress-strain relationship of tensile test

The tensile test gave a 610 MPa yield strength, which is well above the minimum value of 550 MPa given in the design and construction guide (BlueScope Steel 2003). Young's modulus of elasticity of sheets calculated from the above plot gave a value of 205,000 MPa.

3.6 Experimental results and discussion

Based on the experimental investigations described in Sections 3.2 and 3.3, this section presents results and discussion for the static tests, forced vibration tests and heel impact tests performed on the six test panels.

3.6.1 Static tests

The main objective of the static test was to obtain the load-deflection curve for the floor panels and thereby derive stiffness values, which were to be used to calibrate the finite element model. The six static tests performed on each panel gave the load deflection graph in Figure 3-29 and Figure 3-30. It is important to note that the deflection described in each graph is the averaged deflection, taken at two mid span locations. The load is the total line load applied on the mid span, which is the summation of the load cell readings, load of the spreader beam and the timber packing. Figure 3-29 presents the load-deflection curves for the panels without top reinforcement, which are Panel 1, Panel 2 and Panel 3, while Figure 3-30 presents the load deflection curves for the panels with top reinforcement, Panel 4, Panel 5 and Panel 6.

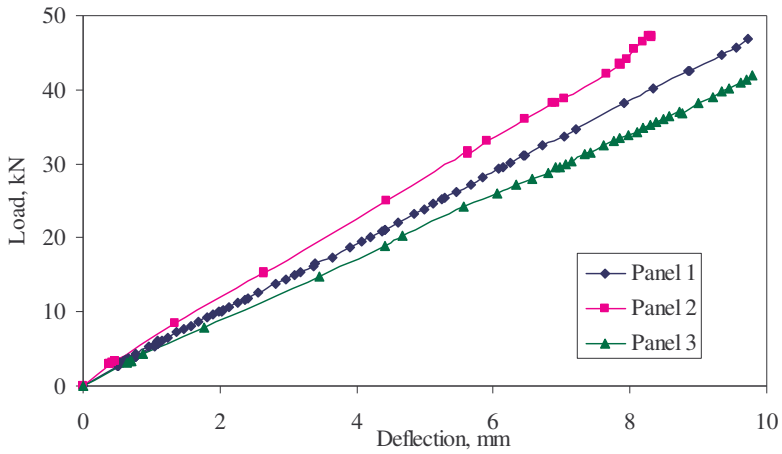

Figure 3-29: Experimental static tests – load deflection curves for panels without top reinforcement

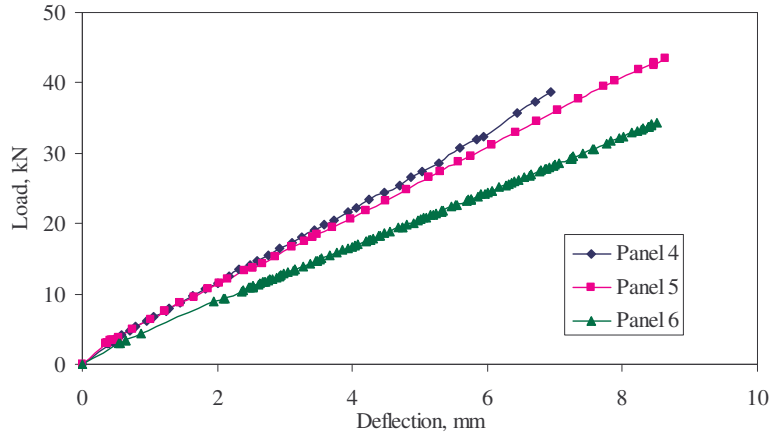

Figure 3-30: Experimental static tests – load deflection curve for panels with top reinforcement

Based on the above load-deflection relationships, stiffness for each panel was calculated and presented in Table 3-4. The stiffness for each panel was calculated using the gradient of the load-deflection curve. The stiffness calculated for each panel was later used to obtain an average stiffness, to represent the panels without top reinforcement and panels with top reinforcement.

The averaged stiffness calculated from this test was used as the stiffness for the plate finite element models. Thus, a stiffness of 5.17 kN/mm was selected for the finite element model, described in Chapter 4, without top reinforcement, while a stiffness of 6.04 kN/mm was chosen for the finite element model with top reinforcement. The results of panel 6 were excluded, since the very low value indicates an error in measurements.

Table 3-4: Stiffness calculation for each panel

	Panel No.	Stiffness (kN/mm)	Average Stiffness (kN/mm)
Without Reinforcement	1	5.16	5.17
	2	5.85	
	3	4.49	
With Reinforcement	4	5.80	6.04
	5	6.28	
	6	4.47	

Overall, as was expected, the results of the static tests show a higher stiffness for the panels with reinforcement, compared with those for the panels without reinforcement. It can be concluded that 15% increase in stiffness was achieved by providing top reinforcement to the composite floor system.

3.6.2 Forced vibration tests

Forced vibration tests were performed on each panel to obtain DAFs. Five different sinusoidal excitation loads, at frequencies starting from 1 Hz to 9 Hz were applied. Figure 3-31 shows typical load-time and deflection-time plots for the panels without top reinforcement for an average sinusoidal load of 10 kN at load frequencies of 1 Hz, 2 Hz, 3 Hz, 4 Hz, 5 Hz, 6 Hz, 7 Hz and 8 Hz. Similar behaviour was observed at and in-between frequencies. Further, similar behaviour was also observed between the panels with top reinforcements. Herein, the load is the total load applied to the system, which is the summation of the load cell reading, load from the spreader beam and the timber packing. The deflection is the average mid span deflection of the slab panel. Figure 3-31 points that the displacement responses were almost in phase, with the dynamic load applied on the floor. This was observed in both cases with and without top reinforcement.

Using the dynamic deflection plots in Figure 3-31, the DAFs for deflection were obtained by dividing maximum deflection obtained during each dynamic load frequency, by the corresponding static deflection. The static deflections were taken from the static test data. The following graphs depict the DAFs versus the ratio of the excitation frequency f_o and the first natural frequency f_1 for the panels without top

reinforcement (refer to Figure 3-32), and panels with top reinforcement (refer to Figure 3-33).

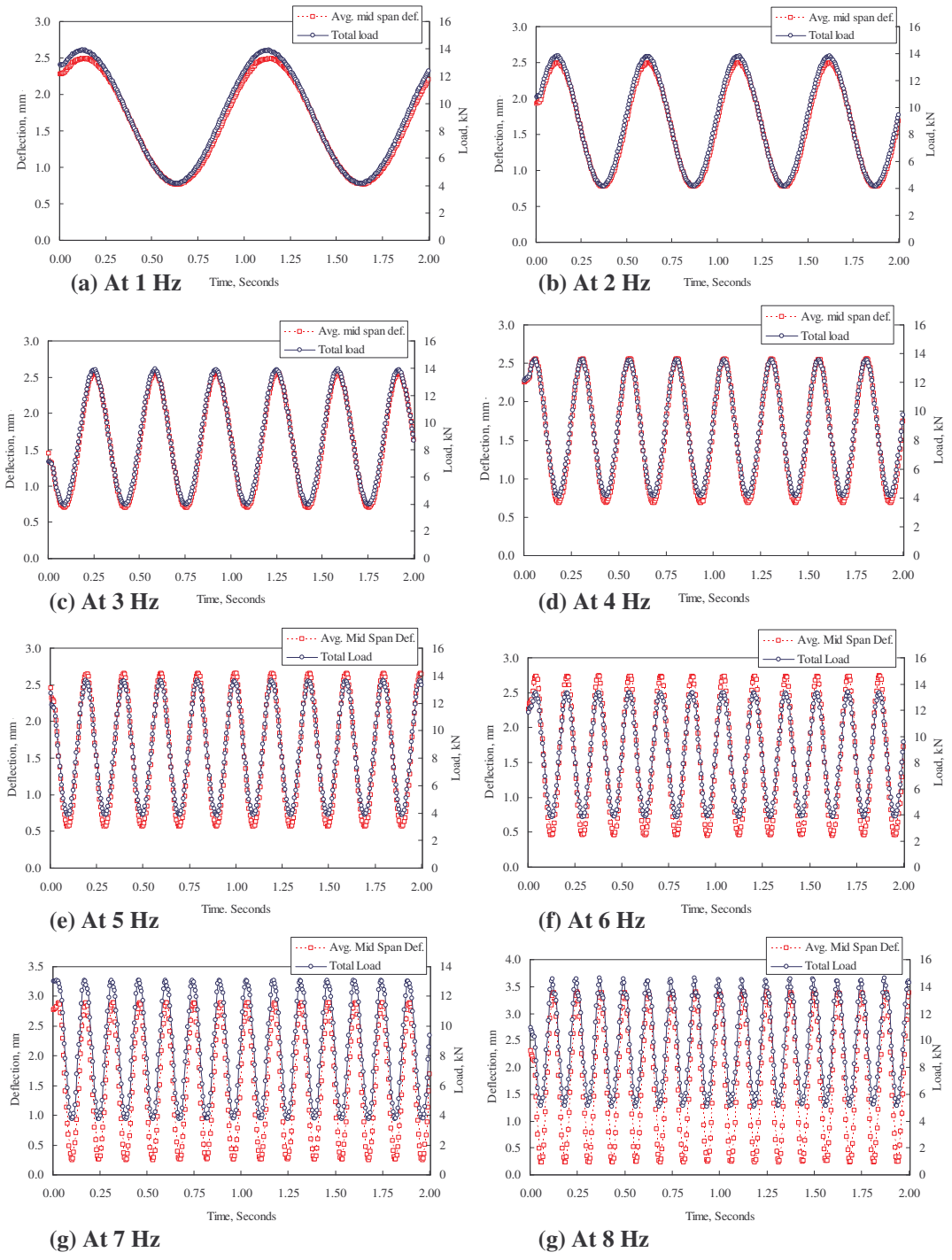

Figure 3-31: Load-time and deflection-time responses for the forced vibration tests for panels <u>without</u> top reinforcement

Plots for different maximum peak loads are also presented in the graphs. The maximum peak load is the highest load that was applied during the sinusoidal forced

excitation, including the load from the spreader beam and the timber packing. The first natural frequencies f_1 used were 14.2 Hz for the panels without top reinforcement and 15.0 Hz for the panels with top reinforcement. The values of these frequencies were obtained from the heel impact test described in Section 3.6.3.

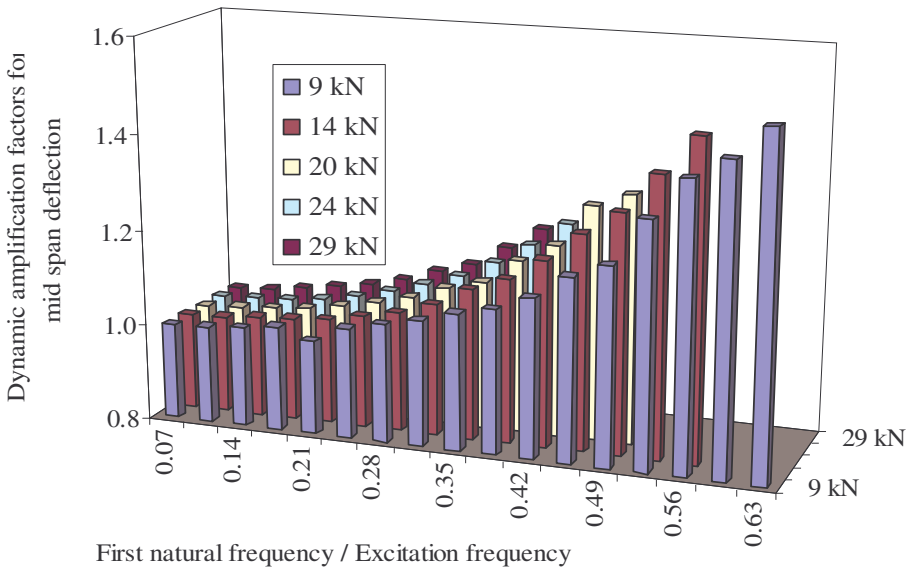

Figure 3-32: Dynamic amplification factors for panels without top reinforcement

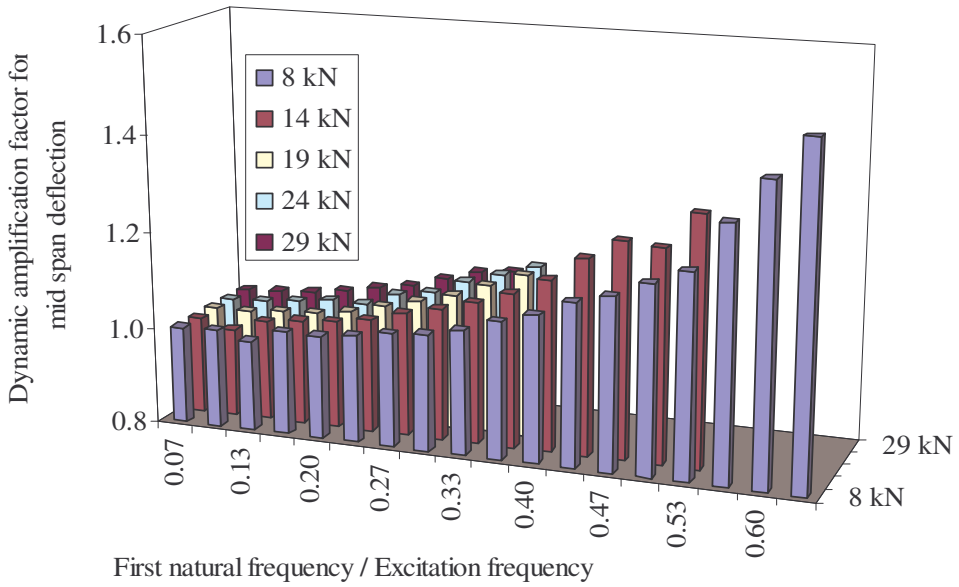

Figure 3-33: Dynamic amplification factors panels with top reinforcement

Due to capacity restrictions of the test equipments, the forced vibration experimental data acquisition was limited to maximum of 9 Hz (i.e. f_o/f_1~0.65). Although the

frequency generator allowed a maximum of 10 Hz of forced excitation, resonance vibration could not be reached since the first natural frequency of the floor was above 10 Hz. Nevertheless, from the above graphs it is evident that the investigated composite floor system provides significant increase in deflection due to dynamic loads, irrespective of the total load in both arrangements with and without top reinforcement. Although, the variation in responses at higher harmonics of the forcing load was not directly identifiable, the forced vibration test produced 1.53 time increase in the deflection compared with the static loads in the panels without reinforcement at a 9 kN peak load and at frequency ratio of 0.63. In addition, it provided 1.49 times increase in the deflection compared with the static loads for the panels with reinforcement at 8 kN peak load and at 0.63 frequency ratio. It is important to note that these DAFs were due forcing loads which were just above half the floor's first natural frequency.

Overall, the experimental analysis provided a supporting evidence for an increased response, where DAF>1 for steel-deck composite floors subjected to dynamic loads. In addition, it provided an evidence of marginal reduction in dynamic response in a slab panel with top reinforcement compared with a slab panel without reinforcement. Thus, embedded reinforcing mesh provides a marginal effect on the dynamic response of composite floors, when considering single panel behaviour. Additionally, it was observed that the DAF for deflection was not effected by the total load applied to the system in both cases of panels, with and without top reinforcement.

3.6.3 Heel impact tests

Heel impact tests were carried out on each test panel to obtain the damping coefficient and the experimental first natural frequency. Three heel impact tests were carried out on each of the six panels, Panel 1, 2, 3, 4, 5 and 6. Altogether 18 tests were performed and data was acquired for 5 seconds at a maximum sampling rate of 1000 samples/second. This enabled a higher accuracy of measured response, and thus a reasonable value of damping coefficient and first natural frequency for the composite floor system was predicted. Heel impact test done on Panel 6 was ignored due to a fault in results.

Typical acceleration responses of two of 5 g accelerometers at mid span and quarter spans for panels without top reinforcement are presented in Figure 3-34 and Figure 3-35 and for panels with top reinforcement in Figure 3-36 and Figure 3-37.

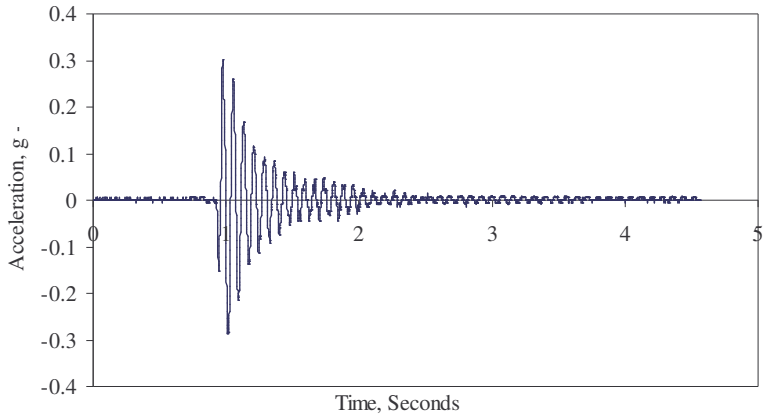

Figure 3-34: Typical heel impact acceleration response at <u>mid span</u> for the panel <u>without</u> top reinforcement

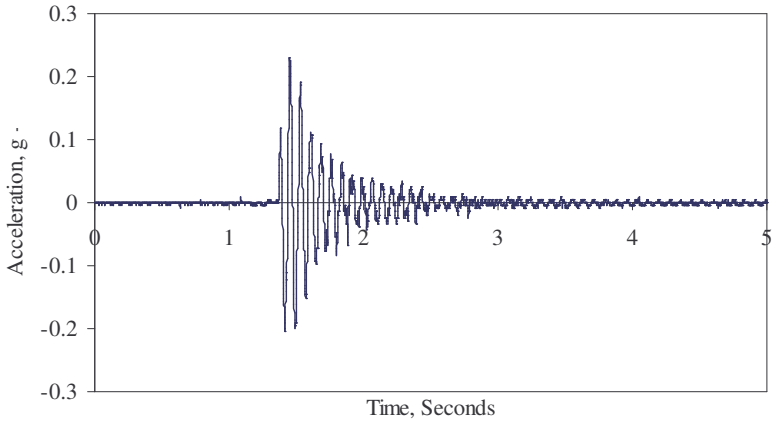

Figure 3-35: Typical heel-impact acceleration responses at <u>quarter span</u> for the panel <u>without</u> top reinforcement

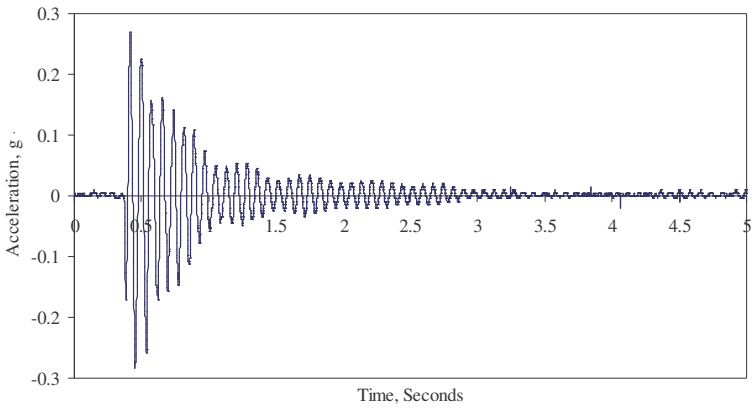

Figure 3-36: Typical heel-impact acceleration response at mid span for the panel with top reinforcement

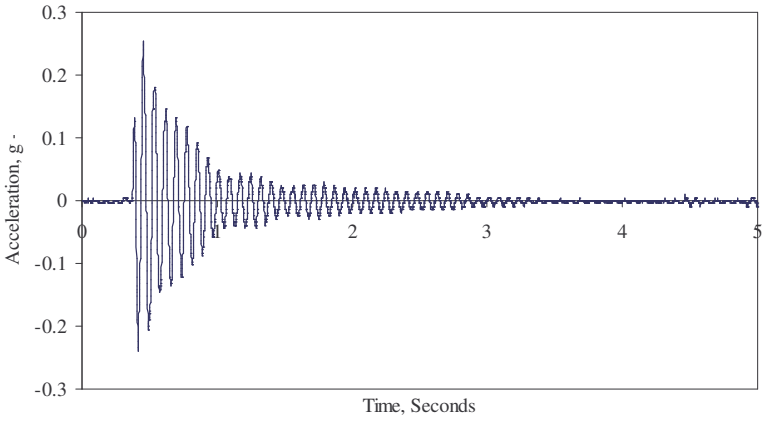

Figure 3-37: Typical heel-impact acceleration response at quarter span for the panels with top reinforcement

Two displacements at mid spans were also used to obtain the time-displacement response for the heel impact excitation. A typical time-displacement behaviour for panels without top reinforcement as seen in Figure 3-38 and for panels with top reinforcement refer Figure 3-39. The deflections used are the averaged values obtained from the experimental test.

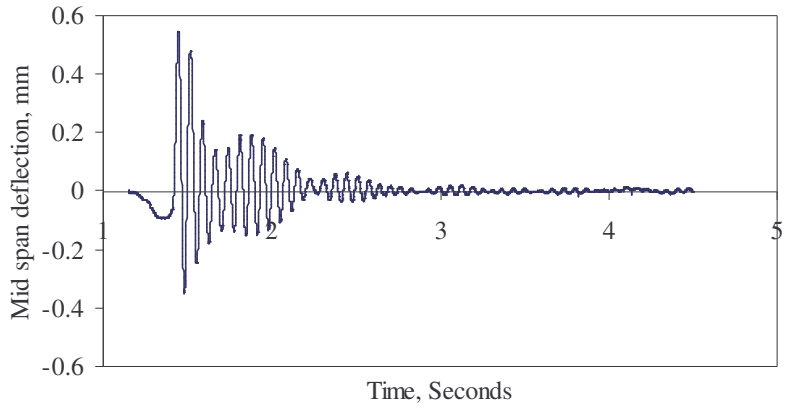

Figure 3-38: Typical heel-drop displacement response at mid span for the panel without top reinforcement

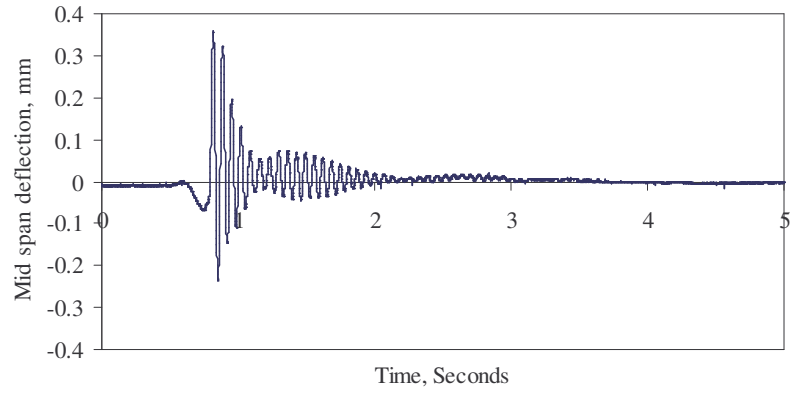

Figure 3-39: Typical heel-drop displacement response at mid span for the panel with top reinforcement

Reductions in the acceleration and displacement responses due to the presence of top reinforcement can be observed from Figure 3-36 to Figure 3-39. This would result a difference in damping and fundamental frequencies in panels with and without top reinforcement.

Using the time-acceleration plots in Figure 3-34 to Figure 3-37 the damping coefficients were calculated using Equation 3-1, presented by Ellis (2001a):

$$\xi = \frac{1}{2n\pi}\log_e \frac{A_o}{A_n}, \qquad \textbf{Equation 3-1}$$

where A_0 and A_n are the amplitudes of "n" successive peaks of the acceleration-time response plot. Damping obtained from this equation is termed "log decrement damping". Murray (2000b) stated that modal damping or true damping is one-half to

two-thirds of the value of the log decrement damping. Herein five initial successive peaks were used in the calculation. Table 3-5 depicts the averaged damping coefficients for each panel.

The damping coefficient calculated for the steel-deck composite system increases marginally with the use of top reinforcement. The presence of reinforcement provides about 0.25% increase in damping coefficient. The calculated experimental damping coefficients were later used in the FE model analysis. Since the damping coefficient is at a critical range according to the design practice, it can be clearly stated that steel-deck composite slab system could give high responses to dynamic excitations. In this context, the resonance response to vibration will produce discomfort to occupants, not only at its first mode of vibration but also at higher modes.

Table 3-5: Damping coefficients for steel-deck composite floors

	Log decrement damping				True damping (0.5 of log decrement damping)
	Centre span acceleration	Quarter span acceleration	Average		
Panel 1	3.8%	3.4%	3.6%		
Panel 2	3.4%	3.7%	3.5%	3.5%	1.75%
Panel 3	3.5%	3.3%	3.4%		
Panel 4	4.2%	3.7%	3.9%		
Panel 5	4.0%	3.9%	4.0%	4.0%	1.98%
Panel 6	-	-	-		

The first natural frequency of the test floor panels was found using the heel impact test results. This was used to validate the FE models described in Chapter 4. The first natural frequency from the heel-drop test was obtained using the Fourier Amplitude Spectrum analysis (Storey) (Paskalov and Reese 2003). These Fourier Amplitude Spectrums for the panels without and with reinforcement respectively are shown in Figure 3-40a and in Figure 3-40b.

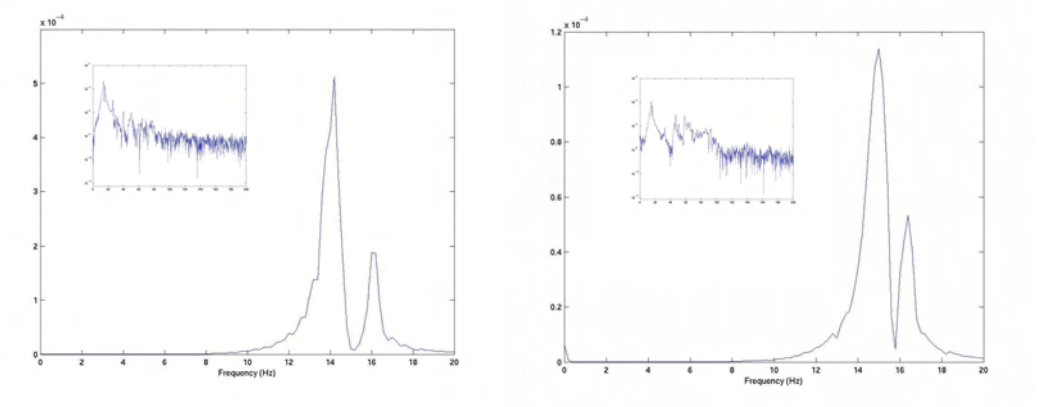

(a) panels without top reinforcement **(b) panels with top reinforcement**

Figure 3-40: **Fourier Amplitude Spectrum analysis for the experimental models**

Two peaks were observed in both Fourier Amplitude Spectrum in Figure 3-40a and in Figure 3-40b. These peaks describe the excitation of two modes, first mode and the second mode. The first peak relates to the first mode and second mode relates to the second mode. Table 3-6 presents the natural frequency for the panel without and panel with top reinforcement.

Table 3-6: Experimental natural frequency of the floor panel

	Fundamental Frequency (Hz)
For panels without reinforcement	14.2
For panels with reinforcement	15.0

Marginal increase in the fundamental frequencies was observed in the panels with top reinforcement. The increase may be due to the increase in the stiffness of the panels due to the additional top reinforcement.

3.7 Summary

This chapter presented a detailed experimental investigation conducted on single panel steel-deck composite floor panels. It included a description of the physical model and the procedures for static tests, forced vibration tests and heel impact tests. It also described the concrete compression test and steel tensile test, the results of which were used in FE modelling.

The results from the static tests were used to calibrate the FE models described in Chapter 4, while the natural frequencies from the heel-impact test results were used to validate the FE models. The initial experimental forced vibration tests at 9 Hz excitation frequency yielded a maximum DAF of 1.53 for the panels without top reinforcement and 1.49 for the panels with top reinforcement. Thus, marginal reductions in DAFs were observed for the panels with top reinforcement compared with the panels without top reinforcement. These reductions are due to the fact that the top reinforcement has no effect on pre-loaded single span bending behaviour of the tested panel.

It became evident, as was expected that response under dynamic loads for steel profiled composite floor panels was higher than that obtained under static loads. DAF's for deflections increased with the increase of the frequency ratio (f_o/f_1) for both panels, with and without top reinforcement. These DAFs were further explored using FEA.

The experimental damping for the steel-deck composite floor system was established using the heel-impact test, which gave values of 1.75% and 1.98% for the panels without and with top reinforcement respectively.

Chapter 4 – Development, Calibration and Validation of FE models

4.1 Introduction

This chapter presents the development of the FE models, which were used for the analytical investigation. Since the dynamic response of composite floor systems under human actions, such as the ones tested in Chapter 3, was not understood enough, analytical investigation of these types of floor systems provides valuable new insight.

Initially, single panel finite element models of various sizes were developed. These finite element models were then calibrated and validated using the experimental data described in the previous chapter. Afterwards, multiple panel FE floor models, which facilitated the investigation of the dynamic response of pattern loading were developed. FE floor models consisted of two models, one with four panels and the other with nine panels.

FE models can be developed using many commercially available FEA programs. The choice of an appropriate program is valuable hence it can reduce the time consumed, and thus increase the efficiency of the research. In this study, the analytical investigation was carried out using the finite element software ABAQUS/Standard version 6.4 by Hibbitt, Karlsson & Sorensen, Inc. (2000). This software was founded in 1978 and hence has become a major tool in structural engineering FEA, especially in research. MSC PATRAN software was used as the pre and post processor, and the analysis was performed on Silicon Graphics Origin 3000 super computers with 28x R14000 MIPS and 32x R12000 processors of 100 GB memory running on the IRIX (SGI version of UNIX) operating system at QUT's high performance computing facility.

4.2 Model description

For the research presented in this thesis, a novel composite floor system produced by a leading Australian manufacturer was chosen. Used in modern floor construction in

Australia, this particular floor system has been used in continuous multiple panel assemblies with varying spans, from 1.5 m to 8.0 m and thicknesses from 100 mm to 250 mm. This floor type is similar to the ones used for the laboratory testing, presented in the previous chapter.

Figure 4-1: Steel-deck floor panels being sep up for construction (BlueScope Lysaght)

Initially, FE models for the experimented single panel model were developed. Afterwards this model was used to develop various model sizes. Herein, two FE models were created and calibrated and they are referred to as "uniform model" and "layered model" hereafter. The uniform model represents behaviour of an equivalent single material model, while the layered model represents dual material model behaviour, using steel and concrete materials. Each of these models was then calibrated using static tests and validated by the heel impact test results.

4.3 Uniform model

The uniform finite element models was developed idealising plate bending behaviour of the slab panel. Thus, shell finite elements were aimed to be used for this scenario. Using simplified methodologies element properties were obtained and are discussed in the following sections.

4.3.1 Elements

In order to simulate the observed experimental behaviour, considerations were given in selection of element types from the ABAQUS element library (Abacus Analysis User's Manual 2003). Since the composite floor system is subjected to surface downward load under static testing, and both upward and downward movement

under dynamic testing, the elements chosen must be able to represent such behaviour and deformations within the slab. As there are bending actions and the thickness of the experimental slab system compared with the length and width is small, shell elements were used for the uniform finite element model. After considering a variety of shell element types available in ABAQUS element library, S4R5 elements were chosen as the most suitable for the uniform finite element model. S4R5 elements are quadrilateral shell elements with four nodes and five degrees of freedom per node.

4.3.2 Material properties

Since, the steel-deck composite floor is bi-material consisting of concrete and steel, and was initially modelled in ABAQUS using shell elements for a uniform model, different definitions on various idealizations were used to obtain material properties. Since the entire set of test panels was simply supported and loaded at mid span, its behaviour was idealised as simply supported beam behaviour, as shown in Figure 4-2.

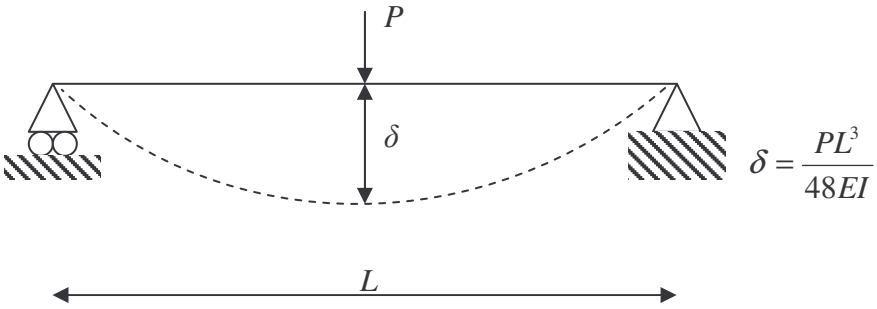

Figure 4-2: Idealization of the experimental model

The idealised structural system as shown in Figure 4-2 has a flexural stiffness of $48EI/L^3$. This idealisation was considered in the FE model calibration and hence, the stiffness of experimental and analytical models were equated to obtain the shell element thickness for the uniform FE model as noted in Equation 4-1.

$$\left(\frac{48EI}{L^3}\right)_{Analytical} = \left(\frac{48EI}{L^3}\right)_{Experimental} \qquad \textbf{Equation 4-1}$$

Since the identical spans L were used in both, experimental and FE models, this equation can be further simplified as follows:

Thus, $(EI)_{Analitical} = (EI)_{Experimental}$ **Equation 4-2**

The experimental panel's stiffness $EI_{Experimental}$, was obtained as:

$$EI_{Experimental} = \frac{kL^3}{48},$$

where k is the gradient of the experimental load deflection plot while the span L is 3200 mm. The gradient k of the load-deflection graphs was calculated as k = 5.17 kN/mm for the panels without top reinforcement in Section 3.6.1. Therefore, $EI_{Experimntal}$ gave a value of 3.5294 x 10^9 N/mm^2.

The modulus of elasticity of concrete is used as the modulus of elasticity of shell elements, $E_{Analytical}$ in uniform FE model. Equation 4-3, presented in Australian standards (AS 3600 Standards Australia 2001), gave a value of $E_{Analytical}$ for the modulus of elasticity of concrete of 31,335 MPa.

$$E_{Analytical} = \sigma^{1.5} 0.043 \sqrt{f_{cm}}\ , \qquad \textbf{Equation 4-3}$$

where σ is the density of concrete and f_{cm} is the mean value of concrete compressive strength. The value for the concrete compressive strength, f_{cm} being 37.1 MPa, as obtained from the cylinder compressive strength tests described in Section 3.4.

Equation 4-2, can now be used to obtain the effective thickness of the shell elements in the FE model. Second moment of area $I_{Analytical}$, of a rectangular section of width b and height d is $I = bd^3/12$. Using Equation 4-2 with $E_{Analytical}$ = 31,335 MPa, b=1800 mm and $I_{Analitical} = (1800)t^3/12$, the equivalent thickness (t) of the FE models can be obtained. This thickness was determined to be t = 90.9 mm.

Hence, the shell element material properties for the uniform FE models are: Young's Modulus $E_{Analytical}$ = 31,335 MPa, Poisson's Ratio = 0.2 and thickness $t_{Analytical}$ = 90.9 mm.

The density of the material in FE models was assumed to be the density of concrete of 2428 kg/m^3, as determined earlier in Table 3-1 and Table 3-2. Table 4-1 summarises the properties used for the uniform FE models.

Table 4-1: Material properties for the uniform finite element model

	Uniform model
Dimensions	3200 x 1800 mm
Element type	Shell elements – 2D, 4 node, 5 DOF per node
Thickness	90.9 mm
Modulus of elasticity	31,335 MPa
Poisson's ratio	0.2
Density	2428 kg/m^3

4.3.3 Loads and boundary conditions

ABAQUS allows the use of various boundary conditions to constrain rotations and translations along global X, Y and Z directions, as needed. In order to comply with the experimental model, the FE model had two supports at either end. At one end, translations in global X, Y, and Z directions and rotations about global X and Y were restrained. At the other end translations in global Y and Z directions and rotations about global X and Y were restrained, to obtain the roller support conditions. Rotations about Z direction were allowed at each end to allow bending.

Figure 4-3 describes the boundary conditions applied, where u and θ were used to describe the restraint conditions for translations and rotations respectively, and the subscripts x, y and z represent the respective global directions.

ABAQUS permits the application of pressure loads on shell elements, perpendicular to the deformed element and not to the initial undeformed configuration. A uniform surface pressure across the corresponding elements, in accordance with the experiments, was considered suitable in representing the static loads adequately. Therefore, for calibration purposes, the loads were applied to the top surface of the corresponding set of shell elements to simulate the actual experimental loading as seen in Figure 4-3.

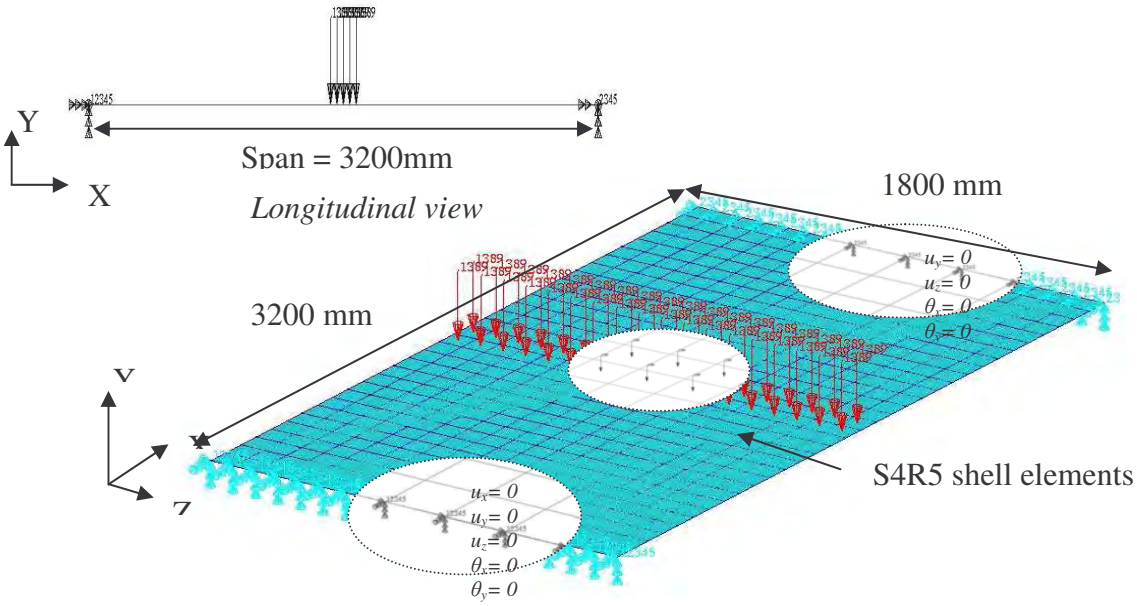

Figure 4-3: Details of uniform FE model

4.3.4 Finite element mesh

In FEA, the selection of mesh size and layout is critical. In the FE models, it's more advantages to use many elements as possible. However, this may lead to increased computational time. Thus, a convergence study was used to obtain the optimal mesh size for the uniform FE models. This study was done for both static analysis, and free vibration analysis. FE mesh configurations with varying number of elements were analysed for maximum deflection at the mid span for the static analysis and first natural frequency for the free vibration analysis. Thereafter, plots of mid span deflection versus number of elements, and first natural frequency versus number of element were obtained. These convergence graphs are depicted in Figure 4-4 and Figure 4-5.

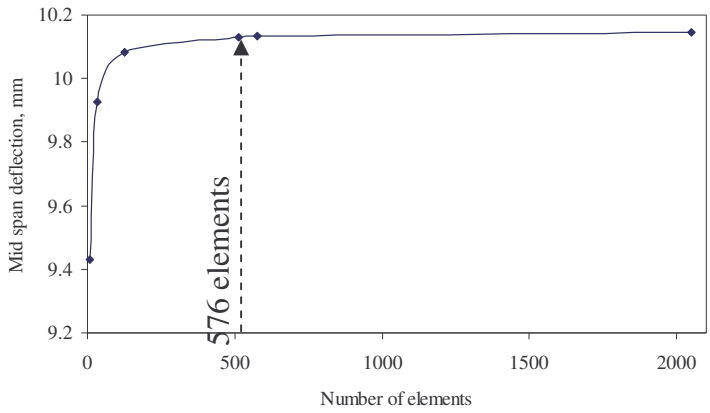

Figure 4-4: Convergence study for uniform model - static analysis

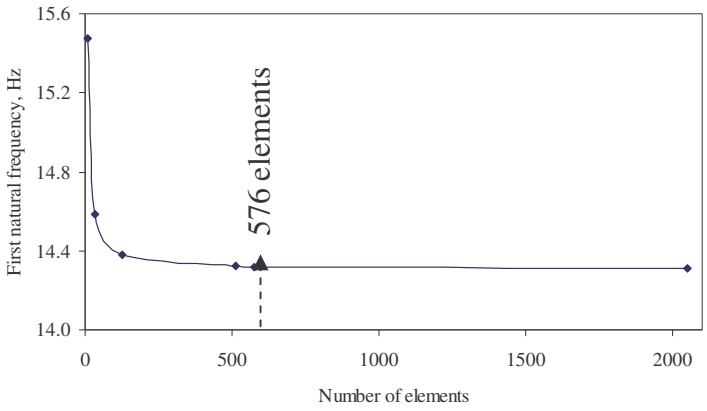

Figure 4-5: Convergence study for uniform model - free vibration analysis

From the above graphs, it was observed that FE models with more than 500 elements converged, to give accurate results for analysis. Furthermore, it is also important to keep the aspect ratio of the shell elements to a unity. Considering all these, a mesh size of 18 x 32 was chosen for the uniform FE model. The mesh had 576 elements, each element was of 100 x 100 mm size.

4.3.5 Analysis

The above described material properties, boundary conditions along with the appropriate mesh density, were used to develop the uniform FE models. Static analysis were used for calibration of the computer models while free vibration analysis were used to validate the models. This process is described in Section 4.5.

4.4 Layered model

Layered three-dimensional FE models offer sophisticated analysis, due to this ability to model two materials separately. The selections of element and material types for analysis in this layered model are based on the true structural system emphasising the future studies. Herein, more importance is placed modelling the experimental slab panels without top reinforcement, since presence of top reinforcement is not very important for the panel's mechanical behaviour (Davison 2003).

4.4.1 Elements

The elements for the layered mode were chosen from the ABAQUS element library. They represent both static and dynamic behaviour, and both materials of steel and

concrete. Since steel in deck-sheet itself is a dovetailed steel-deck profile, which carries bending deformations, it was modelled using S4R5 shell elements. S4R5 elements in ABAQUS are 4 nodes, 5 degrees of freedom/node elements. The concrete core was modelled using C3D8, solid elements available for stress analysis. C3D8 elements are single homogenous 3D, elements with eight nodes and with six degrees of freedom per each node. Perfect bond is assumed to occur between steel plates and concrete core, during the loading. This is achieved by equivalencing the nodes in shell and solid element mesh distributions.

4.4.2 Material properties

Since the layered model represents two separate materials, two sets of material properties were used. They are material properties for the steel sheets or shell elements and material properties for the solid concrete or solid elements. The modulus of elasticity of the steel sheets, the shell elements, was obtained from tensile tests done on the specimens obtained by process described in Section 3.5. The thickness of the shell elements was set to 1.0 mm, to match that of the steel-deck sheets. The density of steel and Poisson's ratio used were 8000 kg/m^3 and 0.3 respectively. The modulus of elasticity of concrete, the solid elements, was set to 22,000 N/mm^2 while the density of concrete and Poisson's ratio were assumed to be 2428 kg/m^3 and 0.2 respectively. Table 4-2 summaries all the properties used for the static and dynamic analysis of the layered model.

Table 4-2: Material properties for the layered FE model

Layered Model		
Dimensions	3200 x 1800 x 100 mm	
Concrete	Element type	3D 6-node hexagonal solid elements
	Modulus of elasticity	22 000 N/mm^2
	Poisson's ratio	0.2
	Density	2428 kg/m^3
	Ultimate strength	37.1 MPa
Steel sheet	Element type	S4R5 quadrilateral shell elements
	Thickness	1.0 mm
	Modulus of elasticity	205 000 N/mm^2
	Poisson's ratio	0.3
	Density	8000 kg/m^3
	Yield stress	610 MPa

Since the original steel-deck is dovetailed profile with flutes and embossments, the analytical model was approximated, as described in Figure 4-6.

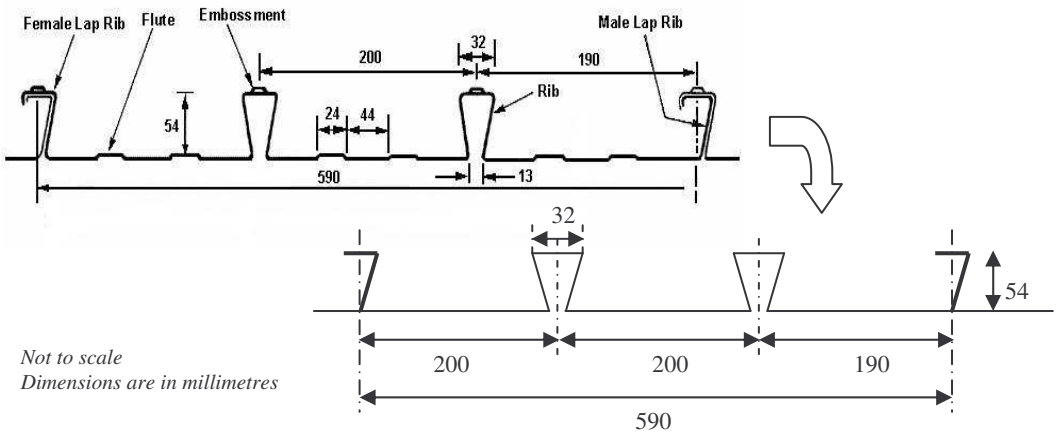

Figure 4-6: Idealized section for the FE model

The geometry of the analytical model consisted of ribs in longitudinal direction, with no flutes or embossments. This reduced the number of elements in the FE model, and as a result decreased the computational time. However, since the mechanical objective of the flutes and embossments is to attain a perfect bond between steel and

concrete, this was achieved by equivalencing the nodes in the shell and solid elements.

4.4.3 Loads and boundary conditions

As described in earlier in Section 4.3.3, in order to comply with the experimental model, the FE model had to have un-restrained rotations about Z, θ_z direction at either ends. To obtain the roller support condition, translations in global X, Y, Z and rotations about global X and Y were restrained on one end, while translations in global Y, Z and rotations about global X and Y were restrained at the other end.

Figure 4-7 describes the boundary conditions used for this model. Herein, u and θ are used to represent the translations and rotations respectively, while subscriptions x, y and z are used to represent the subjective global directions.

Similarly, to the uniform model and in accordance with the experiments a uniform surface pressure across the corresponding solid elements was considered suitable in representing the static loads as seen in Figure 4-7.

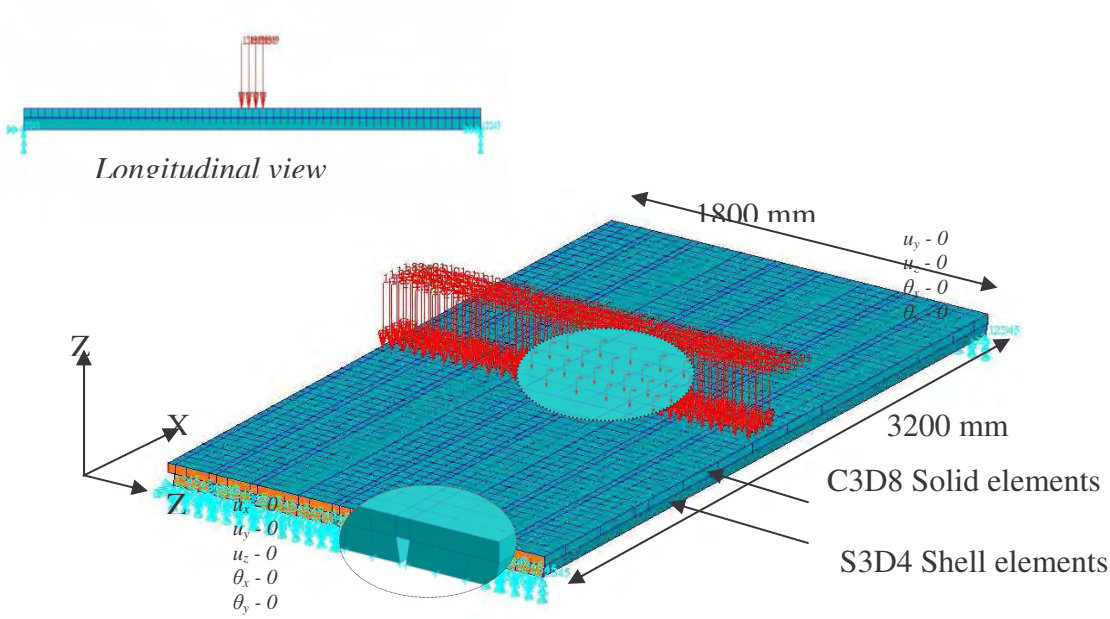

Figure 4-7: Details of layered FE model

4.2.4 Finite element mesh

Convergence studies for the layered model, for both static and free vibration analyses were used in order to obtain sufficient accuracy in analysis. FE mesh configurations

varying the number of elements were analysed, for maximum deflection at the mid span for the static analysis and first natural frequency for the free vibration analysis. These were plotted against the number of elements. Figure 4-8 and Figure 4-9 depicts the convergence study plots for static analysis and free vibration analysis respectively.

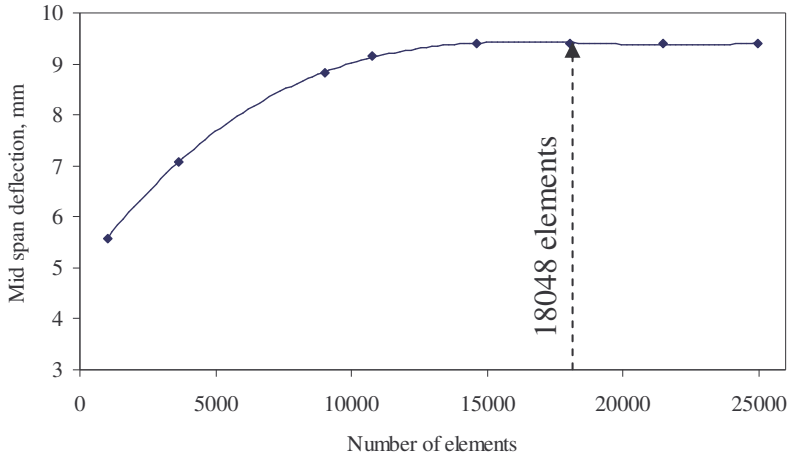

Figure 4-8: Convergence study for layered model - static analysis

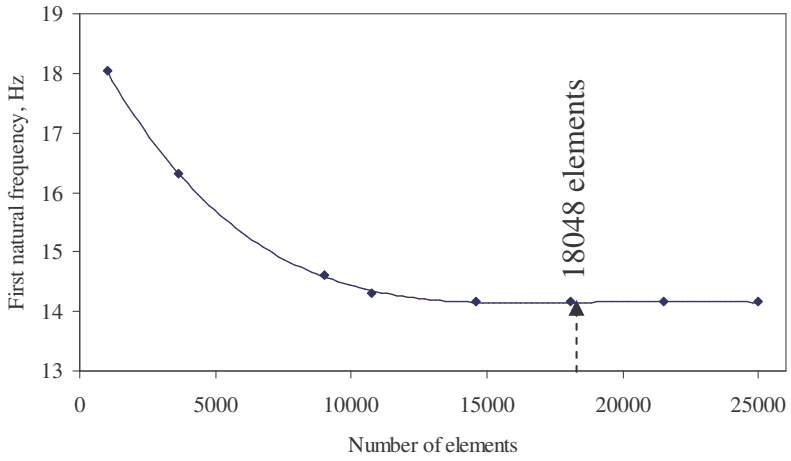

Figure 4-9: Convergence study for layered model - free vibration analysis

It was observed that more than 15,000 elements were appropriate for accurate results in layered model. Also, consideration was given to select a mesh distribution, which gives coinciding nodes in steel surface mesh and solid concrete mesh. A suitable mesh size was selected, with a surface mesh size starting from 25 x 32 mm to 35 x 50

mm, while a solid mesh was of 25 x 32 x 50 mm size each providing 18048 elements.

4.4.5 Analysis

The layered FE model was developed using the above material properties as detailed in Table 4-2 and mesh configurations as seen in Figure 4-8 and Figure 4-9. Then the model for calibration was analysed statically while the validation was done through free vibration analysis.

4.5 Model calibration and validation

Before extensive studies were carried out, it was important to calibrate the FE models described in Section 4.4, to match experimental behaviour. Calibration of the FE model was done using results of static analysis, and validation was done using the heel impact tests undertaken on the experimental test panels. Although the exact behaviour of the constructed floor system is impossible to model, they were calibrated using the available test data.

4.5.1 Calibration by static tests

Mean experimental mid span deflections at various loads were obtained from the panels without top reinforcement, and were compared with FE model mid span deflections for the calibration. Similarly, the mid span deflections at various loads were obtained from the developed layered and uniform FE models. This load-deflection data was then plotted in the graph, as seen in Figure 4-10.

Both uniform and layered FE models generated results were well distributed on the mean load–deflection curves. Thus, the calibration produced a satisfactory agreement in all situations, and all subsequent investigations were done using these FE models.

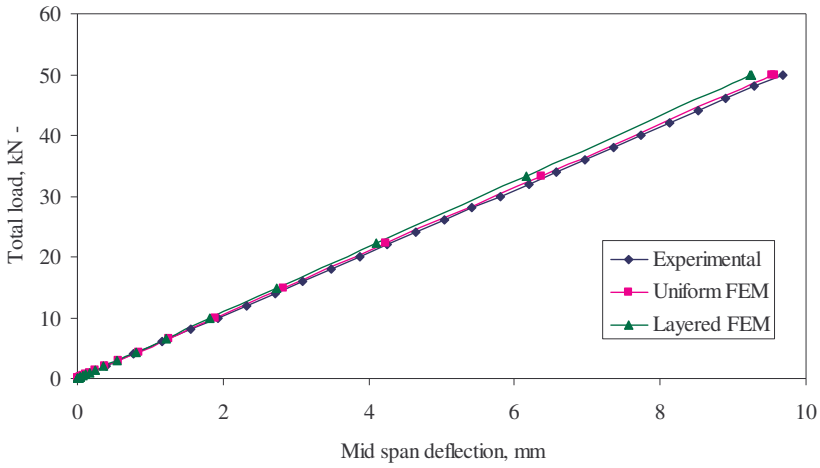

Figure 4-10: Calibration of FE models

4.5.2 Validation by heel impact tests

Heel impact tests can be used, not only to uncover the damping coefficients, but also to obtain the first natural frequency of the floor system. Herein first natural frequencies obtained by heel-impact tests were used to validate the FE models. The procedure for obtaining the first natural frequency from the heel-impact tests was described in Section 3.6.3. Free vibration analysis was done on all the generated FE models to obtain the first natural frequency of the system. The following Table 4-3 compares the first natural frequencies from heel impact tests and from FEA.

Table 4-3: Variation comparisons of FE models with experimental models using heel-impact test

	Fundamental frequency (Hz)
Experimental - Averaged	14.2
Uniform FE model	14.3
Layered FE model	14.1

From the Table 4-3, it can be clearly seen that the fundamental frequency obtained by the experimental investigation was well predicted by the FE models. The FE model, therefore adequately validates experimental test panels. Thus, the calibrated and validated FE models were used for further analysis, to determine the dynamic performance including DAFs and acceleration response, in different human-activities at different damping levels. Additionally, the calibrated and validated FE models were used to develop different model sizes for further investigation.

4.6 Development of single panel models

Vibration problems in floor system occur in longer floor spans that has lesser natural frequencies. Thus, the layered FE model as described in Section 4.4 and hereafter referred to as "Layered model 1" was used to develop series of FE models of various sizes. This model reflected the realistic behaviour of the steel-deck composite floor and was calibrated and validated using the experiments. Herein, commonly used seven model sizes, which gave lower fundamental natural frequencies than those of the experimental model size, were considered. Sizes were selected in such a way, as to give a range of rectangular and square panel sizes. Table 4-4 presents dimensions of the selected panel sizes.

Table 4-4: Selected panel dimensions

	Length (mm)	Width (mm)	Thickness (mm)
Model 1 (experimental model)	3200	1800	100
Model 2	4800	2400	140
Model 3	4800	4800	140
Model 4	6000	3000	190
Model 5	6000	6000	190
Model 6	7200	3600	250
Model 7	7200	7200	250

For each of these generated layered FE models, a corresponding uniform FE model of similar size was generated. The uniform FE models ensure true structural behaviour corresponding to that of layered FE models, by calibrating and validating against respective layered FE models. The main objective of having a layered FE model and uniform FE model was to co-relate their results, and thereby use the uniform FE model in computer simulations. This helped to reduce the time consumed by expensive laboratory investigations and especially reduced the time in performing the dynamic FEA. The flow chart described in Figure 4-11 depicts the methodology used in developing uniform FE models.

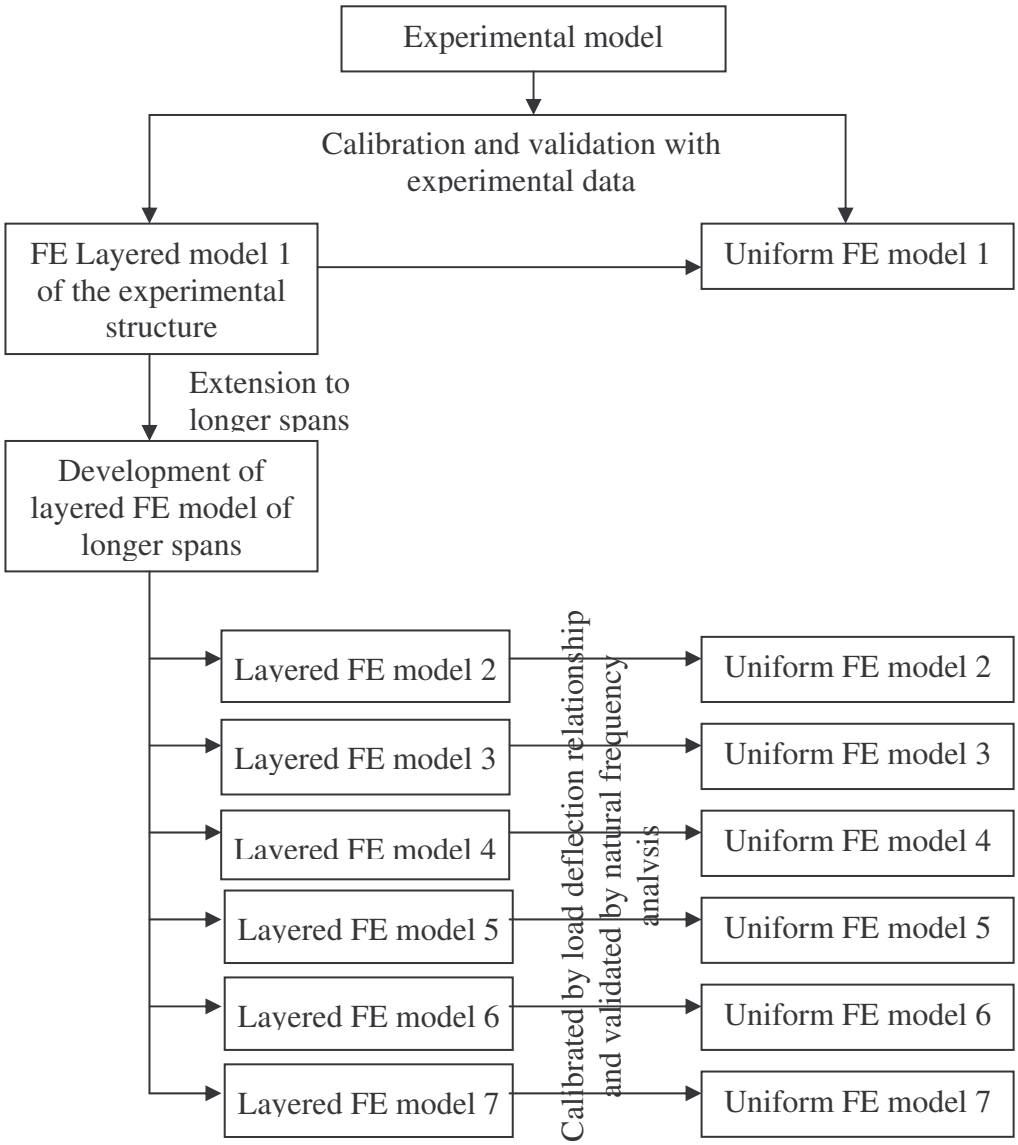

Figure 4-11: Sequence of development of uniform FE models for dynamic analysis

4.6.1 Layered FE models to uniform FE models

For each selected model size, the layered FE models were developed first and corresponding uniform FE models were developed second. The layered FE models used the similar material properties of the model described in the Section 4.4. The material properties were presented in Table 4-2. The model used two materials, steel and concrete, similar to experimental FE model, the layered model 1. Steel-deck was modelled using S4R5 shell elements, while the concrete was modelled using 3D8 solid elements.

During the analysis it was discovered that layered models, modelled in full scale, used a large number of elements that caused errors and thus terminated the analysis process. Therefore, using symmetricity, quadric FE models were used instead as shown in Figure 4-12, to obtain the data needed for calibration and validation. The quadric FE model uses appropriate boundary conditions along the edges to model full scale FE model.

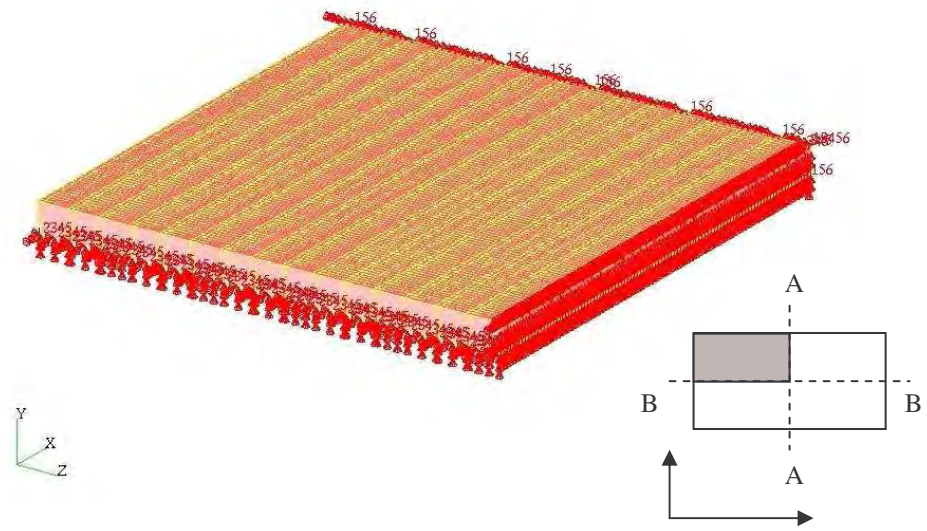

Figure 4-12: Quadric layered FE model for calibration and validation

The boundary conditions used along the section A-A, restrain the translations in X direction, rotations about Y direction and rotations about Z direction. The boundary conditions used along the section B-B, restrain translations in Z direction, rotations in X direction and rotations in Y direction. This set of boundary conditions, along with the boundary conditions used at the supports, gave the required quadric behaviour for the full scale model.

The uniform FE model, on the other hand, modelled in full scale with simply-supported boundary conditions. Figure 4-13 presents a typical uniform FE model used in analysis.

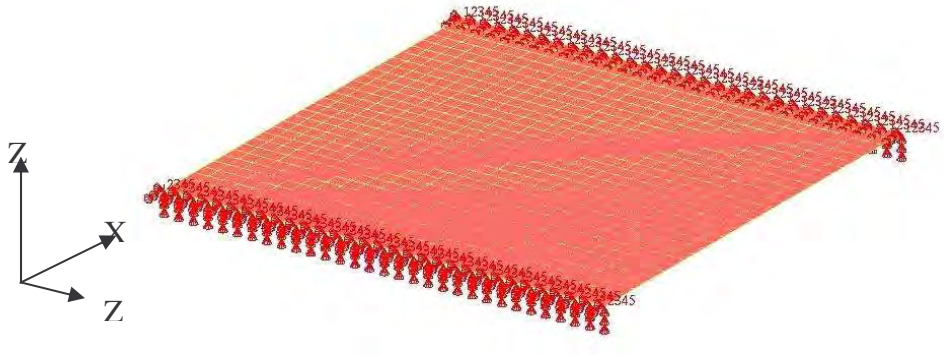

Figure 4-13: Typical uniform FE model

The properties used for the S4R5 shell elements in uniform FE models were the properties of concrete, detailed in Table 4-2. Equivalent thicknesses were obtained by considering the beam behaviour of the respective layered FE model as described in the Section 4.3.2. Table 4-5 presents the effective thickness of the uniform FE models obtained after using the above-described idealization.

Table 4-5: Equivalent shell element thickness for uniform FE models

	Equivalent thickness (mm)
Model 2	132.4
Model 3	132.5
Model 4	186.8
Model 5	186.8
Model 6	238.6
Model 7	239.2

To obtain appropriate mesh distributions, all the layered and uniform FE models undergone a convergence study. These convergence studies yielded the minimum total number of elements required to obtain accurate results for calibration with the uniform FE models.

4.6.2 Calibration of uniform FE models

The uniform FE models were then calibrated against the layered FE models. Load deflection characteristics of corresponding FE models were compared for the calibration purpose. Mid span line load was applied to both types of FE models and

the mid-span deflections were recorded at different loads. Figure 4-14 describes the comparison of load-deflection characteristics of layered and uniform FE models.

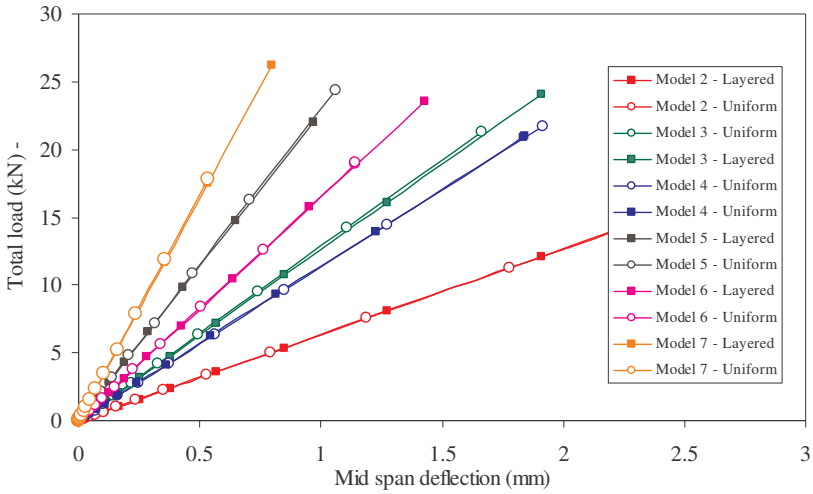

Figure 4-14: Calibration of FE models

The uniform models have given similar load-time characteristics to those of layered models confirming the calibration.

4.6.3 Validation of uniform FE models

The validation of uniform FE models was found by comparing the natural frequency analysis carried out on each model. Table 4-6 presents the comparison of the two models.

From the comparison in Table 4-6 it can be observed that the uniform FE models clearly predict the natural frequency of the layered finite element models. Furthermore, uniform FE models can be used for the more complex and time consuming dynamic analysis, which are described in Chapter 5.

Table 4-6: Validation of FE models

Model notation	First natural frequency of layered FE model (Hz)	First natural frequency of uniform FE model (Hz)
Model 2	9.37	9.41
Model 3	9.37	9.46
Model 4	8.32	8.48
Model 5	8.32	8.54
Model 6	7.28	7.54
Model 7	7.27	7.57

4.7 Development of multiple panel models

The major objective of this research is to evaluate the dynamic response of multiple panel floor systems under pattern loads. Thus, full-scale FE models of multiple panel floors comprising of different number of panels were developed. These models were then used for computer simulations of varied human-induced loadings under different pattern loads.

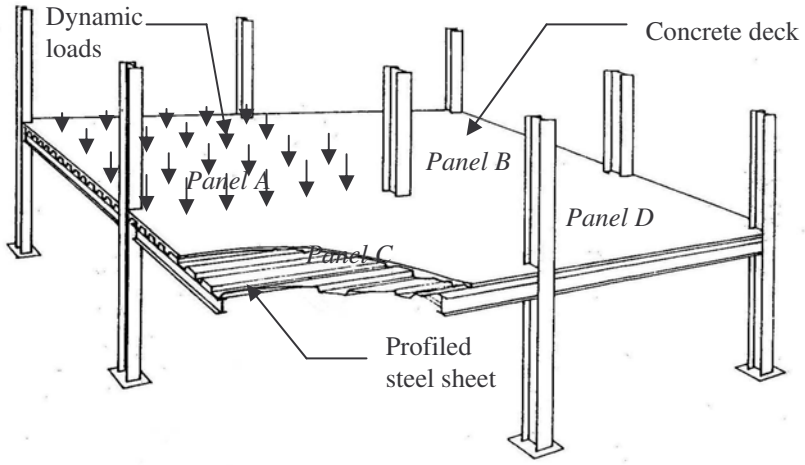

Figure 4-15: Typical pattern loading case on multiple panel floor system

Figure 4-15 illustrates a four panel floor system. Herein, pattern loading occurs when different panels are subjected to different loads. For example, when Panel A is subjected to human-induced dynamic loads, the adjacent floor panels Panel B, Panel C and Panel D will be subjected to loads other than human-induced dynamic loads. To investigate such pattern loading cases, different multiple panel configuration were used in this research study.

4.7.1 Multiple panel configurations

Two multiple panel configurations were used for the investigation. Starting with the extensive examination of a 2 x 2 panel, 4 panel configuration, which is referred to as the structural configuration 1, then followed by investigation involving 3 x 3 panel, 9 panel configuration, which is referred to as the structural model 2. Both these configurations are very common in steel-frame building construction, which uses steel-deck composite floor systems. The structural elements of slab thickness, spans, beam sizes and column sizes, were kept the same for both structural models. The fundamental natural frequency of these configurations observed using Dunkerly's approximate methods was also found to be 4.28 Hz (Fielders Australia Pty. Ltd.) and hence, less than 7 Hz and hence they are classified as low frequency floors (Wyatt 1989). This property is ideal for this research and thus was used extensively for the exploration with pattern loading.

4.7.1.1 The structural configuration 1

The configuration used for the structural model 1 consisted of 4 panels as described in Figure 4-16.

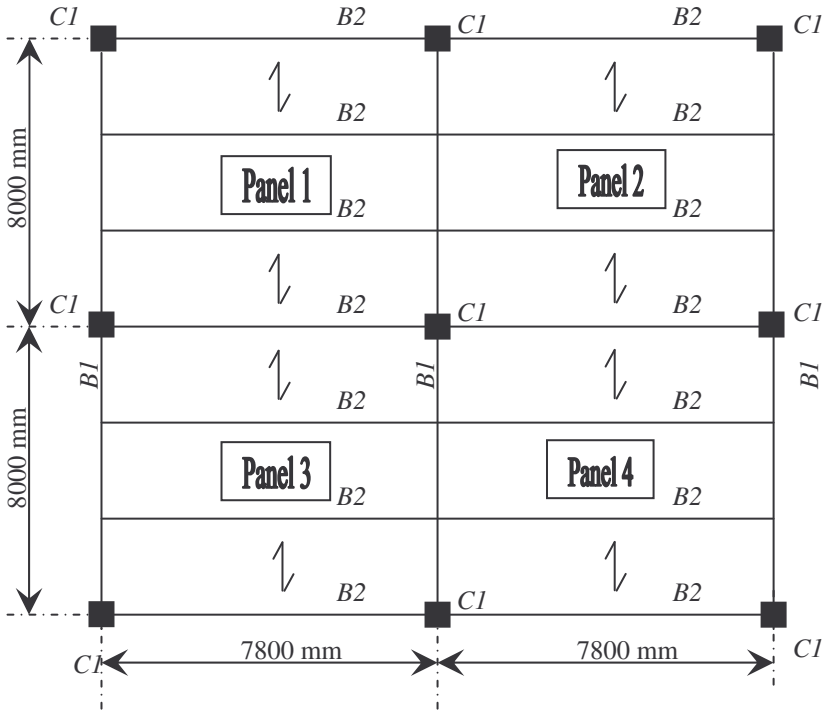

Figure 4-16: Structural configuration of the 2 x 2 steel-deck composite floor model

Configuration 1, consisted of 2 x 2 panel model of floor area 16 m x 15.6 m, having columns C1 placed in a grid of 8.0 m x 7.8 m. Beams B1 of 530 UB 82 act as primary beams in the two continuous spans and beams B2 of 360 UB 45 act as secondary beams, simply supported across the primary beams. The columns C1 were of a similar size of primary beams B1. The slab comprised of 150 mm thick concrete slab laid on 1 mm steel-deck dovetail profiled steel-deck, which was in-situ formwork in one-way spaning direction, as described in Figure 4-16.

4.7.1.2 The structural configuration - 2

The structural model 2 configuration used is similar to the structural model 1 described in Section 4.7.1.1, except for the number of panels. Figure 4-17 illustrates the model configuration.

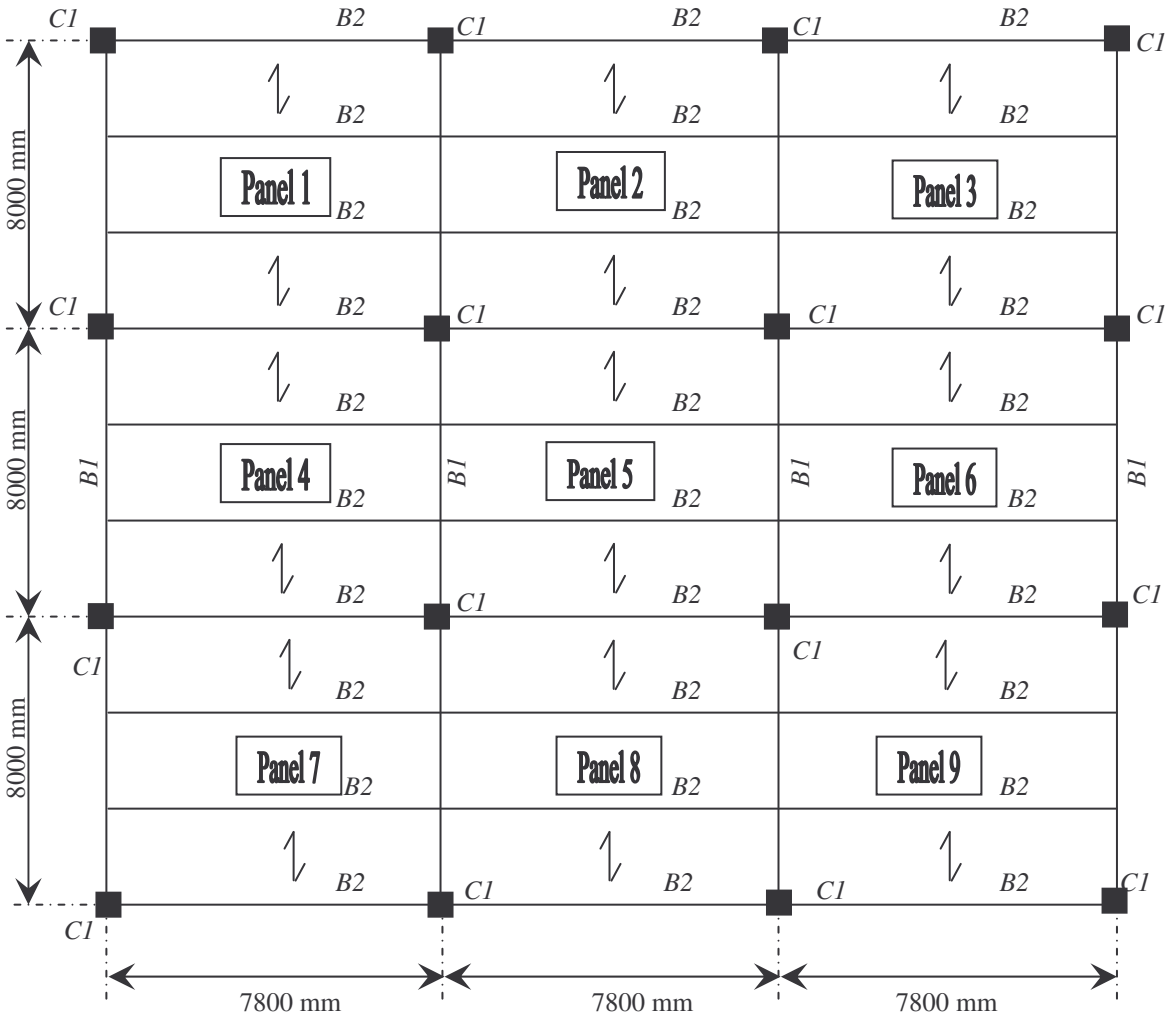

Figure 4-17: Structural configuration of the 3 x 3 steel-deck composite floor model

The 3 x 3 panel configuration covered a floor area of 24 m x 23.4 m, with primary beams B1, of 530 UB 82 and secondary beams B2, of 360 UB 45. The slab thickness was 150 mm with steel-deck of 1 mm. The columns C1 were of similar size of the primary beams B1.

4.7.2 Finite element modelling of multiple panel models

The FE models for the two configurations described in Section 4.7.1 were developed using MSC PATRAN 2004, a pre and post processing software, from which the input codes were generated and were executed in ABACUS solver.

Initially, the structural configuration 1 was modelled as a layered FE model and also as a uniform FE model. The natural frequencies and mode shapes were compared, to determine which are of the two models was more suitable for analysis. Uniform FE models presented by El-Dardirly and Ji. T. (2005) are isotropic flat plate models. Compared to the 3D composite layered FE model the main advantage of using uniform FE model is that it uses less computational time. In this study a comparable study of the two models were performed and proved a significant saving in computational time in favour use of uniform FE model. However, El-Dardirly and Ji T (2005) stated that it is necessary to consider the modelling of steel sheet, in a 3D layered model as its contribution to the global stiffness is about 16%. This section looks at both these model types in terms of fundamental natural frequency and mode shapes. The results were used to identify an accurate FE model for the multiple panel investigation from examination of the uniform plate models and 3D layered composite models.

Floor-column model was considered to be the most appropriate in order to investigate the dynamic behaviour of multiple panel steel-deck composite floors. This reduces the additional stiffness provided by either pinned or fixed supports and thus the false observations (El-Dardiry, Wahyuni et al. 2002). The floor-column model comprised of composite floor, main beams, girder beams and columns, modelled as described in the sections to follow. The column was 1.5 m long on both sides, which was half of the floor heights and fixed boundary conditions were assumed at the two ends. However, necessary boundary conditions restrained by x and z translations at beam-column nodes, were provided to prevent rigid body

movements in the floor plane. Composite floor was modelled using bi-material, concrete and steel in layered model and equivalent properties in uniform model.

4.7.3 Layered FE model and uniform FE model (Configuration 1)

Layered FE model consisted of concrete slab modelled using solid elements, and steel-deck modelled using shell elements. The main steel beams, secondary steel beams and columns of the model were modelled using beam elements, providing a 3D configured computational model. True representation of structural elements in performing their tasks was modelled using solid elements 6 DOF – hexagonal solid 3S6 for concrete, as seen in Figure 4-18a, shell elements 5 DOF – quadrilateral shell S4R5 taking account both membrane and flexural deformations in the steel-deck as seen in Figure 4-18b and beam elements 3 DOF – linear beam 3B2 taking the bending, shear and axial deformations in respective directions. The material properties for the solid elements and beam elements were the properties of the concrete while the material properties for the shell elements were the properties of steel (refer to Table 4-7).

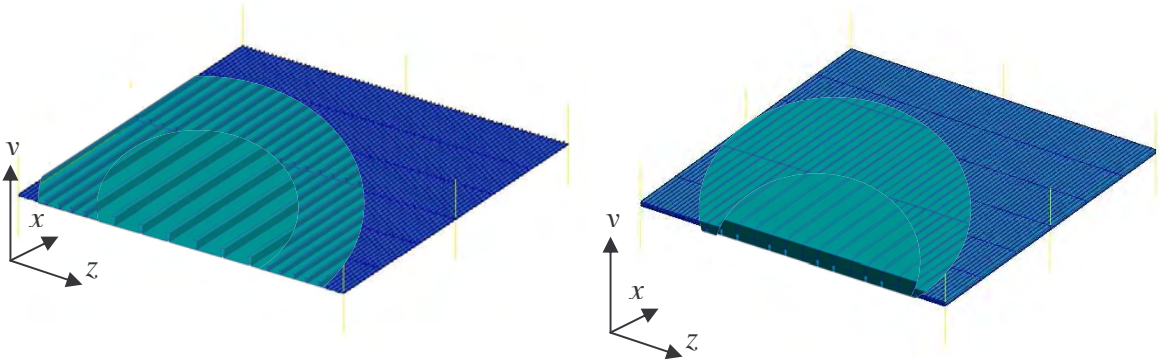

(a) Shell elements for steel-deck **(b) Solid elements for concrete**

Figure 4-18: Components of the layered FE model

The uniform FE model, on the other hand, used shell elements 5 DOF – quadrilateral shell S4R5, to model the slab, whilst beam elements 3 DOF – linear beam 3B2 to model the main steel beams, secondary steel beams and columns. The properties of the elements used in the uniform model were the material properties for the concrete (refer to Table 4-7). The thickness of the shell elements was chosen to be 150 mm, to represent the thickness of the slab. Figure 4-19 illustrates the uniform FE model.

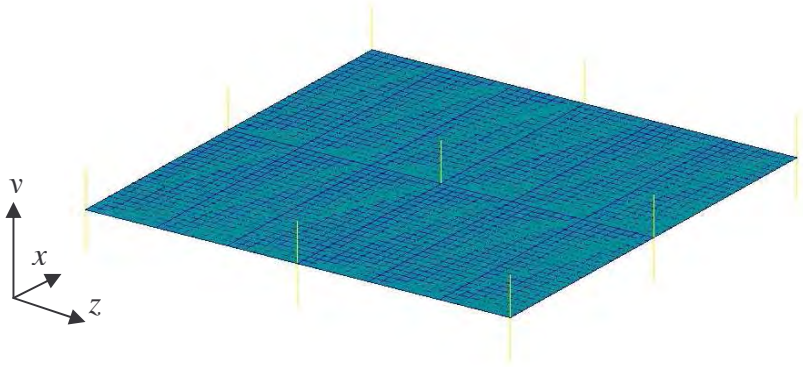

Figure 4-19: Uniform FE model for the 2 x 2 panel configuration

The material properties of the different elements used are presented Table 4-7. These material properties were obtained by the laboratory testing as described in the Chapter 3.

Table 4-7: Material properties used in the FE models

Material	Young's modulus (GPa)	Poisson's ratio	Material density (kg/m^3)
Steel	205	0.3	8000
Concrete	31.335	0.2	2428

4.7.4 Layered FE model versus uniform FE model (Configuration 1)

Natural frequency analyses of the layered FE model (on left column) and the uniform FE model (on right column) described in Section 4.7.3 were carried out. The first six natural frequencies and corresponding mode shapes for both, layered and uniform model, were obtained and presented in Figure 4-20 for comparison. This comparison was carried out to verify the differences of mode shapes and natural frequencies of layered and uniform FE models. These differences are further examined to determine the suitability of using the uniform FE model in the pattern loading, in place of layered model, which consumed more processing time for analysis.

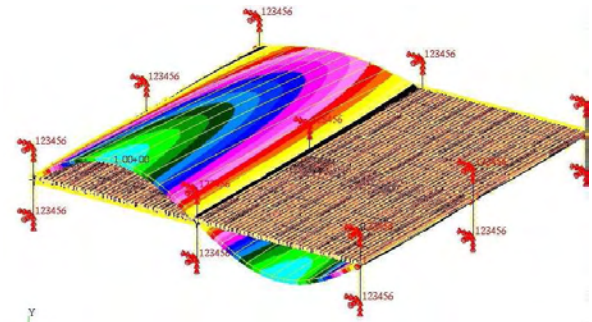

1st mode f_1 = 4.0321 Hz

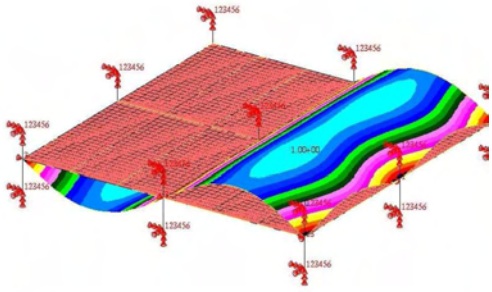

1st mode f_1 = 3.4614 Hz

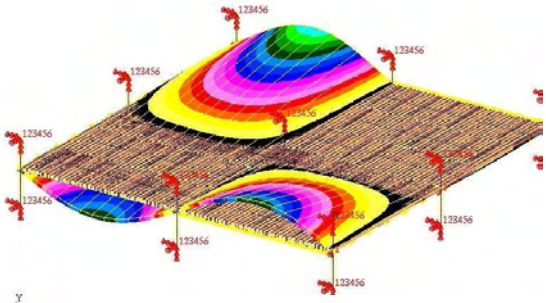

2nd mode f_2 = 5.3545 Hz

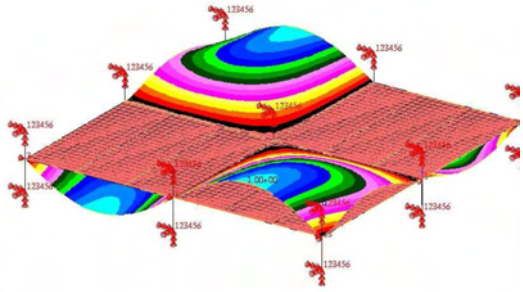

2nd mode f_2 = 4.0843 Hz

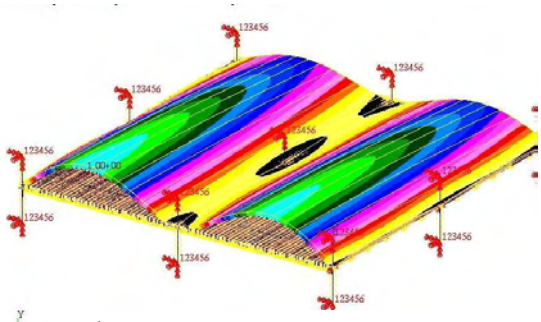

3rd mode f_3 = 5.926 Hz

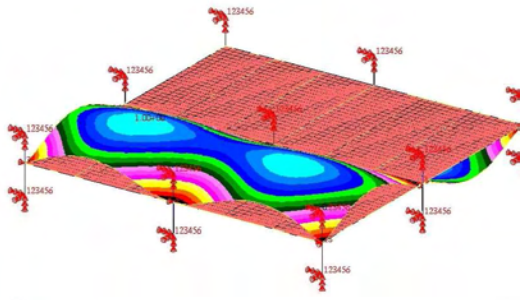

3rd mode f_3 = 4.2977 Hz

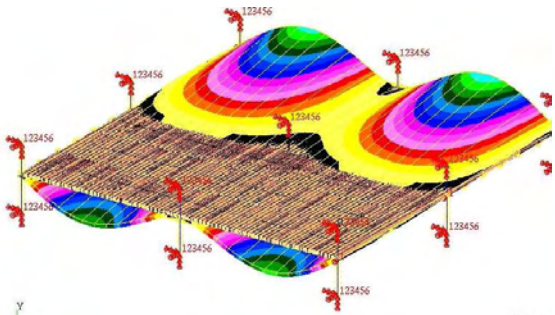

4th mode f_4 = 6.8545 Hz

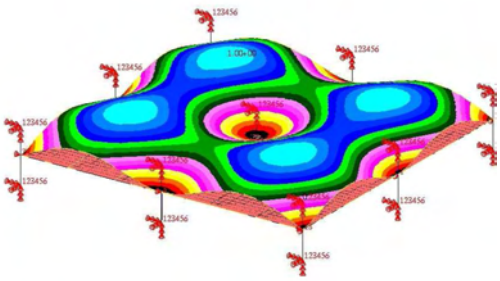

4th mode f_4 = 4.3652 Hz

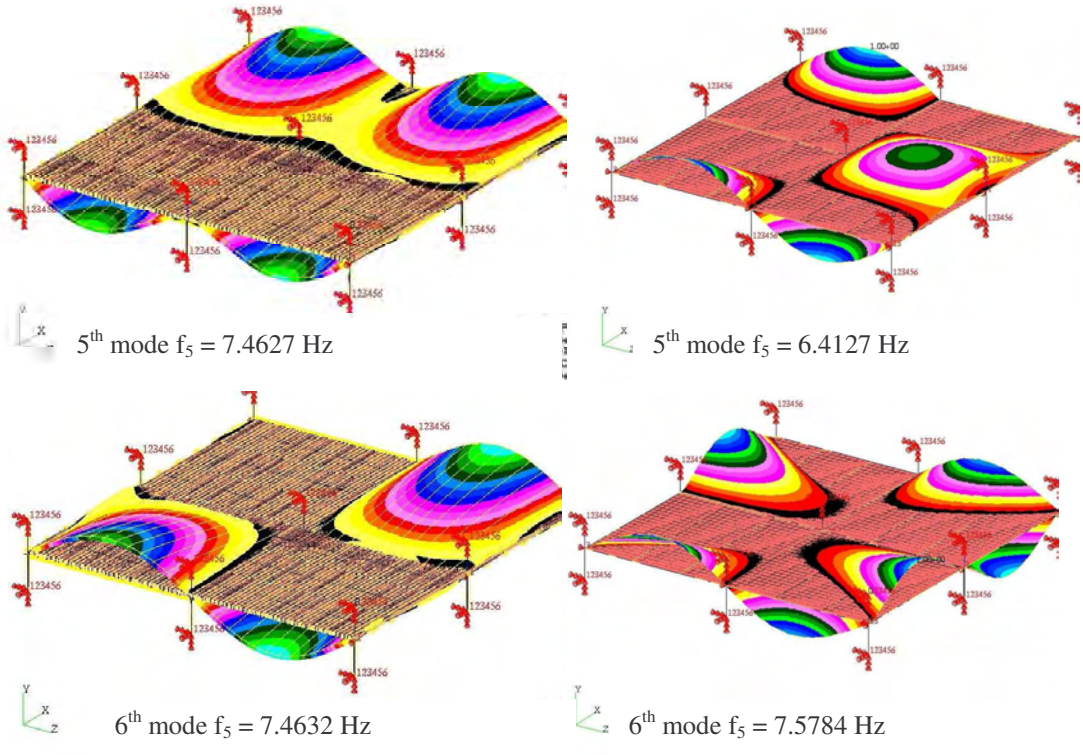

Figure 4-20: Comparison of natural frequencies and corresponding modes of layered model and uniform model

It was observed that all the mode shapes and natural frequencies of the layered model differed from those of the uniform model. Although the first mode and second mode shapes were the same, the other mode shapes were found different. Therefore, the use of uniform FE model, as an approximated model, for investigation under pattern loading was ruled-out. Hence, the layered FE model, which is more precise model, was thus proposed and used hereafter to determine the responses under various pattern loads. In order to reduce the computational time for analysis multiple CPUs were used and analysis jobs were performed in parallel.

4.7.5 Layered FE model for configuration 2

Based on the fact that the possible use of an approximated uniform FE model may cause incompatible natural frequencies and mode shapes, as was demonstrated in Section 4.7.4 for configuration 1, only a layered FE model was developed for the configuration 2. This configuration comprised of 3 x 3 bays of 9 panels of similar properties of the configuration 1. Thus, using extruding techniques available in MSC PATRAN, the configuration 1 was transformed into the configuration 2, saving time

on calibration and validation. The following Figure 4-21 illustrates the 3 x 3 panel model.

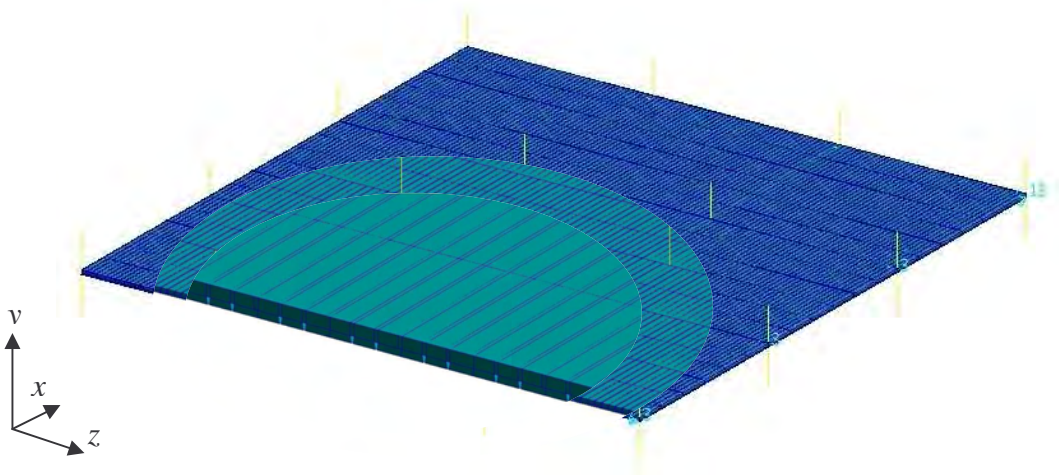

Figure 4-21: Uniform FE model for the 3 x 3 panel configuration

The 3 x 3 FE model is again a floor-column model, with fixed boundary conditions at the end-nodes of the columns. However, similarly to the of 2 x 2 floor model, translations in x and z directions were restrained at beam-column joints to prevent rigid body movements.

Natural frequency analysis of this model was carried out to determine the natural frequencies and the associated mode shapes as depicted in Figure 4-22.

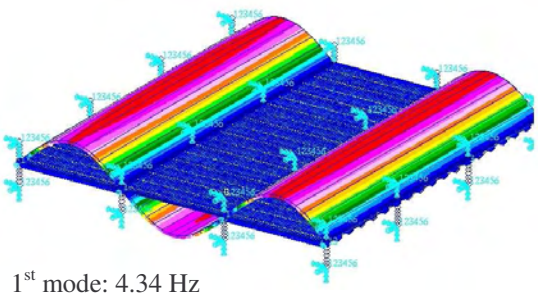

1st mode: 4.34 Hz

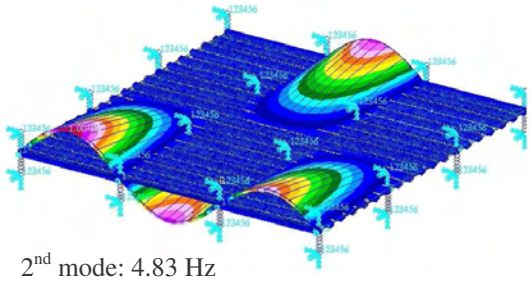

2nd mode: 4.83 Hz

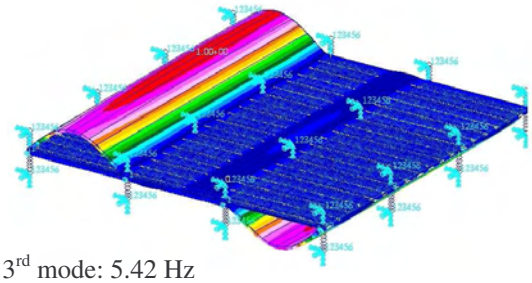

3rd mode: 5.42 Hz

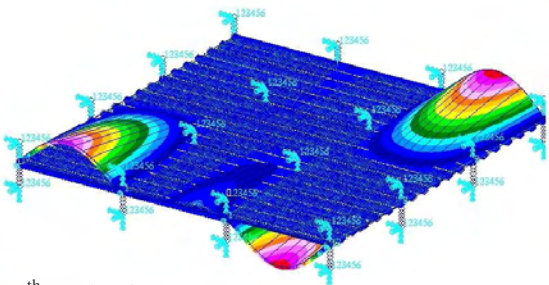

4th mode: 5.93 Hz

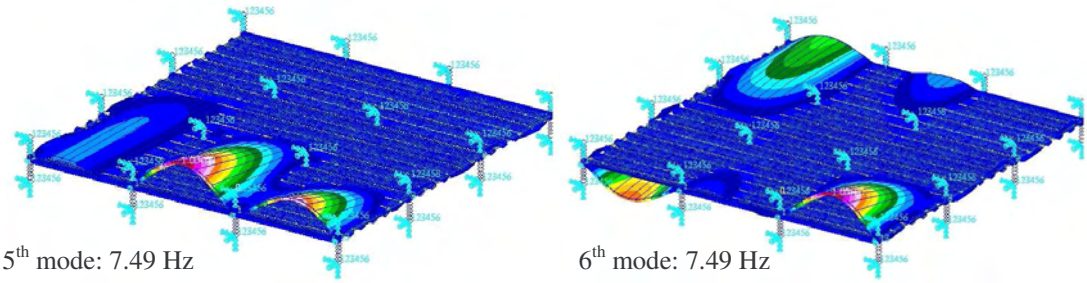

5th mode: 7.49 Hz 6th mode: 7.49 Hz

Figure 4-22: Natural frequencies and associated mode shapes for 3 x 3 panel FE model

The natural frequencies of the 3 x 3 panel model gave similar mode shapes to those of 2 x 2 model, which included bending modes as well as twisting modes. The first mode and the third mode gave symmetric bending behaviour, while other modes gave both symmetric and axis-symmetric twisting modes of vibration.

4.8 Summary

This chapter presented the development, calibration and validation of FE models used for the investigation presented in this thesis. It comprised of development of single panel FE models, as well as multiple panel FE models. Both types of models were verified to have lower fundamental frequencies, which is the main cause to human discomfort under human-induced loads.

Seven single panel FE models with various sizes and stiffness were developed to investigate the structural behaviour under human-induced dynamic loads. Calibrated and validated by the experimental results, these uniform FE models were made suitable for further investigation.

Two multiple panel FE models were developed for the investigation of dynamic response under pattern loading. They comprised of floor-column models, first of 2 x 2 panel model - four panel model and second of 3 x 3 panel model - 9 panel model. The FE models' natural frequencies and associated mode shapes were verified and used for further investigation.

Chapter 5 - Dynamic analysis on single panel FE model

5.1 Introduction

The behaviour of single panel steel-deck composite floors under human-induced loads was investigated and this chapter presents the methodology used and the results obtained. Single panel models are very common in residential apartments and townhouses (e.g. patio, veranda, etc.). These panels in such situations can be subjected to various in-house human-induced dynamic loads such as walking, aerobics, etc. As a result, it could give rise to excessive responses than that to static responses in both displacement and acceleration, similar to that witnessed by the experimental investigation described in Chapter 3. This could give human discomfort to the occupants causing panic and could change their lifestyle to suit and moreover may have to spend extra money on retrofitting. Thus, the main objective of this chapter is to investigate and assess their dynamic amplifications and acceleration responses.

FE models developed for single panel steel-deck composite floors in Chapter 4 were used for this cause. The dynamic loads taking place during aerobics/jumping event, which considered giving the most onerous load was used in the this investigation. These loads are applied on different activity frequencies and at different damping levels. Consequent dynamic responses under these loads were obtained. Finally, these dynamic responses were compared and contrasted with serviceability limits and used to develop empirical relationships.

5.2 Single panel configuration and properties

5.2.1 Geometric configuration

The single panel configurations used were the simply supported single panel FE models calibrated, validated and presented in Chapter 4. Table 5-1 presents the dimensions of these single panel models. These models gave square panels of span to width ratio of 1, as well as rectangular panels of span to width ratio of 2.

Table 5-1: Geometric properties of single panel models

	Length, mm	Width, mm	Thickness, mm
Model 1 (experimental model)	3200	1800	100
Model 2	4800	2400	140
Model 3	4800	4800	140
Model 4	6000	3000	190
Model 5	6000	6000	190
Model 6	7200	3600	250
Model 7	7200	7200	250

Model 1, 2, 4, and 6 are rectangular panels while, Model 3, 5 and 7 are square panels. The thickness of the single panel models were obtained by the design charts which most of the commercial producers published (BlueScope Steel 2003). The longest span limited at 7200 mm with thickness of 250 mm, while the shortest span limited to 3200 mm with thickness of 100 mm giving seven models, including the experimental model size.

5.2.2 Fundamental frequencies from FEA

These FE models have given variety of natural frequencies. Table 5-2 presents the first and second natural frequencies obtained by FEA. The associated mode shapes for first natural frequency was the simple bending mode (refer Figure 5-1a) while the second natural frequency is associated with the twisting modes (refer Figure 5-1b). The higher mode shapes are not important as this single panel model was excited in its fundamental mode (described later). However, the second natural frequencies for the FE models were obtained, as they were used for the calculation of damping coefficients (refer Section 5.3.3 and 5.3.4).

It was observed that the fundamental frequencies of Model 2 and Model 3 were almost equal irrespective of their difference in the transverse length. In like manner, panel Model 4 and Model 5, Model 6 and Model 7 did not vary their fundamental natural frequencies. Thus, the difference in transverse length of the panel has not provided a significant effect on the fundamental frequency.

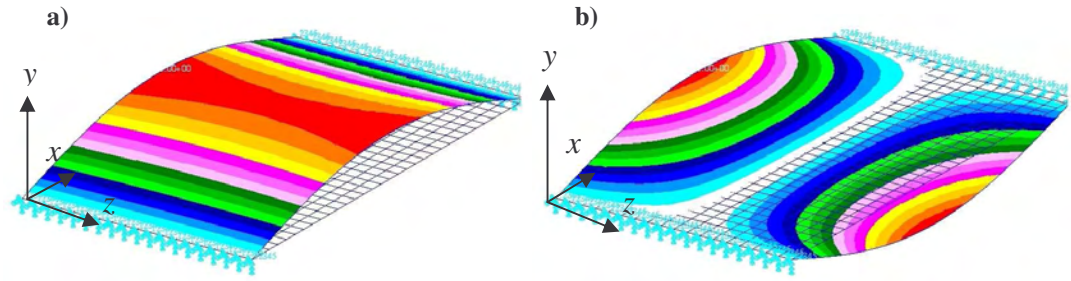

Figure 5-1: Mode shapes of single panel models

Table 5-2: Natural frequencies of the FE model

	First natural frequency, f_{1FEA} (Hz)	Second natural frequency, f_{2FEA} (Hz)
Model 1	14.5	39.0
Model 2	9.4	27.9
Model 3	9.5	15.8
Model 4	8.5	25.1
Model 5	8.5	14.6
Model 6	7.5	22.3
Model 7	7.6	13.0

5.2.3 Verification of fundamental frequency with Wyatt et. al. (1989) method

Fundamental natural frequency of the floor panels, presented in Table 5-2 were compared for verification with the generally used analytical solution in Design Guide on Vibration of Floors (Wyatt 1989). This analytical solution for fundamental natural frequency is given is per Equation 5-1.

$$f_{Analytical} = C_B \left(\frac{EI}{mL^4} \right)^{1/2}, \qquad \textbf{Equation 5-1}$$

where m is the mass per unit length (note: units in tons/m if EI expressed in kNm^2, or kg/m if EI expressed in Nm^2), L is the span (in meters), E is the modulus of elasticity, I is the second moment of area (Wyatt 1989). The values of C_B for various end conditions are 1.57 for the pinned supports (simply supported), 2.45 for fixed/ pinned supported, 3.56 for fixed both ends and 0.56 is for fixed/free (cantilever)

ends. Since the investigated panels were simply supported, the value for C_B is taken as 1.57 (or in mathematical terms $\pi/2$). The modulus of elasticity, E is taken as 31.335 MPa, I, second moment of area taken idealising the panel section to a rectangular beam section (i.e. $bd^3/12$), mass, m is calculated using the concrete density of 2428 kg/m^3 and L is the actual span of the model. Using these values the fundamental natural frequency of the floor models was calculated using Wyatt et al. (1989)'s method and compared with the fundamental frequencies obtained by FEA (refer Figure 5-2).

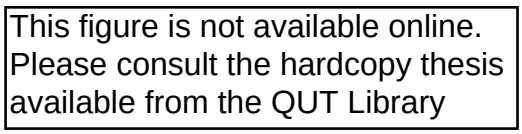

Figure 5-2: Comparison of fundamental frequency obtained using FEA and using the method presented by Wyatt et al. (1989) .

It was observed that the two methodologies have given similar results. Thus, Wyatt et al. (1989) method can be used in determining the fundamental natural frequency in single panel models without using sophisticated finite element modelling. This also validates the single panel FE models.

5.2.4 Derivation of DAF limits of displacement

The results of dynamic analysis on the seven models gave DAFs which were more than unity underlaying that the DAF for displacement under dynamic loading is more than the static loading. These DAFs need to be verified with a DAF limit in order to investigate whether it has reached the serviceability DAFs (or DAF limits). These DAF limits for the current floor configuration were predetermined by load-deflection characteristics obtained by static analysis. Un-factored loads were applied statically over the entire floor panel and deflections at mid-span nodes were obtained. Herein,

live-load of 0.4 kPa was used as the static load posed by the occupants, assuming average weight of person to be 70 kg (Allen 1990b). These loads gave static deflections Δ_{Static} while serviceability deflection limit for static design (Δ_{Max}) was reported to take as lesser of span/250 or 20 mm for composite floor design (British Standard : BS5950 : Part 4 1994; AS 3600 2001). Using these two deflections the DAF limit for displacement has been calculated by dividing Δ_{Max} by Δ_{Static}, which gave values of 4.68, 4.54, 4.54, 5.13, 5.13, 5.46 and 5.47 for the panel models 1, 2 3,4,5 6 and 7 respectively.

5.3 Dynamic analysis of FE models

Linear transient dynamic analysis was done on all single panel FE models to obtain the DAFs and acceleration responses. The load model representing the aerobics/jumping activity presented by other researchers was used for this analysis. This load model is described in Section 5.3.1. This load model was incorporated to FE models in their execution in the ABAQUS solver and the methodology used is described in Section 5.3.2. Furthermore, four damping levels were considered for this research study and they were obtained by referring to publications made by various researchers and are described in Section 5.3.3.

5.3.1 Human-induced forces

Mathematical model (load-time history or load model) describing aerobics/jumping event was used in exciting the single panel FE models. This human event was particularly chosen as it produces higher loads unlike people walking and running. This mathematical model has been described by Equation 5-2 (ISO 10137 1992), (Ginty, Derwent et al. 2001) (Bachmann and Ammann 1987), (Smith 2002).

$$F(t) = G\left[1 + \sum_{i=1}^{\infty} r_i \sin\left(2\pi f_p t + \phi_i\right)\right], \qquad \textbf{Equation 5-2}$$

where $F(t)$ is the force, G is the static weight of the occupant, r_i is the Fourier Coefficients, f_p is the pacing frequency, t is the time and φ_i is the phase lags and $i = 1 \ldots n$.

The above equation can also be used to foam different loads for different human activities of walking and running by using different Fourier coefficients r_i, pacing frequencies f_p and phase lags φ_i. The Fourier coefficients are also termed the harmonic components or the load factors which have been obtained by dividing the dynamic force time history of by the weight of the participants (Willford 2001). The current investigation used the human-actions of aerobics/jumping and thus the corresponding Fourier coefficients used were 1.5 (first Fourier coefficient, r_1), 0.6 (second Fourier coefficient, r_2) and 0.1 (third Fourier coefficient, r_3) (Ginty, Derwent et al. 2001) (Bachmann and Ammann 1987).

The load-time history also varies with pacing frequency (or activity frequency), which again depend upon the human action. Various activity frequencies for different human activities have been published in the literature and the current work used the activity frequencies in the rage of 2.2 Hz to 2.8 Hz, which were predominant frequencies under aerobics/jumping loads (Bachmann and Ammann 1987). Thus, current work used pacing frequencies starting from 2.2 Hz to 2.8 Hz in steps if 0.2 Hz.

It was assumed that all the Fourier components of the load-time history are in-phase during the human activity and thus the phase lag, φ is zero. Thus, perfect coordination between the occupants posing the activity is considered.

5.3.2 Incorporation of load-time functions to FE models

The load-time functions developed using the formula given in Equation 5-2, was needed to be incorporated in to the finite element code which is generated by the MSC PATRAN. This is to acquire data for the computer simulation of human-activity. Initially, these data of the load-time function was created in MS EXCEL (".xls" and ".prn" file format) and a special MATLAB program developed by High Performance Computing (HPC), of QUT was used to convert (".prn" files) to ABAQUS readable ".dat" files. These ".dat" files were then referred in the MSC PATRAN input code that linked the load-time data to be used in its execution with ABACUS (refer Figure 5-3)

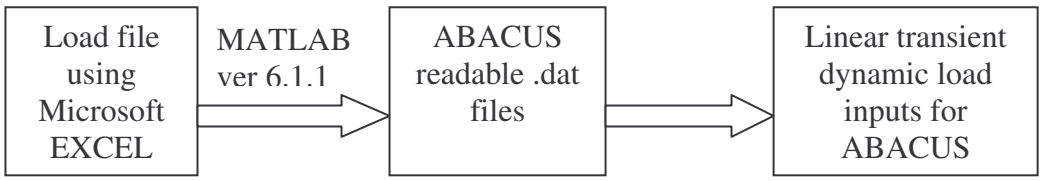

Figure 5-3: Incorporation sequence of load-time functions

5.3.3 Damping for the FE models

Specific damping levels on floor systems is hardly predictable before-hand as they tend to vary with cause (Chen 1999). Thus, the current work looked at four damping levels for the analysis narrowing this variation (refer Table 5-3).

Table 5-3: Damping levels used for the single-panel behaviour

Damping level	Damping ratio (%)
Low damping	1.6
Mild damping	3.0
Medium damping	6.0
High damping	12.0

These four damping levels were identified after referring to investigations made in various publications and their credibility are discussed in the subsequent paragraphs.

Damping level of 1.6 % was used for the damping level for a bare floor which can be classified as “low damping”. In general, damping for bare composite floors has been reported to be between 1.5% - 1.8% (Bachmann and Ammann 1987). Osborne et al. (1990) used slightly higher damping values of 2%~3.0% for the bare floor (full composite construction) for the Super Holorib composite floor system. Damping coefficient of 1.5% was used by Wyatt et al. (1989) for a composite deck floor. Further the heel impact test performed on the tests panels (refer Chapter 4) has also provided a damping of 1.75%, close to this value. However, it should be noted that this would be a rare case as the external force-causing object and other standing objects on the floor will provide additional damping that is not included in this value. Also using partitions on the finished floor system could yield higher damping (Wyatt 1989).

Another level of damping of 3.0% had been identified as “mild damping” which has been used to classify a office without permanent partitions or electronic / paperless offices Hewitt et al. (2004b) and Murray (2000a).

Higher damping could arise in a floor with permanent (full height partitions), drywall partitions where it could be as much as 5.0% - 6.0% (Murray 2000a). Elnimeiri (1989) recommended a damping coefficient of 4.5% - 6.0% for finished floors with partitions. A similar amount of damping can be observed in the older floor systems constructed in 1970’s and 1960’s (Hewitt and Murray 2004b). A floor with this situation can be classified as having a “medium damping” condition.

Brownjohn (2001) showed that the damping could increase to 10% depending on occupant posture. This also would happen in an environment with an old office floor with cabinets, bookcases and desks. On the other hand, Sachse (2002) proved that the presence of stationary humans will increase the damping of the structure. This phenomena is called human-structure interaction and previous investigations by Sachse et al. (2002) (2003) Ji, (2003) has provided that this causes a significant increase in damping which could increase the damping up to 12.0% and thus can be classified as floors with “high damping”.

With this justification of four damping levels, the computer simulation incorporated these flour damping levels using the mass proportional damping, a and the stiffness proportional damping, b (the calculation is described in Section 5.3.4). The seven models gave different mass proportional damping, a and the stiffness proportional damping, b and are presented in Table 5-4. It was assumed that variation of damping ratios were negligible for the first and the second natural frequencies (refer Table 5-2) when calculating the mass and stiffness proportional damping coefficients.

5.3.4 Calculation of mass and stiffness proportional damping

The damping of structural system is more conveniently defined in terms of model damping ratios or levels ζ (as described in Section 5.3.3). However, in a transient dynamic analysis problem, the damping matrix can not be defined by damping ratios and needed to be pre-defined in some other way to solve the problem for displacements or stresses.

In solving the structural system the damping matrix can not be expressed by the damping ratios, instead an explicit damping matrix is used (Clough and Penzien 1993). Thus, a method by Reyleigh which the damping is assumed to be proportional to the combination of mass and stiffness matrix is used. This is described in the Equation 5-3.

$$[C] = a[M] + b[K] \qquad \textbf{Equation 5-3}$$

where [*C*] is the system damping matrix, [*M*] is the mass matrix, [*K*] is the stiffness matrix, *a* is the mass proportional damping and *b* is the stiffness proportional damping. This Reyleigh's damping leads to the following relationship (refer Equation 5-4) between damping ratio ζ and frequency f_n of n^{th} mode.

$$\zeta_n = \frac{a}{2f_n} + \frac{bf_n}{2}. \qquad \textbf{Equation 5-4}$$

The solution for the mass proportional damping coefficient, *a* and stiffness proportional damping, *b* were obtained by a pair of Equation 5-4 simultaneously for the m^{th} and n^{th} mode.

Thus,

$$\begin{Bmatrix} \zeta_m \\ \zeta_n \end{Bmatrix} = \frac{1}{2}\begin{bmatrix} 1/f_m & f_m \\ 1/f_n & f_n \end{bmatrix}\begin{Bmatrix} a \\ b \end{Bmatrix}. \qquad \textbf{Equation 5-5}$$

Assuming, the variation of damping ratio with frequency is minor, the proportional factors were given by, (i.e. $\zeta_m = \zeta_n = \zeta$). Thus, Equation 5-5 can be rearranged to give Equation 5-6 as formulae for calculation for mass and stiffness proportional damping.

$$\begin{Bmatrix} a \\ b \end{Bmatrix} = \frac{2\zeta}{f_m + f_n}\begin{Bmatrix} f_m f_n \\ 1 \end{Bmatrix}. \qquad \textbf{Equation 5-6}$$

Given the damping level ζ and two natural frequencies f_m *and* f_n, ratios mass and stiffness proportional damping can be calculated. The natural frequencies can be

found by using natural frequency analysis while damping needed to be assumed considering structural use and its intended purpose.

Table 5-4: Mass proportional and stiffness proportional damping for the seven models

	Damping 1.6%		Damping 3.0%		Damping 6.0%		Damping 12.0%	
	a	*b*	*a*	*b*	*a*	*b*	*a*	*b*
Model 1	0.3388	5.98E-04	0.6353	1.12E-03	1.2706	2.24E-03	2.5412	4.49E-03
Model 2	0.2252	8.58E-04	0.4223	1.61E-03	0.8445	3.22E-03	1.689	6.44E-03
Model 3	0.1856	1.28E-03	0.3479	2.41E-03	0.6959	4.81E-03	1.3919	9.63E-03
Model 4	0.203	9.52E-03	0.3806	1.78E-03	0.7612	3.57E-03	1.5223	7.14E-03
Model 5	0.1726	1.38E-03	0.3236	2.59E-03	0.6472	5.18E-03	1.2943	1.04E-02
Model 6	0.1805	1.07E-03	0.3384	2.01E-03	0.6767	4.02E-03	1.3534	8.03E-03
Model 7	0.1529	1.56E-03	0.2867	2.92E-03	0.5734	5.84E-03	1.1468	1.17E-02

(a – mass proportional damping, b – stiffness proportional damping)

5.4 Response of FE models under dynamic loads

This section of the chapter presents the responses of displacements, stresses and accelerations obtained from the computer simulated aerobics / jumping loads on the single panel FE models. Linear transient dynamic analysis was performed to obtain these responses. Herein the activity has simulated for 6 seconds with a time step of 0.005 and the respective responses were obtained. This simulation time has given sufficient time to reach steady state conditions.

5.4.1 DAF for displacement for aerobics/jumping loads

The DAFs for displacement were obtained by dividing the dynamic deflection by the corresponding static deflection. The deflection at the mid span node was considered adequate to obtain for this cause. The dynamic deflections were obtained using displacement-time history while the static deflections were obtained using the static analysis done prior to dynamic analysis. Figure 5-4 depicts a typical displacement-time history response of single panel subjected to aerobics/jumping loads.

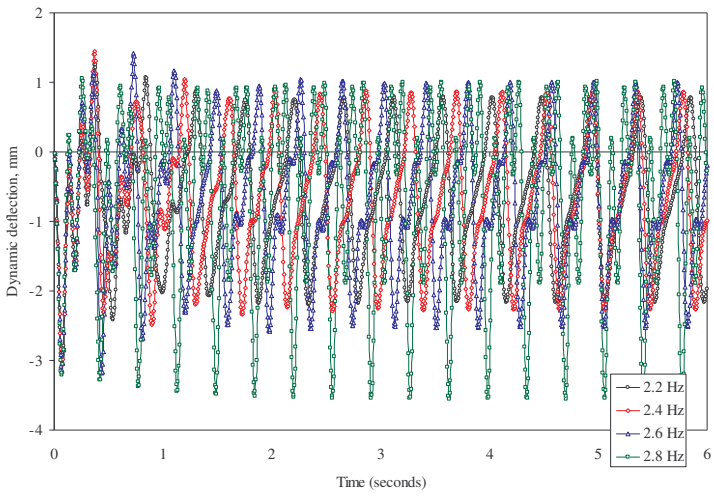

Figure 5-4: Typical displacement time history under aerobics/jumping loading (Span 4 – 1.6% damping)

Using these displacement time histories DAFs were calculated and the results are discussed hereafter. Figure 5-5a, Figure 5-5b, Figure 5-5c, Figure 5-5d represents the DAF for displacements at different damping levels of 1.6%, 3.0%, 6.0% and 12.0% respectively.

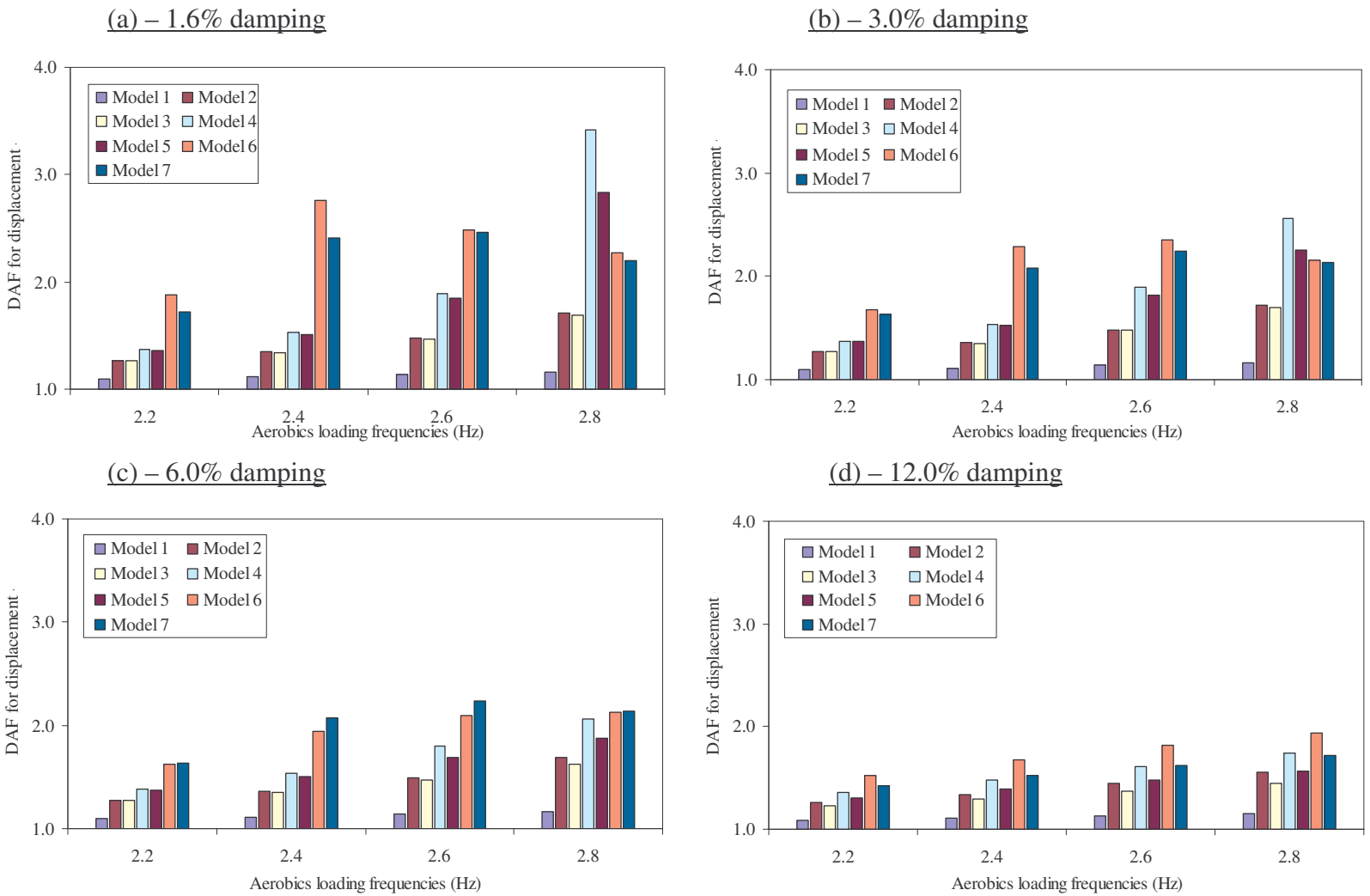

Figure 5-5 Dynamic amplification factors for aerobics in single panel loading

It was observed that the DAFs have not yielded beyond the DAF limits presented in Section 5.2.4. The DAFs for displacement were given maximum at lower damping levels while higher damping levels provided the lowest DAF for displacement. The variations of DAF for displacement were wide from 1.09 to 3.4 under aerobics/jumping loads. By the observation of the trends of the responses described in the above figures the following were noted:

- The DAF for displacement responses were found to be increasing with the increase of the activity frequency (which is expected and standard) in contrast to abnormal jumps in DAFs for displacement in:
    - Model 4 at 1.6% and 3.0% damping at activity frequency of 2.8 Hz,
    - Model 5 at 1.6% and 3.0% damping at activity frequency of 2.8 Hz,
    - Model 6 at 1.6% and 3.0% damping at activity frequencies of 2.4 Hz and 2.6 Hz,
    - Model 7 at 1.6% and 3.0% damping at activity frequencies of 2.4 Hz and 2.6 Hz.
- In contrast to the observations stated above (which were found to be present in the panels with damping of 1.6% and 3.0%), the panels with 6% and 12.0% damping, the DAF for displacement did not drift drastically to give additional peaks.
- Panel model 1, having the highest fundamental frequency was given the lowest DAFs, in contrast to its lowest stiffness. Panel Models 6, 7 are the panels which had the lowest fundamental frequency contrast to its stiffness, but provided higher DAF of all panels (at most times). This concludes that the fundamental frequency's major role in dynamic responses.
- Within equal span models of different transverse span models, the panel model with lower transverse spans was given the highest DAFs for displacement.

5.4.2 DAF for Stresses for aerobics/jumping loads

The stress responses obtained for aerobics/jumping loads were used to determine the DAF for stresses in a similar manner to that of DAF for displacement, by dividing the dynamic stresses by the corresponding static stress. These DAF for stresses were

compared with the DAF for displacement to observe any significant variations. Figure 5-6 presents of such variations, in-fact it came out exactly the same. This is due to the linear transient dynamic analysis procedure adopted for the current work. Nevertheless, this noted the un-necessity to obtain DAF for stresses as such, as it will be the same as the DAF for displacement and thus will not be used in the impending sections of the thesis.

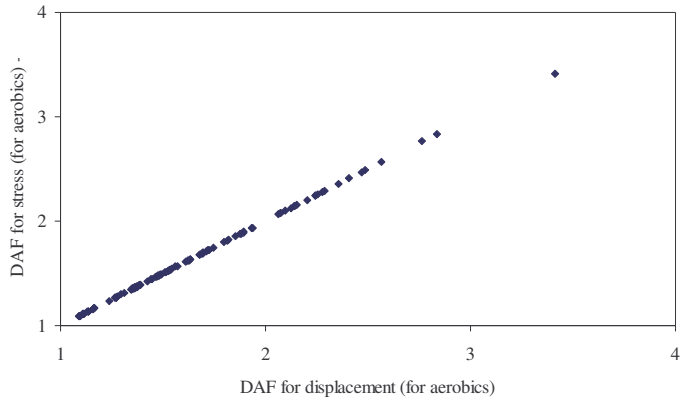

Figure 5-6: The variation of DAF for displacement and DAF for stresses for aerobics/jumping loads

5.4.3 Development of relationships for DAF

With the results described in the above Sections 5.4.1 and 5.4.2 this section intends to determine a possible relationship for dynamic amplification under aerobes/jumping loads which can be used to calculate the same beforehand with known terms of frequency ratio and damping level for a single panel steel-deck composite floor. The basic principals for a system subjected to human excitation triggered the selection of the two non-dimensional parameters of fundamental natural frequency (or the frequency ratio, f_o/f_1) and the damping level. This equation development was done by curve fitting methods and then using the "solver" in MS EXCEL, which is based on the method of least squares and linear programming for the best equation that fits the FEA results.

5.4.3.1 Variation of DAFs with frequency ratio

The averaged DAF (of each panel) at each frequency ratio was used in obtain the variation of DAF with respect frequency ratio and is presented in Figure 5-7.

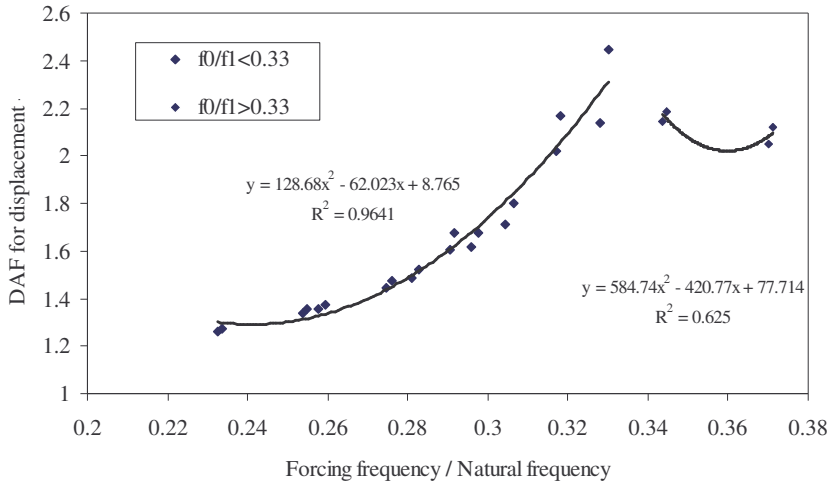

Figure 5-7: Variation of DAFs with frequency ratio

From the above plot, a peak in response was observed at f_o/f_1=0.33. This can be verified as the floors have been excited by the third harmonic of the activity frequency. As a sigule relationship for the DAF for displacement response can not be obtained, two second order polynomials were used, as shown above. The polynomial functions were selected after checking the suitability of other functions eg. exponential, logarithmic, power etc. The functions which gave the R-squared value (also known as coefficient of determination) close to unity and thus was selected. This was considered to give the most reliable estimation to represent the values. The second order polynomials selected gave an R-squired value of 0.9641 and 0.625 for the two functions respectively.

The coefficients of these chosen polynomials were derived by using "Solver", the MS Excel's curve fitting add-in. These two equations after rearranging gave:

$$DAF = \left(A - B\frac{f_0}{f_1} \right)^2 + C, \qquad \textbf{Equation 5-7}$$

where A = 2.73, B = 11.34, C = 1.29 when $f_o/f_1 < 0.33$ and A = 8.70, B = 24.18, C = 2.02 when $f_o/f_1 > 0.33$

The DAFs predicted by formula given in Equation 5-7 was then compared with the same obtained from FEA. This comparison is presented in Figure 5-8. It gave a standard deviation of 0.025842 and COV of 2.6%, which were within the acceptable variations.

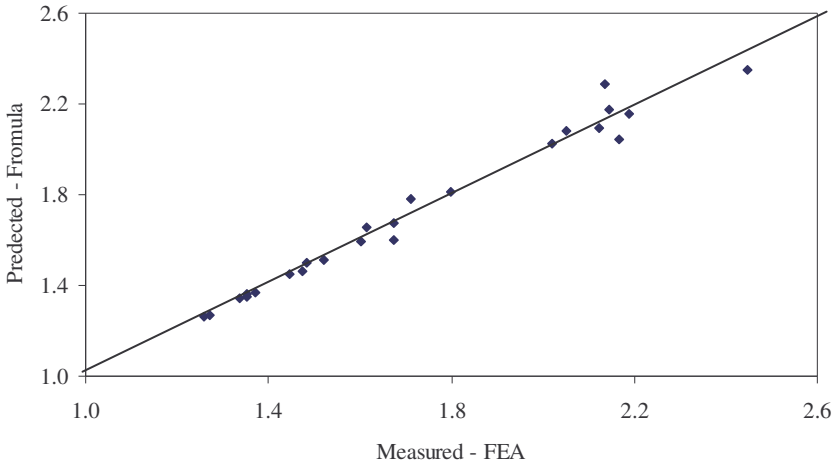

Figure 5-8: Predicted vs measured DAFs

This developed formula can be used in to predict the DAF that occur due the most energetic event of doing aerobics/jumping on a for single panel steel-deck composite floor. However, it should note that this prediction would be limited to excitation in the fundamental mode by the third harmonic of the activity frequency. Given the possible frequencies (of human-activity) and the fundamental natural frequency (obtained using Wyatt et al. (1989) method presented in Section 5.2.3 or by FEA), the above formulae determines directly the DAF risen under a aerobics/jumping event.

5.4.3.2 Variation of DAFs with damping

This investigation considered four damping levels, and thus the DAF were averaged on each damping level of each panel model to obtain the variation of DAF with respect to the damping level and presented in Figure 5-9.

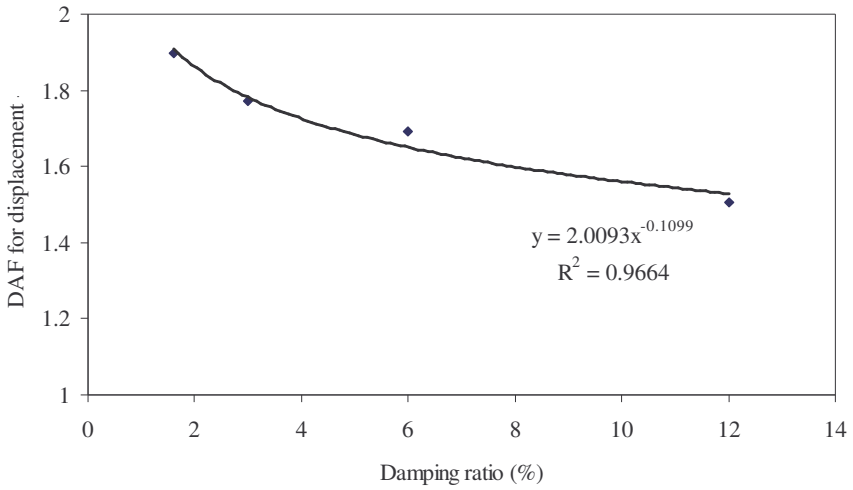

Figure 5-9: Variation of DAFs with damping

The relationship between the damping level and the DAF response can be fitted to a power function that has been developed and presented in the following Equation 5-8:

$$DAF = D(\zeta)^{y}\ , \qquad \textbf{Equation 5-8}$$

where D and y are constants.

The constants D and y were found to be 2 and -0.11 respectively giving a standard deviation of 0.018013 and Coefficient of Variation (COV) 1.8% when compared with the FEA results. Thus results from the formula is well within the standard limits of COV (i.e. 10%) and thus can be used to obtain a DAFs (approximate) due to an aerobics/jumping event when the structural damping level is known in the floor system.

5.4.4 Acceleration responses for aerobics/jumping loads

Acceleration responses for aerobics loads on the single panel FE models were also obtained. Steady state acceleration responses of mid span nodes were obtained on the seven FE models under different damping conditions. A typical acceleration response observed is presented in Figure 5-10.

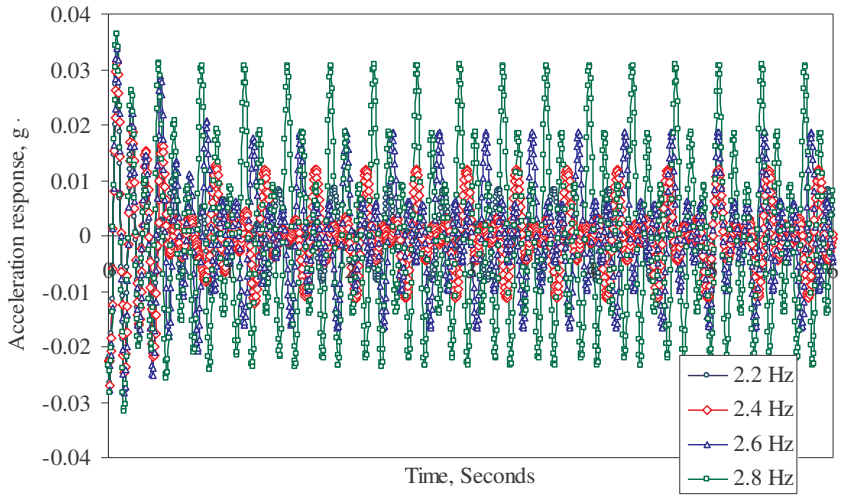

Figure 5-10: Typical acceleration time history under aerobics/jumping loading (Span 4 –3.06% damping)

The acceleration response considered in this was limited to for a human density of 0.4 kPa (single person occupying area of 1.75 m^2 - nominal weight of a single person is taken as 70 kg) which, was considered achieve the maximum human-density performing the activity. Figure 5-11a, Figure 5-11b, Figure 5-11c, and Figure 5-11d depict the acceleration response observed for each floor model under the four damping levels respectively.

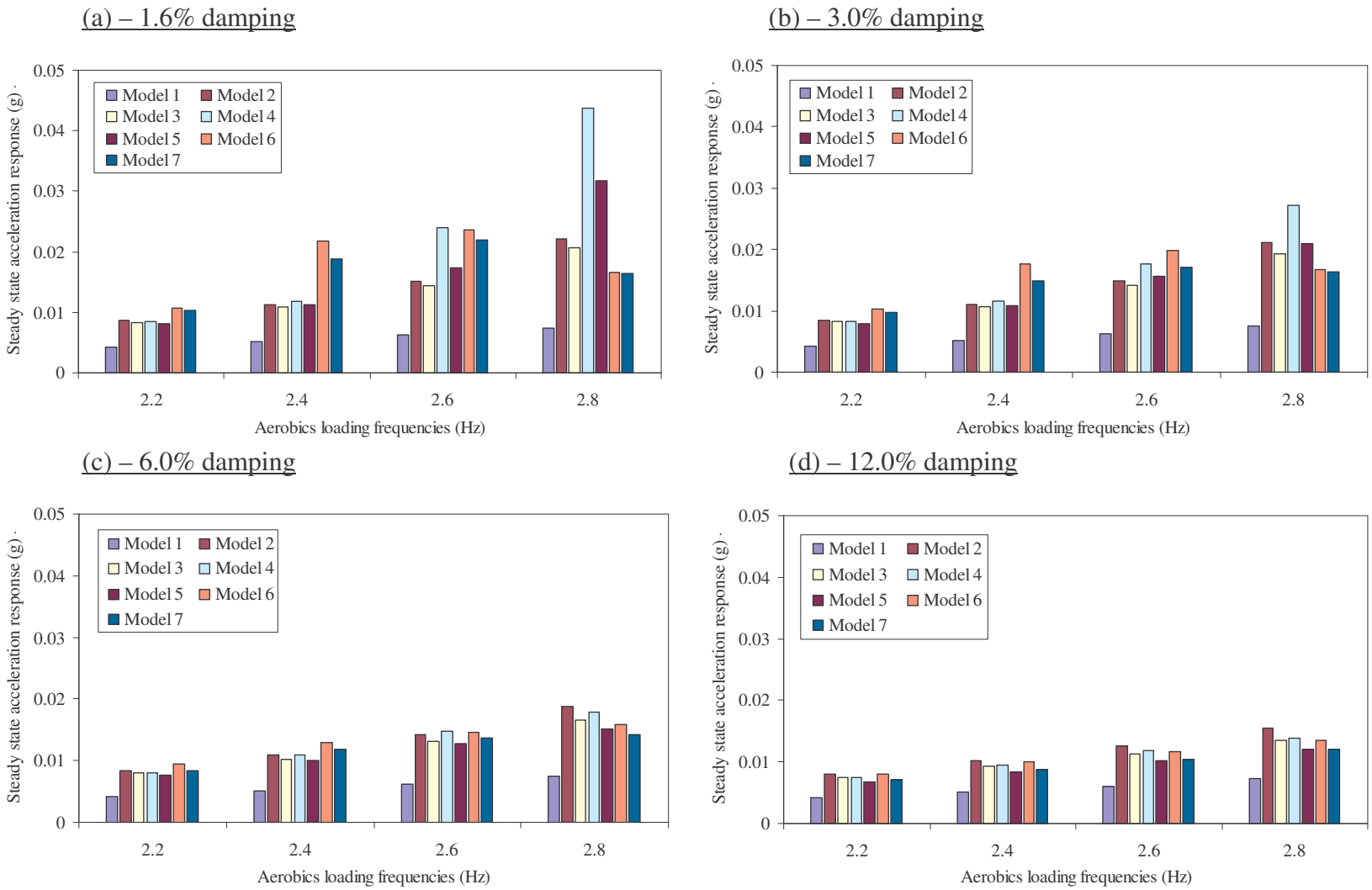

Figure 5-11: Acceleration response for aerobics in single panel loading

The acceleration response observed for the aerobics/jumping were given similar trends to that of the trends observed for DAF for displacement. In an human perceptibility prospective, the acceleration responses were well within the AISC Design Guide 11 (Murray, Allen et al. 1997) of 0.05g (for rhythmic activity), concluding that single panel models have not caused vibration problems to the occupants.

These acceleration responses were then compared with the equation that used in design of floors against vibrations. This equation was discussed in Chapter 2, Equation 2-10 by Murray, Allen et al. (1997). It yields the acceleration response after a rhythmic excitation. The current floor models yielded the response in the third harmonic of the activity frequency thus α_i dynamic amplification factor of 0.1 was used in the above-mentioned Equation 2-10. The effective weight per unit area of participants distributed over the floor panel w_p, is the effective distributed weight per unit area w_t were calculated for the floor model. The natural frequency of the floor f_n were presented in Table 5-2 and the response were observed at various forcing frequencies f and at four damping levels (ζ – Refer Table 5-3*)*. Figure 5-12a, Figure 5-12b, Figure 5-12c and Figure 5-12d depicts the comparison of results obtained using Equation 2-10 of Chapter 2 and FEA for damping levels of 1.6%, 3.0%, 6.0% and 12.0% respectively.

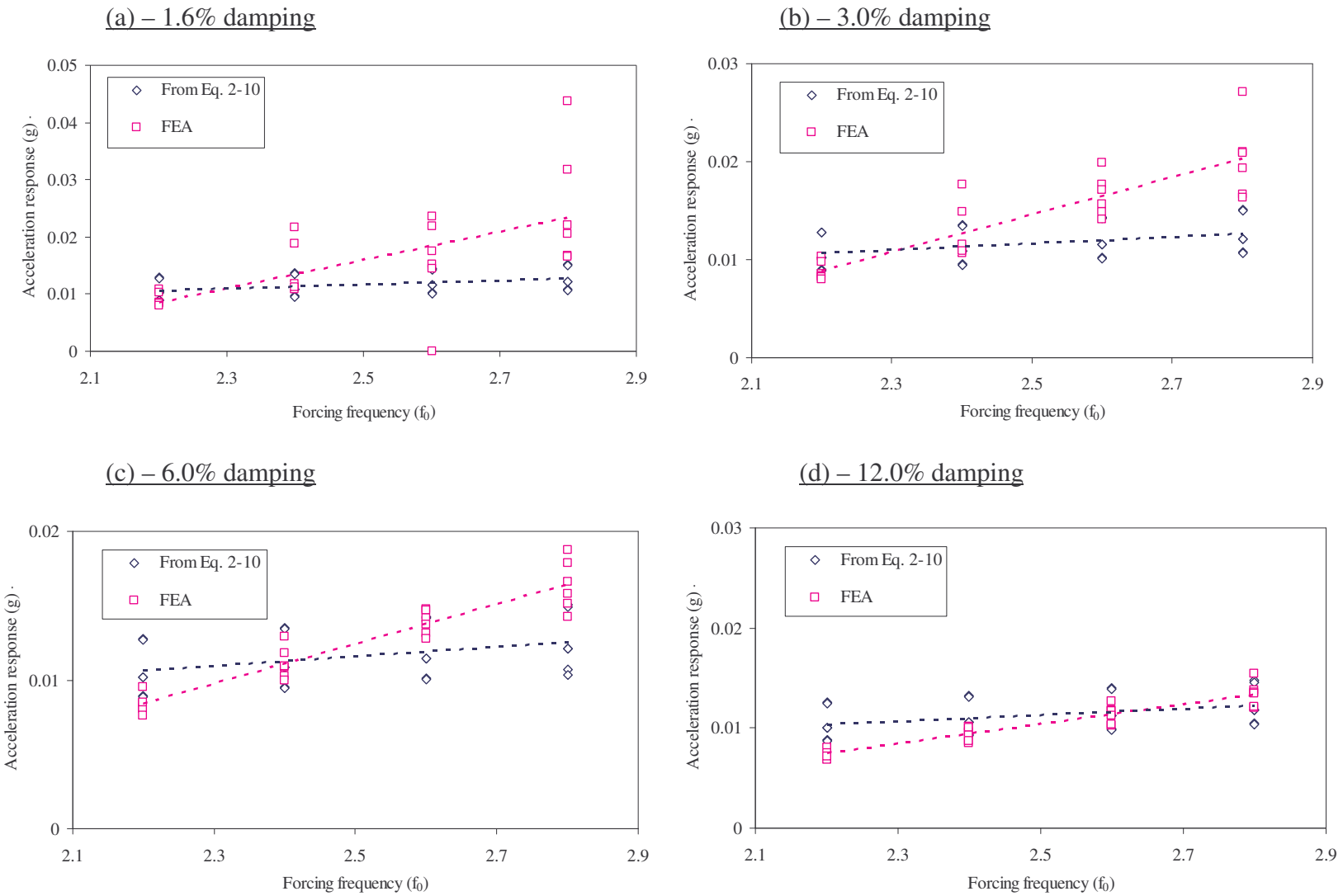

Figure 5-12: Acceleration response comparison with literature and FEA

Equation 2-10's predictions were reasonable close to the FEA results in cases of 6.0% and 12.0% damping. However, there were under-predictions of acceleration response especially at lower damping levels of 1.6% and 3.0%.

5.5 Summary

This chapter of the thesis presented FEA carried out on single panel steel-deck composite floor slabs. Seven of floor model sizes were used for this investigation and linear transit dynamic analysis were carried out.

The finite elements models were subjected to human-induced aerobics/jumping loads to establish DAFs for displacement and acceleration responses. The simulations were carried out on different human-induced forcing frequencies as well as four damping levels. Using the responses obtained by FEA, formulae for the DAFs were established by considering the parameters of frequency ratio and damping levels.

The acceleration responses observed were within current human perceptibility limits and thus have not caused discomfort problems to the occupants. The comparison of acceleration response with the current design equitation's for human comfort yielded reasonable agreement, especially for floors with 6.0% or higher damping levels.

Chapter 6 - Dynamic analysis on four panel FE model

6.1 Introduction

Modern building systems are inhabited by multiple-occupancy floor set-outs in combinations of office/commercial floors and leisure activity halls, such as aerobics halls, gymnasiums etc. These types of floor set-outs generate various pattern loading cases. The floor panels that are occupied for aerobics and gymnasium activities are subjected to dance-type loading, while the adjacent floor panels serve as office/commercial or residential occupancy. Such pattern loading cases can result in excessive vibrations that cause discomfort to the occupants in the adjacent floor panels as well as to the occupants in the panels posing the activity. As a consequence, people can be reluctant to use the floor for their chosen activities, causing severe serviceability problems. Its is the lack of knowledge and understanding of the phenomenon of floors subjected pattern loads that have caused the above mentioned consequences in the past. To address this problem, this chapter investigates the performance of floors under various pattern loading cases.

Four pattern loading cases were identified and their responses were assessed. Linear transient dynamic analyses were carried out for the four pattern loading cases at various operating conditions. These operating conditions included damping levels, human-excitation events based on various load frequencies and contact ratios and human-densities posing the activity. The dynamic responses of deflections and accelerations were obtained and compared with the serviceability deflection limits and human comfort levels for accelerations. Accordingly, possible occupancies and operating conditions that can be used in fit-out for the multiple panel floor system were determined. Finally, empirical formulae which can be used to determine DAFs and acceleration responses were developed.

6.2 Four panel configuration and properties

The four panel FE model developed and described in Chapter 4, Section 4.7 was used for investigation presented in this chapter. It is a two-bay, four-panel floor system supported on primary and secondary beams that generally is found in steel-

frame building construction. This type of floor system is ideal for the current investigations, as they provide large clear space with no conventional walls in between columns. Moreover it has a low fundamental frequency of 4 Hz, which can be easily excited by the human activity frequencies. This FE model was termed "configuration 1" and was used extensively for various operating conditions such as different human-induced activities, activity frequencies (refer Section 6.3), damping (refer Section 6.4) on several pattern loading cases (refer Section 6.5) as reported in this chapter.

6.3 Human-induced activities/loads

In order to investigate the response of floors under various human-induced dynamic loads a mathematical model designed by other researches was used (Ellis and Ji 1994). Generally, human-induced dynamic loads on floors can vary from simple walking to onerous dance-type loads. A general classification for these human actions can be obtained by splitting them into two categories one of continuous and the other of discontinuous ground contact activities (Bachmann, Pretlove et al. 1995). For example, human actions such as walking were considered as continuous ground contact activity, while running, aerobics dance-type activities like activities as discontinuous ground contact activities.

Dance-type activities have been the most pronounced events, which generate higher dynamic forces than those of walking loads, and hence cause a multiple panel floor system to give excessive responses. Modern floor fit-outs accommodate spaces for such activities mainly to enable their residents to engage leisurely in their day-to-day life. Thus, dance-type loads, which can include aerobics/jumping are the most important to be considered in the current investigation to obtain the dynamic responses of multiple panel floor system subjected to pattern loading.

Dance-type loads produce discontinuous load time history, which are similar to human activities of running and aerobics and are more onerous (Ji and Ellis 1994). The load time history of dance-type loads were described by, contact duration which measures both feet in-contact with the structure for a time phase followed by a zero force when both feet leave the floor. This can be described by a half-sinusoidal curve. To represent an entire event of dance-type load activity, a sequence of half-

sinusoidal pluses can be used. Equation 6-1 presents a mathematical model for dance-type activity, followed by Figure 6-1 depicting its graphical representation.

$$F(t)=\begin{cases} K_P G Sin(\pi t/t_p) & 0 \le t \le t_p \\ 0 & t_p \langle t \le T_P \end{cases}, \qquad \textbf{Equation 6-1}$$

where K_p is the impact factor defined by the ratio of peak dynamic load per unit area F_{max} and static weight of occupant weight per unit area G, t_p is the contact duration, and T_p is the duration of the human activity.

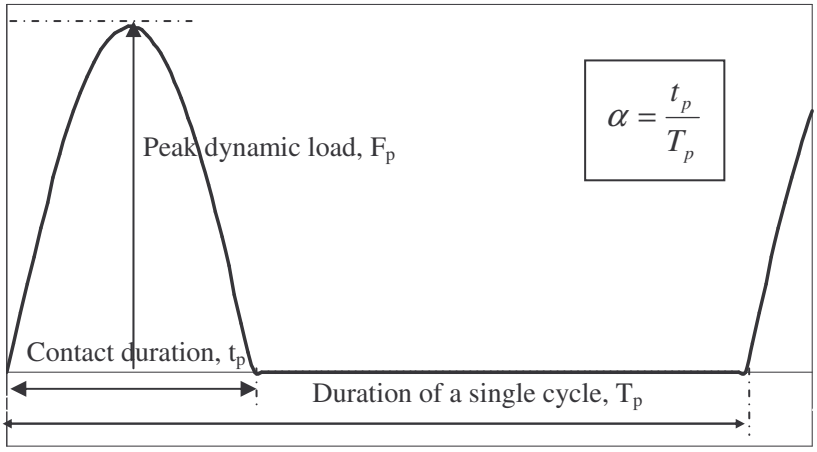

Figure 6-1: Graphical representation of dance-type loads (Bachmann, Pretlove et al. 1995)

The dynamic impact factor K_p is calculated using Equation 6-2 presented by Ellis et al. (Ellis and Ji 1994):

$$K_p = \frac{\pi}{2\alpha}. \qquad \textbf{Equation 6-2}$$

The contact duration t_p of dance-type activity plays a major role in defining the mathematical formulation and hence on the floor's response. Generally, contact duration (contact ratio) is represented by a proportion of the period of the activity (i.e. $\alpha = t_P/T_P$). In a way, the contact ratio provides information on how energetic is the human activity. For example, higher contact ratio leads to a conclusion that the feet in-contact with ground for a longer period and implies that the activity is less energetic. In order to understand the effect of various contact ratios, four different

contact ratios were used for the current analysis i.e. 0.25, 0.33, 0.50 and 0.67. These contact ratios describe different activities of high jumping, normal jumping, rhythmic exercise such as high impact aerobics and low impact aerobics respectively (Ji and Ellis 1994).

The activity frequencies (f_p or $1/T_p$) associated with dance-type activities were reported to vary from 1.5 Hz to 3.5 Hz, depending upon the posture of the activity (Eriksson 1996). For example, dance-type activities which include jumping in a rock or hip-hop music concert can have activity frequencies of up to 3.5 Hz. The current study explored the responses of all these activity frequencies.

6.4 Damping for FE model

The damping for the FE models was incorporated by using the explicit damping matrix presented by Reyleigh (Clough and Penzien 1993). This involved calculation of mass and stiffness proportional damping coefficients using the natural frequencies and damping levels of the structure. Four damping levels were considered in this investigation i.e. 1.6%, 3.0%, 6.0% and 12.0% and the corresponding mass and stiffness proportional damping coefficients were used in FE models. For more details refer Section 5.3.3 in Chapter 5. Table 6-1 presents the respective mass and stiffness proportional damping coefficients. The methodology for calculation of these values was presented in the Section 5.3.4 of Chapter 5. When calculating these mass and stiffness proportional coefficients, it was assumed that damping remains constant in its first and second mode.

Table 6-1: Mass and stiffness proportional damping coefficients for configuration 1

	Mass proportional damping	Stiffness proportional damping
Damping 1.6%	0.0736	0.00340843
Damping 3.0%	0.1380	0.00639080
Damping 6.0%	0.2760	0.01278159
Damping 12.0%	0.5521	0.02556319

6.5 Pattern loading cases for configuration 1

Four pattern loading cases were used to investigate the dynamic responses of the 2 x 2 panel floor system in configuration 1. They are further being referred to as pattern loading 1 (PL1-1), pattern loading 2 (PL2-1), pattern loading 3 (PL3-1) and pattern loading 4 (PL4-1). PL1-1 corresponds to a single panel excitation, while PL2-1, PL3-1 and PL4-1 describe excitation of two panels. The two panels excited were selected to represent the panels on the spaning, transverse and diagonal directions. The single panel excited can be either one of four panels, as the configuration is symmetrical. The mode shapes obtained from free vibration analysis were also considered in selecting the pattern loading cases. The following Figure 6-2 illustrates a graphical representation of the selected pattern loading cases.

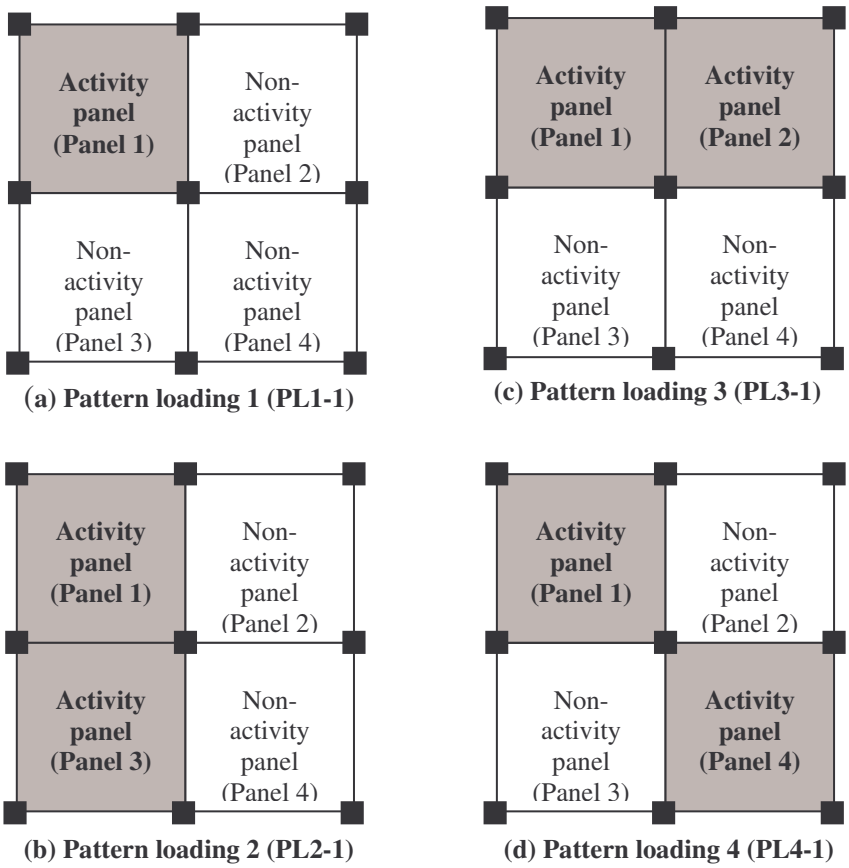

Figure 6-2: Patten loading cases for the 2 x 2 panel FE model in configuration 1

The PL1-1 corresponds to the human activity performed on panel 1 (the shaded area of Figure 6-2a), PL2-1 corresponds to the human activity performed on panels 1 and 3 (the shaded area of Figure 6-2b), the PL3-1 corresponds to the human activity

performed on panels 1 and 2 (the shaded area of Figure 6-2c) and PL4-1 corresponds to the human activity on panel 1 and panel 4 (the shaded area of Figure 6-2d). The "activity panels" (or shaded bays) in the above Figure 6-2 are the panels subjected to human-induced dance-type activities. Consequently, the "non-activity panels" referred in the above Figure 6-2 are assumed to be used for various occupancy fit-outs other than dance-type activities. These fit-outs are mainly governed by the acceleration response raised by the human events in the "activity panels.

6.6 DAF limits for serviceability (deflection limits)

The dynamic amplification factor (DAF) limits for serviceability imply the ratio of maximum dynamic to static deflection, allowable for serviceability limit state (SLS) design. These limits were used in the following sections to assess serviceability deflection arisen from various dance-type human actions. The DAF limits for the current floor configuration were predetermined by load-deflection characteristics obtained by static analysis. For each pattern load case un-factored loads were applied statically over the entire floor span and deflections at mid-span nodes of each panel were obtained. Herein, the live-load was considered as the static load posed by the occupants posting the activity. Two live-loads were considered in this investigation; i) human density of 1.75 m^2 per person (i.e. Q = 0.4 kPa); ii) human density of 3.5 m^2 per person (i.e. Q = 0.2 kPa); assuming average weight of person to be 70 kg (Allen 1990b). The dead load G for the current structure was assumed to be 3.5 kPa. These loads gave static deflections Δ_{Static} for each pattern loading case on each panel (refer to Figure 6-3). These deflections were then used to obtain the DAF limits by using the Equation 6-3.

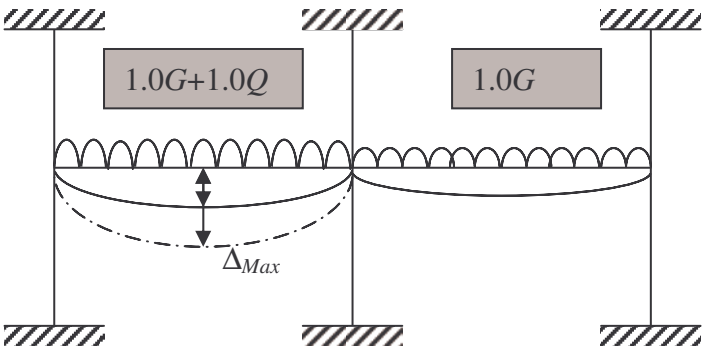

Figure 6-3: Un-factored loading pattern for the panel in configuration 1

$$DAF \cdot Limit = \frac{\Delta_{Max}}{\Delta_{Static}}$$ **Equation 6-3**

Serviceability deflection limit for static design Δ_{Max} has been reported to take as lesser of span/250 or 20 mm for composite floor design (British Standard : BS5950 : Part 4 1994; AS 3600 2001). The current structural model has a span of 8 m which suggested to use the Δ_{Max} as 20 mm to calculate the serviceability deflection limits.

To reduce the complexity of presenting the results, two DAF limits were calculated:

1. DAF limits for panels which cause the floor system to vibrate, termed "activity panels".
2. DAF limits for adjacent panel which is being vibrated by the "activity panel", termed "non-activity panels".

The static deflections Δ_{Static} used are the average deflections obtained in "activity panels" and "non-activity panels". The DAF limits were calculated for each pattern loading case and are presented in Table 6-2.

Table 6-2: DAF limits for activity panels and non-activity panels in configuration 1

		Activity panel(s)		Non-activity panel(s)	
		Static deflection	DAF Limit	Static deflection	DAF Limit
Pattern loading 1 (PL1-1)	Q = 0.4kPa	9.80	2.04	8.33	2.40
	Q = 0.2kPa	9.20	2.17	8.33	2.40
Pattern loading 2 (PL2-1)	Q = 0.4kPa	9.88	2.02	7.93	2.52
	Q = 0.2kPa	9.13	2.19	8.20	2.44
Pattern loading 3 (PL3-1)	Q = 0.4kPa	9.44	2.12	8.39	2.38
	Q = 0.2kPa	9.05	2.21	8.29	2.41
Pattern loading 4 (PL4-1)	Q = 0.4kPa	9.33	2.14	8.47	2.36
	Q = 0.2kPa	8.86	2.26	8.46	2.36

It was observed that DAF limits in "activity panels" were of lesser value those than of "non-activity panels" in all four pattern loading cases. This was because for the

"non-activity panels" to reach the maximum allowable SLS deflection it needed to deflect more.

6.7 Acceleration limits for occupancy

Floor systems normally fit-out different occupancies at before and after construction. For human conformability, these occupancy fit-outs need to comply with acceleration limits. These limits have been published by many researchers (Ellingwood and Tallin A. 1984). Many design guidelines such as International Standards Originations (1992), Canadian Standards (1995), American Institute of Steel Construction (1997), (1999) have also used to guide the design to resolve the floors acceptability against the vibrations caused by various human-induced activities. These limits were discussed in Section 2.3 of Chapter 2 and the work reported in this thesis used these acceleration limits to fit-out occupancies. Table 6-3 summarises these limits considering all the possible occupancies, dividing them into four categories termed: occupancy 1, occupancy 2, occupancy 3 and occupancy 4.

Table 6-3: Acceleration limits for various occupancies

Occupancy category	Acceleration limit, a_o (g)	Occupancy
Occupancy 1	0.05	Rhythmic activities / aerobics / dance-type loads
Occupancy 2	0.02	Shopping malls (centres) / weightlifting / stores / manufacturing / warehouse / walkaways / stairs
Occupancy 3	0.005	Office / residencies / hotels / multi - family apartments / school rooms / libraries
Occupancy 4	0.002	Hospitals / laboratories / critical working areas (e.g. operating theatres, precision laboratories)

These acceleration limits will be used in this and the following chapters to distinguish the occupancies suited under each pattern loading case.

6.8 Dynamic analysis – Pattern loading 1 (PL1-1)

This section presents the results of DAFs as well as acceleration responses in configuration 1, after computer simulations of dance-type activities under PL1-1.

PL1-1 corresponds to the simulated dance-type activities being performed on panel 1. In the PL1-1 configuration the panel 1 is the "activity panel" and panels 2, 3 and 4 are the "non-activity panels". The steady state dynamic defection at the mid location of each panel, which was the point that gave the maximum deflection was observed in determining the DAFs. These DAFs were then used to attain the DAFs for "activity panels", which are basically the DAFs of panel 1. The DAFs for "non-activity panels" were obtained by averaging the DAFs of panel 2, panel 3 and panel 4. The variations of DAFs with activity frequency were then plotted with respect to "activity panel" and "non activity panels". The DAF limits for PL1-1 has been distinguished in figures used in this Section by discontinues red line for "activity panel" and a discontinuous blue for "non-activity panels".

The acceleration responses are plotted using human perceptibility scales. In the case of PL1-1, the floor system was found to resonate in the second harmonic of the activity frequency and is discussed in Section 6.8.5. These harmonics were found to excite various mode shapes under PL1-1, from which the first mode and the third mode are more predominant. Thus acceleration responses underlying these mode frequencies were used to differentiate the floor fit-outs. The respective results are presented in a graphical format distinguishing the location of "activity panel" and "non-activity panels".

6.8.1 High impact jumping activity – PL1-1

The variation of DAF with activity frequency for high impact jumping activity of occupant density of 0.4 kPa under PL1-1 is presented in Figure 6-4.

DAF responses, in "activity panel" and "non-activity panels" gave the maximum peaks of 3.73 and 3.04 respectively, for an activity frequency of 2 Hz. The human activity of 2 Hz not only produced peaks in DAF response, but also exceeded the serviceability deflection limits. Secondary peaks were also observed near activity

frequency of 2.9 Hz, though they did not exceed the limits. The magnitudes of the peaks reduced with the increase of damping. The DAF responses observed were below the DAF limits for serviceability deflection in the cases of, "activity panel" with 12.0% or higher damping and "non-activity panels" with 3.0% or higher damping.

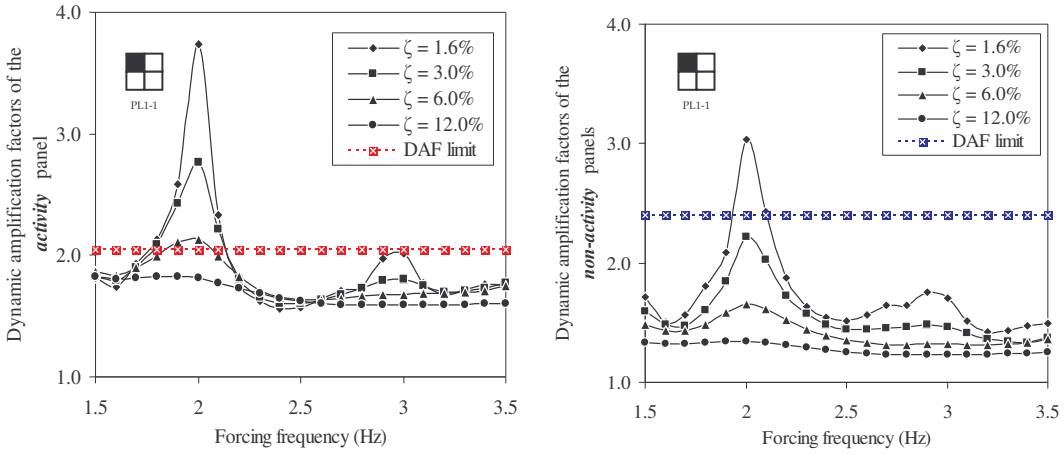

Figure 6-4: DAFs due to high impact jumping event in PL1-1 for Q=0.4 kPa

In most nominal cases 3.0% damping is realistic in "activity panels", although this damping level exceeded the serviceability deflection limit. Thus, a remedial solution was proposed to reduce the human-occupancy density performing the current activity. Prior to that, the acceleration response observed for the current density was plotted to identify the occupancy fit-outs.

The acceleration responses observed for the current case were plotted using the human perceptibility scales (refer to Figure 6-5). The peak accelerations were found to be occurring at similar frequencies to those resulting in maximum DAFs, i.e. at 2.0 Hz and 2.9 Hz and thus were used in these perceptibility scales.

It was observed that the responses under high impact jumping activity in the "activity panel" would not perform within the occupancy 1 acceleration limits. Also the "activity panel" had earlier shown to exceed the serviceability defection limits under high impact jumping event at damping of 6.0% or higher and therefore had to be restricted. The acceleration responses in the adjacent "non-activity panels" indicate that they can be fit-out to occupancy 2 with a provided damping level of 12 %.

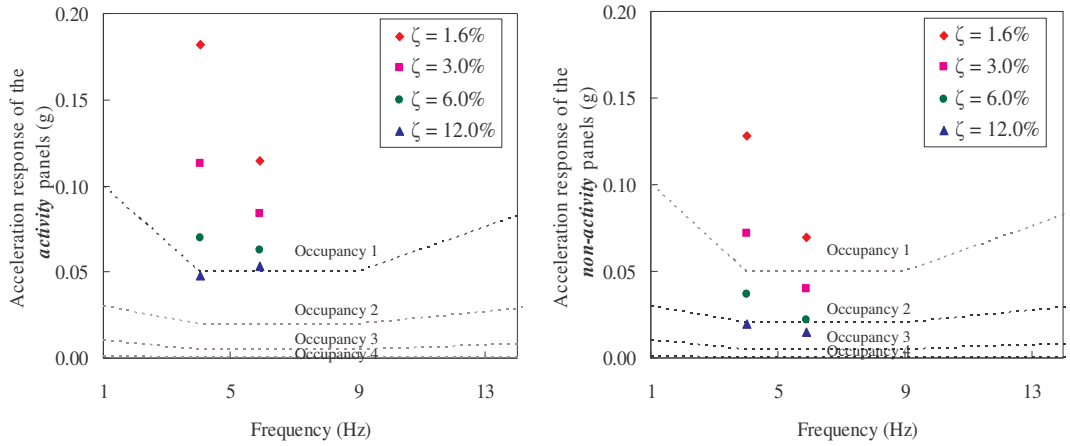

Figure 6-5: Acceleration response due to high impact jumping event in PL1-1 for Q=0.4 kPa

Under these circumstances, either high-jumping activity must be restricted or an alternative method must be used to strengthen the structure to perform better. This could include placement of passive damping devices to resist an excessive deflection that occurs from high impact jumping event. The use of passive damping devices and their role for the current case of high impact jumping under PL1-1 is described in Chapter 8. Another solution, as indicated earlier is to reduce the human density performing the activity.

The human density was reduced by half (i.e. Q = 0.2 kPa - single person occupying an area of 3.5 m^2) and analyses were performed again to obtain the DAFs and acceleration responses. The DAFs plots provided the trends shown in Figure 6-6 and the acceleration responses are presented in Figure 6-7.

The DAFs observed under the half density human activity load reduced with peaks of 2.46 and 2.02 in "activity panels" and "non-activity panels" respectively, both occurring at a activity frequency of 2 Hz. Similarly to a full human density load, a secondary peak was observed near 2.9 Hz, which is lesser in magnitude and well below the limits. The DAF responses observed were below the DAF limit for serviceability deflection in the cases of, "activity panel" with 3.0% or higher damping and "non-activity panels" with 1.6% or higher damping.

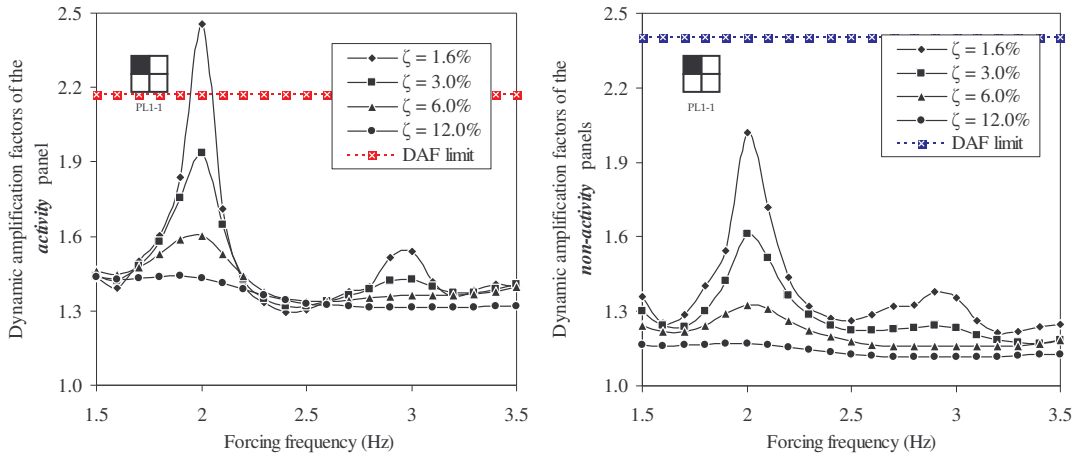

Figure 6-6: DAFs due to high impact jumping event in PL1-1 for Q=0.2 kPa

It was observed that the occupant density of 0.2 kPa posing the activity in "activity panels" improved the performance needing lesser damping levels. The acceleration response in this case gave similar trends with 0.4 kPa human densities, however in lesser magnitude with the peaks occurring at 2.0 Hz and 2.9 Hz. These acceleration responses are plotted in the perceptibility graphs in Figure 6-7.

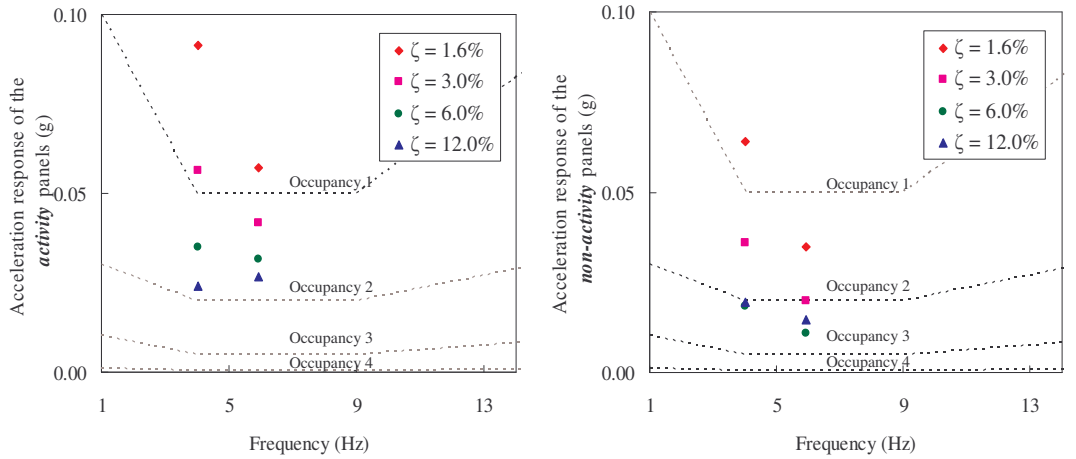

Figure 6-7: Acceleration response due to high impact jumping event in PL1-1 for Q=0.2 kPa

It was observed that the "activity panels" can now fit-out with occupancy 1, the current activity at damping of 6.0%. The "non-activity panels" on the other hand, can be used for occupancy 2 with 6.0%, or higher damping. However, other occupancies can not be fit-out as the yielded acceleration responses are much higher than the

limits. In conclusion, the recommended levels of human density in "activity panel", when high impact jumping is 0.2 kPa, along with necessary damping levels.

6.8.2 Normal jumping activity – PL1-1

The DAF responses observed for normal jumping with contact ratio of 0.33 for an occupant density of 0.4 kPa is presented in Figure 6-8.

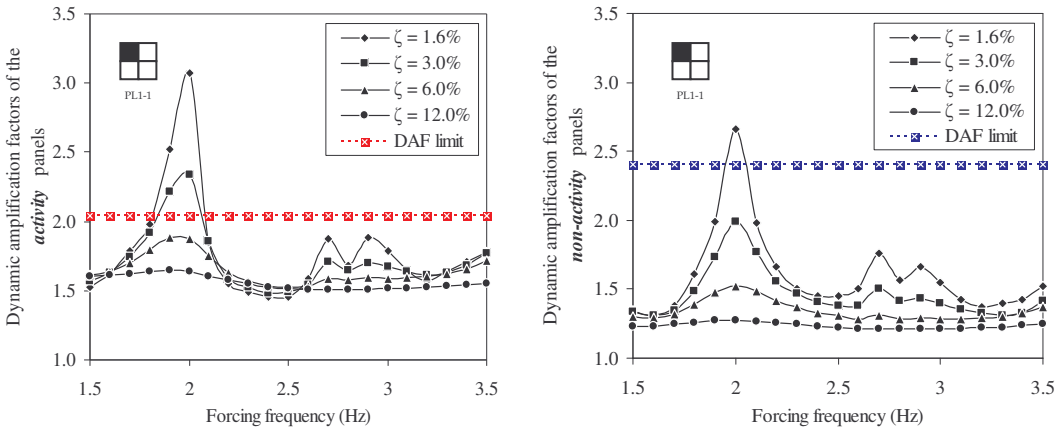

Figure 6-8: DAF due to normal jumping event in PL1-1 for Q=0.4 kPa

Under normal jumping activity, a maximum DAF of 3.07 was produced in the "activity panel", while DAF of 2.66 resulted in the "non-activity panels". Both these maximums occur at an activity frequency of 2.0 Hz and are lower than those of high-jumping activity in the previous case. This is because the events described by normal jumping provide lower impact forces resulting from footsteps that stay in contact with the floor for a higher period of time than there is high jumping event. At the same time, two additional peaks were also observed for normal-jumping activity at activity frequencies of 2.7 Hz and 2.9 Hz. These additional peaks were more predominant at lower damping levels of 1.6% and 3.0%. In contrast to the latter activity frequencies, the normal jumping activities performed at 2 Hz have exceeded the serviceability deflection limits. However, "activity panel" with 6.0% or higher damping and "non-activity panels" with 3.0% or higher damping were seen to be within the serviceability deflection limits. Thus, for the floor system to be within the serviceability deflection limits for the human density of a single person occupying an area of 1.75 m^2, it can be stated that the normal jumping event in an aerobics class

would be permissible only for 6.0% or higher damping levels for the "activity panel" and 3.0% for the "non-activity panels".

The acceleration response for the normal jumping activity was investigated for human-density of 0.4 kPa (1.75 m^2 / person). Figure 6-9 presents the maximum acceleration responses observed for the second harmonics of 2.0 Hz, 2.7 Hz and 2.9 Hz activity frequencies.

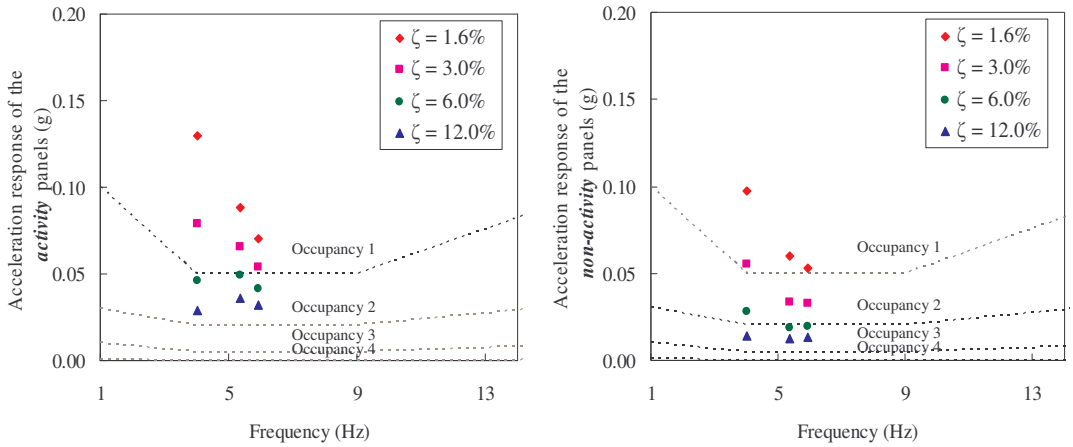

Figure 6-9: Acceleration response due to normal jumping event in PL1-1 for Q=0.4 kPa

With respect to the acceleration response in the "activity panel", as presented in Figure 6-9 it can be observed that vibration serviceability limits are not exceeded in a case where the event is performing at damping of 6.0% or higher. Lesser damping levels yield however was beyond limits of occupancy 1, which could provide discomfort to the occupants. The "non-activity panels", on the other hand, were seen as capable of fitting into occupancy 2 for damping levels more than 12.0%. Lower damping levels though were not seen to fit into occupancy 2. Neither occupancy 3 nor occupancy 4 in the adjacent panels were permissible as their thresholds were much lower.

In summary, the normal jumping activity under PL1-1 in the "activity panel" with a damping level of 6.0% or higher was observed to be within both serviceability limits of deflection and acceleration. In the case of "non-activity panel(s)", occupancy 2 with 12.0% or higher damping was within the acceleration limits. Reduced human

density of 0.2 kPa was also tested and the following Figure 6-10 represents the variation of DAFs with respect to activity frequency.

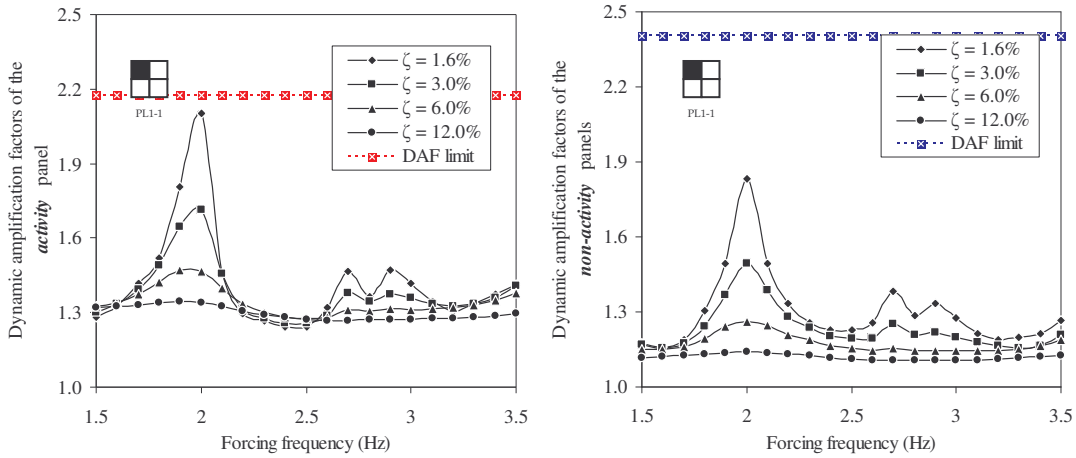

Figure 6-10: DAF due to normal jumping event in PL1-1 for Q=0.2kPa

With maximum DAFs of 2.10 and 1.83 in "activity panels" and "non-activity panels" respectively, both occurring at an activity frequency of 2 Hz occupant density of 0.2 kPa had not exceeded the DAFs limits. Consequently, normal jumping activity by an occupant density of 0.2 kPa would not cause any serviceability deflection problems at any of the damping levels. However, the acceleration responses were observed in order to fit-out the suitable occupancies. The maximum accelerations were seen at activity frequency of 2.0 Hz and 2.9 Hz, as plotted in the perceptibility graphs in Figure 6-11.

With the human-density of 0.2 kPa, the "activity panels" can be operated at 3.0% or higher damping, where 0.4 kPa human density needed 6.0% or higher damping. The "non-activity panels" can be fit-out to occupancy 2 with 6.0% or higher damping, where 12.0% or higher damping was needed with a human density of 0.4 kPa in "activity panels". However, neither occupancy 3 nor occupancy 4 can be fit-out under these circumstances.

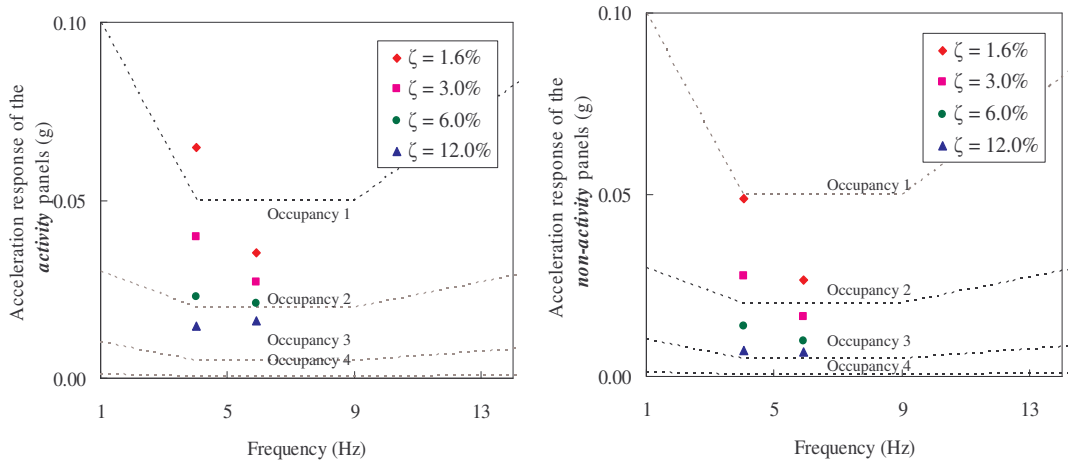

Figure 6-11: Acceleration response due to normal jumping event in PL1-1 for Q=0.2 kPa

6.8.3 Rhythmic exercise / high impact aerobics – PL1-1

The DAF response observed for the rhythmic exercise / high impact aerobics with a contact ratio of 0.5 for occupant density of 0.4 kPa is presented in Figure 6-12.

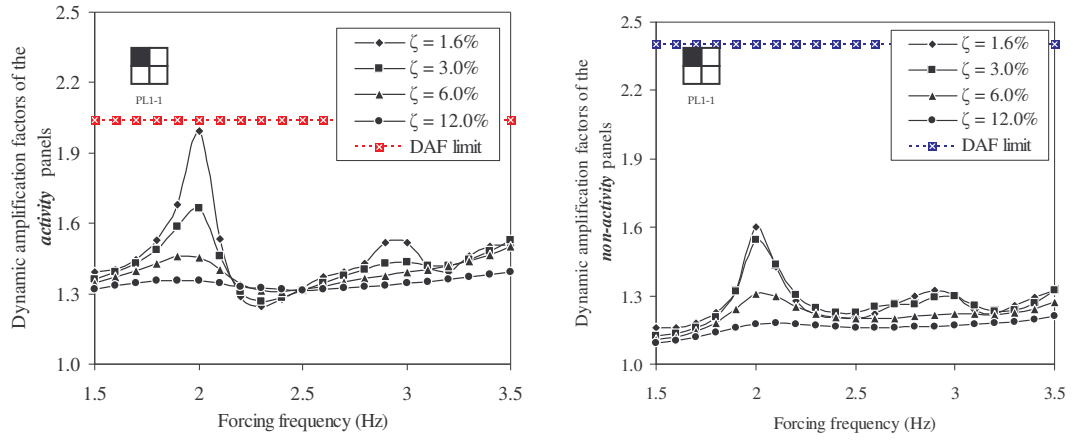

Figure 6-12: DAF due to rhythmic exercise, high impact aerobics event in PL1-1 for Q=0.4 kPa

Rhythmic exercise / high impact aerobics in PL1-1 yielded maximum DAFs of 1.99 in "activity panel" and 1.60 in "non-activity panel(s)", both occurring at a activity frequency of 2 Hz. These DAFs in both "activity panel" and "non-activity panels" did not exceed the serviceability deflection limits. Also, the DAFs obtained were much lower than those from previously described cases. Additional to peak occurring at 2 Hz, another peak in DAFs response was observed near 2.9 Hz. This secondary peak did not cause any concerns as it was much lower than the peaks occurring at 2

Hz. Thus, it can be stated that dance-type event described by rhythmic exercise, high impact aerobics of the human density of 0.4 kPa did not cause problems in the serviceability deflection limits. However, this activity may create discomfort to the occupants in floor fit-outs, is described in the next paragraph.

The maximum acceleration responses for rhythmic exercise / high impact aerobics under PL1-1 were seen at activity frequency of 2.0 Hz and 2.9 Hz. These acceleration responses were plotted in the perceptibility scales as presented in Figure 6-13 to verify the floor fit-outs.

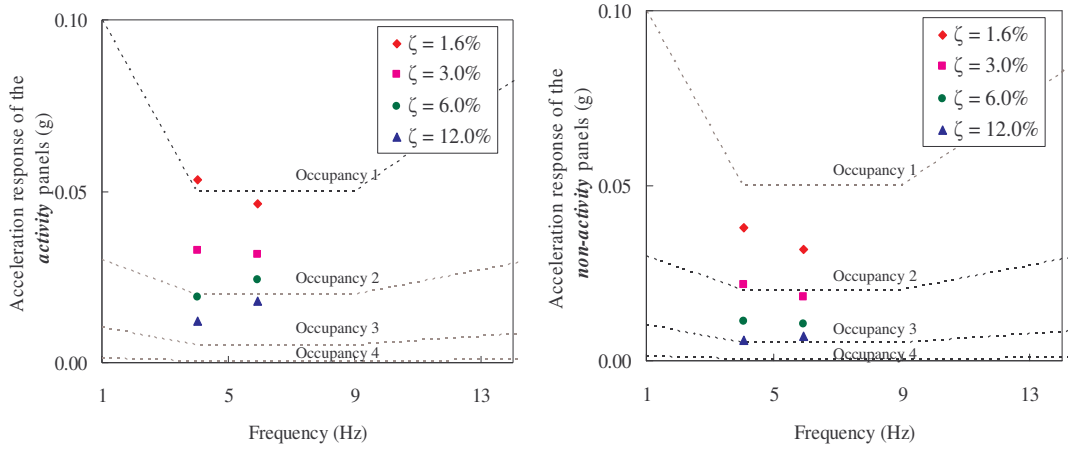

Figure 6-13: Acceleration response due to rhythmic exercise / high impact aerobics in PL1-1 for Q=0.4 kPa

Acceleration response observed at 2 Hz at 1.6% damping level caused to restrict occupancy 1 in "activity panel". This provides the evidence that the "activity panel" is serviceable at all other higher damping levels as well as all other activity frequencies. The "non-activity panels" can fit-out to occupy the occupancy 2 at 3.0% or higher damping. However, it was observed that in the event of rhythmic exercise / high impact aerobics activity the adjacent floor panels will not meet the limits of acceleration for both two occupancies, occupancy 3 and occupancy 4.

6.8.4 Low impact aerobics – PL1-1

Low impact aerobics with contact ratio of 0.67 for human density of 0.4 kPa, gave the DAFs trends presented in Figure 6-14 .

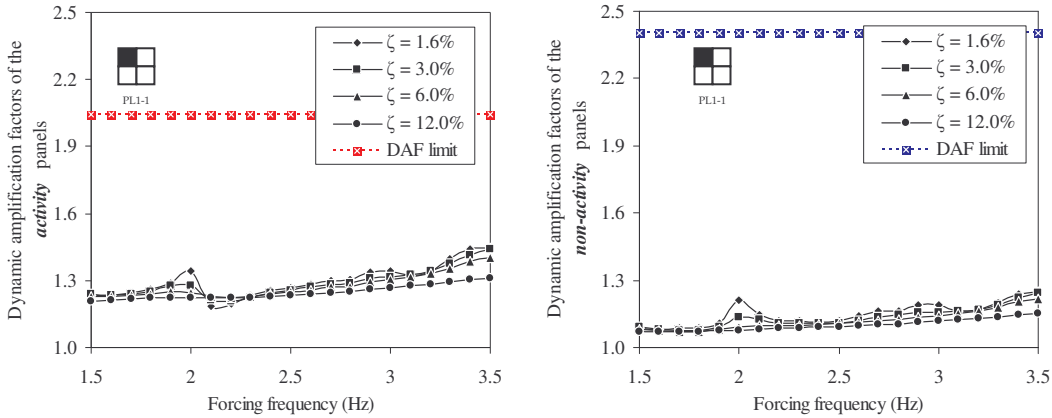

Figure 6-14: DAF due to low impact aerobics event in PL1-1 for Q=0.4 kPa

Similar to the previous activity of rhythmic exercise / high impact aerobics, the DAFs obtained for this event did not exceed the serviceability deflection limits at any of the investigated damping levels. Furthermore, it can be seen in Figure 6-14 that DAF responses between the different damping levels yielded coinciding trends, except for minor deviations at activity frequency of 2 Hz and those above 2.5 Hz. The maximum DAF of 1.45 in the "activity panel" and 1.35 in the "non-activity panels" was found in the maximum activity frequency used in the analysis. However, peaks in DAF responses were seen at activity frequency of 2.0 Hz and 2.9 Hz, which were lower than the maximum DAFs observed in the previous cases.

The acceleration response observed at activity frequency of 2 Hz and 2.9 Hz for the low impact aerobics activity is presented in Figure 6-15.

The acceleration responses observed in the "activity panel" were well within the serviceability acceleration limits of occupancy 1 at all damping levels, and thus no discomfort is predicted for the occupants. In the case of "non-activity panels", occupancy 2 would be easily fit-out all damping levels. Furthermore, it is quite appropriate to state that the adjacent panels can be used in the occupancy described by the occupancy 3 for of 6.0% or higher damping. However, occupancy 4 cannot be accommodated under the circumstances described in this section.

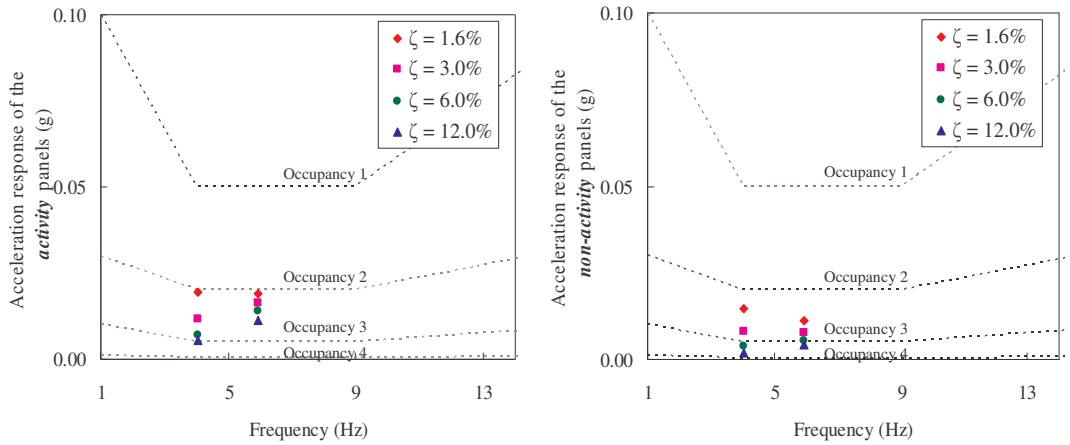

Figure 6-15: Acceleration response due to low impact aerobics in PL1-1 for Q=0.4 kPa

6.8.5 Results summary and discussion in PL1-1

The results under PL1-1, presented in the previous sections with respect to serviceability deflection and human comfortably criteria gave mixed responses. The results varied with respect to the dance-type event, human occupant density in the activity panel and the damping considered for the floor system. More onerous activities occurred under low damping conditions giving serviceability problems.

In a summation of DAFs for the PL1-1, it was found that the most onerous activities of high impact and normal jumping dance-type activity under low damping conditions resulted in unfavourable serviceability deflections causing the structure to give unfavourable responses. This can be mitigated by employing a reduced human density in the "activity panels", accompanied by appropriate damping levels. However, it needs to be stressed that such responses can only occur during continuous excitation event which is practically vary, since cases of high impact jumping dance-type of activity normally occur only in a short period of time. The most interesting responses observed under this pattering loading case were the sudden jumps, which occurred regardless of the type of event. Two peaks were more prominent, with one occurring at 2 Hz and the other occurring near 2.9 Hz. Furthermore, these jumps were highly distinguishable at lower damping conditions in contrast to the higher damping conditions.

Using the DAF responses obtained under PL1-1 testing, a summary of favourable operating conditions of the floor system was obtained and is presented in Table 6-4.

This tabulation distinguishes the permissible combinations that comply with the serviceability deflection criteria for damping, human density and type of activity for PL1-1.

Table 6-4: Operating conditions for serviceability deflection in PL1-1

Dance-type activity in AP	Human density in AP	AP	NAP
High impact jumping	0.4 kPa	$\zeta >$ 12.0%	$\zeta > 3.0\%$
	0.2 kPa	$\zeta > 3.0\%$	$\zeta > 1.6\%$
Normal jumping	0.4 kPa	$\zeta > 6.0\%$	$\zeta > 3.0\%$
	0.2 kPa	$\zeta > 1.6\%$	$\zeta > 1.6\%$
Rhythmic exercise / high impact aerobics	0.4 kPa	$\zeta > 1.6\%$	$\zeta > 1.6\%$
Low impact jumping	0.4 kPa	$\zeta > 1.6\%$	$\zeta > 1.6\%$

The human-induced activities along with the human-densities and damping levels that complied the human perceptibility under PL1-1 are summarised in the Table 6-5.

One fact that identified in DAFs and acceleration responses under PL1-1 was that their peaks in responses occurred at 2 Hz and near 2.9 Hz (Figure 6-10). In addition, peaks of response near activity frequency of 2.7 Hz at normal jumping of contact ratio of 0.5 were also noticed. These peaks in response had mainly led to unfavourable responses, which made the floor system unusable for the intended purpose. The reasons that initiated such responses were examined using Fourier spectrum analysis for respective acceleration response data.

The Fourier amplitude spectrum obtained for the acceleration response at 2 Hz, yielded two peaks, one at 4 Hz, and the other at / near 6 Hz as presented in Figure 6-16. Comparison of these two peaks with the natural frequencies highlights that due to current pattern loading PL1-1, two vibration modes have been excited. The first mode to excite is the primary mode which is commonly known as the fundamental mode and the second mode to excite is the third modes, all of which is bending modes and are further discussed in Section 4.7.4. Therefore, the PL1-1 battering had

excited both these mode shapes, causing jumps in the DAFs and acceleration responses and hence limiting its use for the intended occupancies.

Table 6-5: Occupancy fit-out for human comfortability in PL1-1

Dance-type activity in AP	Human density in AP	AP	NAP
High Impact Jumping	0.4 kPa	Occupancy 0	Occupancy 2 $\zeta > 12.0\%$
	0.2 kPa	Occupancy 1 $\zeta > 6.0\%$	Occupancy 2 $\zeta > 6.0\%$
Normal Jumping	0.4 kPa	Occupancy 1 $\zeta > 6.0\%$	Occupancy 2 $\zeta > 12.0\%$
	0.2 kPa	Occupancy 1 $\zeta > 3.0\%$	Occupancy 2 $\zeta > 6.0\%$
Rhythmic exercise / high impact aerobics	0.4 kPa	Occupancy 1 $\zeta > 3.0\%$	Occupancy 2 $\zeta > 3.0\%$ Occupancy 3 $\zeta > 12.0\%$
Low impact jumping	0.4 kPa	Occupancy 1 $\zeta > 1.6\%$	Occupancy 2 $\zeta > 1.6\%$ Occupancy 3 $\zeta > 6.0\%$

Occupancy 0	Uncomfortable
Occupancy 1	Rhythmic activities / aerobics / dance- type loads
Occupancy 2	Shopping malls (centres) / weightlifting / stores / manufacturing / warehouse / walkaways / stairs
Occupancy 3	Office / residencies / hotels / multi - family apartments / school rooms / libraries
Occupancy 4	Hospitals / laboratories / critical working areas (eg. operating theatres, precision laboratories)

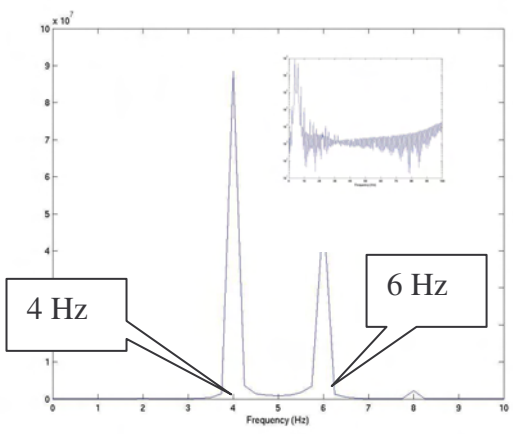

Figure 6-16: Fourier Amplitude spectrum for acceleration response at 2 Hz at 1.6% damping for contact ratio of 0.25

The Fourier amplitude spectrum analysis for the acceleration response at 2.9 Hz at 1.6% damping resulted in the curve depicted in Figure 6-17. It can be seen that the floor system gave resonant response near 6.0 Hz, illustrating the excitation of the third mode shape. Consequently, it can be stated that the due to the dance-type activity of 2.9 Hz the third mode of the floor system was excited to give vibration problems under PL1-1.

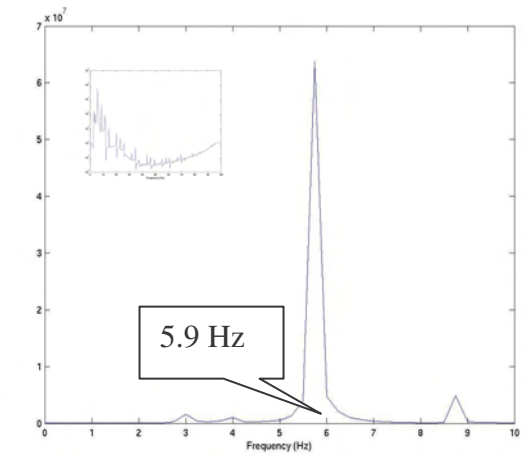

Figure 6-17: Fourier amplitude spectrum for acceleration response at 2.9 Hz at 1.6% damping for contact ratio of 0.25

In summary, the floor system under PL1-1 pattern loading was deemed unsuitable for its intended used for some human dance-type activities. This was due to its increased deflections under dynamic loading as well as acceleration response causing vibration problems. The cause being the excitation of various mode shapes: where the excitation of first and third modes were found behind this cause. The former mode of excitation was found to be dominant. The possible occupancies for this type of loading were also illustrated in this section.

6.9 Dynamic analysis – Pattern loading 2 (PL2-1)

This section presents the DAFs as well as acceleration reposes of multiple panel configuration 1 after computer simulations of dance-type activities under pattern loading 2 noted as PL2-1, defined in Section 6.6.

PL2-1 constituted of two panels subjected to dance-type activity. These two panels are Panel 1 and Panel 3 (refer to Figure 6-2) which were termed the “activity panels” and Panel 2 and Panel 4, termed the “non-activity panels”. Dynamic analyses were

carried out on this constitution with different damping levels identified in Section 6.4 and human densities posing the activity. Using the dynamic analysis it was found that the percentage variation of displacement / acceleration responses between activity panels, Panel 1 and Panel 3 was ±10% and between the "non-activity panels", Panel 2 and Panel 4 < ±1%, in most cases. Thus, this gave the flexibility to use averaged responses of each set of panels (i.e. Panel 1 and Panel 3 – "activity panels"; Panel 2 and Panel 4 – "non-activity panels"), which also reduced the complexity of presented results. Using this data, the DAF responses against the activity frequencies were plotted and their features and significances under each dance-type activity were discussed.

The acceleration responses under PL2-1 were obtained in order to distinguish the occupancies. The acceleration limits presented in the Section 6.7 were used for to distinguish the occupancies. The results for each event are presented under two scenarios: the "activity panels" and the "non-activity panels".

6.9.1 High-impact jumping activity – PL2-1

The DAFs for the high impact jumping under PL2-1 for activity density Q of 0.4 kPa gave the trends with respect to the activity frequency as seen in Figure 6-18.

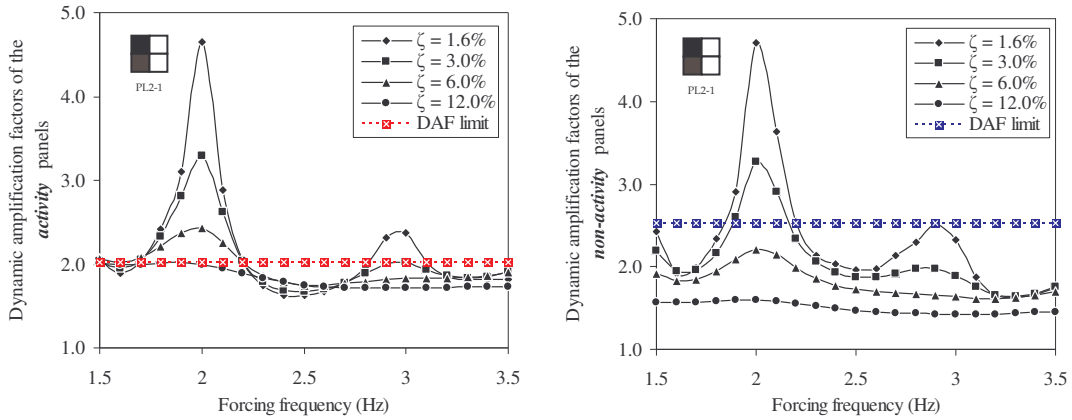

Figure 6-18: DAF due to high impact jumping event in PL2-1 for Q=0.4 kPa

The trends gave higher DAFs than to serviceability deflection limits at lower damping levels, in-fact the DAFs were the highest of all the pattern loading cases investigated in this Chapter. One reason for this may be the onerous trends of this

activity, which caused to pound the floor with a higher dynamic force. Another reason may be the dance-activity being performed in panels which reflected excitation of the fundamental mode shape. This activity gave the maximum DAFs of 4.66 and 4.70 for "activity panels" and "non-activity panels" respectively occurring at a activity frequency of 2 Hz. Additionally, another peak in DAF response was observed near 2.9 Hz, but its DAF was less than that observed at 2.0 Hz.

In summary, high impact jumping in PL2-1 was seen to be within the serviceability deflection limit for:

- 12.0% or higher damping in "activity panels", and
- 6.0% or higher damping in "non-activity panels".

It should be noted that 12.0% or higher damping in "activity-panels" may be too high and thus passive methodology or reduction of occupant density are proposed. However, the acceleration responses were observed regardless of the defection response and are presented in the perceptibility scales in Figure 6-19. As observed in the DAFs response, peaks of acceleration responses were observed at activity frequency of 2.0 Hz and 2.9 Hz. These frequencies excited the first mode at 4.0 Hz and third mode at 5.9 Hz by the second harmonic and thus are used in perceptibility plots.

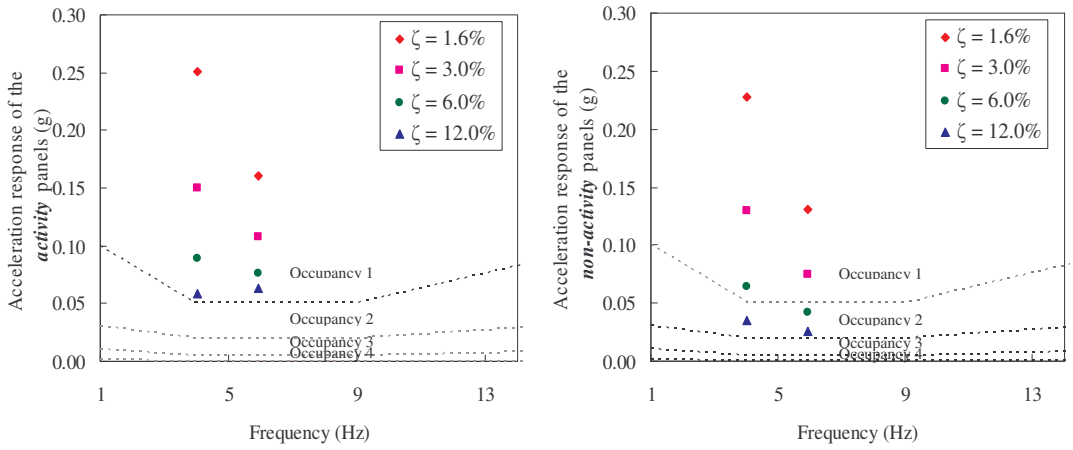

Figure 6-19: Acceleration response due to high impact jumping event in PL2-1 for Q=0.4 kPa

The peak acceleration responses in the "activity panels" were above the acceleration limits probing occupant's comfortableness. Thus, high impact jumping in PL2-1 will cause discomfort to occupants posing the activity. The "non-activity panels", on the other hand, can be fit-out to occupancy 2 in floors with 12.0% or more damping. Since the "activity panels" did not comply with the perceptibility criteria at all damping levels, it's advisable to take remedial measures to enhance the structures performance. The remedy in this case can either be a reduction in the load-density or a use of passive damping mechanism. The use of passive damping mechanism will be discussed in Chapter 8, by employing a VE damping device to the structural system. The former which is to use lower human density performing this event is addressed by simulating the activity in a reduced density. The selected density for this case was half of the original density, i.e. 3.5 m^2/person (0.2 kPa). The dynamic analysis was carried out again and the DAFs responses observed are presented in Figure 6-20.

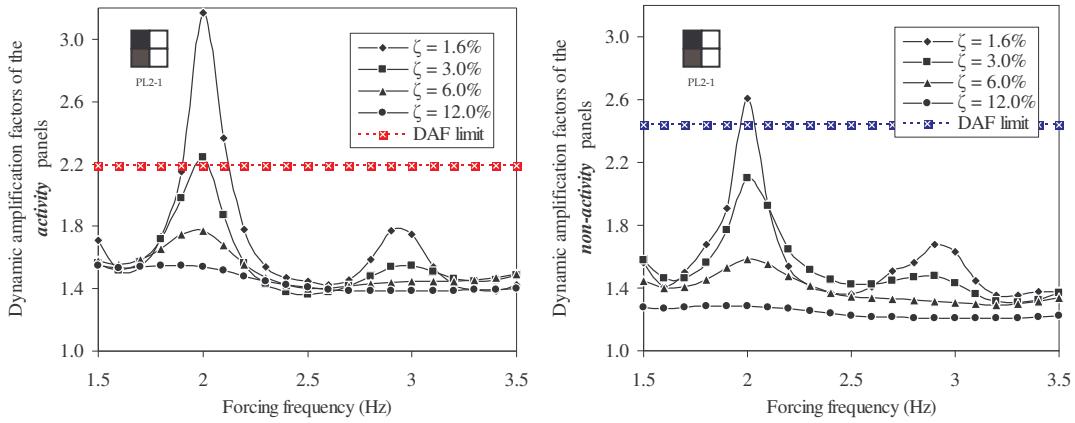

Figure 6-20: DAF due to high impact jumping event in PL2-1 for Q=0.2 kPa

The DAFs observed for this case gave peaks of 3.17 and 2.61 in "activity panels" and "non-activity panels" respectively, both occurring at an activity frequency of 2 Hz. The suitable operating damping levels identified were:

- activity panels with 6.0% or higher damping, and
- non-activity panels with 3.0% or higher damping.

This was an improvement compared with the previous damping levels. The acceleration responses for this case were also investigated. The following Figure 6-21 presents their occurrences in perceptibility scales.

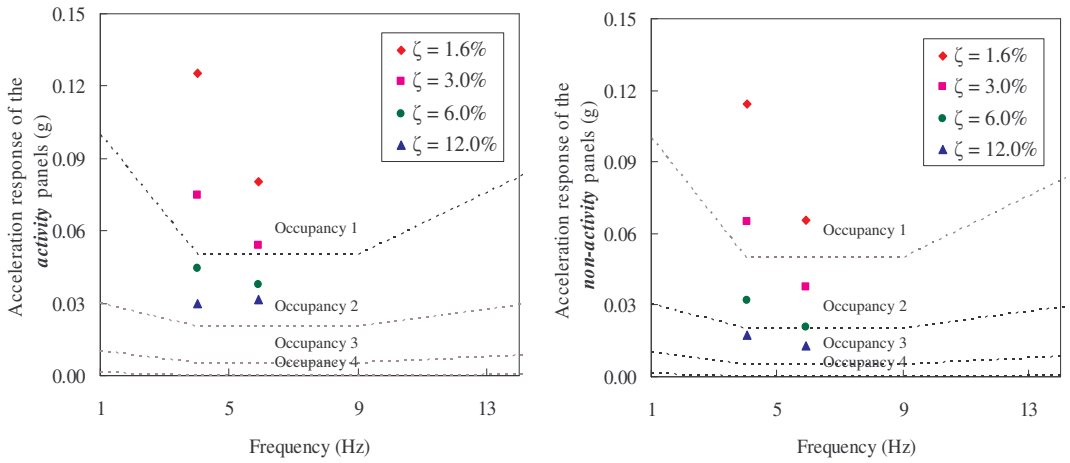

Figure 6-21: Acceleration response due to high impact jumping event in PL2-1 for Q=0.4 kPa

The acceleration responses in "activity panels" have fallen within the human perceptibility limits with 6.0% or higher damping. On the other hand the "non-activity panels" can be used for occupancy 2 with 12.0% or higher damping.

6.9.2 Normal jumping activity – PL2-1

The DAFs for normal jumping event by human density of 0.4 kPa under PL2-1 gave the trends depicted in Figure 6-22.

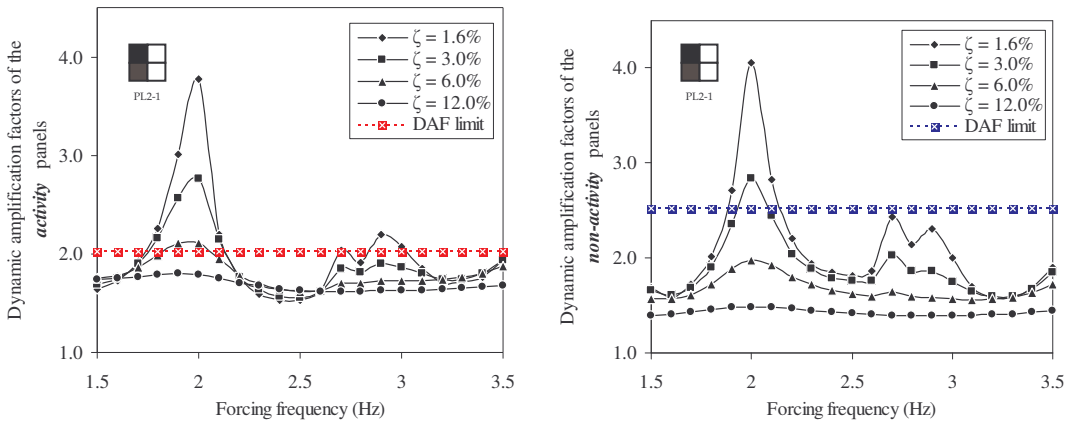

Figure 6-22: DAF due to normal jumping event in PL2-1 for Q=0.4 kPa

It can be seen that, at a damping level of 12.0% or higher in "activity panels" the DAFs for normal jumping activity have not exceeded the limits. In the case of "non-activity panels", it was observed to be within the deflection limits at 6.0% or higher damping levels. However, the magnitudes of the DAF responses were lower than those in the previous section. There were three peaks of DAF responses observed under normal-jumping activity i.e. at 2.0 Hz, 2.7 Hz and 2.9 Hz. These peaks were distinguishable at lower damping levels and were the main cause of exceeding the serviceability deflection limits.

The acceleration responses were seen to give the maximum responses in the above-described activity frequencies of 2.0 Hz, 2.7 Hz and 2.9 Hz. The following Figure 6-23 presents those acceleration responses in the perceptibility graphs.

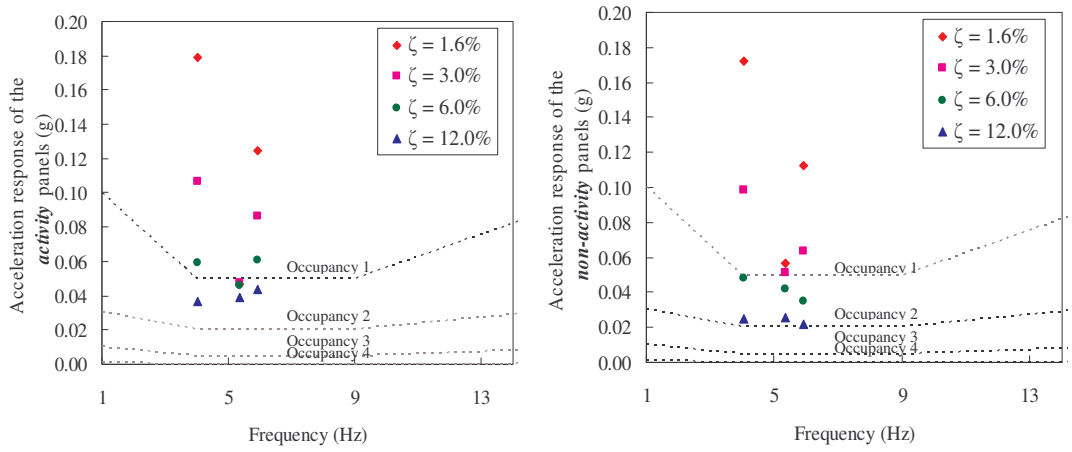

Figure 6-23: Acceleration response due to normal jumping event in PL2-1 for Q=0.4 kPa

Observed by the perceptibility scales, the "activity panels" subjected to normal jumping under PL2-1 was within the perceptibility limits when 12.0% or higher damping. The "non-activity panels" can be fit-out to occupancy 2 when 12.0% more damping. However, as occupants posing the activity can not gain damping levels of 12.0% in the "activity panels", alternative methods are needed to fit-out the occupancies. These methods may either employ a passive damping mechanism, described in the Chapter 8 or reduce the human-density performing the activity. After simulating the normal jumping activity at a reduced density of 0.2 kPa (3.5 m^2/person) the trends in DAFs were observed and depicted in Figure 6-24.

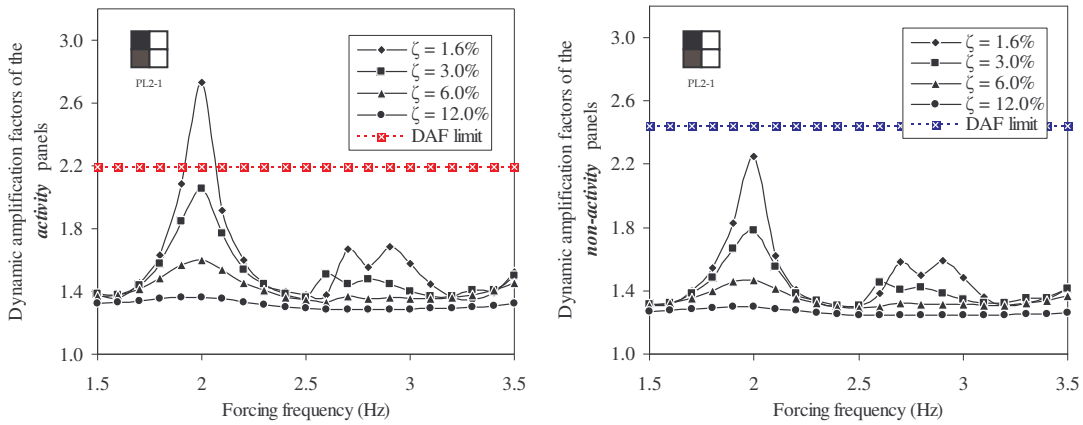

Figure 6-24: DAF due to normal jumping event in PL2-1 for Q=0.2 kPa

The density of 0.2 kPa gave lower DAFs, with maximum of 2.73 and 2.25 in "activity panels" and "non-activity panels" respectively, both occurring at an activity frequency of 2.0 Hz. Similarly to the cases with density 0.4 kPa, secondary peaks in DAFs were observed at activity frequencies of 2.7 Hz and 2.9 Hz. However, this density gave operating damping levels of 3.0% or higher in the "activity panels" and 1.6% or higher damping in the "non-activity panels". The acceleration responses gave similar trends to those of DAFs and peak values found at 2.0 Hz and 2.9 Hz. These were plotted in human perceptibly scales as presented in Figure 6-25.

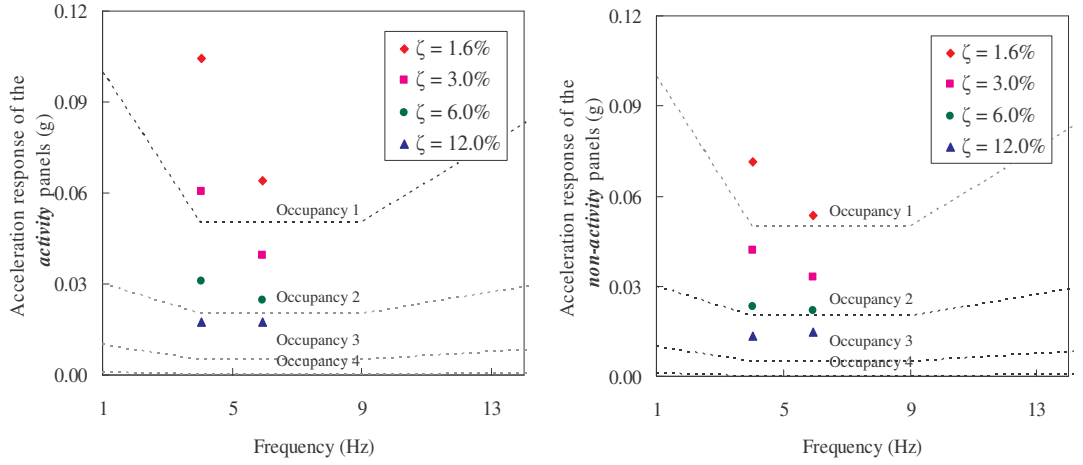

Figure 6-25: Acceleration response due to normal jumping event in PL2-1 for Q=0.2 kPa

To avoid human discomfort to occupants posing the activity in "activity panels" damping levels of 6.0% or higher was observed. The "non-activity panels", on the other hand needed 12.0% or higher damping to fit-out occupancy 2. In summary, the

normal jumping activity of occupant density of 0.2 kPa is recognised as the asking damping levels are achievable with non-structural elements, partitions etc.

6.9.3 Rhythmic exercise / high impact aerobics – PL2-1

The DAFs for the rhythmic exercise / high impact aerobics of human density 0.4 kPa under PL2-1 is presented in Figure 6-26.

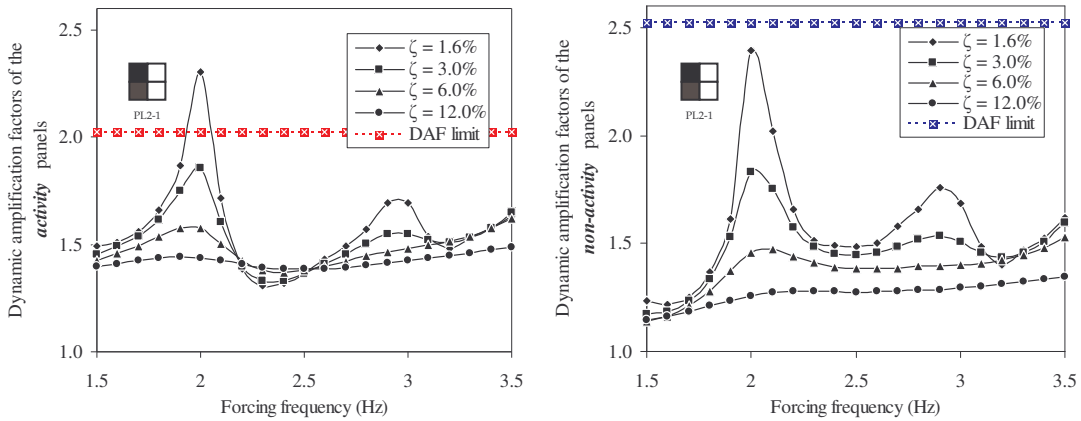

Figure 6-26: DAF due to rhythmic exercise / high impact aerobics event in PL2-1 for Q=0.4 kPa

Rhythmic exercises / high impact aerobics under PL2-1, yielded results with the DAFs within the limit at 6.0% or higher damping level in the "activity panels". In the case of "non-activity panels" it was found that the panels would perform within the serviceability deflection limits when 3.0% or higher damping. The magnitudes of the DAFs observed were much lower than in previous two cases, with maximum occurring at 2 Hz. In addition the usual secondary peaks were observed near the activity frequency of 2.9 Hz. The acceleration responses were found to give the maximum at these two frequencies. The respective values are plotted in the perceptibility scales as seen in Figure 6-27.

The perceptibility scales for the rhythmic exercise / high impact aerobics shows that occupancy 1 can be set out in the "activity panels" under PL2-1 with damping levels higher than 3.0%. In the case of "non-activity panels", it is suitable for occupancy 2 at 6.0% or higher damping.

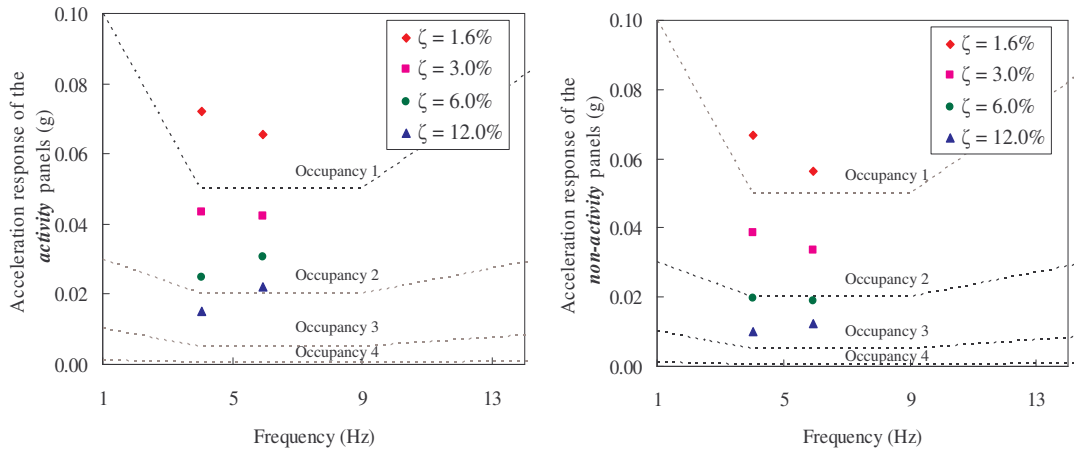

Figure 6-27: Acceleration response due to rhythmic exercise / high impact aerobics in PL2-1 for Q=0.4 kPa

6.9.4 Low impact aerobics – PL2-1

The DAFs for low impact aerobics of occupant density 0.4 kPa in "activity panels" are presented in Figure 6-28.

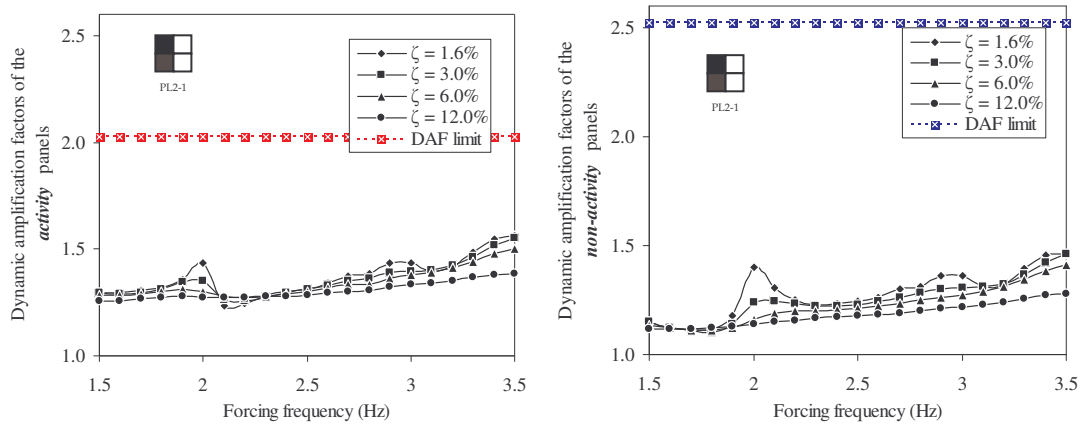

Figure 6-28: DAF due to low impact aerobics event in PL2-1 for Q=0.4 kPa

It was observed that the low impact aerobics in the "activity panel" did not cause DAFs to exceed the DAF-limits for any of the frequencies or damping levels in both "activity panels" and adjacent "non-activity panels". Though, the previously observed two peaks of responses at 2.0 Hz and near 2.9 Hz occurred at this event also. These peaks did not seem to give the maximum DAFs as in previous cases, the maximum was observed at the maximum activity frequency applied. However, the

acceleration responses were obtained at 2.0 Hz and 2.9 Hz and were plotted in the perceptibility scales in order to determine the fit-outs (refer to Figure 6-29).

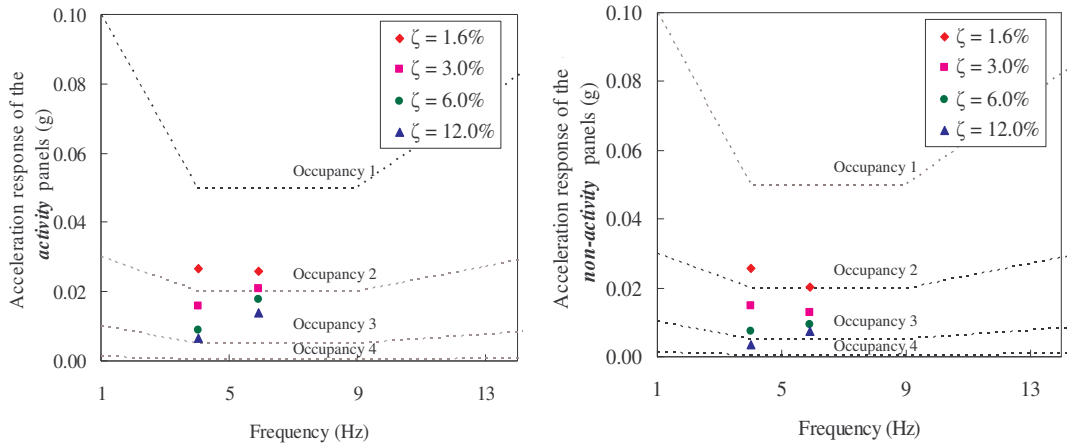

Figure 6-29: Acceleration response due to low impact aerobics in PL2-1 for Q=0.4 kPa

Since acceleration responses plotted in the perceptibility scales were well below the limits, occupancy 1 can be fit–out under PL2-1 even in floors with only 1.6% damping. The "non-activity panels", was determined suitable for occupancy 2 at 3.0% or higher damping levels.

6.9.5 Results summary and discussion in PL2-1

In summary, the PL2-1 caused much higher DAFs than those in PL1-1 cases. This may be due the fact that in PL2-1 simulated dance-type activities reflected the excitation of fundamental mode. In most cases, the responses occurred at 2.0 Hz and caused the floor system exceed the serviceability state limits. In addition the secondary peaks near 2.9 Hz sometimes gave similar response. Based on these observations, the Table 6-6 summarises the type of activity, activity density and necessary damping levels that would comply with the serviceability deflection criteria.

In the same way, Table 6-7 summarises the suitable occupancies that can be set-out along with occupant densities and activity types in "activity panels" and damping levels under PL2-1 that complied with the human comfortability levels.

Table 6-6: Operating conditions for serviceability deflection in PL2-1

Dance-type activity in AP	Human density in AP	AP	NAP
High impact jumping	0.4 kPa	$\zeta > 12.0\%$	$\zeta > 6.0\%$
	0.2 kPa	$\zeta > 6.0\%$	$\zeta > 1.6\%$
Normal jumping	0.4 kPa	$\zeta > 12.0\%$	$\zeta > 6.0\%$
	0.2 kPa	$\zeta > 3.0\%$	$\zeta > 1.6\%$
Rhythmic exercise / high impact aerobics	0.4 kPa	$\zeta > 3.0\%$	$\zeta > 1.6\%$
Low impact jumping	0.4 kPa	$\zeta > 1.6\%$	$\zeta > 1.6\%$

Table 6-7: Occupancy fit-out for human comfortability in PL2-1

Dance-type activity in AP	Human density in AP	AP	NAP
High impact jumping	0.4 kPa	Occupancy 0	Occupancy 0
	0.2 kPa	Occupancy 1 $\zeta > 6.0\%$	Occupancy 2 $\zeta > 12.0\%$
Normal jumping	0.4 kPa	Occupancy 1 $\zeta > 12.0\%$	Occupancy 2 $\zeta > 12.0\%$
	0.2 kPa	Occupancy 1 $\zeta > 6.0\%$	Occupancy 2 $\zeta > 12.0\%$
Rhythmic exercise / high impact aerobics	0.4 kPa	Occupancy 1 $\zeta > 3.0\%$	Occupancy 2 $\zeta > 6.0\%$
Low impact jumping	0.4 kPa	Occupancy 1 $\zeta > 1.6\%$	Occupancy 2 $\zeta > 3.0\%$

Occupancy 0	Uncomfortable
Occupancy 1	Rhythmic activities / aerobics / dance-type loads
Occupancy 2	Shopping malls (centres) / weightlifting / stores / manufacturing / warehouse / walkaways / stairs
Occupancy 3	Office / residencies / hotels / multi - family apartments / school rooms / libraries
Occupancy 4	Hospitals / laboratories / critical working areas (e.g. operating theatres, precision laboratories)

PL2-1, was prone to the most onerous response with respect to both deflection and acceleration criteria, restricting or needing higher damping levels to comply with both serviceability state limits. The main reasons for the unusability of the floor system as described above Tables 6-6 and 6-7 is due to sudden jumps that were found to be occurring at activity frequency of 2.0 Hz and near 2.9 Hz. These types of responses were also seen under PL1-1. However, the reason for the occurrence of this type of peaks is due to the excitation of the modes shapes of the floor system. The Fourier Amplitude Spectrum obtained for a typical acceleration response shown

in the following Figure 6-30 at 2.0 Hz and Figure 6-31 at 2.9 Hz described the excitation of the respective mode shapes.

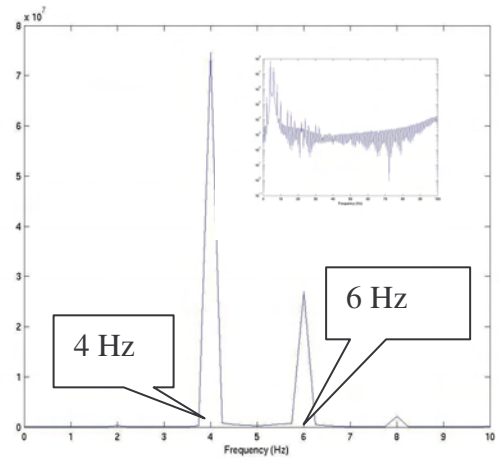

Figure 6-30: Fourier Amplitude Spectrum for acceleration response at 2.0 Hz at 1.6% damping for contact ratio of 0.25 in PL2-1

Figure 6-30 depicts the floor model excited at 4.0 Hz and 6.0 Hz due to an activity frequency of 2.0 Hz. These frequencies correspond to the first and third modes. Consequently, this analysis suggests that PL2-1 exited two mode shapes, which caused the floor system to vibrate exceeding the current serviceability criteria.

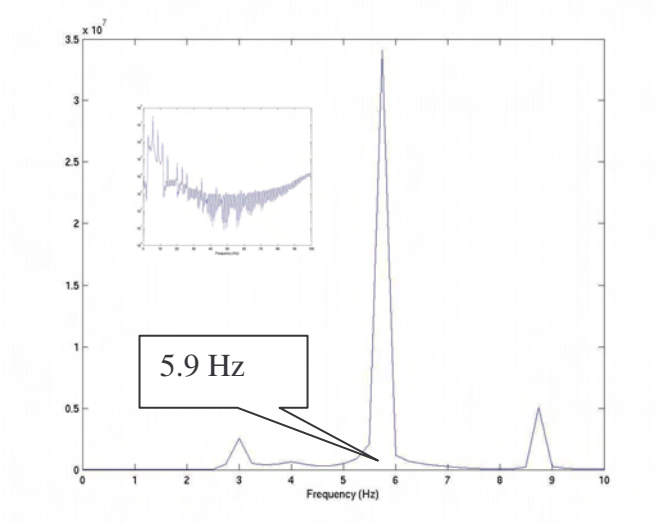

Figure 6-31: Fourier Amplitude Spectrum for acceleration response at 2.9 Hz at 1.6% damping for contact ratio of 0.25 in PL2-1

Similarly, the Fourier Amplitude Spectrum observed at 2.9 Hz suggested that the floor system was responding at 5.9 Hz. This frequency relates to the third mode shape frequency of the structure. In conclusion, PL2-1 caused the floor system to vibrate in its first and third mode shapes, restricting the use of some of the activities performed.

6.10 Dynamic analysis – Pattern loading 3 (PL3-1)

This section presents the results of DAFs and acceleration responses observed under pattern loading 3 noted as PL1-3. PL3-1 constituted of two panels subjected to dance-type activity. These two panels were panel 1 and panel 2 as seen in Figure 6-2 which were termed "activity panels" and as a result panel 3 and panel 4 became the "non-activity panels". The dynamic displacement and acceleration analysis found that the percentage variation between the "activity panels" was less than 10%. Similarly, this variation between the "non-activity panels" was less than 1%. Thus, to reduce the complexity the results were presented in averages for both "activity panel" and "non-activity panels".

Similarly, as in previous two cases of PL1-1 and PL2-1, PL3-1 used data of DAF responses to discuss its consequences in terms of serviceability deflection limit noted by red dotted line for "activity panels" and by blue dotted line for "non-activity panels". In like manner, the acceleration responses under PL3-1 were obtained in-order to distinguish the suitable occupancies. As in the earlier sections, the results are again presented in two scenarios, i.e. "activity panels" and "non-activity panels" under each case of event.

6.10.1 High-impact jumping – PL3-1

The DAFs for high impact jumping activity of 0.4 kPa in "activity panels" under PL3-1 are presented in Figure 6-32.

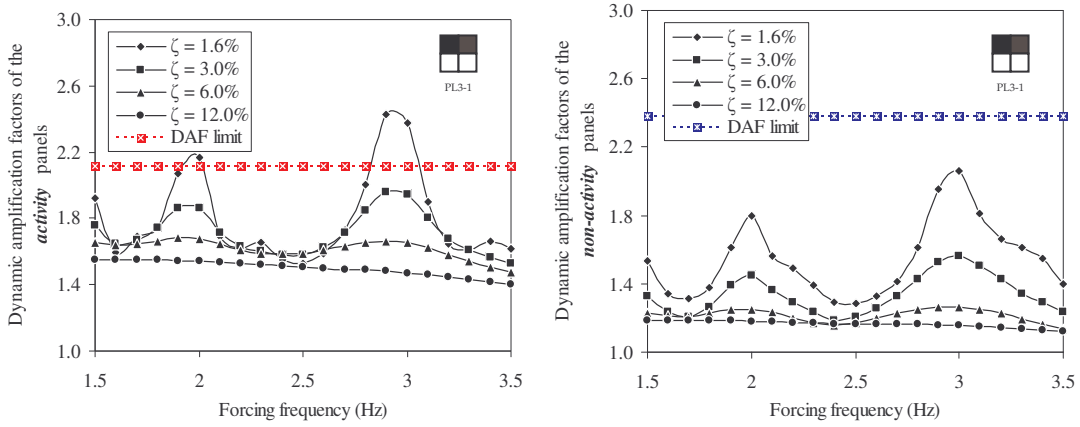

Figure 6-32: DAF due to high impact jumping event in PL3-1 for Q=0.4 kPa

The DAFs in "activity panels" observed under this scenario met the serviceability deflection limits at 3.0% or higher damping levels. With respect to "non-activity panels", DAFs were well below the deflection limits at all the investigated damping levels. The DAF trends found under PL3-1 were lower than those in PL2-1, although both pattern loadings used two loaded panels. However, in contrast to the primary peaks observed at 2.0 Hz in the previous two pattern loadings, PL3-1 produced primary peak near 2.9 Hz, although a secondary peak was observed at 2.0 Hz. Since the most important peak was observed at activity frequency of 2.9 Hz, it suggested the floors suitability with 3.0% or higher damping levels.

To determine the possible occupancy fit-out the human-perceptibility for this activity is investigated next. The acceleration responses which gave the peaks at 2.0 Hz and 2.9 Hz where thus used in the perceptibility charts.

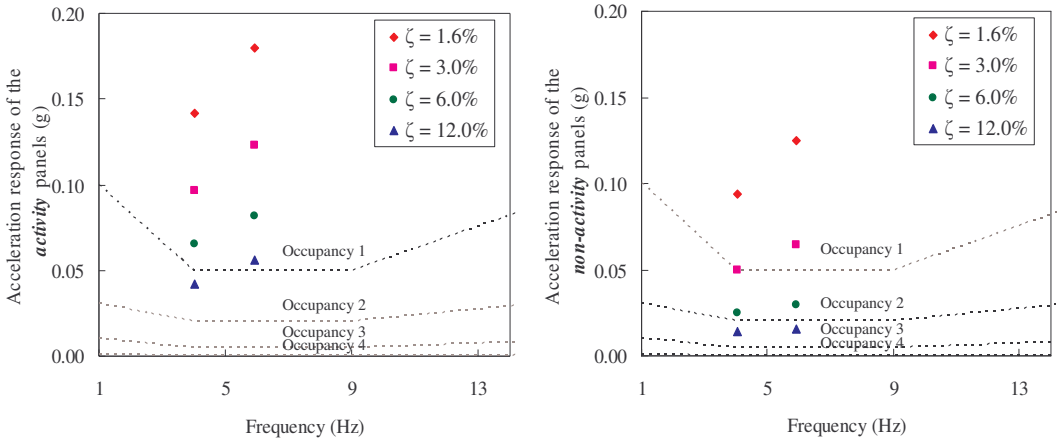

Figure 6-33: Acceleration response due to high impact jumping event in PL3-1 for Q=0.4 kPa

The acceleration response observed in the "activity panels" was only suited for occupancy 1 at 12.0% or higher damping, although it did pass the severability deflection limits at a lower damping level of 3.0%. The "non-activity panels", on the other hand, can be fit-out to occupancy 2 with 12.0% or higher damping and they passed the serviceability deflection limits at 1.6 % or higher damping.

A human density of 0.2 kPa posing the high jumping activity in "activity panels" was investigated next. Figure 6-34 presents the variation of DAF responses with respect to activity frequency.

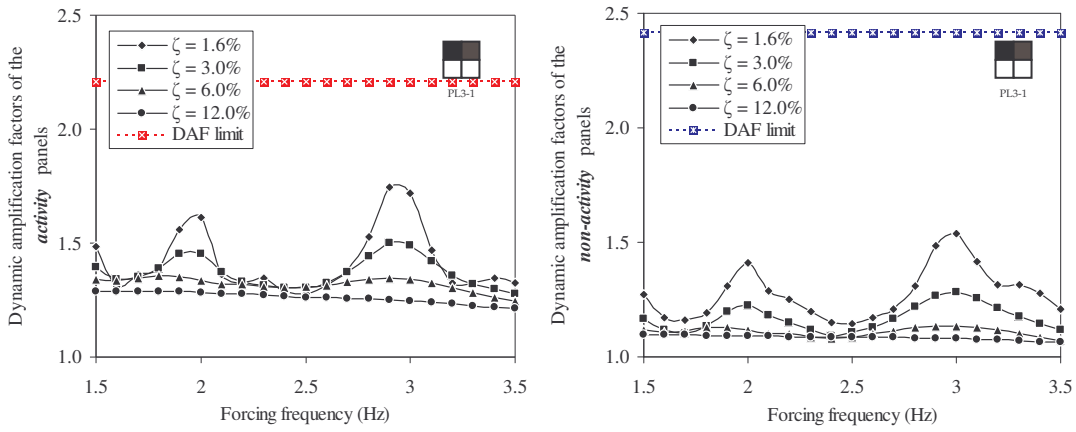

Figure 6-34: DAF due to high impact jumping event in PL3-1 for Q=0.2 kPa

The DAFs observed at occupant density of 0.2 kPa were well below the DAF limits at all damping levels. The maximum DAFs 1.74 and 1.54 were observed in "activity panels" and "non-activity panels" respectively, both occurring at activity frequency of 3.0 Hz. Similar to the previous case, a secondary peak of DAF response was observed at a step frequency of 2.0 Hz. The acceleration responses resulted in a behaviour similar to that of DAFs, with maximum occurring at 3.0 Hz and secondary maximum occurring at 2.0 Hz. These acceleration responses were recorded in human perceptibility scales and are presented in Figure 6-35.

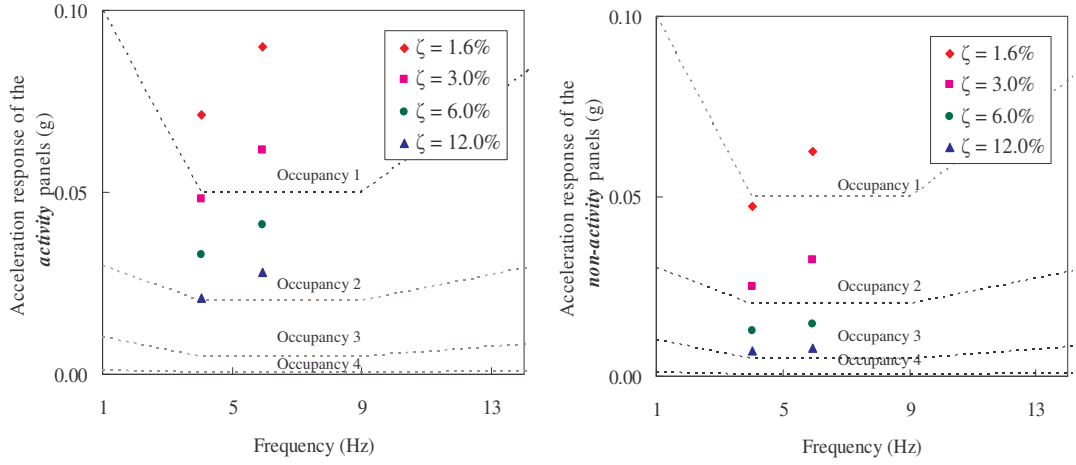

Figure 6-35: Acceleration response due to high impact jumping event in PL3-1 for Q=0.2 kPa

The reduced human density reduced the operating damping levels to 6 % or higher in the "activity panels". Under this density the "non-activity panels" can be fit-out to occupancy 2 with 6.0% or higher damping. This is an improvement since with

human density of 0.4 kPa, more than 12.0% damping was needed to comply with the serviceability acceleration criteria. Thus, human density of 0.2 kPa is recommended with appropriate damping levels in the "activity panels".

6.10.2 Normal jumping activity – PL3-1

The DAFs for the normal jumping in "activity panels" for occupant density 0.4 kPa are presented in Figure 6-36.

In summary, the normal jumping activity in PL3-1 did not cause the dynamic deflection to exceed the limiting values. The peaks occurred at 2.0 Hz and near 2.9 Hz. The peak near 2.9 Hz reached the maximum DAFs, 1.80 in "activity panels" and 1.46 in "non-activity panels", both at 1.6% damping. The acceleration responses were found to give similar trends with maximums at 2.0 Hz and 2.9 Hz. These values were plotted in the perceptibility graphs to investigate the human discomfort levels as seen in Figure 6-37.

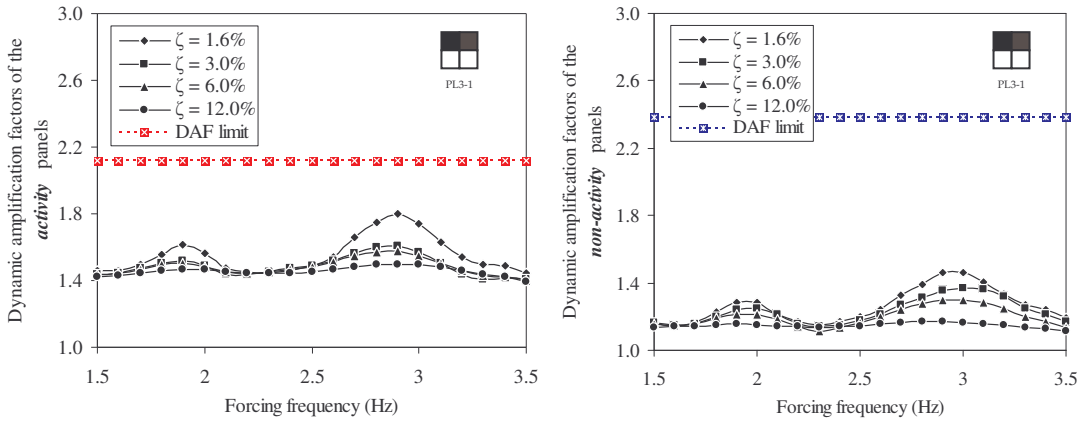

Figure 6-36: DAF due to normal jumping event in PL3-1 for Q=0.4 kPa

Even though this occupant density passed the serviceability deflection limits at all damping levels, it can be seen that the "activity panels" would fit in human perceptibility limits when 12.0% or higher damping is provided. The "non-activity panels", can be fit-out to occupancy 2 with 12.0% or higher damping.

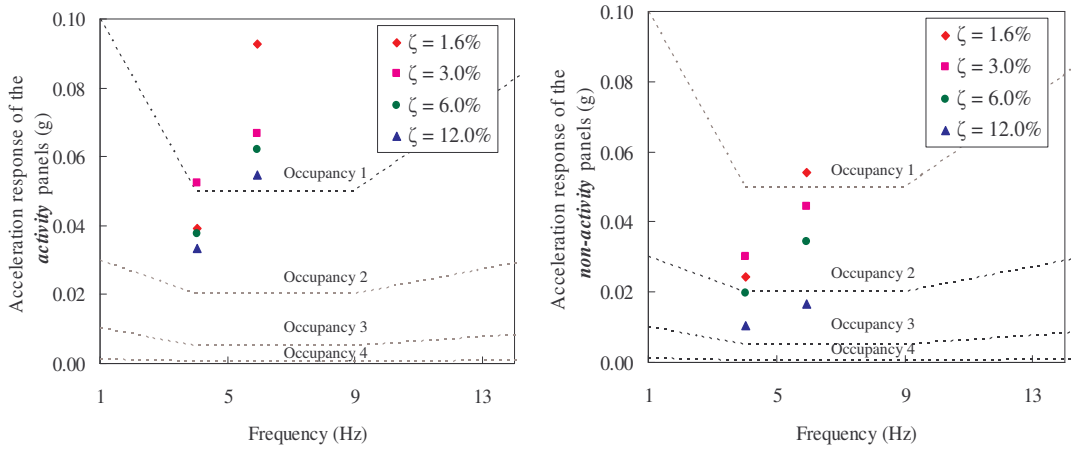

Figure 6-37: Acceleration response for normal jumping event in PL3-1 for Q=0.4 kPa

The normal jumping activity by human density of 0.2 kPa was also investigated. Figure 6-38 presents the variation of DAF with respect to activity frequency.

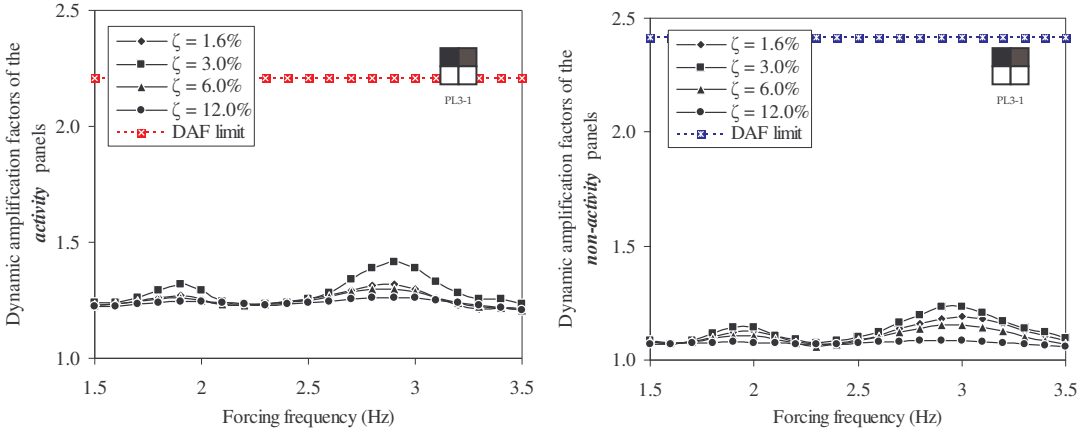

Figure 6-38: DAF due to normal jumping event in PL3-1 for Q=0.2 kPa

As expected, similarly to DAFs in human density 0.4 kPa the DAFs for human density of 0.2 kPa did not exceeded the DAF limits. The maximum DAFs observed were 1.32 and 1.19 in "activity panels" and "non-activity panels" respectively, both occurring at the activity frequency of 3.0 Hz. The acceleration response gave peaks at activity frequencies of 2.0 Hz and 3.0 Hz. Figure 6-39 represents those in perceptibility scales.

It was observed that under the human density of 0.2 kPa the "activity panels" in normal jumping can be used for occupancy 1 even at 1.6% damping. In the case of

"non-activity panels", occupancy 2 can be fitted-out at 6.0% or higher damping, whereas with human density of 0.4 kPa, 12.0% or higher damping was needed. Neither occupancy 3 nor occupancy 4 is suitable under the loadings described in this section.

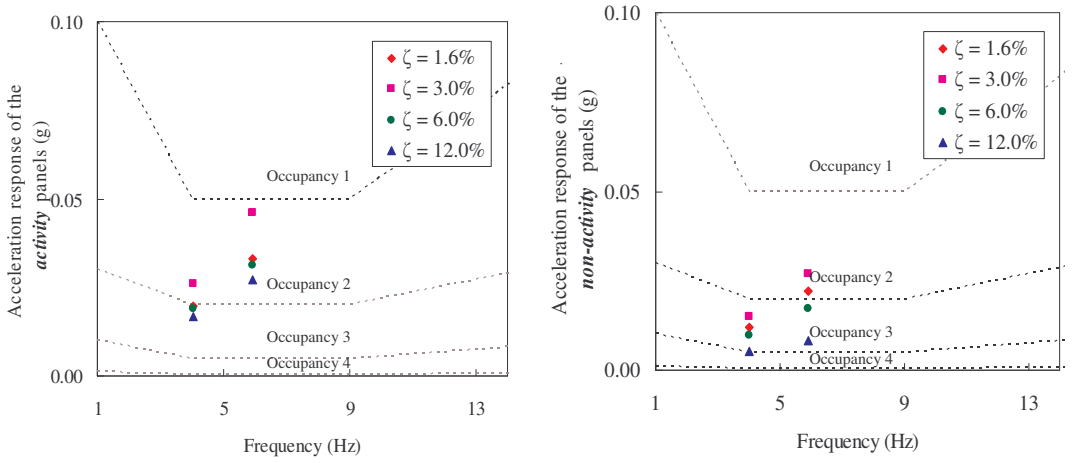

Figure 6-39: Acceleration response due to normal jumping event in PL3-1 for Q=0.2 kPa

6.10.3 Rhythmic exercise / high impact aerobics – PL3-1

The DAF responses for rhythmic exercise / high impact aerobics for occupant density of 0.4 kPa in "activity panels" are presented in Figure 6-40.

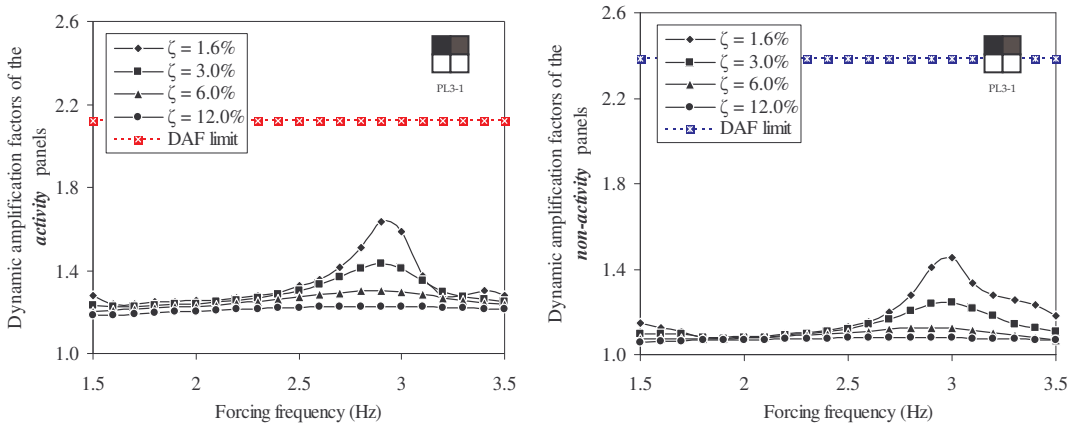

Figure 6-40: DAF due to rhythmic exercise / high impact aerobics event in PL3-1 for Q=0.4 kPa

It can be seen that rhythmic exercise / high impact aerobics under PL3-1 did not cause any problems in serviceability deflection at any damping levels. This agreed with the expected outcome since rhythmic exercise / high impact aerobics were

classified as less onerous activity than normal jumping activity. Also, the peak of DAFs, occurring near 2.0 Hz in the previous cases disappeared in this activity and the peak occurring near 2.9 Hz became more prominent. The maximum DAF occurred are 1.63 and 1.46 in "activity panels" and "non-activity panels" respectively, both occurring at 1.6% damping.

The acceleration response for rhythmic exercise / high impact aerobics events in both "activity panels" and "non-activity panels" were seen to yield a curve similar to that of DAFs with the maximum occurring at an activity frequency of 2.9 Hz. These values were plotted in the perceptibility graphs depicted in Figure 6-41.

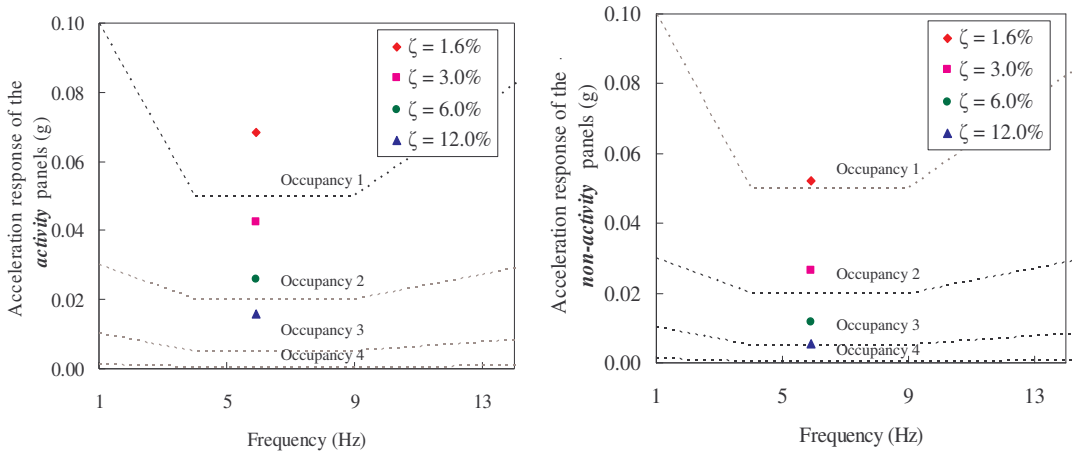

Figure 6-41: Acceleration response due to rhythmic exercise, high impact aerobics in PL3-1 for Q=0.4 kPa

The acceleration responses in the "activity panels" fit-out the occupancy 1 with 3.0% or higher damping. On the other hand, the "non-activity panels" would fit-out the occupancy 2 with 6.0% or higher damping. In addition, it was observed that the "non-activity panels" with 12.0% or higher damping can also be used to fit-out occupancy 3.

6.10.4 Low impact aerobics – PL3-1

Figure 6-42 describes the DAF responses obtained for low impact aerobics of activity density 0.4 kPa under PL3-1 conditions.

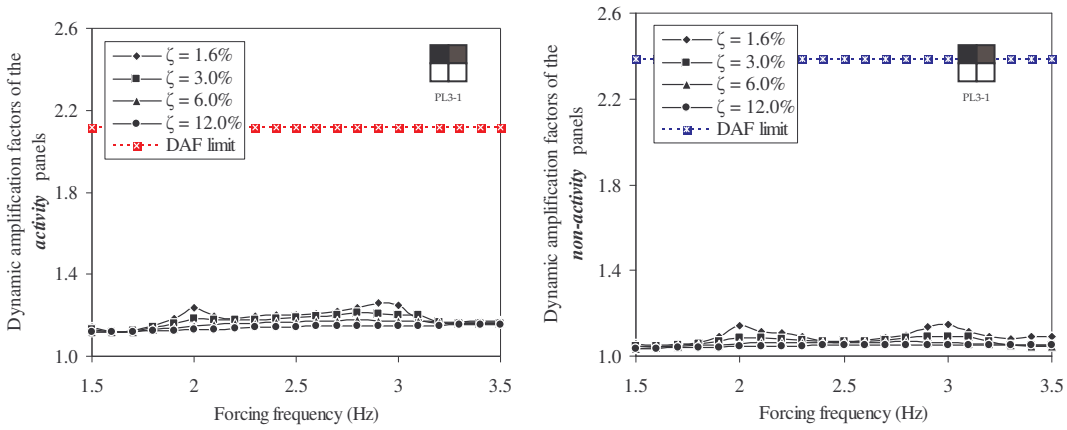

Figure 6-42: DAF due to low impact aerobics in PL3-1 for Q=0.4 kPa

As observed in the above two graphs, dance-type activity described by the low impact aerobics did not exceed the serviceability deflection criteria in both, "activity panels" and "non-activity panel", under all damping conditions. The maximum DAFs observed were 1.26 in the "activity panels" under 1.6% damping and 1.15 in the "non-activity panel" under 1.6% damping. Both of these maximum were observed at an activity frequency of 2.9 Hz, although other peaks in DAFs responses were seen at an activity frequency of 2.0 Hz. To determine and to find out suitable occupancies the acceleration responses with maximum values were plotted in the perceptibility graphs depicted in Figure 6-43. The acceleration response in the "activity panels" revealed that it would not cause discomfort to the occupants due to performing low impact aerobics at damping levels as low as 1.6%. The acceleration response in the "non-activity panels" revealed that it would fit-out occupancy 2 at damping levels as low as 1.6%. However, the occupancy 3 would only be suitable under the damping levels higher than 6.0%. The occupancy 4 cannot be fitted-out since its acceleration limits more were higher than the limits provided in the design guidance.

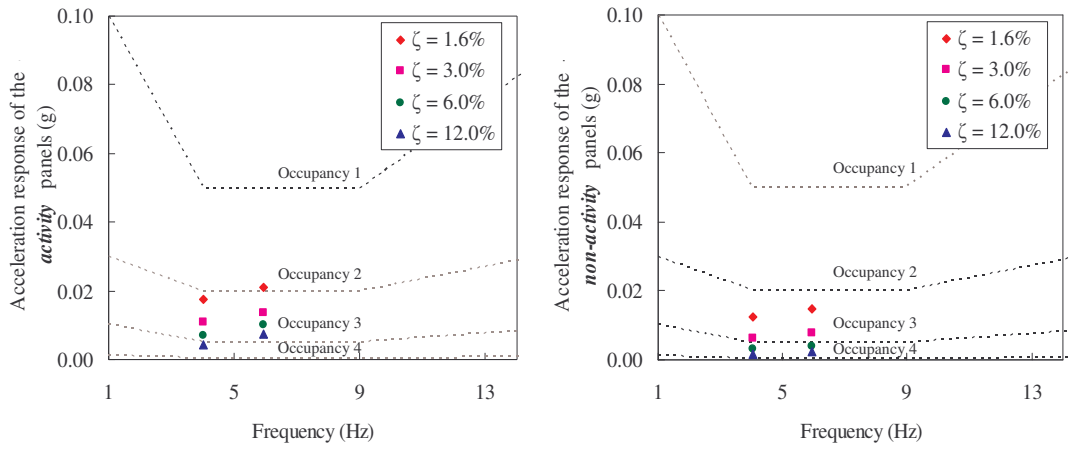

Figure 6-43: Acceleration response due to low impact aerobics in PL3-1 for Q=0.4 kPa

6.10.5 Results summary and discussion in PL3-1

In summary, the DAFs for PL3-1 gave lower readings than those in cases observed in PL2-1. PL3-1, being similar to PL2-1 in each case two panels were loaded, however the location of the loads varied. PL3-1 showed improved performance under the most onerous dance-type activities. For example, most onerous activity of high impact jumping when performed in PL3-1 configurations resulted in DAFs response well within the limits where as the same activity under PL2-1 did not. Similar outcomes were observed in other human-induced activities under these two pattern loadings.

The peaks occurring near the activity frequency of 2.9 Hz made the floor system unable to hold the dynamic effects. Although other peaks occurred at 2.0 Hz, the peak at 2.9 Hz was the major peak that helped to decide possible events, event densities and damping levels for PL3-1, which complied with the serviceability deflection limits as presented in Table 6-8.

The occupancy fit-out that complies with the acceleration criteria observed under PL3-1 is summarised in Table 6-9.

In the deflection PL3-1, gave moderate structural response compared to that of PL2-1. The sudden peaks that occurred near 2.9 Hz were the most pronounced responses that gave the indication of limits for some of the activities. In the PL1-1 and PL2-1 pattern loading cases the most pronounced response occurred near activity frequency of 2.0 Hz. In contrast, PL3-1 gave the deciding response at an activity frequency of

2.9 Hz. Fourier amplitude spectrum for this pattern loading observed at activity frequency of 2.9 Hz at 1.6% damping is presented in Figure 6-44.

Table 6-8: Operating conditions for serviceability deflection in PL3-1

Dance-type activity AP	Human density in AP	AP	NAP
High impact jumping	0.4 kPa	$\zeta > 3.0\%$	$\zeta > 1.6\%$
	0.2 kPa	$\zeta > 1.6\%$	$\zeta > 1.6\%$
Normal jumping	0.4 kPa	$\zeta > 1.6\%$	$\zeta > 1.6\%$
	0.2 kPa	$\zeta > 1.6\%$	$\zeta > 1.6\%$
Rhythmic exercise / high impact aerobics	0.4 kPa	$\zeta > 1.6\%$	$\zeta > 1.6\%$
Low impact jumping	0.4 kPa	$\zeta > 1.6\%$	$\zeta > 1.6\%$

Table 6-9: Occupancy fit-out for human comfortability in PL3-1

Dance-type activity AP	Human density in AP	AP	NAP
High impact jumping	0.4 kPa	Occupancy 1 $\zeta > 12.0\%$	Occupancy 2 $\zeta > 12.0\%$
	0.2 kPa	Occupancy 1 $\zeta > 6.0\%$	Occupancy 2 $\zeta > 6.0\%$
Normal jumping	0.4 kPa	Occupancy 1 $\zeta > 12.0\%$	Occupancy 2 $\zeta > 12.0\%$
	0.2 kPa	Occupancy 1 $\zeta > 1.6\%$	Occupancy 2 $\zeta > 6.0\%$
Rhythmic exercise / high impact aerobics	0.4 kPa	Occupancy 1 $\zeta > 3.0\%$	Occupancy 2 $\zeta > 6.0\%$ Occupancy 3 $\zeta > 12.0\%$
Low impact jumping	0.4 kPa	Occupancy 1 $\zeta > 1.6\%$	Occupancy 2 $\zeta > 1.6\%$ Occupancy 3 $\zeta > 6.0\%$

Occupancy 0	Uncomfortable
Occupancy 1	Rhythmic activities / aerobics / dance - type loads
Occupancy 2	Shopping malls (centres) / weightlifting / stores / manufacturing / warehouse / walkaways / stairs
Occupancy 3	Office / residencies / hotels / multi - family apartments / school rooms / libraries
Occupancy 4	Hospitals / laboratories / critical working areas (e.g. operating theatres, precision laboratories)

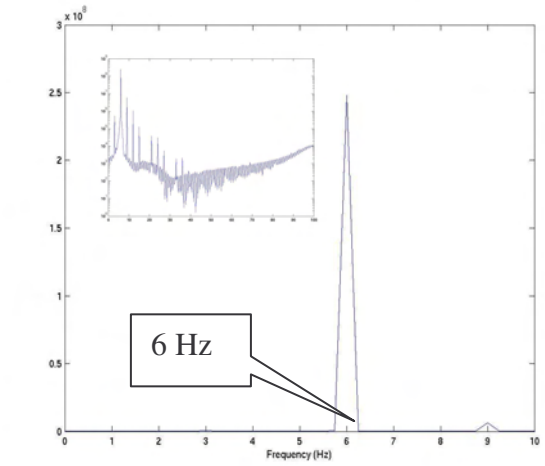

Figure 6-44: Fourier Amplitude spectrum for acceleration response at 2.9 Hz at 1.6% damping for contact ratio of 0.25 in PL3-1

The Fourier Amplitude Spectrum shows that due to the activity event frequency of 2.9 Hz of its second harmonic the floor has been excited near 5.9 Hz. This vibration frequency correlates to the third mode of vibration, which implies discomfort to the occupants. On the other hand, another peak observed in the deflection and acceleration response was at the activity frequency of 2.0 Hz. The Fourier Amplitude Spectrum for this frequency as seen in Figure 6-45 shows the floor system excited at 6 Hz. This again corresponds to the excitation of third mode of vibration.

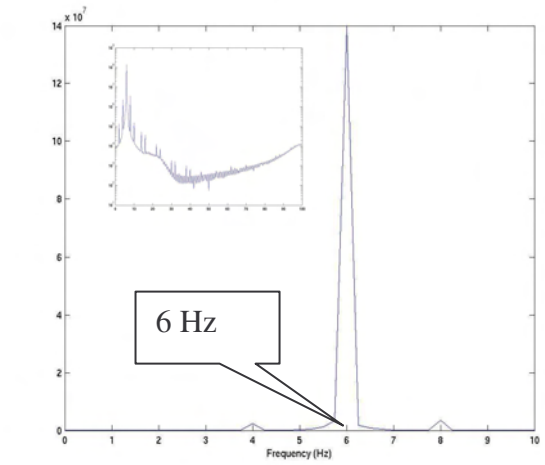

Figure 6-45: Fourier Amplitude spectrum for acceleration response at 2 Hz at 1.6% damping for contact ratio of 0.25 in PL3-1

In an overall conclusion the pattern loading in PL3-1, caused the excitation of third mode of vibration. This mode of vibration was excited by the second and third

harmonics of the activity frequency. Also this mode of vibration was the main cause for the reluctance to use the floor structure for the intended occupancy. The suitable occupancies and its operating conditions were illustrated in Table 6.8 and Table 6.9.

6.11 Dynamic analysis – Pattern loading 4 (PL4-1)

This section presents the results of DAFs as well as acceleration responses of multiple panel configuration 1 after computer simulations of dance-type activities under PL4-1, identified in the Section 6.6. To reduce the complexity of using results from every panel, the results are presented in terms of "activity panels" and "non-activity panels". Herein the Panel 1 and Panel 4 are termed the "activity panels" while Panel 2 and Panel 4 the "non-activity panels". Such notation was possible since the deference in results for "activity panels" and "non-activity panels" was less than 10% for DAFs and less than 5% for accelerations.

6.11.1 High impact jumping

The DAF response in PL4-1 observed under the high impact jumping for occupant density 0.4 kPa is presented in Figure 6-46.

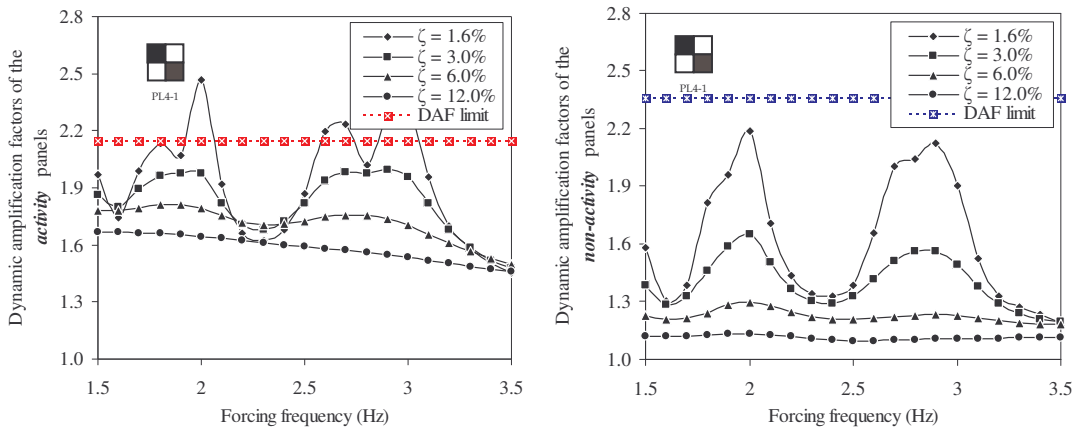

Figure 6-46: DAF due to high impact jumping event in PL4-1 for Q=0.4 kPa

The maximum observed DAFs for "activity panels" and "non-activity panels" were 2.47 and 2.19 respectively. The DAF responses observed in "activity panels" were within the serviceability deflection limits in cases with 3.0% or higher damping. In "non-activity panels" the DAFs responses were well within the limits at all damping

levels. The peaks observed at activity frequencies 1.7 Hz, 2.0 Hz, 2.6 Hz and 2.9 Hz were the cause of exceeding the limits in "activity panels". However, all these peaks were not distinguishable at damping levels higher than 3.0%. Since the more predominant peaks were the ones occurring near 2.0 Hz, 2.6 Hz and 2.9 Hz, the acceleration response at these frequencies was plotted in the perceptibility scales in Figure 6-47.

It can be seen that the acceleration response of the "activity panels" would not fit-out occupancy 1 at any of the damping levels. However, the acceleration response in the "non-activity panels" gave results suitable for occupancy 2 at 12.0% or higher damping. Lower damping levels in "non-activity panels" exceeded giving human comfort problems to the occupants in respective occupancies.

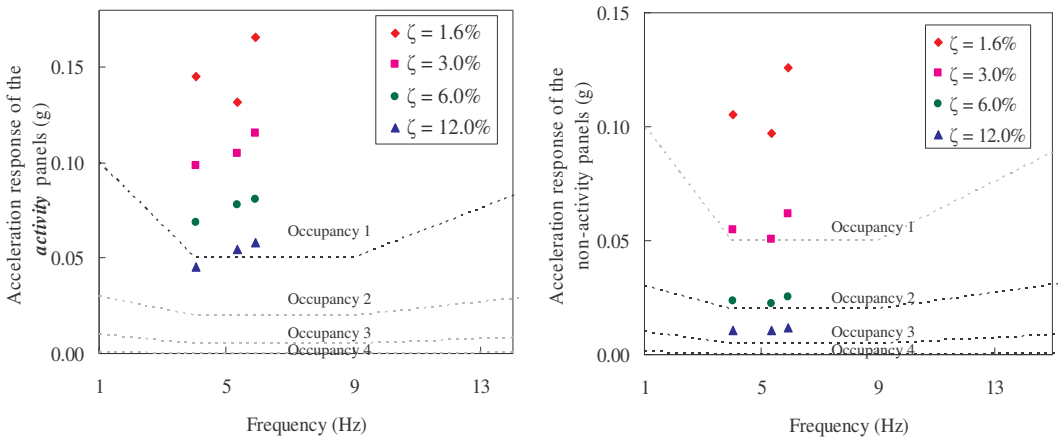

Figure 6-47: Acceleration response due to high jumping activity in PL4-1 for Q=0.4 kPa

The same jumping activity under in "activity panels" PL4-1 was simulated with a reduced human density of 0.2 kPa. Figure 6-48 presents the variation of DAF responses with activity frequency.

It can be seen that the DAF responses were well within the DAF limits at all damping levels. The maximum DAFs were 1.77 and 1.60 in "activity panels" and "non-activity panels" respectively, occurring at activity frequency of 2.0 Hz. However, secondary peaks in DAF responses were observed at activity frequency of 2.6 Hz and 2.9 Hz. These activity frequencies gave the maximum acceleration responses used in the perceptibility scales presented in Figure 6-49.

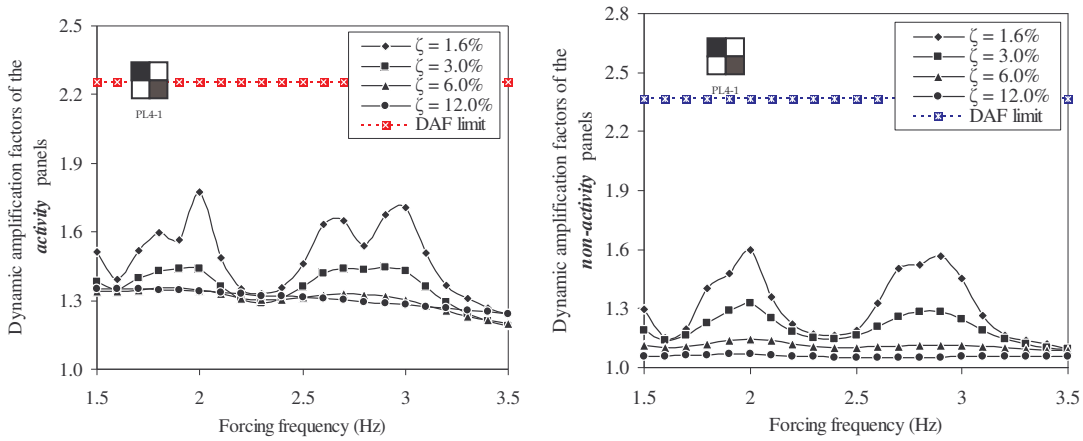

Figure 6-48: DAF due to high impact jumping event in PL4-1 for Q=0.2 kPa

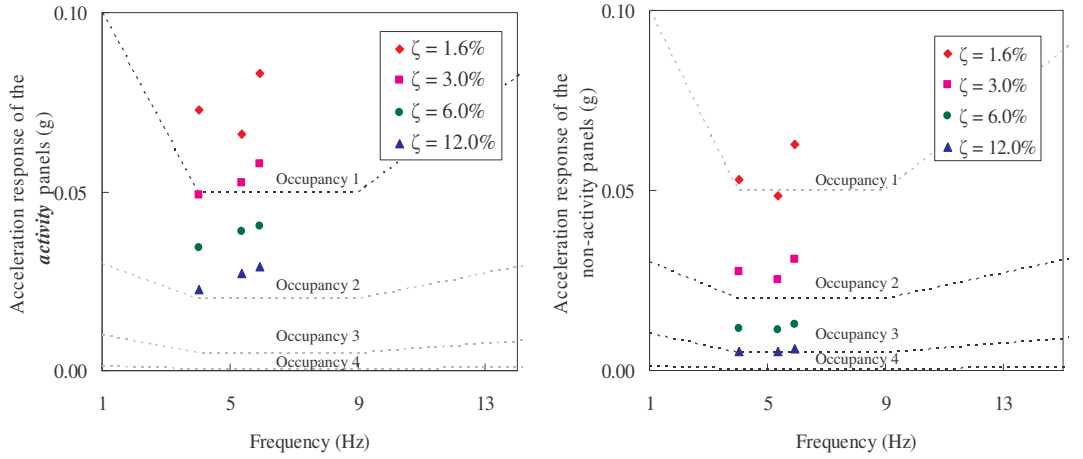

Figure 6-49: Acceleration response due to high jumping activity in PL4-1 for Q=0.2 kPa

The acceleration response in the "activity panels" yielded to fit-out occupancy 1, at 6.0% or higher damping. The "non-activity panels" can be used for occupancy 2 with 6.0% or higher damping and for occupancy 3 with 12.0% or higher damping.

6.10.2 Normal jumping activity – PL4-1

The normal jumping activity under PL4-1 for occupant density of 0.4 kPa gave the trends in DAFs presented in Figure 6-50.

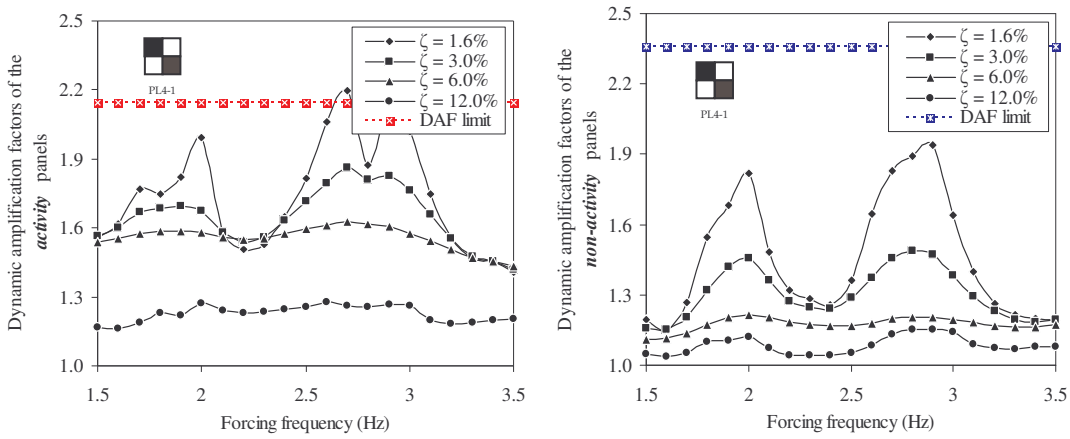

Figure 6-50: DAF due to normal jumping in PL4-1 for Q=0.4 kPa

The DAFs responses for normal jumping activity gave maximum of 2.2 for the "activity panels" and 1.9 for the "non-activity panels". It can be seen that the "activity panels" performing at 3.0% or higher damping and non-activity panels performing at 1.6% or higher damping would not cause issues related to serviceability deflection criteria.

The acceleration response for normal jumping activities under PL4-1 was plotted in the human perceptibility scales and is shown in Figure 6-51. The maximum acceleration response data that occurred near 2.0 Hz, 2.6 Hz and 2.9 Hz were used in these plots.

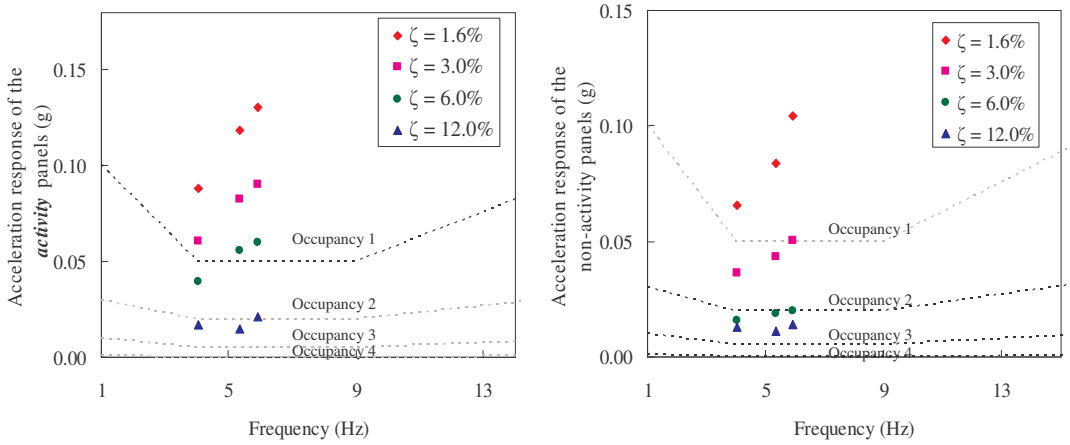

Figure 6-51: Acceleration response due to the normal jumping activity in PL4-1 for Q=0.4 kPa

The “activity panels” can be fit-out for occupancy 1 with 12.0% or higher damping where as the “non-activity panels” would fit-out occupancy 2 with 6.0% or higher damping.

The analyses were also performed for a human occupant density of 0.2 kPa performing the activity in “activity panels”. Following Figure 6-52 presents the variation of DAFs with activity frequency.

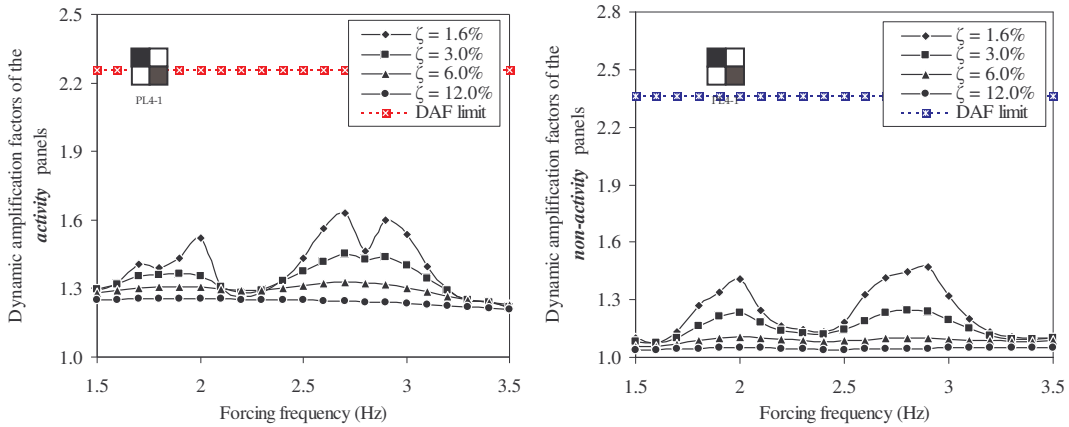

Figure 6-52: DAF due to normal jumping in PL4-1 for Q=0.2 kPa

The DAFs were well within the DAF limits for all the damping levels and thus have not caused serviceability deflection problem. The maximum DAFs of 1.63 and 1.42 were observed at 1.6% damping at activity frequency of 2.6 Hz. Similar with the previous cases of high impact jumping secondary peaks were observed at activity frequencies of 2.0 Hz and 2.9 Hz. The peaks of acceleration responses at frequencies 2.0 Hz, 2.6 Hz and 2.9 Hz were used in human perceptibility scales in Figure 6-53.

The acceleration responses for human comfortability induced a suitable damping of 3.0% or higher in the “activity panels”. The “non-activity panels” can be used for occupancy 2 at 6.0% or higher damping, as well as occupancy 3 at 12.0% or higher damping.

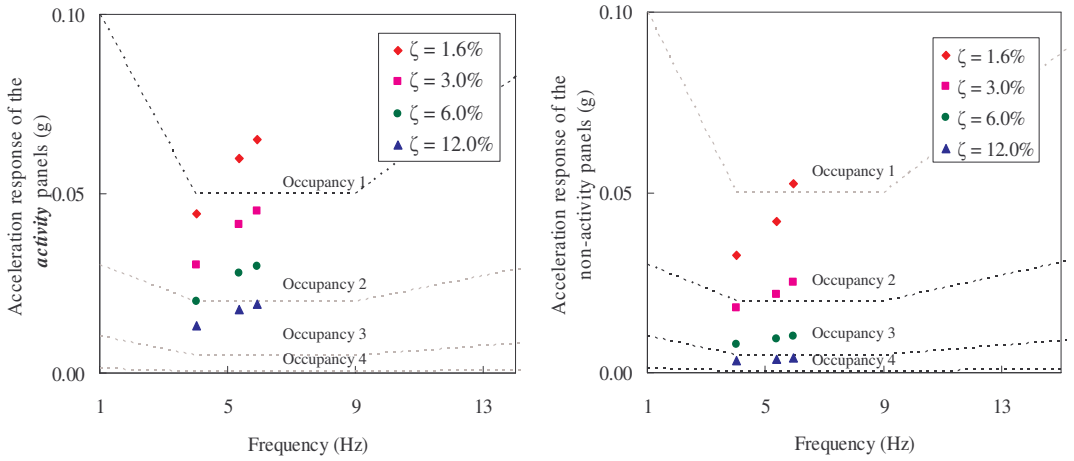

Figure 6-53: Acceleration response due to the normal jumping activity in PL4-1 for Q=0.2 kPa

6.11.3 Normal rhythmic exercise / high impact aerobics – PL4-1

The rhythmic exercise / high impact aerobics activity under PL4-1 for occupant density of 0.4 kPa gave the trends in DAFs presented in Figure 6-54.

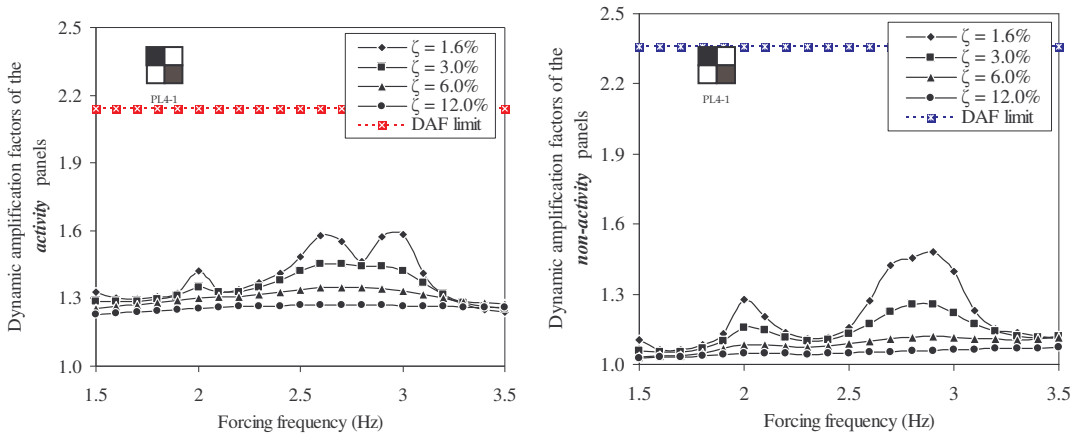

Figure 6-54: DAFs due to rhythmic exercise / high impact aerobics in PL4-1 for Q=0.4 kPa

It can be seen that neither the "activity panels" nor the "non-activity panels" exceeded the DAF limits. However, peaks in DAF responses were observed in 2.0 Hz 2.6 Hz and 2.9 Hz. These were distinguishable at lower damping levels, however disappeared with increased damping. The maximum DAF of 1.6 was found in the "activity panels" and a maximum of 1.4 in the "non-activity panels". Similarly to the DAF response, the maximum acceleration responses for the rhythmic exercise / high

impact aerobics were observed at activity frequencies of 2.0 Hz, 2.6 and 2.9 Hz and were used to plot perceptibility scales in Figure 6-55.

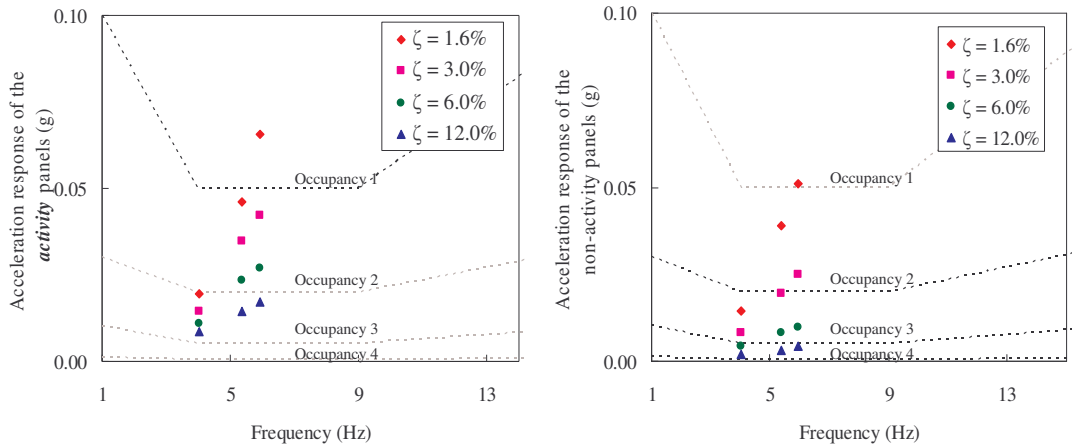

Figure 6-55: Acceleration response due to the rhythmic exercise / high impact aerobics activity in PL4-1 for Q=0.4 kPa

The acceleration responses in the "activity panel" were within the limits of occupancy 1 for 3.0% or higher damping. The resulting acceleration responses in the "non-activity panels" are suitable for occupancy 2 with damping levels of 6.0% or higher, and for occupancy 3 with damping levels of 12.0% or higher.

6.11.4 Low impact aerobics – PL4-1

The DAFs response observed for low impact jumping of occupant density 0.4 kPa performing the activity in "activity panels" under PL4-1 presented in Figure 6-56.

The DAF responses for the low impact aerobics, in both "activity" and "non activity panels" did not exceed the DAF limits at all damping levels. Thus, events decided by the low impact aerobics do not cause any serviceability deflection problems. The acceleration response for the low impact aerobics produced the perceptibility charts given in Figure 6-57.

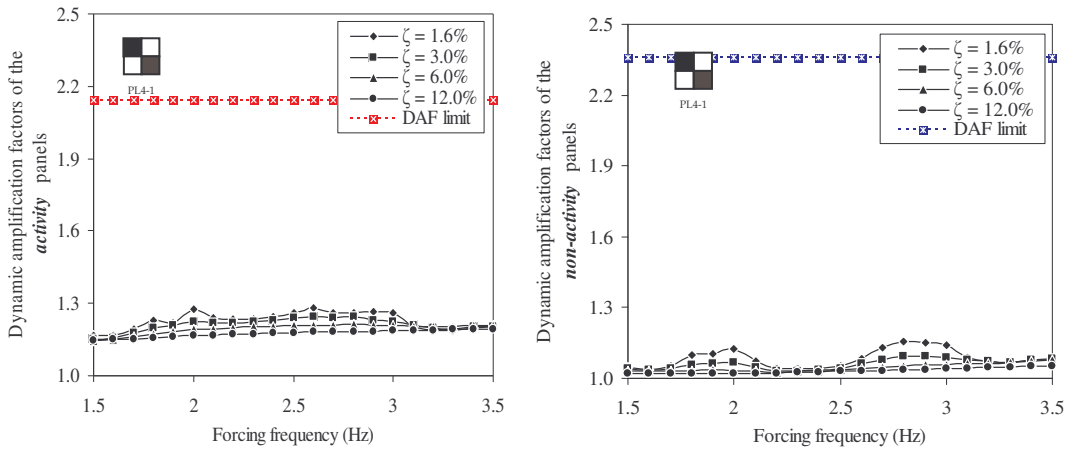

Figure 6-56: DAFs due to low impact aerobics in PL4-1 for Q=0.4 kPa

Low impact aerobics in the "activity panels" did not cause any discomfort to the occupant fitting out the occupancy 1 at any of the damping levels. Similarly, resulting acceleration response in the "non-activity panels", can be fitted with occupancy 2 at all the damping levels, and with occupancy 3 at 3.0% or higher damping levels.

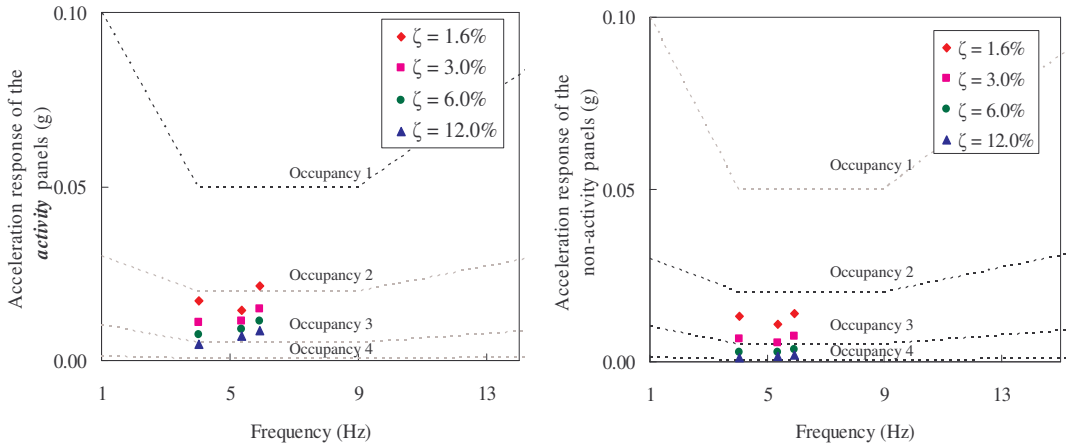

Figure 6-57: Acceleration response due to low impact aerobics activity in PL4-1 for Q=0.4 kPa

6.11.5 Results summary and discussion in PL4-1

In summary, the dance-type activities performed under PL4-1 did not exceed the serviceability deflection limits at almost all the damping levels and human densities. Table 6-10 summaries the events and damping levels that complied the for serviceability deflection limits.

Table 6-10: Operating conditions for serviceability deflection in PL4-1

Dance-type activity AP	Human density in AP	AP	NAP
High impact jumping	0.4 kPa	$\zeta > 3.0\%$	$\zeta > 1.6\%$
	0.2 kPa	$\zeta > 1.6\%$	$\zeta > 1.6\%$
Normal jumping	0.4 kPa	$\zeta > 3.0\%$	$\zeta > 1.6\%$
	0.2 kPa	$\zeta > 1.6\%$	$\zeta > 1.6\%$
Rhythmic exercise / high impact aerobics	0.4 kPa	$\zeta > 1.6\%$	$\zeta > 1.6\%$
Low impact jumping	0.4 kPa	$\zeta > 1.6\%$	$\zeta > 1.6\%$

The acceleration response for various dance-type loads observed under PL4-1, distinguished the occupancies summarised in Table 6-11.

PL4-1 showed the best fit-out for occupancies of all investigated pattern loads. However, there were few instances where it did not comply with the serviceability state limits. The reason for not complying was due to peak acceleration responses observed at 2.0 Hz, 2.6 Hz and 2.9 Hz. These excitation frequencies caused the floor structure to vibrate at different mode shapes. The most vigilant activity frequency under PL4-1 was 2.6 Hz. The Fourier Amplitude Spectrum taken at this frequency, as seen in Figure 6-58, clarified the floor structures frequency response.

Table 6-11: Occupancy fit-out for human comfortability in PL4-1

Dance-type activity AP	Human density in AP	AP	NAP
High impact jumping	0.4 kPa	Occupancy 0	Occupancy 2 $\zeta > 12.0\%$
	0.2 kPa	Occupancy 1 $\zeta > 6.0\%$	Occupancy 2 $\zeta > 6.0\%$ Occupancy 3 $\zeta > 12.0\%$
Normal jumping	0.4 kPa	Occupancy 1 $\zeta > 12.0\%$	Occupancy 2 $\zeta > 6.0\%$
	0.2 kPa	Occupancy 1 $\zeta > 3.0\%$	Occupancy 2 $\zeta > 6.0\%$ Occupancy 3 $\zeta > 12.0\%$
Rhythmic exercise / high impact aerobics	0.4 kPa	Occupancy 1 $\zeta > 3.0\%$	Occupancy 2 $\zeta > 6.0\%$ Occupancy 3 $\zeta > 12.0\%$
Low impact jumping	0.2 kPa	Occupancy 1 $\zeta > 1.6\%$	Occupancy 2 $\zeta > 1.6\%$ Occupancy 3 $\zeta > 6.0\%$ Occupancy 4 $\zeta > 12.0\%$

Occupancy 0	Uncomfortable
Occupancy 1	Rhythmic activities / aerobics / dance - type loads
Occupancy 2	Shopping malls (centres) / weightlifting / stores / manufacturing / warehouse / walkaways / stairs
Occupancy 3	Office / residencies / hotels / multi - family apartments / school rooms / libraries
Occupancy 4	Hospitals / laboratories / critical working areas (e.g. operating theatres, precision laboratories)

The Fourier Amplitude Spectrum shows a peak response at frequency of 5.4 Hz. This frequency coincides with the second natural frequency of the floor system and thus it can be stated that the floor system was vibrating in the second mode shape.

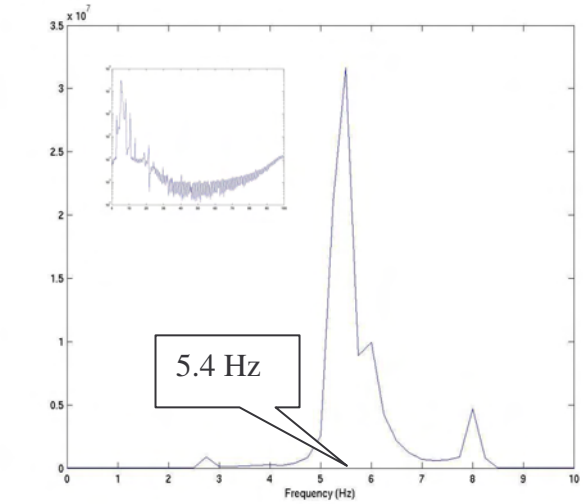

Figure 6-58: Fourier Amplitude Spectrum for acceleration response at 2.7 Hz at 1.6% damping for contact ratio of 0.25 in PL4-1

Similarly the Fourier Amplitude Spectrum observed at the activity frequency of 2.9 Hz as seen in Figure 6-59 showed similar behaviour. It was observed that the floor system was vibrating in its third mode.

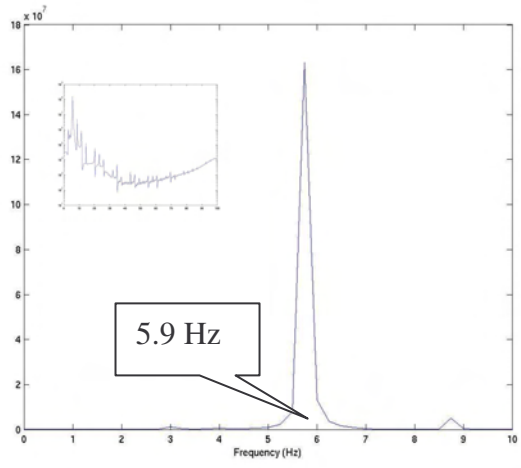

Figure 6-59: Fourier Amplitude Spectrum for acceleration response at 2.9 Hz at 1.6% damping for contact ratio of 0.25 in PL4-1

From an overall prospective, PL4-1 gave wider control in vibration of the floor system. However, PL4-1 caused the floor structure to vibrate predominately at second mode of vibration. Third mode of vibration was also observed by the higher harmonics of the activity frequencies. Nevertheless, it produced the lowest DAFs and acceleration responses of all the pattern loadings. As a result, PL4-1 provided

relaxation of the vibration response so that wider occupancies can be fit-out to the floor system.

6.12 Development of empirical formulae

This section of the Chapter 6 presents the development of relationships for DAFs and acceleration responses. The data extracted from the maximum DAFs and acceleration responses in each pattern loading case were used. The damping ratio, contact ratio and mode of vibration were the parameters used.

The relationships between the DAFs and acceleration responses when developed, can be used to estimate the DAFs and acceleration responses for known contact ratio of dance-type activity, damping levels and location of event being performed or the mode of vibration. However, an occupant density of 1.75 m^2 per person which was considered to be the maximum possible density of people in which they won't cause problems to each other was used. Consequently, the results obtained from the formulae can be considered to be the highest predicted.

6.12.1 Formulae for DAF

The maximum DAFs observed in four pattern loading cases and their variations with respect to the contact ratio and damping ratio were used to derive the relationships. These relationships were obtained by MS EXCEL's curve fitting techniques and using the "solver" add-in. A format for the formulae was initially taken from observing the trends of DAFs and contact ratios. These trends show an exponential function captured in Equation 6-4 where the '*A's* and '*N's* are coefficients which depend on the damping ratio:

$$DAF = Ae^{-N\alpha}. \qquad \textbf{Equation 6-4}$$

The variation of DAFs with contact ratio was observed for each pattern loading case and respective values for '*A*'s and '*N*'s were obtained after substituting into the above Equation 6-4. This was done for both "activity panels" and "non-activity panels" and for all the pattern loads.

The PL1-1, excited the first mode of vibration, that gave the maximum DAFs at an activity frequency of 2 Hz. Thus, DAF responses at 2 Hz were used in Equation 6-4

to obtain values for '*A's* and '*N's*. The following Figure 6-60 represents the variation of DAF with contact ratio along with the coefficients '*A*' and '*N*' generated (for each damping ratio).

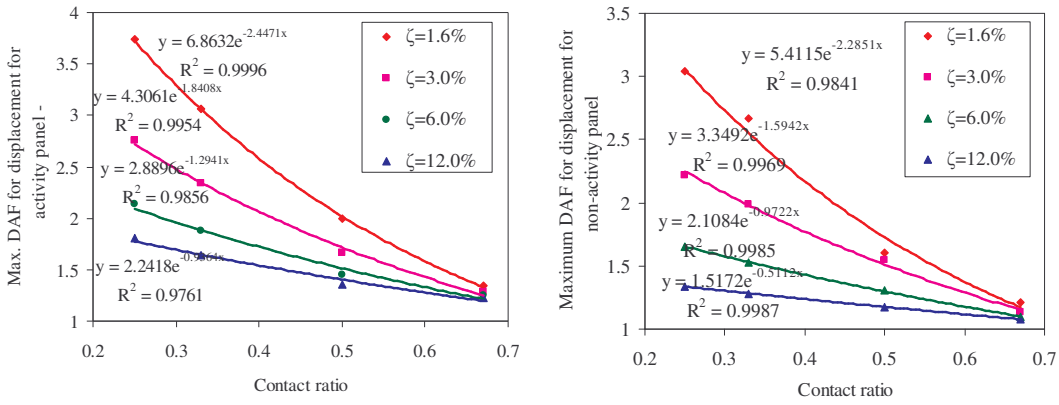

Figure 6-60: Variation of DAF with contact ratio in PL1-1

The values generated for coefficients '*A's* and '*N's* as shown in Figure 6-60 were compared with the original values, which gave a standard deviation of 0.020356 and 0.02512, and COV of 2.04% and 2.51% for the "activity panels" and "non-activity panels" respectively.

Similarly for the PL2-1, the variation of maximum DAF at activity frequency of 2 Hz with respect to contact ratio was observed and presented in Figure 6-61. Herein, as in previous pattern loading case PL1-1 the maximum DAFs observed were found in the first mode of excitation and were plotted against different contact ratios.

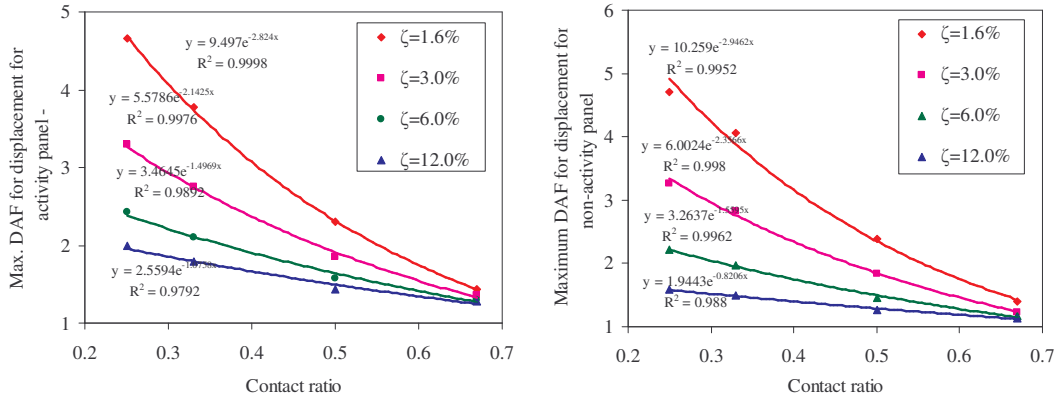

Figure 6-61: Variation of DAF with contact ratio in PL2-1

The curve fitting for PL2-1 using the MS EXCEL solver generated set of '*A*'s and '*N*'s and gave standard deviation of 0.021123 and 0.024891 and COV of 2.11% and 2.50% for the "activity panels" and "non-activity panels" respectively.

Thereafter, results for PL3-1 were used to obtain the set of '*A*'s and '*N*'s. This pattern loading excited the first mode as well as third mode. However, the third mode gave the maximum DAFs for the four contact ratios and Figure 6-62 presents their variation with contact ratio.

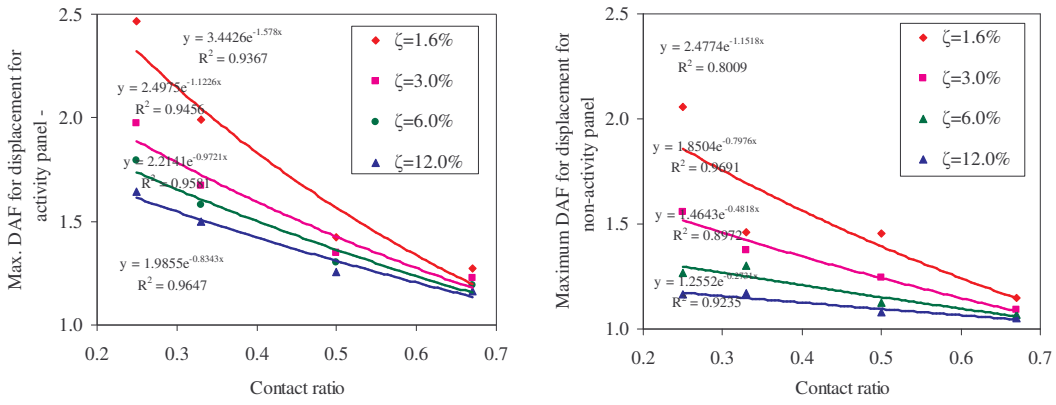

Figure 6-62: Variation of DAF with contact ratio in PL3-1

The curve fitting for the PL3-1 gave standard deviation of 0.047577 and 0.048703, and COV of 4.74% and 4.87% for the "activity panels" and "non-activity panels" respectively.

Finally, the variation of DAFs with contact ratio was observed PL4-1. In contrast to the previous pattern loading cases this loading excited various mode shapes. The maximum DAFs were given at an activity frequency 2.7 Hz, which excited the second mode of the FE model. The following Figure 6-63 presents the corresponding variation with contact ratio.

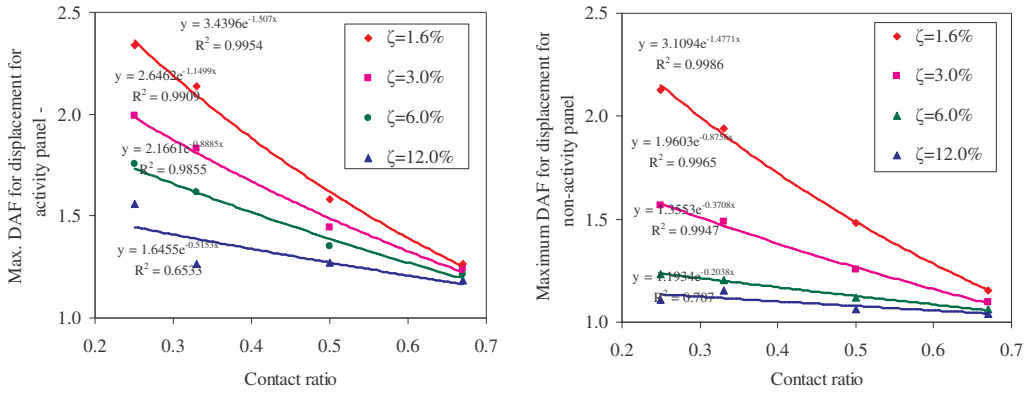

Figure 6-63: Variation of DAF with contact ratio in PL4-1

The curve fitting for the PL4-1 gave set of '*A*'s and '*N*'s which gave standard deviations of 0.033516 and 0.0125797, and COV of 3.35% and 1.26% for the "activity panels" and "non-activity panels" respectively.

The values obtained for '*A*'s and '*N*'s was a function of damping ratio. A general format for the formulae for '*A's* and '*N's* as recorded in Equation 6-5 and Equation 6-6 was initially taken after observing the trends of '*A's* and '*N's* versus damping ratios for the four pattern-loading cases:

$$A = k_1 \zeta^{k_2} . \qquad \textbf{Equation 6-5}$$

$$N = k_3 \zeta^{k_4} . \qquad \textbf{Equation 6-6}$$

Herein, the constants k_1, k_2, k_3 and k_4 were obtained by MS EXCEL's curve fitting techniques and by using the "solver" add-in. The constants k_1 and k_3 are multification to the base which is the damping ratio while the k_2 and k_4 are the exponents of the base. These constants were obtained by observing the variation of *A*'s and *N*'s with damping ratio. Figure 6-64 presents these variations, multifications k_1, k_3 and exponents k_2, k_4 for the four pattern loading cases for the "activity panels".

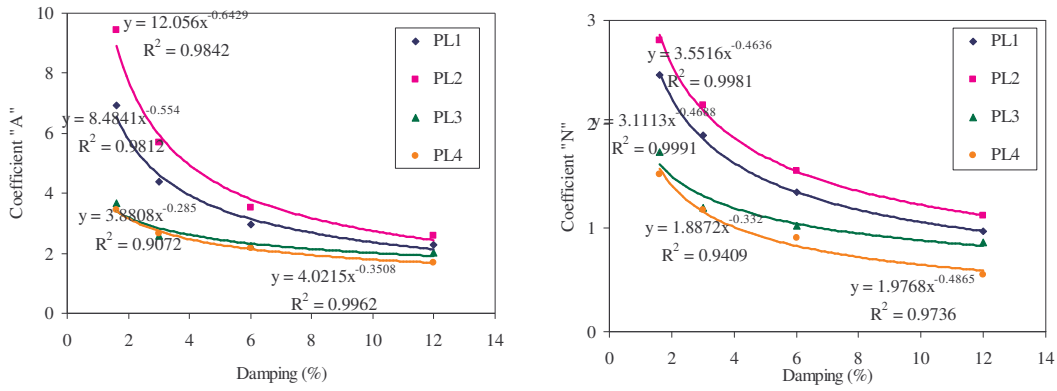

Figure 6-64: Variation of coefficients '*A's* and '*N's* for "activity panels"

The curve fitting for "activity panels" gave standard deviation and COVs of 0.073624 and 7.31%, 0.05145 and 5.13% for coefficients '*A's* and '*N's* respectively. Similarly, for "non-activity" panel's variation of coefficients *A* and *N* with damping ratio was plotted in Figure 6-65 and the constants k_1, k_2, k_3 and k_4 were found. This gave a standard deviation and COV of 0.067869 and 6.84%, 0.07323 and 7.20 for coefficients '*A's* and '*N's* respectively.

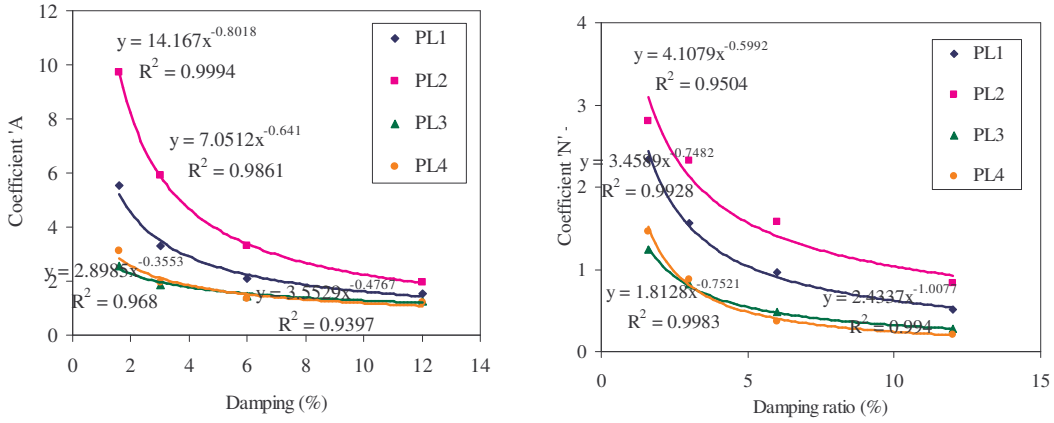

Figure 6-65: Variation of coefficients '*A*'s and '*N*'s for "non-activity panels"

Using the obtained coefficients k_1, k_2, k_3 and k_4 the final formulae for DAFs for various pattern loading cases is presented in Equation 6-7:

$$DAF = Ae^{-N\alpha}\ , \qquad \textbf{Equation 6-7}$$

where $A = k_1\zeta^{k_2}$ and $N = k_3\zeta^{k_4}$.

The proposed multifications k_1 and k_3 and the exponents k_2 and k_3 are presented in the following Table 6-12. The standard deviations and coefficient of variations calculated for each pattern loading case was also are also presented in the table.

Table 6-12: Proposed coefficients of k_1, k_2, k_3 and k_4 for DAF response

	Activity panel(s)				Standard deviation	COV
	k_1	k_2	k_3	k_4		
PL1-1	9.03	-0.61	3.09	-0.46	0.078	7.94%
PL2-1	12.97	-0.71	3.51	-0.45	0.088	9.01%
PL3-1	4.06	-0.32	1.98	-0.37	0.065	6.52%
PL4-1	4.02	-0.35	1.89	-0.45	0.043	4.29%
	Non-activity panel(s)					
PL1-1	7.57	-0.70	3.28	-0.70	0.095	9.68%
PL2-1	14.23	-0.81	4.11	-0.60	0.100	9.97%
PL3-1	3.01	-0.38	1.76	-0.72	0.080	8.06%
PL4-1	3.25	-0.39	1.50	-0.44	0.075	7.45%

Herein, PL1-1 can be referred to as a single panel loaded vibrating at the first mode, PL2-1 can be referred to as two panels loaded, vibrating at the first mode, PL3-1 can be referred to as vibrating at the third mode and PL4-1 can be referred to as vibrating in the second mode.

6.12.2 Formulae for acceleration response

Similar steps that were used for formulating the DAF responses were also used in the cause of developing the formulae for acceleration response a. The acceleration responses used were the maximum accelerations observed in each pattern loading case. Initially, the variations of acceleration responses with contact ratio were observed. These variations were then transformed in to an exponential function in Equation 6-8:

$$a = A' e^{-N'\alpha}. \qquad \textbf{Equation 6-8}$$

The values for 'A''s and 'N''s were dependent upon the damping ratio.

The values for 'A''s and 'N''s were obtained by MS EXCEL's curve fitting techniques and using the "solver" add-in. For each pattern loading case, sets of 'A''s and 'N''s were obtained for both "activity panels" and "non-activity panels".

The following Figure 6-66 presents the variation of acceleration response with contact ratio in PL1-1.

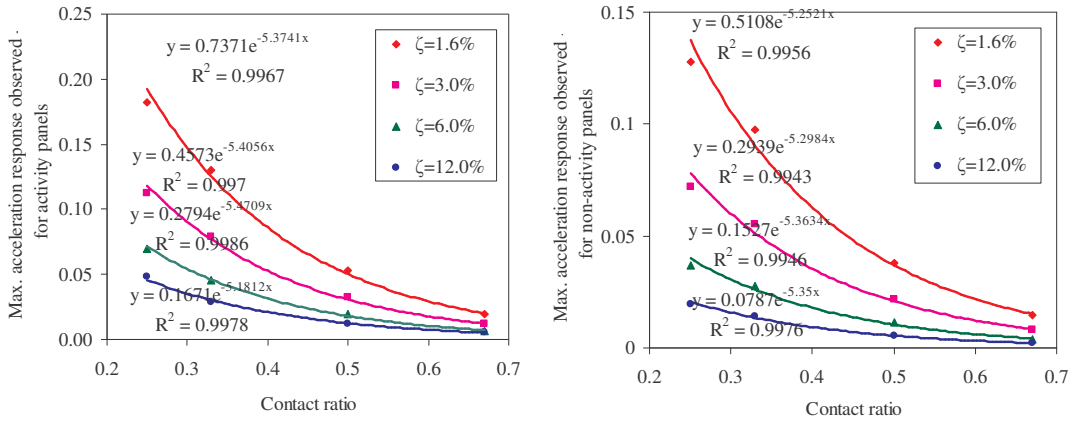

Figure 6-66: Variation of acceleration response with contact ratio in PL1-1

In Figure 6-67 the exponential functions gave 'A''s and 'N''s for different damping ratio for both "activity panel" and "non-activity panels". Standard deviations for Equation 6-5 of 0.087581 and 0.059641 and COVs of 8.85% and 5.95% were observed for "activity panels" and "non-activity panels" respectively.

For PL2-1, the variations of acceleration responses with the contact ratio were presented in Figure 6-67.

The MS EXCEL's curve fitting techniques captured in Figure 6-67 gave various values for 'A''s and 'N''s with standard deviations of 0.080554 and 0.056896, and COVs of 8.19% and 5.68% for "activity panels" and "non-activity panels" respectively.

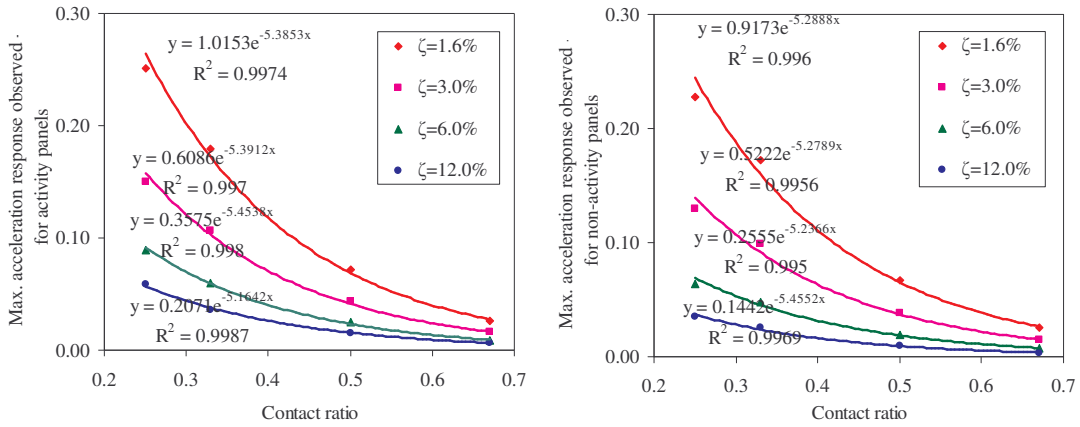

Figure 6-67: Variation of acceleration response with contact ratio in PL2-1

Similarly, PL3-1 produced variations of acceleration response with contact ratios and values for 'A''s and 'N''s were obtained and depicted in Figure 6-68.

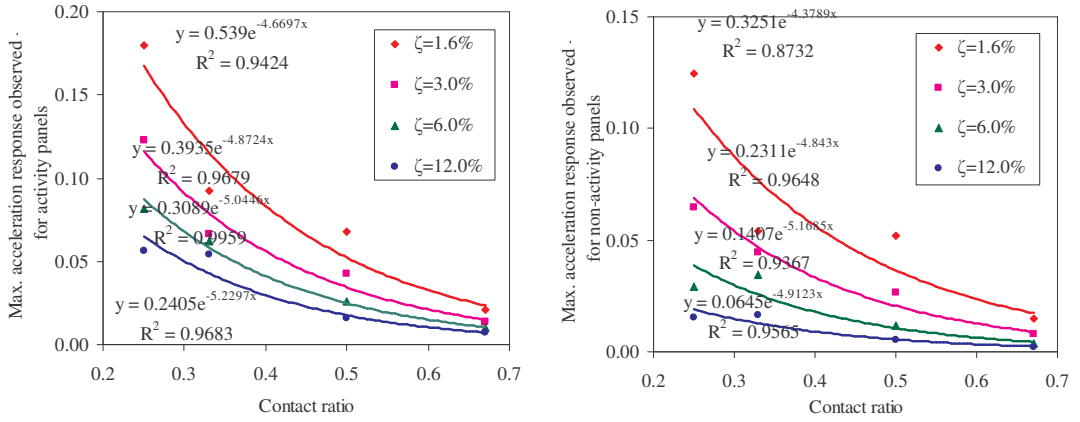

Figure 6-68: Variation of acceleration response with contact ratio in PL3-1

The PL4-1 gave the maximum acceleration response at an activity frequency 2.7 Hz and its variations with contact ratio are presented in Figure 6-69.

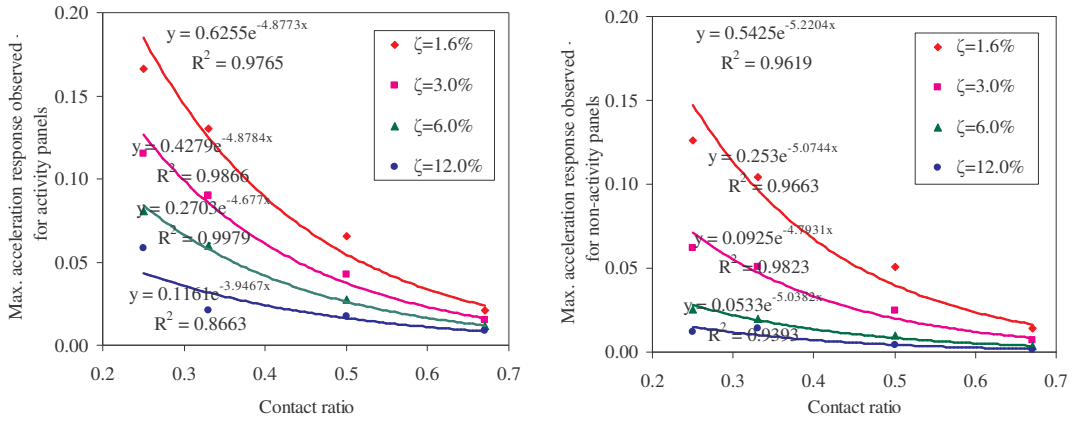

Figure 6-69: Variation of acceleration response with contact ratio in PL4-1

The examination of acceleration response versus contact ratio for the four pattern loading cases resulted in varied values for both coefficients 'A''s and 'N''. The coefficient 'A'' was a function of the damping ratio and coefficient 'N'' came out as a constant. Thus a general format for 'A'' for the formulae was taken by observing the trends and keeping 'N''constant, as noted in Equation 6-9 and Equation 6-10:

$$A' = k_1' \zeta^{k_2'} \qquad \textbf{Equation 6-9}$$

$$N = Cons\tan t \qquad \textbf{Equation 6-10}$$

Constants k_1' and k_2' , were again obtained by MS EXCEL's curve fitting techniques and the using the "solver" add-in. The constant k_1' denotes a multification to the base which is the damping ratio, while k_2' is the exponents of the base. The following Figure 6-70 presents the variation of multifications k_1' and exponents k_2' in "activity panels" for the four pattern loading cases.

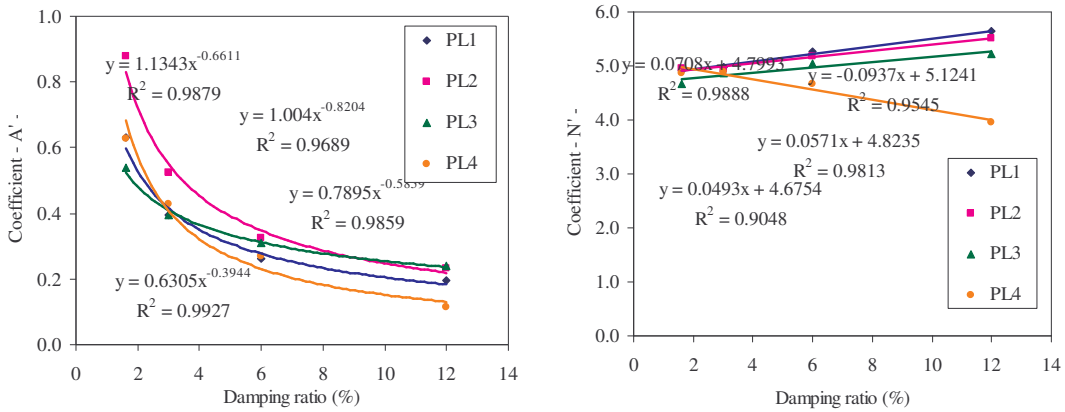

Figure 6-70: Variation of coefficients 'A''s and 'N''s for "activity panels"

In this search of appropriate values for the multifications factors and exponents the COVs were seen to be less than 10%. The constant for N' for the "activity panels" was found to be 4.97.

Similarly for "non-activity panels", the variation of coefficients 'A''s and 'N''s with damping ratio were plotted and the constants k_1 and k_2 were found as seen in Figure 6-71. Constant value for 'N'' was found to be 5.33 (for PL1-1, PL2-1), 4.78 (for PL3-1) and 4.84 (for PL4-1).

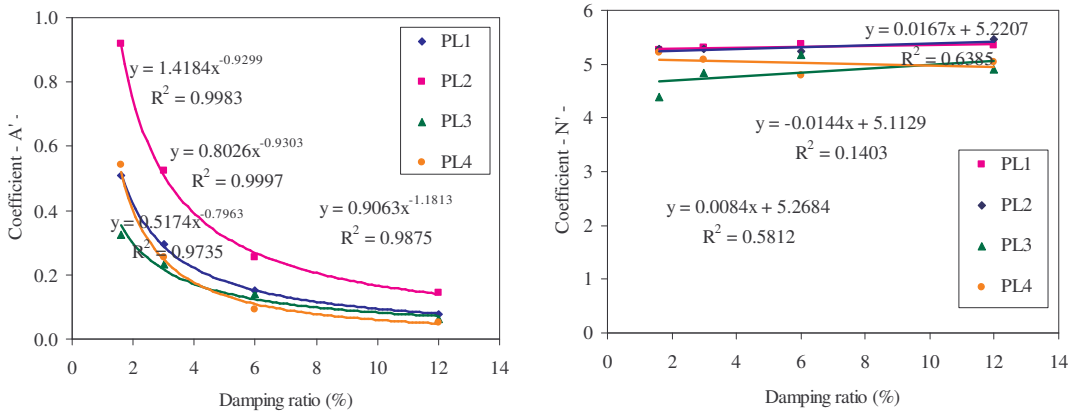

Figure 6-71: Variation of coefficients 'A''s and 'N''s for "non-activity panels"

Finally, the general solution for acceleration response a for various pattern loading cases can be stated as:

$$a = A' e^{-N'\alpha}$$ **Equation 6-11**

where $A' = k_1' \zeta^{k_2'}$ and $N' = Constant$**.**

The proposed multifications k_1' exponents k_2' and constants N' are presented in Table 6-13. It also presents the standard deviations and coefficient of variations observed in this case.

Table 6-13: Proposed coefficient for k_1' and k_2' for acceleration response

	Activity panel(s)			Standard deviation	COV
	k_1'	k_2'	N'		
PL1-1	0.83	-0.70	4.97	0.094	9.37%
PL2-1	1.16	-0.75	4.97	0.091	9.14%
PL3-1	0.85	-0.60	4.97	0.087	8.65%
PL4-1	0.79	-0.54	4.97	0.096	9.57%
Non-activity panel(s)					
	k_1'	k_2'	N'		
PL1-1	0.80	-0.93	5.33	0.063	6.35%
PL2-1	1.42	-0.93	5.33	0.065	6.56%
PL3-1	0.69	-1.03	4.78	0.129	12.90%
PL4-1	0.75	-1.16	4.84	0.129	12.93%

Herein, PL1-1 can be referred to as a single panel loaded and vibrating it the first mode, PL2-1 can be referred as to two panels loaded, vibrating in the first mode, PL3-1 can be referred to as a vibrating the third mode and PL4-1 can be referred to as vibrating in the second mode.

In conclusion, it can be stated that the derived formulae can be used for estimating the DAF response and acceleration response that occur in multi-modal vibration in multiple panel floor panels. Since the COV in all the examined cases was less than 10%, it proves that the results derived by using the formulae agree with those of FE models. Consequently the formulae can be used to predict both deflection and acceleration responses that occur in a human-induced dynamic event in a known type of activity, damping, and mode of excitation. This reduces the complexity of obtaining the dynamic responses in multi-modal vibration under various types of dance-type events on various damping levels.

6.13 Summary

Chapter 6 of the thesis illustrated a comprehensive investigation of a four panel steel-deck composite floor system subjected to different pattern loading cases. Four pattern loading cases were identified and investigated for deflection and acceleration response under different human-induced events. These different human-induced events namely high-jumping, normal jumping, rhythmic exercise, high impact aerobics and low impact aerobics, differentiated by different contact ratios were simulated at different damping levels, activity frequencies and human-densities posing the activity. The floor responses to each pattern loading and human activity were obtained and critiqued with respect to the serviceability design criteria of deflection and human discomfort criteria of accelerations. Thereafter, these results were used to nominate suitable damping levels and human densities in the "activity panels" and suitable occupancies in the "non-activity panels" that comply with the two serviceability state design criteria.

An important conclusion arrived at from investigations presented in this chapter was that the floor was exited in the higher modes of vibration in contrast to the common belief of vibrating in its primary mode. The pattern loading cases examined caused this kind of multi-modal behaviour resulting in restriction and control of some of the human activities. This finding highlights that in floor systems subjected to pattern loading, the knowledge of not only the primary mode of vibration but also of the higher mode of vibration needs to be attained.

The equations developed in this chapter can be used as guidance to determine serviceability deflection and acceleration responses of floors subjected to multi-modal vibration. Due to varying properties of the real-type floor structure, both statically and dynamically exact values are difficult to determine. However, by using the equations developed in this chapter reasonably accurate estimation can be obtained by the user. These equations can be used as a pre-estimation tool as well as a retrofitting tool.

Chapter 7 - Dynamic analysis on nine panel FE model

7.1 Introduction

The previous chapter presented a comprehensive investigation of a four panel floor system subjected to pattern loading. This chapter extends the investigation in to a nine panel model, where linear transient dynamic analysis was carried out on two human-induced pattern loads and their responses were recorded. As in the previous chapter the responses due to human-induced dance-type loads at different activity frequencies, damping levels and human densities posing the activity were investigated. The resulting DAFs and acceleration responses were observed and were used to nominate suitable occupancies that complied with the serviceability design criteria.

7.2 Nine panel configuration and properties

The nine panel FE model developed and presented in Section 4.7.5 was used for the investigation described in this chapter. This FE model was termed “configuration 2” and different human-induced activities, activity frequencies, damping, human densities on several pattern loading cases were studied.

The natural frequency analysis for the nine panel model was already done in Section 4.7.5, which gave values of 4.34 Hz, 4.83 Hz 5.42 Hz and 5.93 Hz for the first four natural frequencies respectively.

7.3 Human-induced activities/loads

The human-induced activities/loads used for the investigation described in this chapter were the same loads described in the Section 6.3 termed dance-type loads. Four dance-type loads with activity frequencies starting from 1.5 Hz to 3.5 Hz were used. These dance-type loads were described by different contact ratios (i.e. 0.25, 0.33, 0.50 and 0.67) (Ji and Ellis 1994) as high impact jumping, normal jumping, rhythmic exercise or high impact aerobics and low impact aerobics respectively. Human load intensity of 0.4 kPa performing the activity, on top of the dead and

imposed loads was simulated in the "activity panels". In cases where initial density had not given favourable responses below the limits human load density of 0.2 kPa performing the activity was used. The dead and the imposed loads used were assumed to be 3.5 kPa.

7.4 Damping for FE model

Four damping levels i.e. 1.6%, 3.0%, 6.0% and 12.0% identified in Section 5.3.3. were considered in this investigation. These damping levels were incorporated into the FE model by using an explicit damping matrix presented by Reyleigh (Clough and Penzien 1993). This required calculation of mass and stiffness proportional damping coefficients using the natural frequencies and damping levels. Table 7-1 presents the respective stiffness proportional damping *a* and mass proportional damping *b* coefficients used. The methodology of calculation of these values was presented in Section 5.3.4.

Table 7-1: Mass and stiffness proportional damping coefficients for configuration 2

	a	*b*
Damping 1.6%	0.00348869	0.0732
Damping 3.0%	0.00654129	0.1372
Damping 6.0%	0.01308258	0.2744
Damping 12.0%	0.02616517	0.5488

When calculating the above-mentioned coefficients the damping was assumed to remain unchanged in the first and second mode of vibration.

7.5 Pattern loading cases for configuration 2

Two pattern loading cases were identified for the current investigation and they are referred to as pattern loading 1, PL1-2 and pattern loading 2, PL2-2. The graphical illustrations of these two pattern loading cases are presented in Figure 7-1. Both pattern loading cases excite three panels, with PL1-2 exciting the consecutive three panels along the rib-spaning direction (refer to Figure 7-1a) and PL2-2 exciting three panels at traverse locations (Figure 7-1b). This configuration aimed to excite not only

the first mode of vibration but also the higher modes of vibration of the floor system. These modes of vibration were presented in Section 4.7.5.

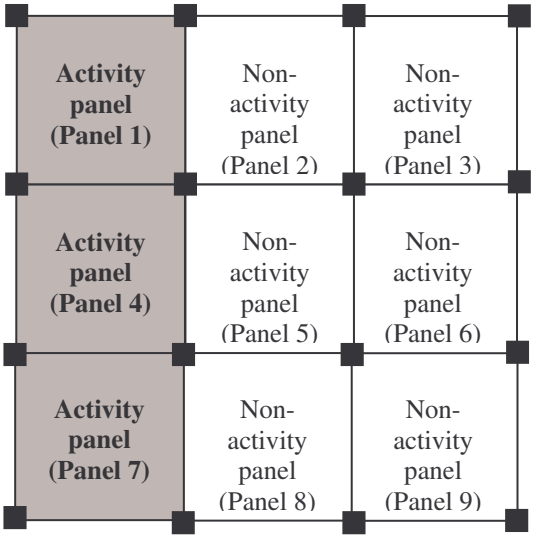

(a) Pattern loading 1 (PL1-2)

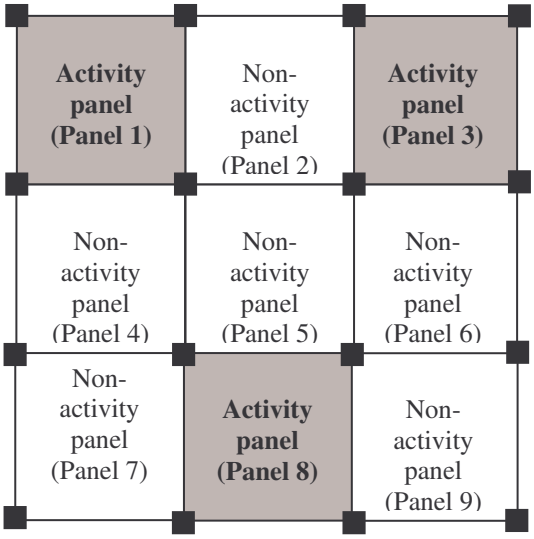

(c) Pattern loading 2 (PL2-2)

Figure 7-1: Patten loading cases for the 3 x 3 panel configuration

The shaded panels in Figure 7-1 were termed the "activity panels", which were referred to as the panels where the human dance-type event was simulated. Consequently, the other panels were used to fit-out various occupancies and were termed "non-activity panels". Herein, it was assumed that "non-activity panels" accommodate human-induced activities, which are less energetic, uncoordinated activities such as walking, running etc.

7.6 Serviceability state limits

The serviceability state limits were set and used as a compliance tool to verify the floors response for its intended purpose of occupancy and to fit-out occupancies. Two serviceability state limits were used for this cause, one is the most regularly used deflection limit for serviceability limit state (SLS) design or DAF limits. The other is the acceleration limits for human perceptibility. The latter was described in Section 6.6, where in Table 6-3, four occupancy categories were defined with various acceleration limits for human comfort. The same categories were used in this chapter to distinguish the suitable occupancies.

The DAF limits were obtained by static analysis for each pattern loading. The maximum allowable serviceability deflection Δ_{Max} is divided by the true serviceability static deflection Δ_{Static} to calculate DAF limits.

Unfactored loads for each pattern load case were applied statically over the entire floor and deflections at mid-span nodes on each panel were obtained. Herein, the live-load is considered as the static load posed by the occupants posing the activity (i.e. Q = 0.4 kPa and Q = 0.2 kPa). The dead load G for the current structure was assumed to be 3.5 kPa. Thus, this gave static deflections Δ_{Static} for each pattern loading case.

Serviceability deflection limits Δ_{Max} for composite floor design were reported to take as lesser of span/250 or 20 mm (British Standard : BS5950 : Part 4 1994; AS 3600 2001). The structural model used has a span of 8 m, which led to take the Δ_{Max} as 20 mm to calculate the serviceability deflection limits. Then, the DAF limits were established by considering two scenarios on each case of pattern loading i.e.:

1. DAF limits for panels, which caused the floor system to vibrate, termed "activity panels".
2. DAF limits for adjacent panels, which are being vibrated by the "activity panel", termed "non-activity panels".

This produced DAFs for the two locations and the DAF limits for individual pattern loads are presented in Table 7-2. It is important to note that the deflections used were averaged to yield a single value.

Table 7-2: DAF limits for activity panels and non-actively panels – Configuration 2

		Activity panel		Non-activity panel	
		Static Deflection	DAF Limit	Static Deflection	DAF Limit
Pattern loading 1 (PL1-2)	Q=0.4 kPa	-10.1	1.99	-8.9	2.24
	Q=0.2 kPa	-9.4	2.12	-8.8	2.26
Pattern loading 2 (PL2-2)	Q=0.4 kPa	-9.1	2.19	-9.1	2.19
	Q=0.2 kPa	-9.0	2.23	-8.9	2.23

The DAF limits in “activity panels” were of lower value than those of “non-activity panels” in all pattern loading cases. This was because the “non-activity panels” were deflected less to reach the maximum deflection.

7.7 Dynamic analysis – pattern loading 1 (PL1-2)

This section of the chapter presents results of dynamic amplifications and acceleration responses observed for the four human events under PL1-2. PL1-2 simulated dance-type loads on three panels; namely panel 1, panel 4 and panel 7 as seen in Figure 7-1. These panels were termed “activity panels”. The remaining six panels did not simulate any dynamic activity and thus were termed “non-activity panels”. The responses in each panel were averaged in their respective categories to reduce the complexity of presented results.

The variations of DAFs were plotted against the activity frequency for each human dance-type activity. The DAF limits presented in Section 7.6 for PL1-2 were plotted by a red discontinuous line for “activity panels” and by a blue discontinuous for “non-activity panels”.

The acceleration responses for each human event were plotted in human perceptibility scales. The maximum acceleration responses observed at different activity frequencies were used in these plots. Accordingly, occupancies from the five occupancies presented in Section 6.7 that complied with the acceleration limits and thus the human perceptibility were nominated.

7.7.1 High impact jumping activity – PL1-2

Figure 7-2 presents the variation of DAFs response with activity frequency when occupant density of 0.4 kPa is simulated under PL1-2.

The DAFs trends gave a complex profile with the maximum of 2.65 occurring at an activity frequency of 2.2 Hz in “activity panels” and “non-activity panels” respectively. Additional peaks in DAF responses were also observed at activity frequencies of 1.8 Hz and 2.7 Hz. These DAF responses were lower than the ones observed at activity frequency of 2.2 Hz. However, high impact jumping under PL1-

2, fell within the serviceability deflection limits when the "activity panels" had 6.0% or higher damping and "non-activity panels" had 3.0% or higher damping.

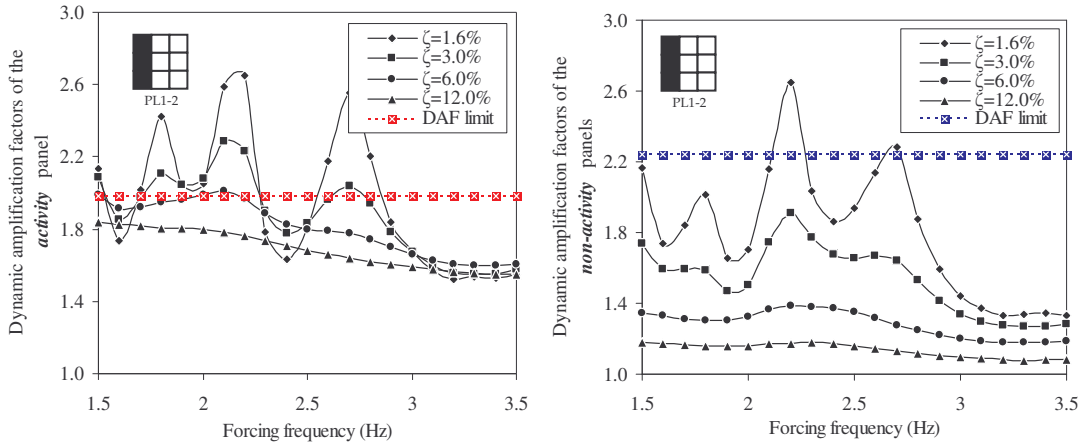

Figure 7-2: DAF response due to high impact jumping activity in PL1-2 for Q=0.4 kPa

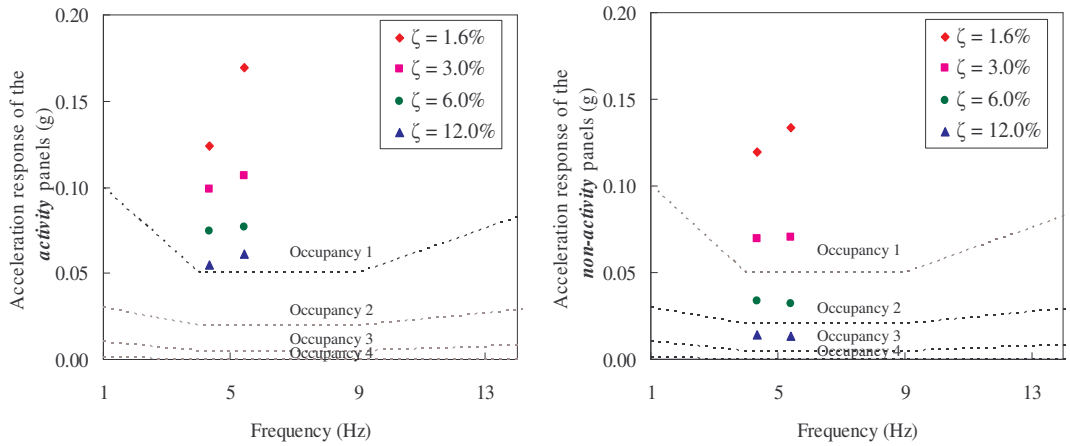

Figure 7-3: Acceleration response due to high impact jumping activity in PL1-2 for Q=0.4 kPa

In order to assess the human comfort due to high impact jumping, the acceleration responses observed at 2.4 Hz and 2.7 Hz were taken and plotted in the human-perceptibility scales as seen in Figure 7-3. It should be noted that the secondary peak acceleration response observed at 1.8 Hz was ignored as it was given lower values than the values obtained at 2.2 Hz and 2.7 Hz. This also reduced the complexity of presenting the results.

It can be observed that, though the "activity panels" would perform satisfactory at 6.0% or higher damping for serviceability deflection criteria. This level of damping may still cause discomfort to the occupants performing the activity. This was because the acceleration responses observed in "activity panels" did not perform within the

occupancy 1 limit, as shown in Figure 7-3. On the other hand, the "non-activity panels" can fit-out occupancy 2 provided with a damping level of 12.0%.

The dynamic analyses were performed again with a human density reduced by half to 0.2 kPa. The DAFs plots provided the trends shown in Figure 7-4 and the acceleration responses are presented in Figure 7-5.

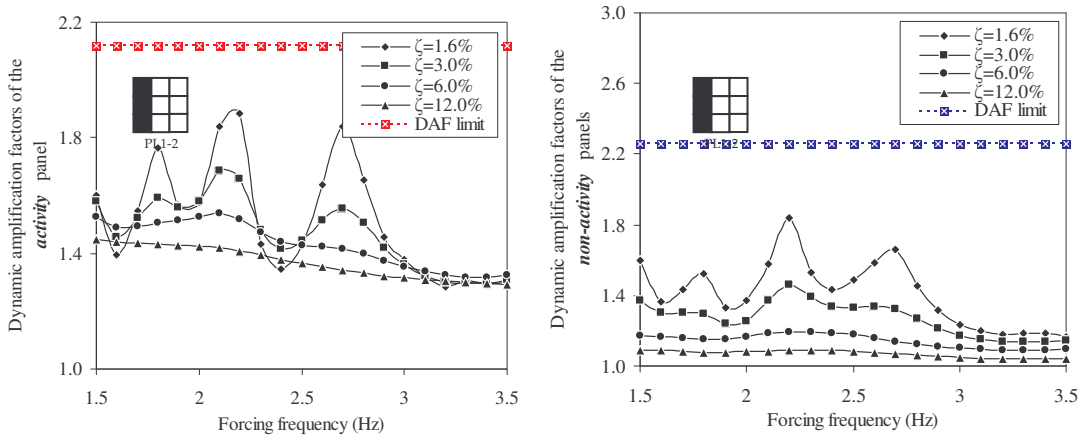

Figure 7-4: DAF response due to high impact jumping activity in PL1-2 for Q=0.2 kPa

With the reduced density of human performing the high impact jumping activity, the DAF responses floated well below the limits. However, peaks in responses were observed at 1.8 Hz, 2.2 Hz and 2.7 Hz with values of 1.76, 1.89 and 1.84 respectively. The acceleration response was given a similar trend with maximum occurring at 2.2 Hz and 2.7 Hz, which were used in the perceptibility plots presented in Figure 7-5.

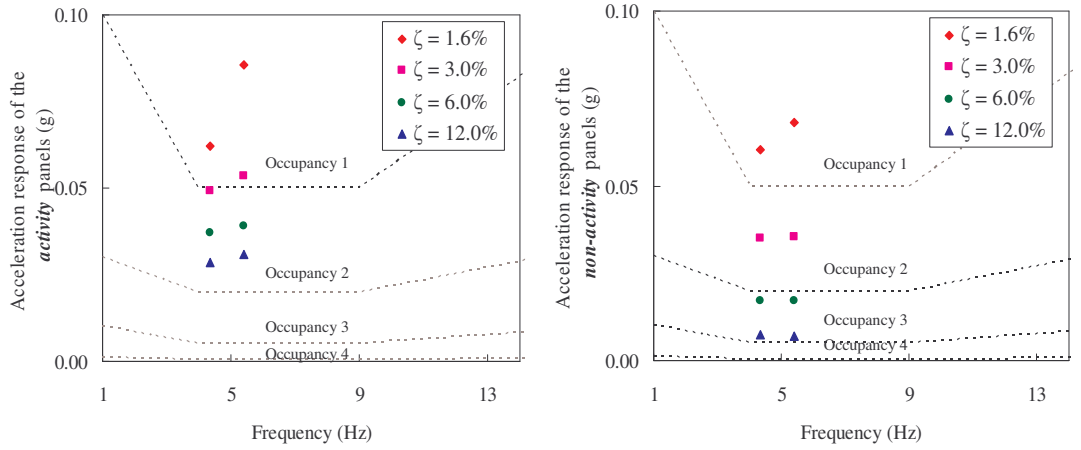

Figure 7-5: Acceleration response due to high-jumping activity in PL1-2 for Q=0.2 kPa

The acceleration response showed that "activity panels" can fit-out occupancy 1, with 6.0% or higher damping. The "non-activity panels" can fit-out occupancy 2 when 6.0% or higher damping is provided. Thus, occupant density of 0.2 kPa (3.5 m^2 per person) performing the high impact jumping under PL1-2 with 6.0% damping is recommended.

7.7.2 Normal jumping activity – PL1-2

The DAF responses observed for normal jumping activity of occupant density of 0.4 kPa are presented in Figure 7-6.

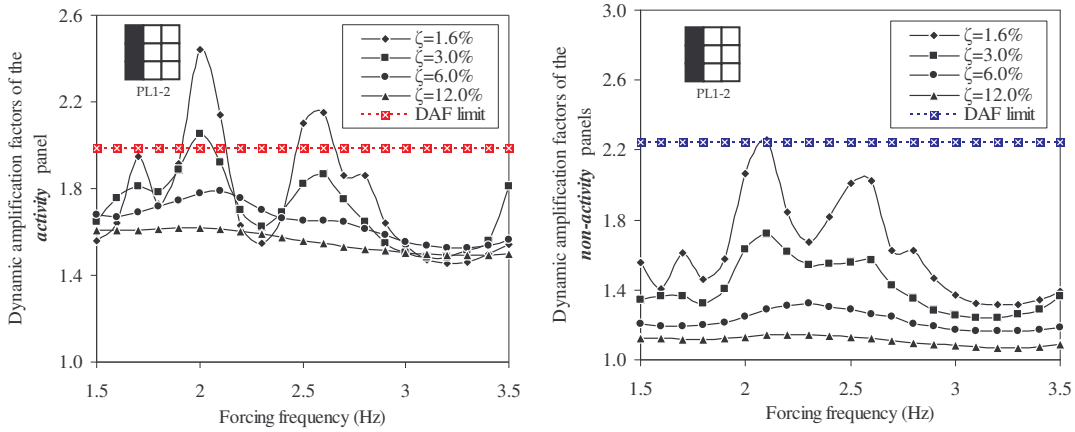

Figure 7-6: DAF response due to normal jumping activity in PL1-2 for Q=0.4 kPa

For normal jumping activity the maximum DAFs observed were 2.14 and 2.26 in "activity panels" and "non-activity panels" respectively, both occurring at 1.6% damping level at an activity frequency of 2.1 Hz. Secondary peaks were also observed at activity frequencies of 1.8 Hz and 2.7 Hz. Although, these secondary peaks were not distinct at damping levels of 6.0% and 12.0%, they only occurred at lower damping levels of 1.6% and 3.0%. However, normal jumping of human density 0.4 kPa posing the activity in "activity panels" were within the serviceability deflection limits when "activity panels" with 6.0% or higher damping and "non-activity panels" with 1.6% or higher damping were used.

In order to assess the level of human discomfort and fit-outs, the maximum acceleration responses were plotted in human-perceptibly scales. Figure 7-7 described below, presents the maximum acceleration responses observed at activity frequencies of 2.1 Hz and 2.7 Hz.

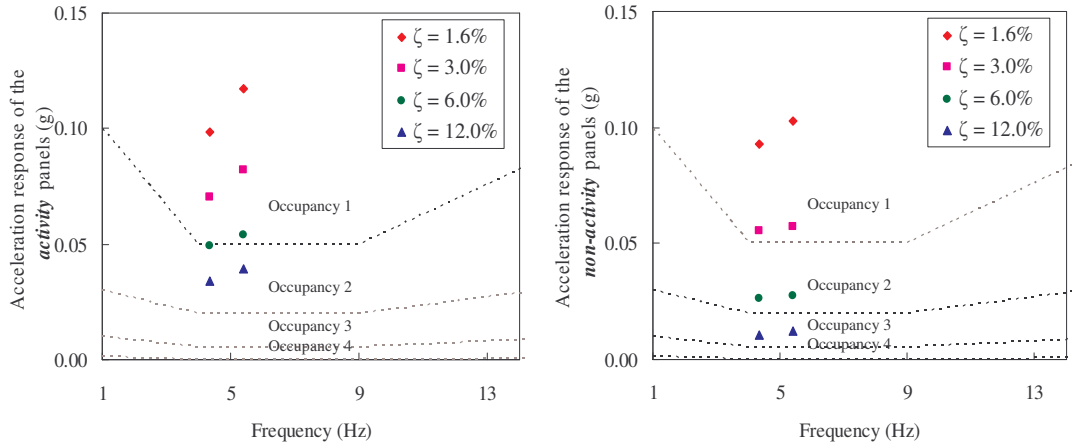

Figure 7-7: Acceleration response due to normal jumping activity in PL1-2 for Q=0.4 kPa

It was observed that the "activity panels" with 12.0% or higher damping would be within the human perceptibility limits. Lesser damping levels yielded discomfort to the occupants. In the case of "non-activity" panels, occupancy 2 can be fitted-out when 12.0% or higher damping is provided. However, neither occupancy 3 nor occupancy 4 can be fitted-out under the circumstances described in this section.

The responses for the normal jumping activity by human density of 0.2 kPa in "activity panels" were obtained. Figure 7-8 presents the DAF response observed for the human density of 0.2 kPa posing the activity in "activity panels".

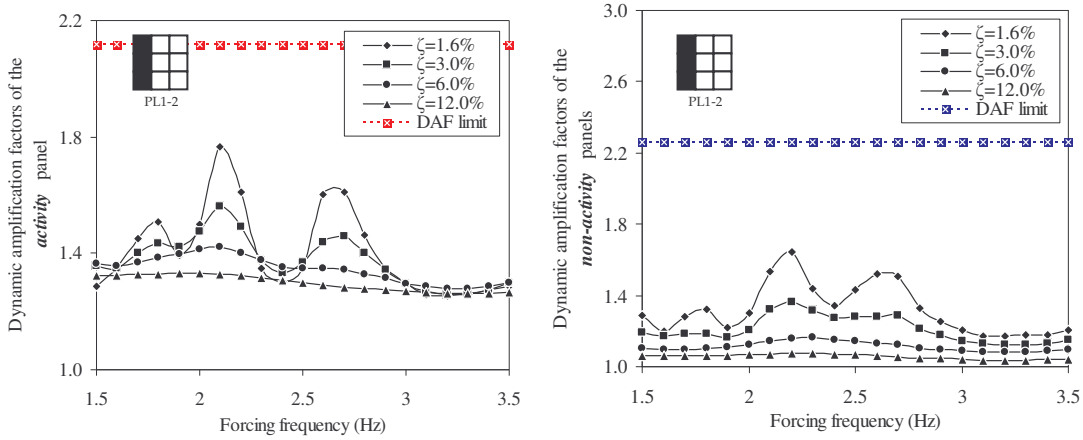

Figure 7-8: DAF response due to normal jumping activity in PL1-2 for Q=0.2 kPa

This human-density performed well within the severability deflection limits. Similar to the previous load density of 0.4 kPa, peaks in acceleration responses occurred at activity frequency of 1.8 Hz, 2.2 Hz and 2.7 Hz and were used to critique the

occupancy fit-out. Figure 7-9 presents the maximum acceleration responses, observed at 2.2 Hz and 2.7 Hz in human perceptibility scales.

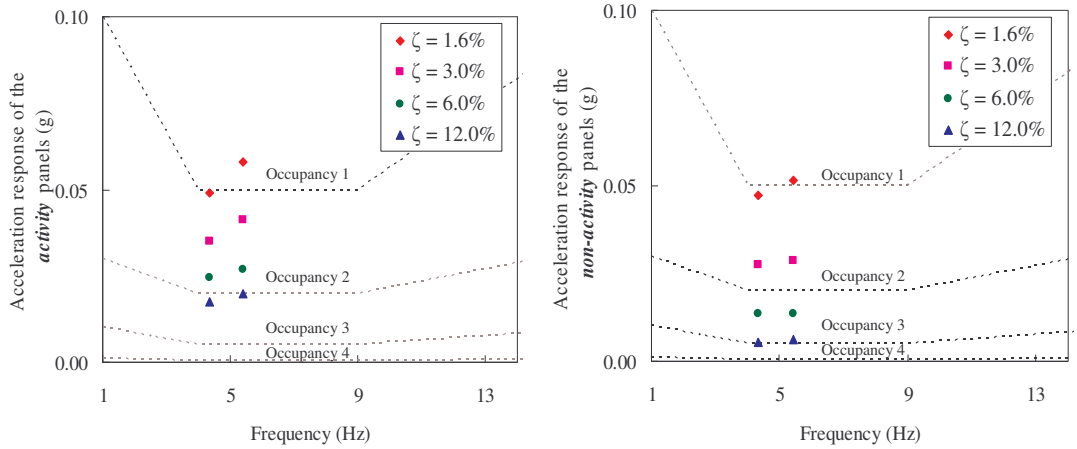

Figure 7-9: Acceleration response due to normal jumping activity in PL1-2 for Q=0.2 kPa

The reduction in human-density performing the current activity improved the performance of the structure allowing to fit-out occupancy 1 at 3.0% or higher damping in the "activity panels". The "non-activity panels" were able fit-out to occupancy 2, with 6.0% or higher damping, which is improvement from 12.0% observed in the 0.4 kPa density.

In summary for normal jumping activity under PL1-2, it is advisable to have a human density of 0.2 kPa (3.5 m^2/person) in the "activity panels". This allowed to fit-out occupancy 2 in "non-activity panels" at 6.0% or higher damping. Human density of 0.4 kPa (1.75 m^2/person) has caused vibration problems and requires to provide other means of mitigating the excessive responses.

7.7.3 Rhythmic exercise / high impact aerobics – PL1-2

The DAF responses observed for rhythmic exercise / high impact aerobics of contact ratio 0.50 by a human density of 0.4 kPa is presented in Figure 7-10.

The rhythmic exercise / high impact aerobics described by contact ratio of 0.50 gave DAFs which were within the serviceability deflection limits for both "activity panels" and "non-activity panels". However, two peaks in responses were seen with one occurring at 2.1 Hz and the other occurring at 2.7 Hz. The maximum DAFs

observed were 1.74 in the "activity panels" and 1.68 in the "non-activity panels". Similar trends in acceleration response were observed with peaks occurring near 2.1 Hz and 2.7 Hz. These peak responses were plotted in the human-perceptibly scales for assessment in human comfort. Figure 7-11 presents these plots in "activity panels" and "non-activity panels".

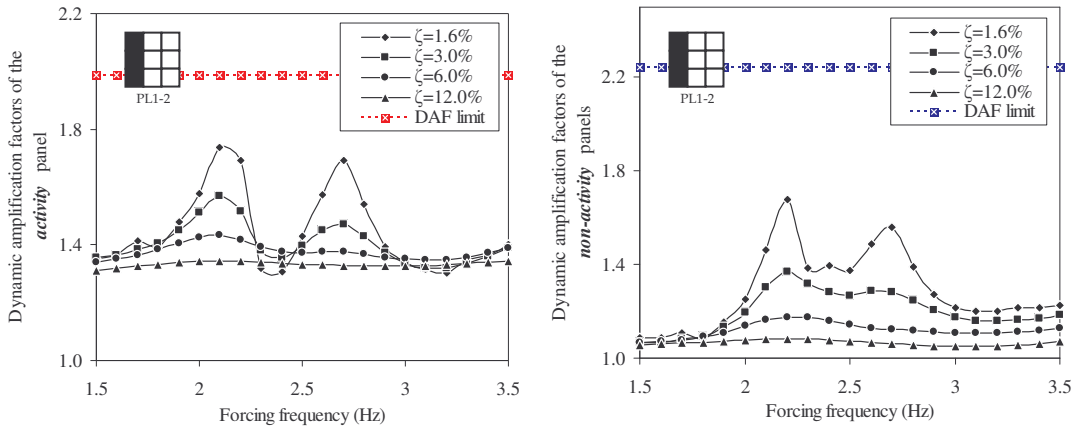

Figure 7-10: DAF response due to rhythmic exercise / high impact aerobics activity in PL1-2 for Q=0.4 kPa

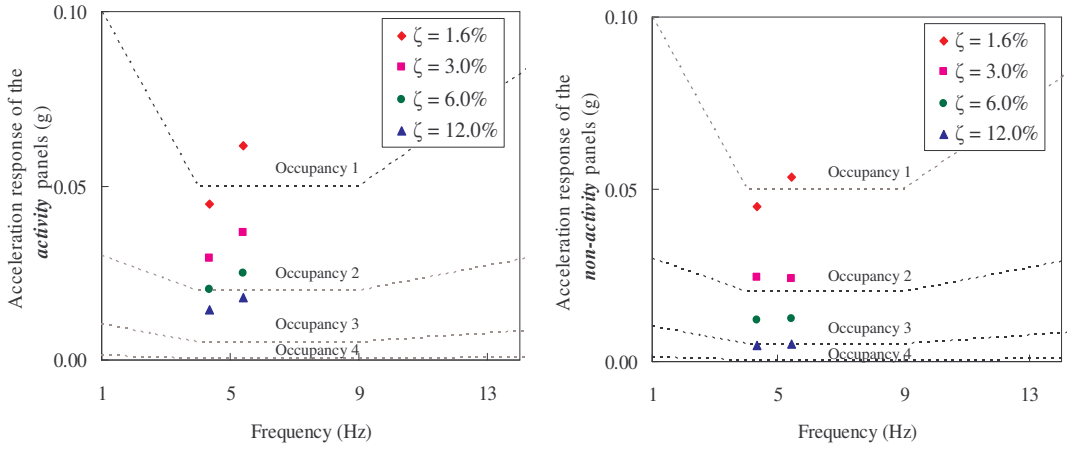

Figure 7-11: Acceleration response due to rhythmic exercise / high impact aerobics activity in PL1-2 for Q=0.4 kPa

It was observed that the activity panels with 3.0% or higher damping can be fit-out to occupancy 1. The "non-activity panels" are able to occupy occupancy 2 when 6.0% or higher damping is provided. However, it was observed that the adjacent floor panels will not meet the limits of acceleration for the other two occupancies,

described by occupancy 3 and occupancy 4, for the event of rhythmic exercise / high impact aerobics activity.

7.7.4 Low impact aerobics – PL1-2

Low impact aerobics described by the human activity contact ratio of 0.67 by a human density of 0.4 kPa, gave the DAF trends in Figure 7-12.

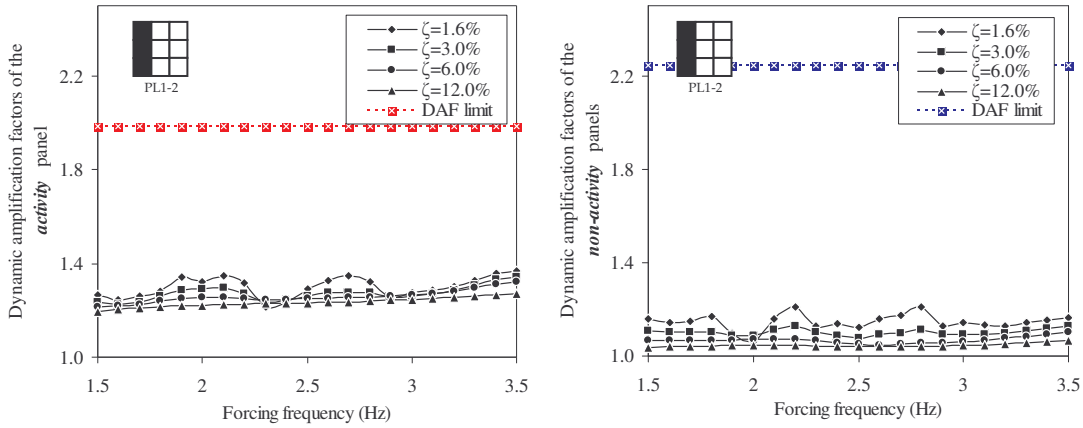

Figure 7-12: DAF response due to low impact aerobics activity in PL1-2 for Q=0.4 kPa

With the maximum DAFs of 1.35 in "activity panels" and 1.21 in "non-activity panels" low impact aerobics did not exceeded the serviceability deflection limits. However, peaks in response were observed at 1.8 Hz, 2.2 Hz and 2.7 Hz. Similarly the acceleration responses gave peaks in the above activity frequencies and the results are plotted in the human-perceptibility scales in Figure 7-13.

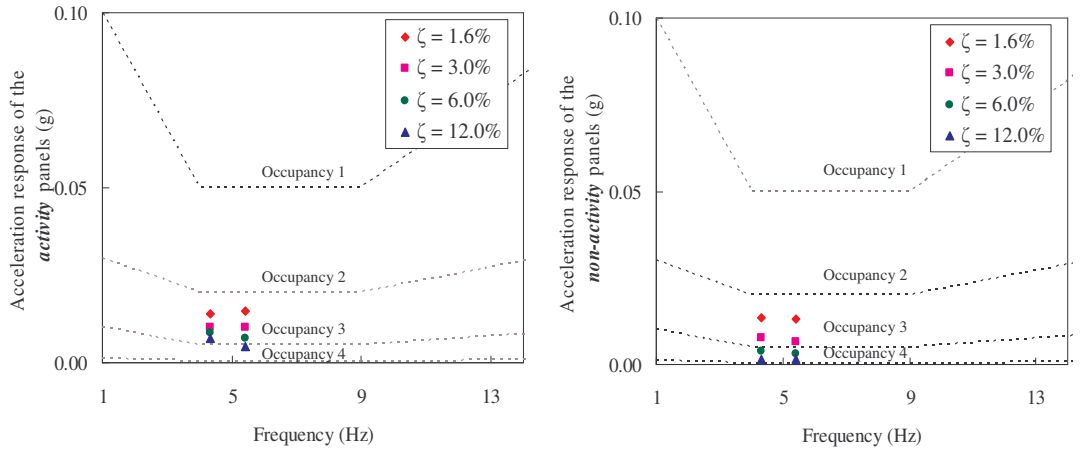

Figure 7-13: Acceleration response due to low impact aerobics activity in PL1-2 Q=0.4 kPa

It was observed that occupancy 1 can be fitted to the "activity panels" under 1.6% or higher damping, without causing any problems in human comfortability. The "activity panels" can accommodate occupancy 2 at 1.6% or higher damping and occupancy 3 at 6.0% or higher damping.

7.7.5 Results summary and discussion for PL1-2

The results under PL1-2 provided a mixed response with respect to deflection and accelerations. These responses varied with the different dance-type loads, activity densities, activity frequencies and structural damping, with more onerous activities in low structural damping conditions giving serviceability problems. However, it should be stressed that such responses can only occur at continuous excitation event which is unlikely from a practical point of view. Also such cases can occur only for a short period of time. The most interesting responses observed under this pattern loading case were the sudden peaks, which occurred regardless of the type of event. In fact, three such peaks were more prominent - occurring at 1.8 Hz, 2.1 Hz and 2.7 Hz. However, the latter two frequencies gave the deciding dynamic responses with the maximum occurring at 2.1 Hz. Typical Fourier amplitude spectrum of an acceleration response of 2.1 Hz activity frequency is presented in Figure 7-14. This Fourier amplitude spectrum gave peak at frequency of 4.2 Hz, which related to the first natural frequency of the floor system. Consequently it was concluded that the floor vibrated in its first mode shape.

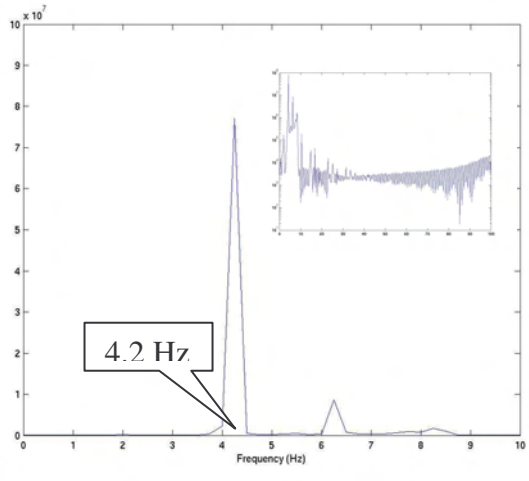

Figure 7-14: Typical Fourier amplitude spectrum for PL1-2 at contact ratio of 0.25 & 1.6% damping

In summary, damping levels, activity types and activity densities that complied with the serviceability deflection criteria under PL1-2 are presented in Table 7-3.

Table 7-3: Operating conditions for serviceability deflection - pattern loading 1 (PL1-2)

Dance-type activity in AP	Human density in AP	AP	NAP
High impact jumping	0.4 kPa	$\zeta > 6.0\%$	$\zeta > 3.0\%$
	0.2 kPa	$\zeta > 1.6\ \%$	$\zeta > 1.6\ \%$
Normal jumping	0.4 kPa	$\zeta > 6.0\%$	$\zeta > 1.6\%$
	0.2 kPa	$\zeta > 1.6\ \%$	$\zeta > 1.6\ \%$
Rhythmic exercise / high impact aerobics	0.4 kPa	$\zeta > 1.6\ \%$	$\zeta > 1.6\ \%$
Low impact jumping	0.4 kPa	$\zeta > 1.6\ \%$	$\zeta > 1.6\ \%$

Table 7-4: Occupancy fit-out for human comfortability – pattern loading 1 (PL1-2)

Dance-type activity in AP	Human density in AP	AP	NAP
High impact jumping	0.4 kPa	Occupancy 0	Occupancy 2 $\zeta > 12.0\%$
	0.2 kPa	Occupancy 1 $\zeta > 6.0\%$	Occupancy 2 $\zeta > 6.0\%$
Normal jumping	0.4 kPa	Occupancy 1 $\zeta > 12.0\%$	Occupancy 2 $\zeta > 12.0\%$
	0.2 kPa	Occupancy 1 $\zeta > 3.0\%$	Occupancy 2 $\zeta > 6.0\%$
Rhythmic exercise / high impact aerobics	0.4 kPa	Occupancy 1 $\zeta > 3.0\%$	Occupancy 2 $\zeta > 6.0\%$
Low impact jumping	0.4 kPa	Occupancy 1 $\zeta > 1.6\%$	Occupancy 2 $\zeta > 1.6\%$ Occupancy 3 $\zeta > 6.0\%$

Occupancy 0	Uncomfortable
Occupancy 1	Rhythmic activities / aerobics / dance- type loads
Occupancy 2	Shopping malls (centres) / dining and dancing / weightlifting / Stores / manufacturing / warehouse / walkaways / stairs
Occupancy 3	Office / residencies / hotels / multi - family apartments / school rooms / libraries
Occupancy 4	Hospitals / laboratories / critical working areas (e.g. operating theatres, precision laboratories)

It must be noted that the above densities and damping levels were not sufficient for human perceptibility. Thus, the acceleration responses were observed for their compliance with human perceptibility criteria. Table 7-4 summarises the human densities, activity types and damping levels that complied with the acceleration limits. It also presents the possible occupancy fit-outs that occur under PL1-2.

The high impact jumping of human density of 0.4 kPa gave unfavourable responses that caused discomfort to the occupants. Same activity performed at a reduced density required 6.0% or higher damping. In the same way, normal jumping of human density of 0.4 kPa required damping levels of 12.0%. However, its performance at a reduced density of 0.2 kPa yielded damping level of 3.0%. Meanwhile, the other activities performed at a density of 0.4 kPa did not give problematic responses as the required damping levels can be achieved using non-structural elements, flooring materials, carpets etc.

In conclusion, it can be stated that with proper human density posing the activity and appropriate damping levels, the structural responses occurring after a human-excitation event under PL1-2 can be brought down to acceptable human comfort levels.

7.8 Dynamic analysis – pattern loading 2 (PL2-2)

This section of the chapter presents the responses of the nine panel model subjected to human-induced activities under PL2-2. PL2-2 constituted three panels simulating human-induced activities and the remaining six panels not simulating any activity. The deflection and acceleration responses were observed for different damping levels, human-densities and type of activity. The results are presented in two scenarios described by “activity panels” and “non-activity panels”, reducing the complexity of presenting the results.

The variations of DAFs were plotted against the activity frequency for dance-type human activity. The DAF limits presented in Section 7.6 for PL2-2 were used in these plots which were a discontinuous red line for “activity panels” and a discontinuous blue line for “non-activity panels”.

The acceleration responses for each human-event were plotted in human-perceptibility scales. The maximum acceleration responses observed at different activity frequencies were used in these plots. Accordingly, occupancies that complied with the acceleration criteria have been nominated from the five occupancies in Section 6.7.

7.8.1 High impact jumping activity – PL2-2

The variation of DAF responses with activity frequency observed for high impact jumping activity by a human density of 0.4 kPa is presented in Figure 7-15.

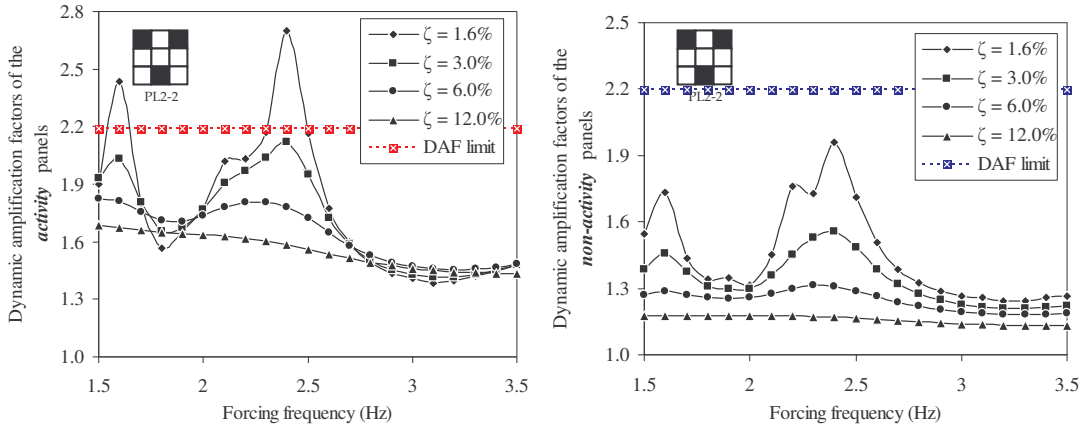

Figure 7-15: DAF response due to high impact jumping activity in PL2-2 for Q=0.4 kPa

The trends gave the maximum DAF of 2.70 in "activity panels" and 1.90 in "non-activity panels". These maximum DAFs were occurring at an activity frequency of 2.4 Hz and at 1.6% or higher damping levels. Additional peaks in DAF responses were observed at activity frequencies of 1.6 Hz and 2.2 Hz. High impact jumping activity by human density of 0.4 kPa under PL2-2, fell within the serviceability deflection limits for "activity panels" with 6.0% or higher damping and for "non-activity panels" with all damping levels.

The acceleration responses for the current activity in the activity panels gave similar trends with peaks occurring at 1.6 Hz, 2.2 Hz and 2.4 Hz. However the maximum response was observed at activity frequency of 2.4 Hz and was used in the perceptibility scales in Figure 7-16.

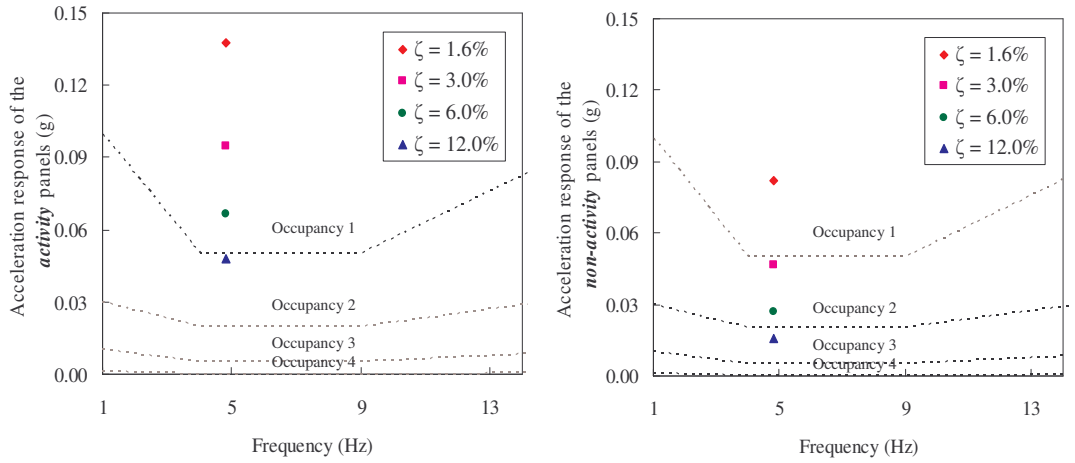

Figure 7-16: Acceleration response due to high impact jumping activity in PL2-2 for Q=0.4 kPa

In order to fit-out occupancy 1 the acceleration responses in perceptibility scales yielded 12.0% or higher damping in the "activity panels". The "non-activity panels" were able to fit-out occupancy 2 with 12.0% or higher damping. However, 12.0% damping in the "activity panels" may not be achievable by the occupants and thus may create discomfort to the occupants. Therefore, a reduced density of occupants posing the activity was studied. Herein an occupant density of 0.2 kPa was investigated. Figure 7-17 describes the variation of DAFs with the activity frequency.

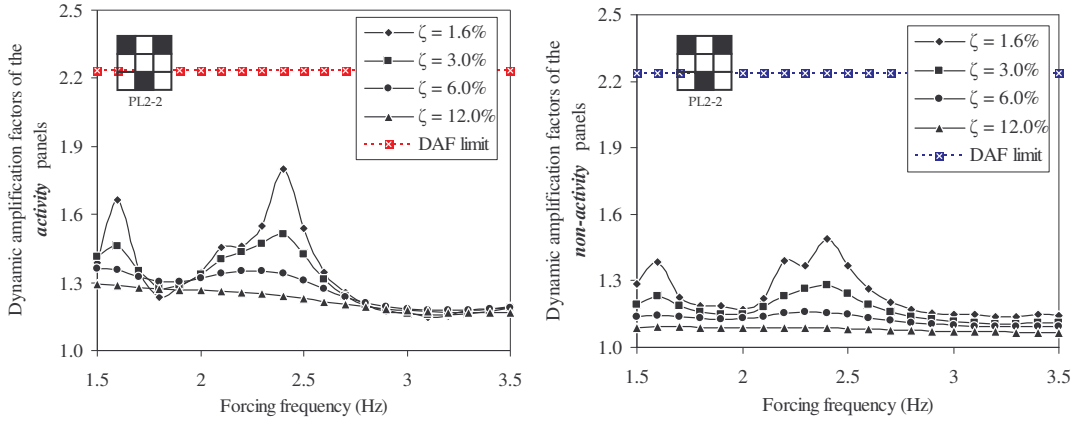

Figure 7-17: DAF response due to high impact jumping activity in PL2-2 for Q=0.2 kPa

The occupant density of 0.2 kPa posing the activity in the "activity panels" yielded the DAFs within the serviceability deflection limits at all damping levels and activity frequencies, unlike the previous human density. However, the peaks in responses of 1.80 and 1.49 were observed at an activity frequency of 2.4 Hz in "activity panels" and "non-activity panels" respectively. Secondary peak was also observed at an

activity frequency of 1.6 Hz. The acceleration responses gave similar trends to that of DAF trends, with primary and secondary maximum responses occurring at activity frequencies of 2.4 Hz and 1.6 Hz respectively. The primary maximum response at 2.4 Hz was plotted in the perceptibility scales in Figure 7-18 to fit-out the occupancies.

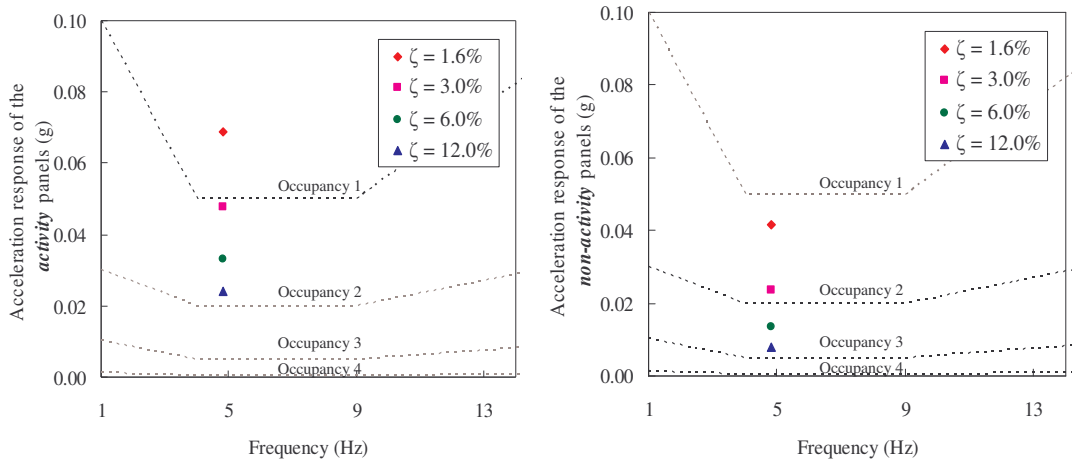

Figure 7-18: Acceleration response due to high impact jumping activity in PL2-2 for Q=0.2 kPa

The acceleration responses in the perceptibility scales resulted in occupancy 1 in "activity panels" with a damping level of 6.0% or higher. In the case of "non-activity panels", these can be fit-out to occupancy 2 with damping levels of 6.0% or higher.

In conclusion, for high impact jumping in PL2-2, an occupant density of 0.2 kPa with appropriate level of damping of at least 6.0%, for human conformability in both activity and non-activity panels is recommended.

7.8.2 Normal jumping activity – PL2-2

The variation of DAF responses observed for normal jumping of human density of 0.4 kPa is presented in Figure 7-19.

The DAF responses for normal jumping activity gave maximum DAFs of 2.38 and 1.77 in "activity panels" and "non-activity panels" respectively. The maximum DAF was observed at 2.4 Hz. Similar to the previous cases, secondary peak was observed at an activity frequency of 1.6 Hz. It was observed that the "activity panels" were

well within the serviceability deflection limits when 3.0% or higher damping was applied. The "non-activity panels" were within the limits at all damping levels.

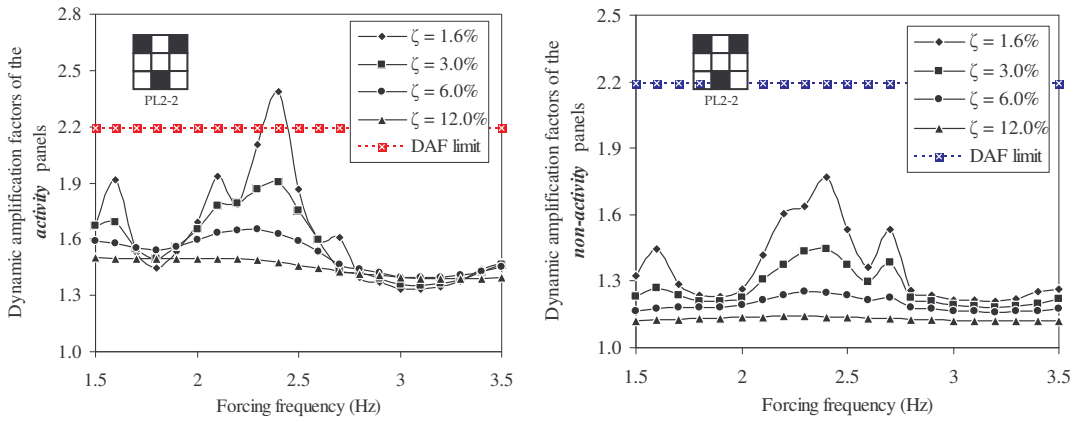

Figure 7-19: DAF response due to normal jumping activity in PL2-2 for Q=0.4 kPa

The acceleration responses gave similar trends to those of DAF responses, with peaks occurring at an activity frequency of 1.6 Hz and 2.4 Hz. The response at activity frequency 2.4 Hz gave the maximum acceleration and thus used in the perceptibility plots shown in Figure 7-20.

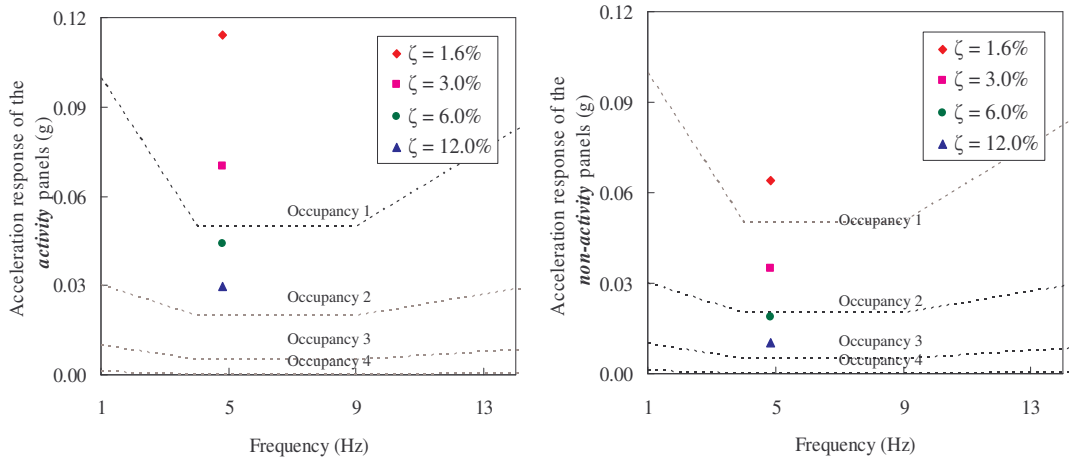

Figure 7-20: Acceleration response due to normal jumping activity in PL2-2 for Q=0.4 kPa

The acceleration responses allowed to fit-out the normal jumping activity in the "activity panels" in the presence of 6.0% or higher damping. In the case of "non-activity panels", these were able to fit-out occupancy 2 at 6.0% or higher damping. These damping levels were used for the human-density of 0.4 kPa posing the activity in the "activity panels". Lower human density of 0.2 kPa posing the activity in the

"activity panels" was investigated also. Figure 7-21 presents the variation of DAF responses with the activity frequency for this lower human density.

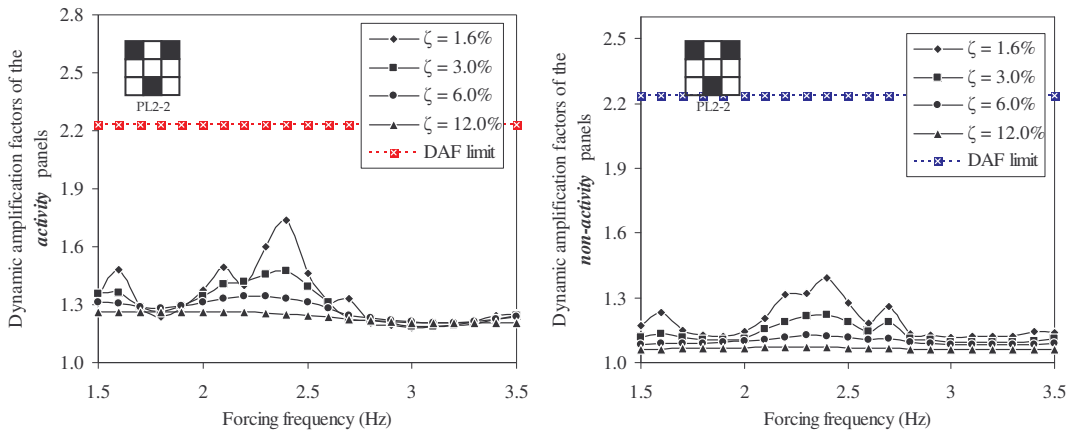

Figure 7-21: DAF response due to normal jumping activity in PL2-2 for Q=0.2 kPa

With maximum peak of 1.74 in "activity panels" and 1.39 in "non-activity panels", the floor system performed within the serviceability deflection limits at all damping levels. However, peaks in DAFs occurred at activity frequencies of 2.4 Hz and 1.6 Hz. The acceleration responses gave similar trends with peaks occurring at 2.4 Hz and are plotted in the perceptibility scales in Figure 7-22.

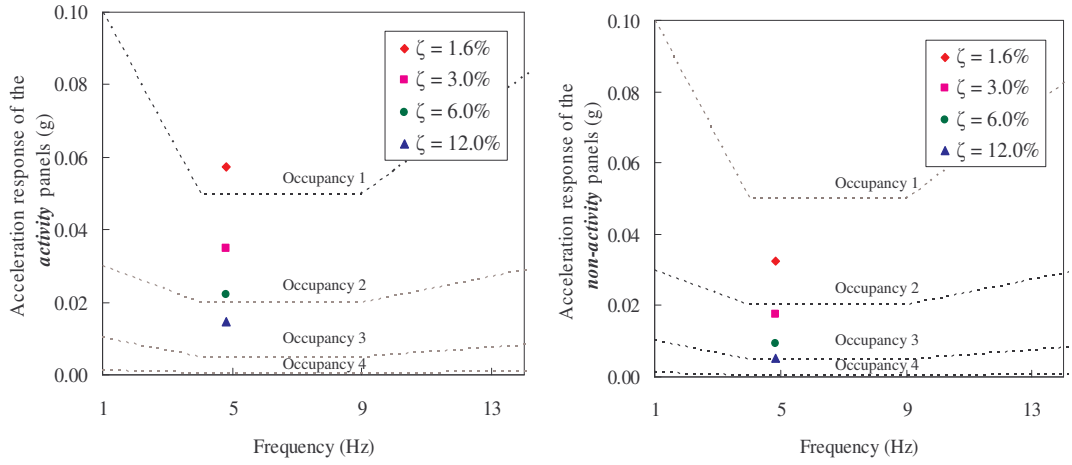

Figure 7-22: Acceleration response due to normal jumping activity in PL2-2 for Q=0.2 kPa

Plots in Figure 7-22 illustrate, that normal jumping activity can be performed in the "activity panels" at damping level of 3.0% or higher. In the case of "non-activity panels", it can fit-out to occupancy 2 at 3.0% or higher damping levels as well.

In conclusion, the normal jumping activity performed in PL2-2, requires occupant density of 0.2 kPa to avoid human discomfort.

7.8.3 Rhythmic exercise / high impact aerobics – PL2-2

The rhythmic exercise / high impact aerobics by human density of 0.4 kPa in PL2-2 gave the variations of DAF as seen in Figure 7-23.

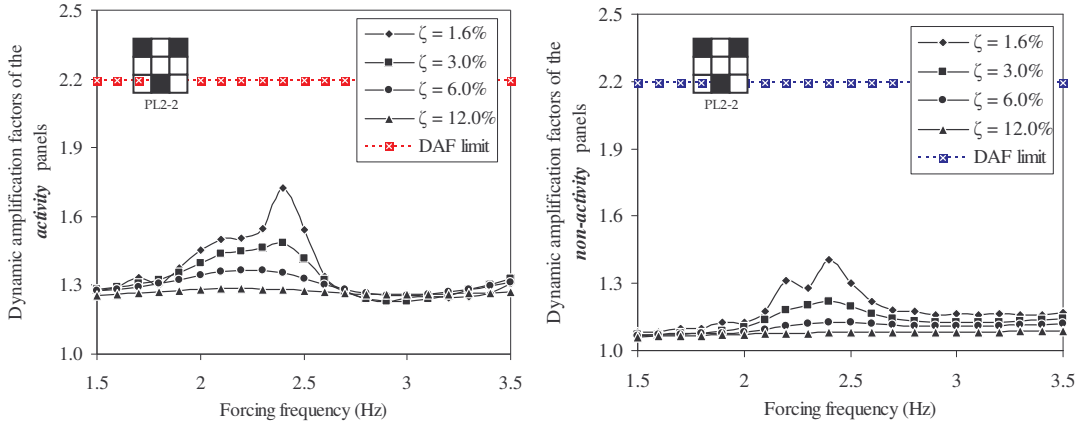

Figure 7-23: DAF response due to Rhythmic exercise / high impact aerobics activity in PL2-2 for Q=0.4 kPa

The rhythmic exercise / high impact aerobics gave DAFs within the limits at all damping levels. This is because this event is less energetic than the previous two activities. This event gave maximum DAFs of 1.72 in "activity panels" and 1.41 in "non-activity panels". These maximum responses were observed at an activity frequency of 2.4 Hz. Similar observations were also found in the acceleration responses. The peaks in responses at the activity frequency of 2.4 Hz are plotted in the perceptibility scales and presented in Figure 7-24.

The rhythmic exercise / high jumping aerobics in the "activity panels" resulted in human conformability with damping levels more than 3.0%. In the case of "non-activity panels", those can be fit-out to occupancy 2, with 3.0% or higher damping and also to occupancy 3 with 12.0% or higher damping.

Finally, it can be concluded that occupant density of 0.4 kPa in the "activity panels" posing the rhythmic exercise / high jumping activity gave responses that were within the limits of human perceptibility. With appropriate damping levels in the "non-activity panels" the floor system it can be fit-out to occupancy 2 and occupancy 3.

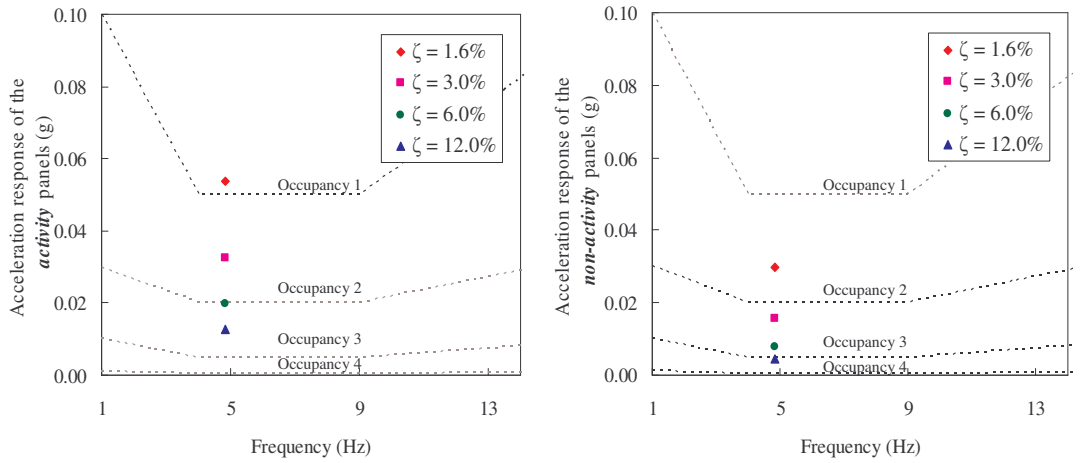

Figure 7-24: Acceleration response due to rhythmic exercise / high impact aerobics activity in PL2-2 for Q=0.4 kPa

7.8.4 Low impact aerobics – PL2-2

The variations of DAFs with respect to activity frequency due to low impact aerobics in activity panels are presented in Figure 7-25. Since the event was the least onerous activity compared to the previous activities the DAFs were within the serviceability deflection limits. However the peaks in responses were observed at activity frequency of 2.4 Hz which gave maximum DAFs of 1.31 and 1.14 in the "activity panels" and "non-activity panels" respectively.

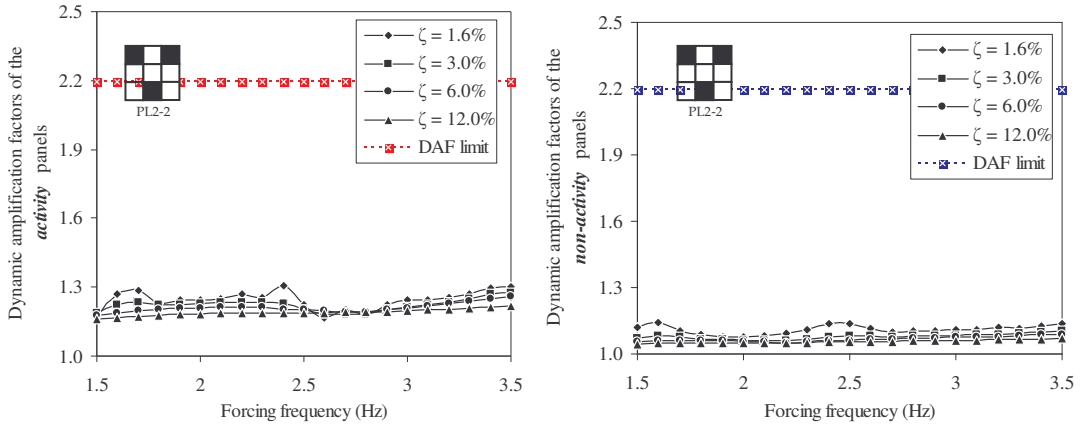

Figure 7-25: DAF response due to low impact aerobics activity in PL2-2 for Q=0.4 kPa

The acceleration responses also gave similar trends with peaks in responses occurring at activity frequency of 2.4 Hz. This acceleration response was plotted in the perceptibility scales in Figure 7-26 to identify the occupancies suited.

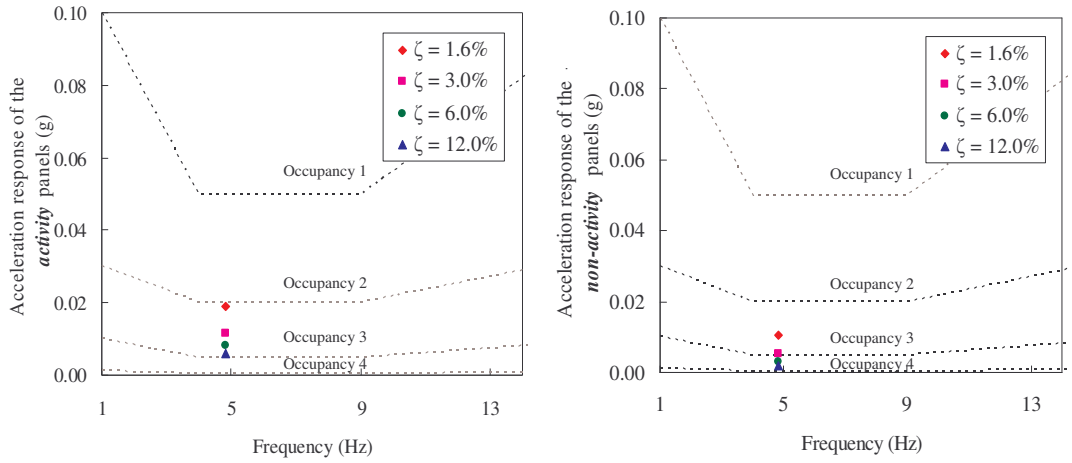

Figure 7-26: Acceleration response due to low impact aerobics activity in PL2-2 for Q=0.4 kPa

The acceleration response allowed performing low impact aerobics in the "activity panels" at any of the damping levels without causing any discomfort to the occupants. The "non-activity panels" fit-out occupancy 2, for all damping levels.

In conclusion, it can be stated that low impact aerobics activity of occupant density of 0.4 kPa gave lower damping levels in "activity panels" and was able to fit-out occupancy 2 and occupancy 3 with appropriate damping in the "non-activity panels".

7.8.5 Results summary and discussion for PL2-2

PL2-2 similarly to PL1-2 gave mixed dynamic responses that did and did not exceed the serviceability limits. Those were varying with different dance-type activities, activity densities, activity frequencies and structural damping.

The peaks in responses, in both DAFs and acceleration, were found at activity frequencies of 1.6 Hz and 2.4 Hz. Fourier Amplitude spectrums of acceleration responses at these frequencies were observed to identify the resonance frequency. Typical Fourier amplitude spectrum of acceleration responses for activity frequency of 1.6 Hz and 2.4 is depicted in Figure 7-27 and Figure 7-28 respectively.

Fourier amplitude spectrums' peaks at frequency of 4.8 Hz were found in both cases of activity frequencies of 1.6 Hz and 2.4 Hz. The frequency of 4.8 Hz relates to the second natural frequency of the floor system. Thus, it is evident that due to the PL2-2 the floor system vibrated in its second mode shape. Consequently the second and third harmonic of the activity frequency caused to excite second mode of the floor

system. As a result, the floor system responded beyond both the serviceability defection limits as well as the human perceptibility limits.

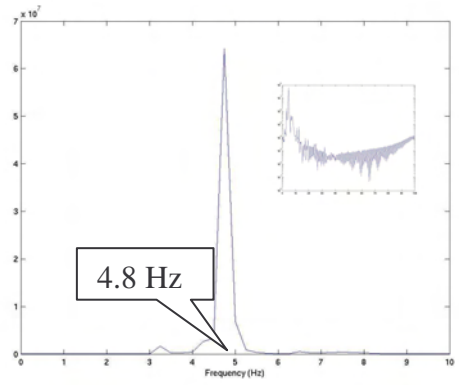

Figure 7-27: Typical Fourier amplitude spectrum for PL2-2 at contact ratio of 0.25 at 1.6 Hz & 1.6% damping

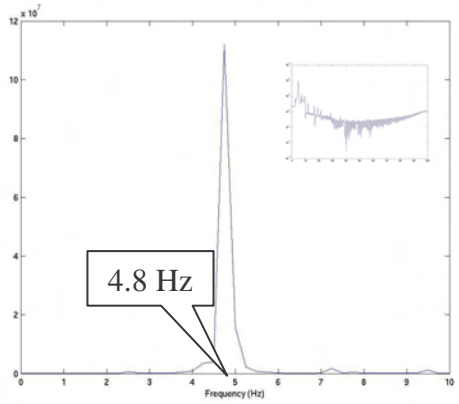

Figure 7-28: Typical Fourier amplitude spectrum for PL2-2 at contact ratio of 0.25 at 2.4 Hz & 1.6% damping

In summary, the human-activities that resulted in compliance with the serviceability deflection criteria with the damping levels and densities in both activity and non-activity panels in PL2-2 are presented in Table 7-5.

The human density of 0.4 kPa posing the activity in the "activity panels" was possible when performing the high impact jumping at 6.0% or higher damping and normal jumping at 3.0% or higher damping. Apart from these two cases, all the other densities and activities gave satisfactory performance for serviceability deflection criteria under all the damping levels.

Table 7-5: Operating conditions for serviceability deflection in PL2-2

Dance-type activity AP	Human density in AP	AP	NAP
High impact jumping	0.4 kPa	$\zeta > 6.0\%$	$\zeta > 1.6\ \%$
	0.2 kPa	$\zeta > 1.6\ \%$	$\zeta > 1.6\ \%$
Normal jumping	0.4 kPa	$\zeta > 3.0\%$	$\zeta > 1.6\ \%$
	0.2 kPa	$\zeta > 1.6\ \%$	$\zeta > 1.6\ \%$
Rhythmic exercise / high impact aerobics	0.4 kPa	$\zeta > 1.6\ \%$	$\zeta > 1.6\ \%$
Low impact jumping	0.4 kPa	$\zeta > 1.6\ \%$	$\zeta > 1.6\ \%$

Table 7-6 presents the summary of the occupancy fit-outs along with the damping, human-density and the human-activity that did not cause discomfort to the occupants.

Table 7-6: Occupancy fit-out for human comfortability in PL2-2

Dance-type activity in AP	Human density in AP	AP	NAP
High impact jumping	0.4 kPa	Occupancy 1 $\zeta > 12.0\%$	Occupancy 2 $\zeta > 12.0\%$
	0.2 kPa	Occupancy 1 $\zeta > 6.0\%$	Occupancy 2 $\zeta > 6.0\%$
Normal jumping	0.4 kPa	Occupancy 1 $\zeta > 6.0\%$	Occupancy 2 $\zeta > 6.0\%$
	0.2 kPa	Occupancy 1 $\zeta > 3.0\%$	Occupancy 2 $\zeta > 6.0\%$
Rhythmic exercise / high impact aerobics	0.4 kPa	Occupancy 1 $\zeta > 3.0\%$	Occupancy 2 $\zeta > 3.0\%$ Occupancy 3 $\zeta > 12.0\%$
Low impact jumping	0.4 kPa	Occupancy 1 $\zeta > 1.6\%$	Occupancy 2 $\zeta > 1.6\%$ Occupancy 3 $\zeta > 3.0\%$

Occupancy 0	Uncomfortable
Occupancy 1	Rhythmic activities / aerobics / dance- type loads
Occupancy 2	Shopping malls (centres) / dining and dancing / weightlifting / stores / manufacturing / warehouse / walkaways / stairs
Occupancy 3	Office / residencies / hotels / multi - family apartments / school rooms / libraries
Occupancy 4	Hospitals / laboratories / critical working areas (e.g. operating theatres, precision laboratories)

High jumping activity at 0.4 kPa in "activity panels" yielded 12.0% or higher damping, which is not achievable and thus has to be restricted or other means of mitigating the responses needs to be provided. Reduced occupant density was used instead which resulted in damping levels of 6.0% and higher. The other activities and densities gave damping levels of 1.6% and 3.0%. Table 7-6 summarises the occupancy fit-out, which in turn would not cause any discomfort to occupants.

7.9 Summary

This chapter extended the knowledge of the dynamic responses under different pattern loading to a nine panel model. It included thorough examination of the responses under the human-induced dance-type events and compared these with the limits of serviceability for deflection and human comfort.

Two pattern loading cases were identified and investigated for deflection and acceleration response. Four human-induced events, namely high-jumping, normal jumping, rhythmic exercise, high impact aerobics and low impact aerobics, were simulated on each pattern loading case. These simulations were carried out at different damping levels, activity frequencies and human-densities posing the activity. The results were used to establish suitable occupancies and operating conditions. These operating conditions involved damping levels, type of human activity and density of humans posing the human activity and were tabulated with respect to each pattern loading case.

It was also observed that depending upon the pattern loading floor responded, not only in the primarily mode but also in higher mode shapes. The respective mode shapes were easily excited by the second or third harmonics of the activity frequency. This caused resonance vibration rising serviceability problems. This phenomenon of multi-modal vibrations was also identified in the previous chapter when a four panel floor system was subjected to pattern loading. Thus, understating of the higher modes of vibration and corresponding natural frequencies was yet again emphasised. This is in contrast to the current practice of using fundamental natural frequency in design against floor vibrations.

Chapter 8 - VE dampers to mitigate floor vibration problems

8.1 Introduction

This chapter investigates the use of VE dampers, to mitigate the excessive deflections and acceleration responses, which caused floor structures to restrict and control human activities such as dance-type activities described in the previous chapters. The use of VE dampers is particularly important from a post-construction prospective as a remedial solution for floor vibration problems.

VE dampers have been used in building construction for mitigating the structural response occurring in a seismic event. The current study on the other hand, uses VE dampers to mitigate the structural response that occur in a human-excitation event. Thus, the main objective of this chapter is to investigate the use of VE dampers to control the excessive responses that occur under human-induced loads. The structural configuration 1, described in Chapter 6, was used for this purpose. VE damper properties were obtained and the reductions in DAF and acceleration responses were calculated. Two damper location configurations were used for the analysis described in this chapter and the one, which gave the higher reduction, was used in computer simulations under pattern loading. The methodology used to obtain the damper properties is discussed and the results demonstrating the effects on the location of damper and the variations of reductions in responses due to structural damping and type of human activity are presented in this chapter.

8.2 Identification of VE damper locations

VE dampers located in high-rise structural systems that counteract the seismic response are usually placed in a bracing of the shear frame or in cut-outs of shear walls (Shen, Soong et al. 1995) (Marko, Thambiratnam et al. 2004). They are sometimes connected to amplifying devices in order to increase their efficiency by increasing the displacements and velocities transferred from the structure to the damper (Ribakov and Reinhorm 2003). In such cases, the seismic loads are applied

horizontally to the column supports, whereas the loads caused by human activity are applied vertically to the floor structure (Bachmann and Ammann 1987). Therefore VE dampers were orientated vertically to gain the most effective behaviour against vertical vibrations.

Two location configurations for VE dampers were investigated. The one with higher reduction in response was chosen and admitted for further analysis with various load frequencies of human-activity, damping levels and pattern loading. These location configurations were termed “location A” and “location B”.

8.2.1 VE damper location A

In damper “location A” the VE dampers were placed underneath the spaning edge of each panel in the four panel model. This particular location was chosen, as it gave the higher deflections under both static and dynamic loads. In this configuration, the VE dampers can be easily inserted inside the ceiling, hanging from the floor. A centre to centre spacing of 250 mm, generally used for service ducts, was considered for placing the VE dampers. Altogether, six VE dampers were allocated and their locations are described in Figure 8-1.

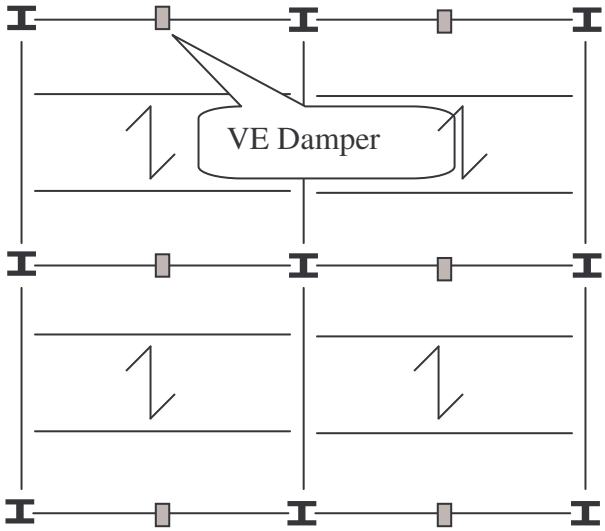

Figure 8-1: VE damper - location A

One end of the VE damper was fixed to the girder beams of size 360 UB 45, spanning along the columns as seen in Figure 8-2. The other end of the damper was attached to the floor slab rigidly. This will efficiently transmit the floor displacements to the dampers.

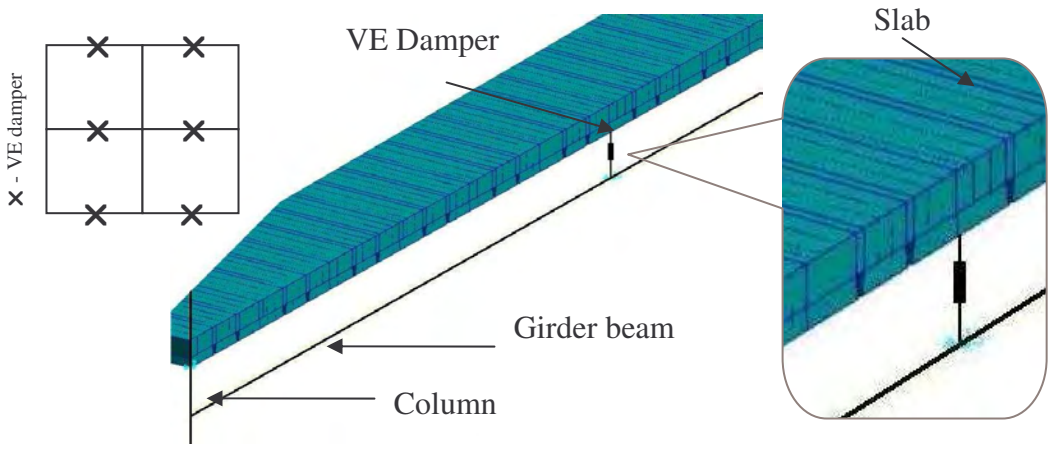

Figure 8-2: Damper location 1: set up

8.2.2 VE damper location B

In damper "location B", the VE dampers were positioned at different locations. Herein the VE dampers were placed underneath the mid-span locations of each panel. This required four VE dampers for the 2 x 2 panel configuration. The mid-span locations were chosen since those locations had the maximum displacement and acceleration responses in the previous analysis without VE dampers. In the structural set-up for this configuration, a supporting beam was used to attach one end of the damper. Then, the other end of the damper was attached to the floor slab using a mechanical fastening method. The supporting beams were of similar size to girder beam and spaned across the main beams of the frame structure as seen in Figure 8-3.

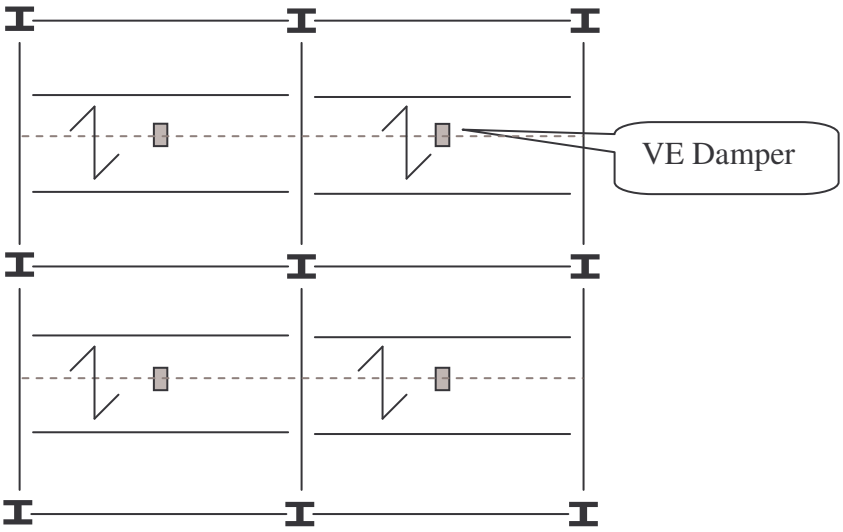

Figure 8-3: VE damper - location B

The "supporting beam" was modelled using beam elements with sectional properties similar to those of the girder beams. The spacing between the floor slab and the supporting beams was set to 100 mm to accommodate the damper. These supporting beams were then connected to the main beams by a rigid link expressed by MPC (multi point constraint) in ABACUS. Figure 8-4 depicts the new FE model's connection configuration with VE dampers. The MPC creates a rigid connection between the supporting beam and the main beam, thereby providing equal deflection constrains for the respective nodes of the main beam and the supporting beam.

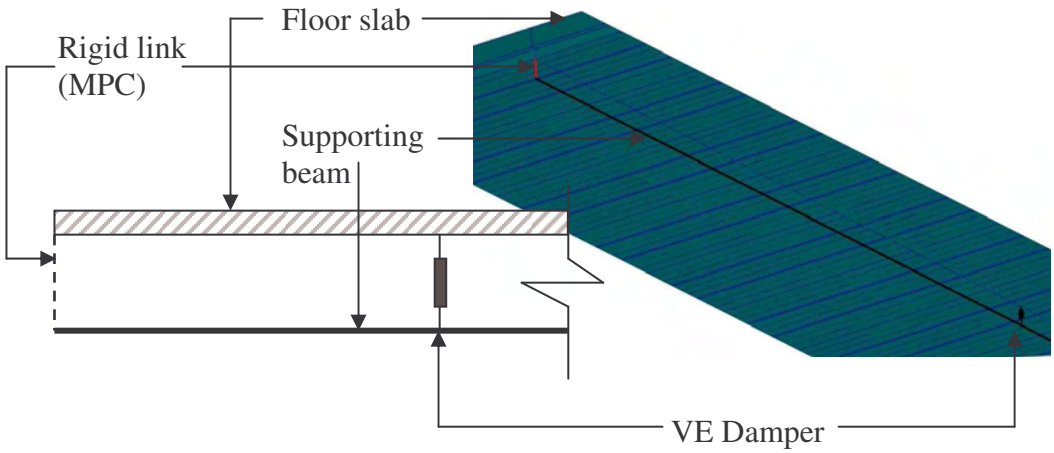

Figure 8-4: Damper location 2: set up

8.3 Properties of VE dampers

This section aims to obtain the properties of VE dampers that reduce the excessive vibration responses occurring under human excitations. The four panel FE model described in Chapter 6 was treated with the attachment of VE dampers at two different locations, as described in Section 8.2. The pattern loading PL2-1 involving high impact jumping with a contact ratio 0.25 gave the maximum responses, at a frequency of 2 Hz. The VE dampers were tuned to this frequency of 2 Hz. The peak values of dynamic deflection and acceleration responses were measured, and the respective spring and dashpot element properties, giving the maximum reduction in response, were used in defining the properties of the damper. The VE dampers were modelled using elastic spring and dashpot in parallel, termed Kelvin model, as described in Section 2.8. Herein, the spring represented the stiffness and the dashpot represented the damping of the VE damper. These stiffness k_d and damping C_d

properties were defined by Abbas and Kelly (Abbas and Kelly J.M. 1993), using the properties of visco-elastic material used in the VE damper. According to Abbas et al. (1993), for a given damper dimensions, the VE material properties of shear storage modulus, G' and shear loss modulus G'' can be obtained using the spring stiffness k_d and dashpot damping parameter C_d of the Kelvin model. An initial derivation of spring stiffness of 996 N/m and dashpot parameter of 708 Ns/m, calculated from the formulae presented by those authors presented in Section 2.8 were used. Herein, the ambient temperature of the VE material was assumed to be 21^{o}C, the shear strain was assumed to remain constant at 100%, loading frequency was taken as 2 Hz, assuming the structure will vibrate in its primary mode. It was assumed that the VE damper has two layers of VE material, each layer 5 mm in thickness and 0.01 m^2 in shear area.

8.3.1 Properties of VE dampers at location A

Linear transient dynamic analyses of the structure were carried out with VE dampers placed at "location A", to obtain the spring stiffness k_d and dashpot damping parameter C_d. The stiffness values k_d used for the spring elements ranged from 1 x 10^{-6} N/m to 1 x 10^{18} N/m and the values for the dashpot C_d elements were ranged from 0.01 Ns/m to 1 x 10^{13} Ns/m. These ranges were selected to cover the initial values of k_d and C_d. Using these values, after about 80 different combinations of analysis optimised values for the springs and the dashpots were taken for the computer simulations under pattern loading.

It was observed that there had been reductions in acceleration response due to employment of VE dampers (refer to Figure 8-5). Similar reductions in displacement responses were also observed. These responses were then used to calculate percentage reductions in displacement and acceleration responses with the values of the un-damped structure for different k_d's and C_d's. Table 8-1 and Table 8-2 present these reductions for the displacements and accelerations respectively. It also describes the percentage reductions obtained for "activity panels" and "non-activity panels".

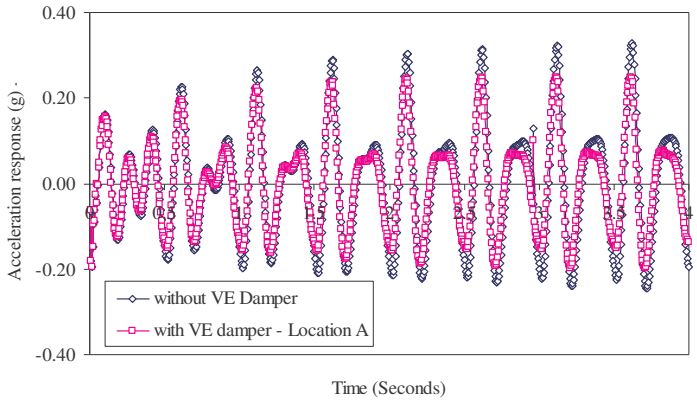

Figure 8-5: Typical acceleration-time history in PL2-1 with contact ratio 0.25 and 1.6% damping at 2 Hz

The results of percentage reduction in both displacements and accelerations appeared at rages of 0%-21% and 0%-24% respectively, depending upon the VE damper material properties.

Overall, it can be stated that the damper "location A" performed well to give an improvement to the structural system in its behaviour under dynamic loads. However, the reductions differed based on the properties of the dashpot and spring elements, giving various performances. The best performance was that of the highset reduction in displacement and accelerations. This was found to be 21% for displacement in the "activity panels", and 24% for acceleration in the "activity panels". Furthermore, reductions of 17% for the displacement and 20% for the acceleration were given in the "non-activity panels". These percentages were found to be valid for a range of k_d starting from 1x 10^{-6} N/m to 1 x 10^3 N/m and C_d of 1 x 10^4 Ns/m.

Table 8-1: Percentage reductions in displacements of VE damper location A

k_d (N/m)	C_d (Ns/m)																
		1.E-02		1.E+00		1.E+03		1.E+04		1.E+05		1.E+07		1.E+11		1.E+13	
		AP	NAP	AP	NAP	AP	NAP	AP	NAP	AP	NAP	AP	NAP	AP	NAP	AP	NAP
	1.E-06	0%	0%	0%	0%	15%	12%	15%	12%	15%	12%	15%	12%	15%	12%	15%	12%
	1.E-02	0%	0%	0%	0%	4%	4%	**21%**	**17%**	16%	12%	15%	12%	15%	12%	15%	12%
	1.E+00	0%	0%	0%	0%	4%	4%	**21%**	**17%**	16%	12%	15%	12%	15%	12%	15%	12%
	1.E+03	0%	0%	0%	0%	4%	4%	**21%**	**17%**	16%	12%	15%	12%	15%	12%	15%	12%
	1.E+04	0%	0%	0%	0%	4%	4%	20%	17%	16%	12%	15%	12%	15%	12%	15%	12%
	1.E+05	16%	12%	16%	12%	16%	12%	16%	12%	16%	13%	15%	12%	15%	12%	15%	12%
	1.E+07	15%	12%	15%	12%	15%	12%	15%	12%	15%	12%	15%	12%	15%	12%	15%	12%
	1.E+11	15%	12%	15%	12%	15%	12%	15%	12%	15%	12%	15%	12%	15%	12%	15%	12%
	1.E+13	15%	12%	15%	12%	15%	12%	15%	12%	15%	12%	15%	12%	15%	12%	15%	12%
	1.E+18	15%	12%	15%	12%	15%	12%	15%	12%	15%	12%	15%	12%	15%	12%	15%	12%

AP - Activity panel

NAP - Non-activity panel

Table 8-2: Percentage reductions in acceleration of VE damper location A

		C_d (Ns/m)															
		1.E-02		1.E+00		1.E+03		1.E+04		1.E+05		1.E+07		1.E+11		1.E+13	
		AP	NAP	AP	NAP	AP	NAP	AP	NAP	AP	NAP	AP	NAP	AP	NAP	AP	NAP
k_d (N/m)	1.E-06	0%	0%	5%	5%	24%	20%	15%	10%	15%	10%	11%	6%	11%	6%	11%	6%
	1.E-02	0%	0%	0%	0%	5%	5%	**24%**	**20%**	15%	10%	11%	6%	11%	6%	11%	6%
	1.E+00	0%	0%	0%	0%	5%	5%	**24%**	**20%**	15%	10%	11%	6%	11%	6%	11%	6%
	1.E+03	0%	0%	0%	0%	5%	5%	**24%**	**20%**	15%	10%	11%	6%	11%	6%	11%	6%
	1.E+04	0%	0%	0%	0%	5%	4%	23%	19%	15%	10%	11%	6%	11%	6%	11%	6%
	1.E+05	15%	10%	15%	10%	15%	10%	15%	10%	15%	9%	11%	6%	11%	6%	11%	6%
	1.E+07	10%	5%	10%	5%	10%	5%	11%	5%	11%	6%	11%	6%	11%	6%	11%	6%
	1.E+11	11%	6%	11%	6%	11%	6%	11%	6%	11%	6%	11%	6%	11%	6%	11%	6%
	1.E+13	11%	6%	11%	6%	11%	6%	11%	6%	11%	6%	11%	6%	11%	6%	11%	6%
	1.E+18	11%	6%	11%	6%	11%	6%	11%	6%	11%	6%	11%	6%	11%	6%	11%	6%

AP - Activity panel

NAP - Non-activity panel

8.3.2 Properties of VE dampers at location B

Using the spring and dashpot element properties obtained in the previous Section 8.3.1, the structural responses were obtained after employing VE dampers at "location B" configuration. Herein, human-activity of high impact jumping at an activity frequency of 2 Hz and contact ratio of 0.25 was simulated. Figure 8-6 presents a comparison of the typical acceleration response without dampers and with VE dampers in "location A" and with VE dampers in "location B".

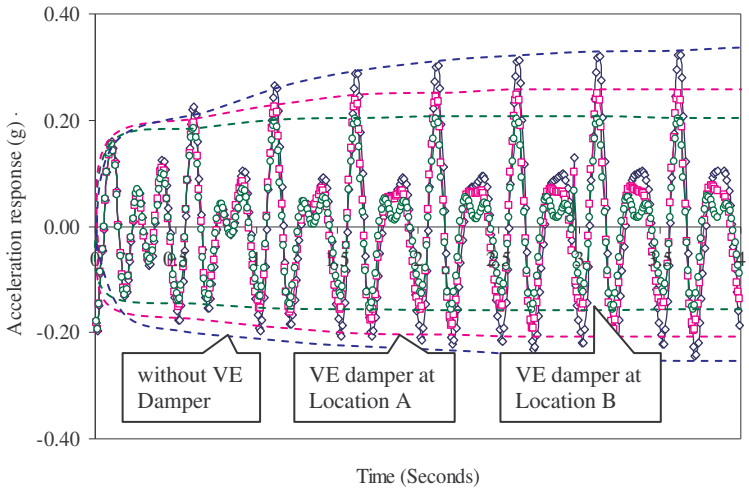

Figure 8-6: Acceleration response comparison for various dampers locations in PL2-1 with 1.6% damping and 0.25 contact ratio

It was observed that VE dampers at "location B" produced better reductions than those at "location A". In fact, the analysis revealed that 31% reduction in DAF and 35% in acceleration can be achieved, compelling "location B's" suitability for using the VE dampers to mitigate floor vibrations.

8.3.3 Effect on natural frequency due to VE dampers

The influence on the natural frequency and the mode shapes of the floor structure due to the introduction of VE dampers was investigated. Table 8-3 compares the natural frequency variations with that of floor system without VE damper.

Table 8-3: Effect on natural frequency due to VE dampers

	Natural frequency (Hz)		
	Without VE dampers	With VE dampers at "location A"	With VE dampers at "location B"
First mode	4.03	4.06	4.07
Second mode	5.35	5.36	5.37
Third mode	5.96	5.96	5.95
Fourth mode	6.85	6.84	6.86

It was observed that the introduction of VE dampers to the structural system did not alter the natural frequencies. The associated mode shapes were also observed to be the same as the modes without VE dampers.

8.3.4 Properties of VE dampers – summary of findings

The VE dampers in the structural system reduced both the DAF for displacement and the acceleration responses. The Figure 8-7 presents a comparison of the DAF with and without dampers.

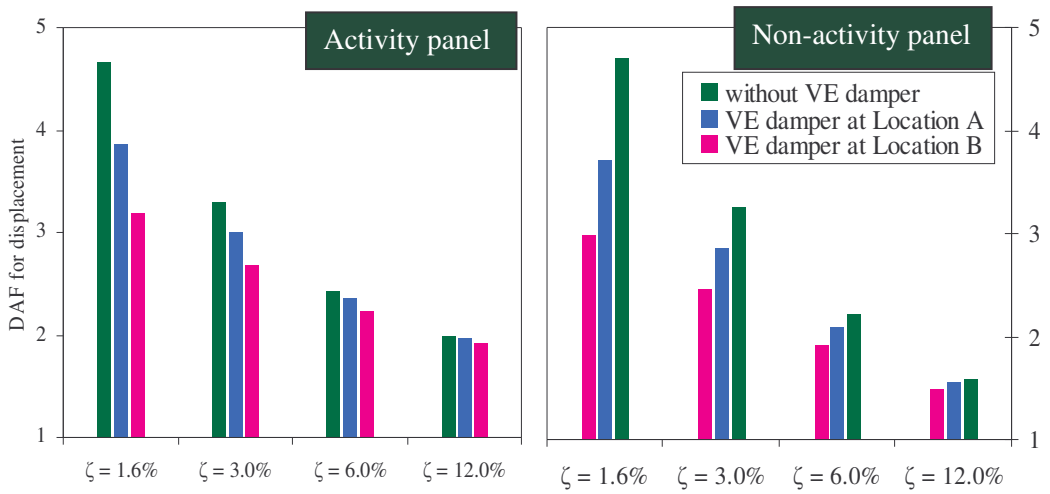

Figure 8-7: Comparison of the DAF with and without dampers

With respect to the results described in the previous Sections 8.3.1 and 8.3.2, the VE damper "location B" configuration was found to give the maximum reductions in both displacement and accelerations. Therefore, "location B" was used to install the VE dampers. The dashpot damping parameter and the stiffness of the spring that was

chosen and used in the current analysis are thus, 1 x 10^4 Ns/m and 1 x 10^3 N/m respectively. Using these VE damper properties at "location B" configuration, computer simulations were carried out for varied different human-induced pattern loading at different structural damping.

8.4 Pattern loading cases with VE dampers

This section, describes the structural response of the four panel floor system in configuration 1 after employing the VE dampers at "location B". Two pattern loading cases were used in this case and analyses were carried out using four human-induced activity contact ratios and four damping levels. The contact ratios, described in Section 6.3 and damping levels, described in Section 6.4 were used for this investigation. The selected pattern loading cases were PL1-1, described in Section 6.8 and PL2-1, described in Section 6.9. These two pattern loading cases were the ones that reflected the vibration problem the most and thus selected for investigation after employing VE dampers. PL3-1 and PL4-1 pattern loading cases of were not considered, as their responses were lower than those of PL1-1 and PL2-1, however, the same methodology can be used for their investigation.

For the two pattern loading cases a human-density of 0.4 kPa was used in the computer simulation in the "activity panels". The dead load, *G* for the current structure was assumed to be 3.5 kPa.

8.5 Dynamic analysis: pattern loading 1 (PL1-1)

PL1-1 gave excessive dynamic responses and thus this section gives a comprehensive description of the improvement in dynamic behaviour after employing VE dampers on each dance-type activity under PL1-1. The responses were compared with the serviceability deflection limits and acceleration limits on the four dance-type activities. After employing the VE dampers the DAF limits were found to be 2.06 and 2.43 for "activity panels and "non-activity panels" respectively. Marginal improvement in the DAF limits was observed after employing the VE damper. The acceleration limits and the respective occupancies used were the ones presented in Section 6.7.

8.5.1 High jumping event – PL1-1 with VE damper

The high jumping event under PL1-1 with VE damper, gave similar trends to that of the floor system without VE damper as depicted in Figure 8-8.

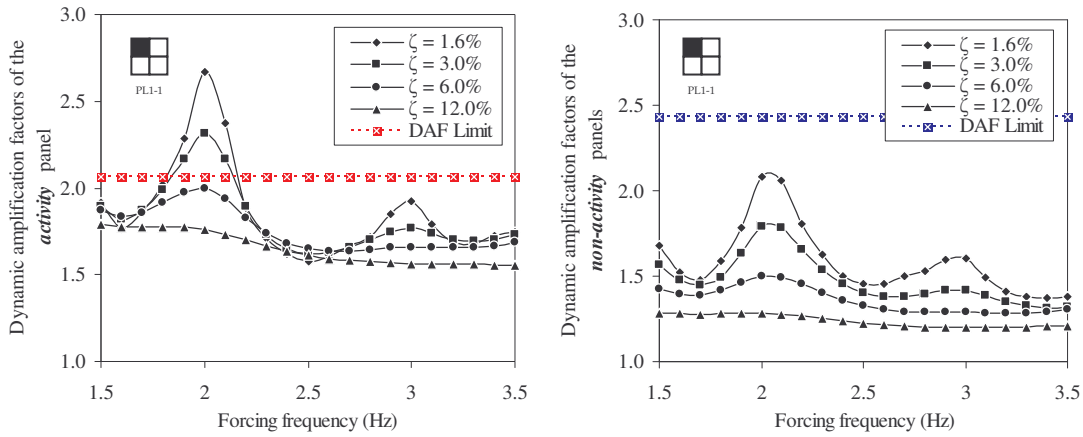

Figure 8-8: DAFs due to high impact jumping event in PL1-1 with VE damper for Q=0.4 kPa

The maximum DAF response was given at an activity frequency of 2 Hz, exciting the fundamental mode by the second harmonic of the activity frequency. These DAFs were 2.67 in the "activity panels" and 2.09 in the "non-activity panels". These maximum DAFs were reduced and the reductions varied from 29% under 1.6% damping to 2.8% under 12.0% damping in the "activity panels" and 31% under 1.6% damping to 4.1% under 12.0% damping in the "non-activity panels".

It was observed that the "activity panels" were within the deflection limits under 6.0% or higher damping and the same applied to "non-activity panels" for all damping levels. This was an improvement in the structure since the model without VE damper needed 12.0% or higher damping in the "activity panels" and 3.0% or higher damping in the "non-activity panels".

The acceleration responses gave similar trends to those of DAFs. Peak acceleration responses were observed at activity frequency of 2 Hz and 2.9 Hz, which excited the first and the second modes of vibration. These acceleration responses in perceptibility scales are presented in Figure 8-9.

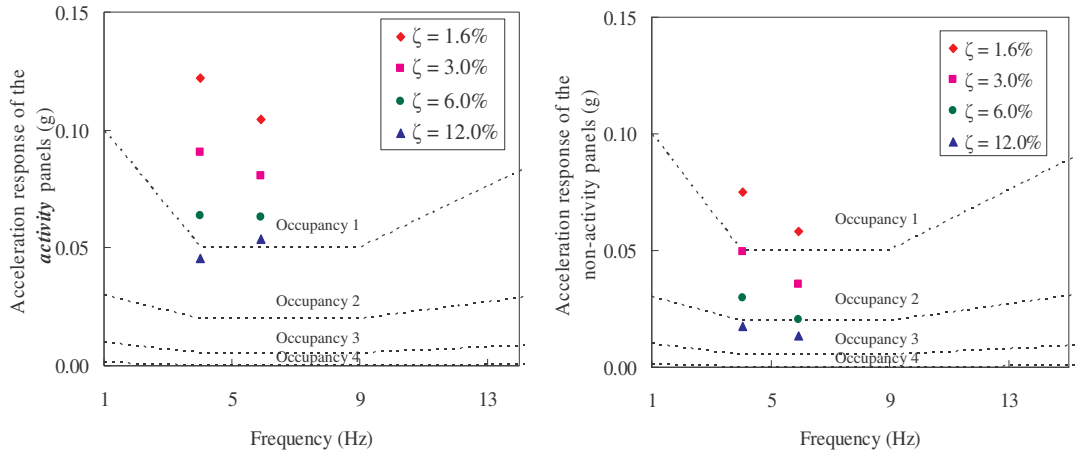

Figure 8-9: Acceleration response due to high impact jumping event in PL1-1 with VE damper for Q=0.4 kPa

The reductions in acceleration response varied form 3.0% under 1.6% damping to 4.9% under 12.0% damping in "activity panels" and 41.2% under 1.6% damping to 12.0% under 12.0% damping in the "non-activity panels". It was observed that the "activity panels" created discomfort to the occupants even at 12.0% damping while the "non-activity panels" can be fit-out to occupancy 2 with 12.0% or higher damping without causing any discomfort.

In comparison with the floor system without VE damper, no improvements in occupancies were observed, though significant reductions in accelerations were obtained. As a result, the occupancies and damping levels in the floor system with VE dampers remained the same as for the floor system without VE dampers. Although, reduced occupant density of 0.2 kPa performing the high jumping activity on the floor, with VE dampers is proposed as a solution that complies with the acceleration criteria.

8.5.2 Normal jumping activity – PL1-1 with VE damper

The variation of DAF responses with activity frequency observed for normal jumping activity under PL1-1 with VE dampers is presented in Figure 8-10.

The normal jumping activities gave maximum DAFs at an activity frequency of 2 Hz in both "activity panels" and "non-activity panels". After employing VE dampers,

the maximum DAFs were brought down to 2.28 and 1.87 in "activity panels" and in "non-activity panels" respectively. These reductions were 26% under 1.6% damping to 2.6% under 12.0% damping in "activity panels" and 30% under 1.6% damping to 3.7% under 12.0% damping in "non-activity panels". These reductions enabled the performance of the floor system to comply with the serviceability deflection criteria at 3.0% or higher damping in the "activity panels" and at all damping levels in the "non-activity panels". This was found to be an improvement from the model without VE dampers which needed 6.0% or higher damping in the "activity panels" and 3.0% or higher damping in the "non-activity panels".

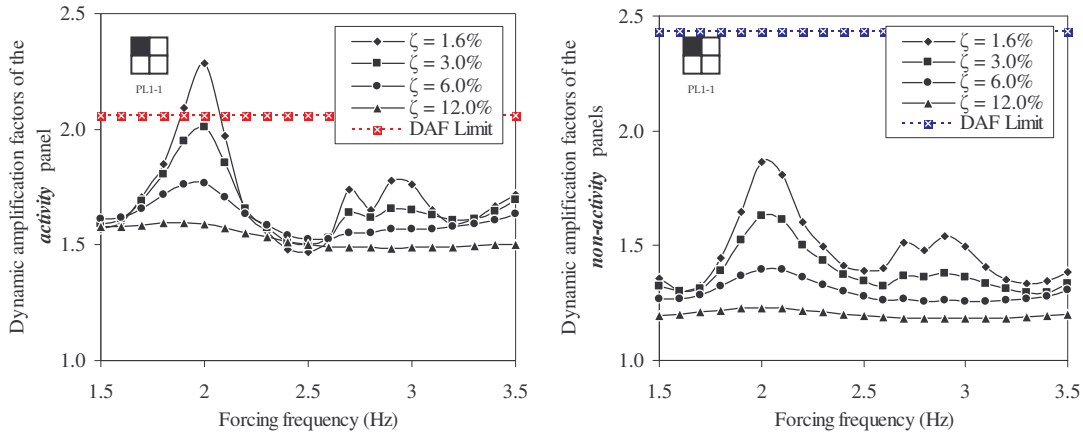

Figure 8-10: DAFs due to normal jumping event in PL1-1 with VE damper for Q=0.4 kPa

The peaks in both acceleration responses were observed at an activity frequency of 2 Hz, with secondary peak occurring near 2.9 Hz. These two values were used in the perceptibility scales in Figure 8-11.

The acceleration responses were observed to be within the limits when 6.0% or higher damping was used in "activity panels". In the case of "non-activity panels", occupancy 2 can be fitted at 6.0% or higher damping. Overall, the maximum reduction in acceleration response varied from 37% under 1.6% damping to 5.8% under 12.0% damping in the "activity panels" and 44% under 1.6% damping to 13.9% under 12.0% damping in the "non activity panels".

In summary, the performance of the structure was improved by using VE damper since it allowed fit-out occupancy 2 at 6.0% or higher damping in the "non-activity panels", where as without VE dampers the model needed more than 12.0% damping.

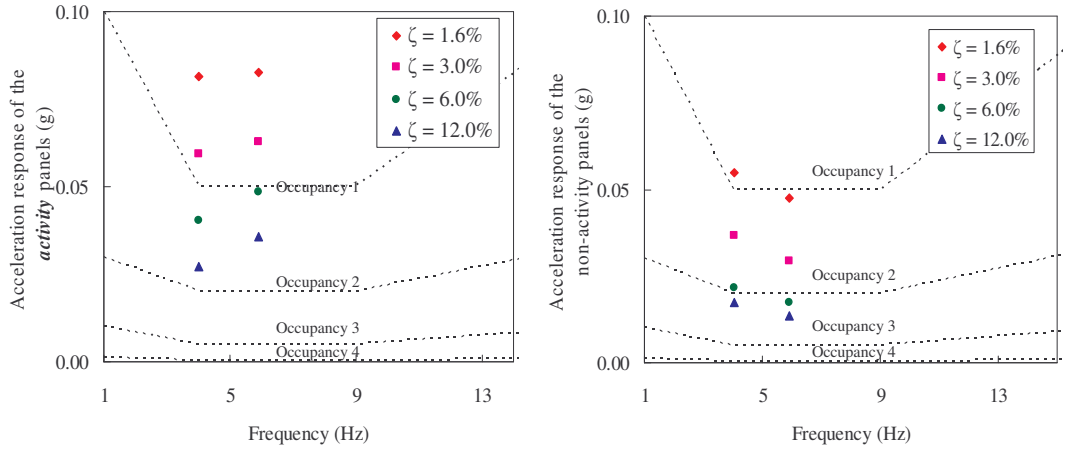

Figure 8-11: Acceleration response due to normal jumping event in PL1-1 with VE damper for Q=0.4 kPa

8.5.3 Rhythmic exercise / high impact aerobics – PL1-1 with VE damper

The variation of DAFs with activity frequency for the rhythmic exercise / high impact aerobics under PL1-1 with the VE damper is presented Figure 8-12.

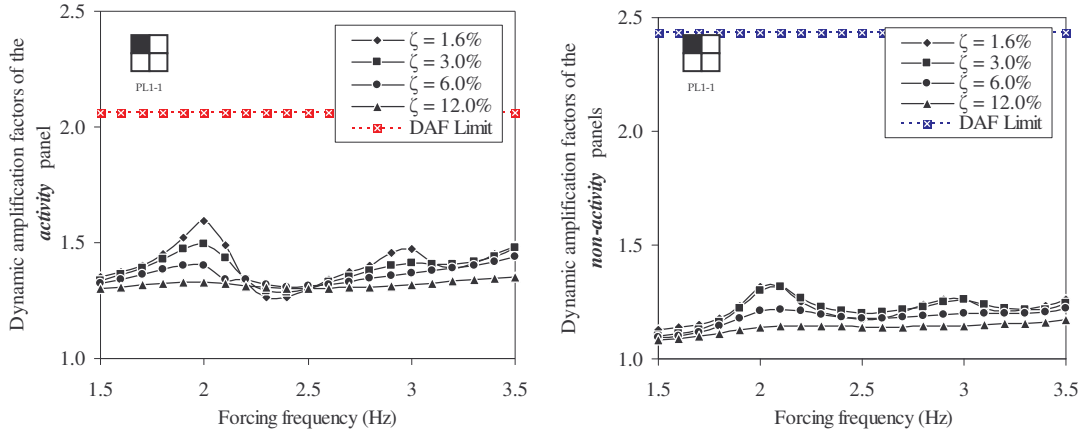

Figure 8-12: DAFs due to rhythmic exercise / high impact aerobics event in PL1-1 with VE damper for Q=0.4 kPa

The rhythmic exercise / high impact aerobics gave maximum DAF of 1.59 in the "activity panels" and 1.31 in the "non activity panels", both occurring at a activity frequency of 2 Hz. Reductions in DAFs varied from 20% under 1.6% damping to 2.0% under 12.0% damping in "activity panels" and 18% under 1.6% damping to

3.2% under 12.0% damping in "non-activity panels". Furthermore, the floor structure performed within the permissible deflection limits of serviceability and thus did not caused problems in serviceability deflection criteria. This was expected, as the structure without VE dampers did not exceed the serviceability deflection limits either. The maximum acceleration responses were observed at 2 Hz and 2.9 Hz same as for the structure without VE dampers, exciting the first and second mode shapes respectively. Figure 8-13 depicts those responses in perceptibility scales.

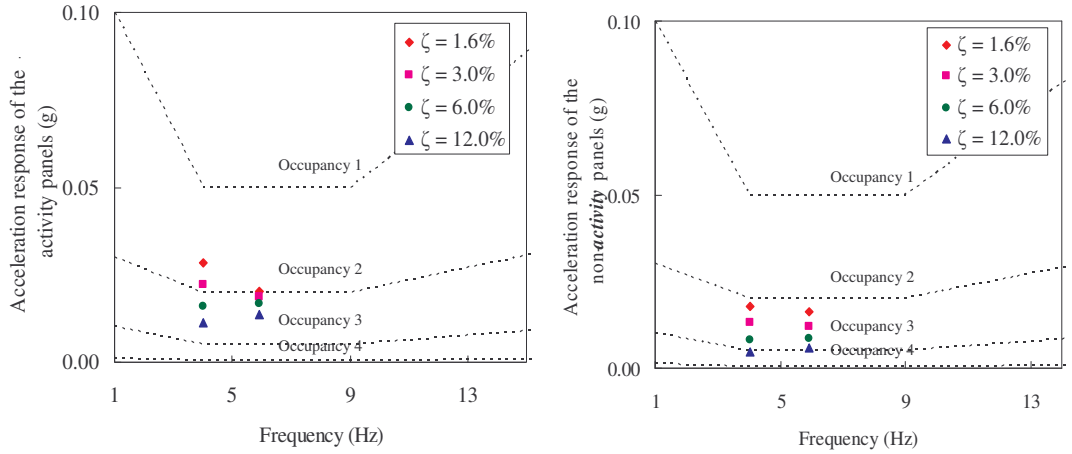

Figure 8-13: Acceleration response due to rhythmic exercise / high impact aerobics event in PL1-1: with VE damper for Q=0.4 kPa

It was observed that "activity panels" gave acceleration responses within the occupancy 1 at all damping levels. The "non-activity panels" however can fit-out the occupancy 2 at 1.6% or higher damping and occupancy 3 at 12.0% or higher damping. The overall reductions in acceleration responses varied from 47% under 1.6% damping to 8.5% under 12.0% damping in the "activity panels" and 53.6% under 1.6% damping to 16.0% under 12.0% damping in the "non-activity panels". These reductions allowed the structure to fit-out occupancy 1 in the "activity panels" and occupancy 2 in the "non-activity panels" at 1.6% damping, both of which were not able fitted-out in the structure without VE dampers.

8.5.4 Low impact aerobics – PL1-1 with VE damper

Low impact aerobics in PL1-1 without VE dampers did not exceeded DAF limits and so was the case with VE damper (refer to Figure 8-14). However, reductions in DAFs were observed due to the presence of the VE dampers.

These reductions varied from 6.2% under 1.6% damping to 1.3% under 12.0% damping in the "activity panels" and 8.9% under 1.6% damping to 1.1% under 12.0% damping in the "non-activity panels". Consequently, the acceleration responses were improved and the maximum observed acceleration responses in perceptibility scales are presented in Figure 8-15.

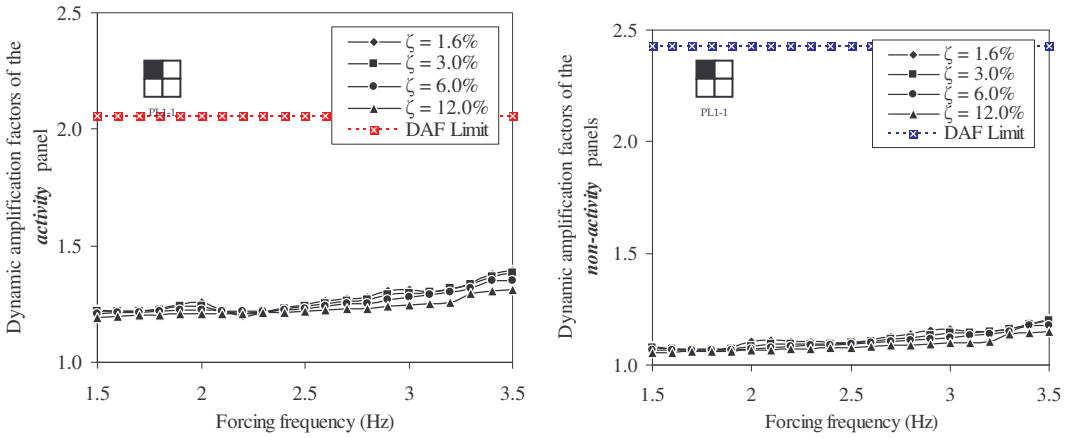

Figure 8-14: DAFs due to low impact aerobics event in PL1-1: with VE damper for Q=0.4 kPa

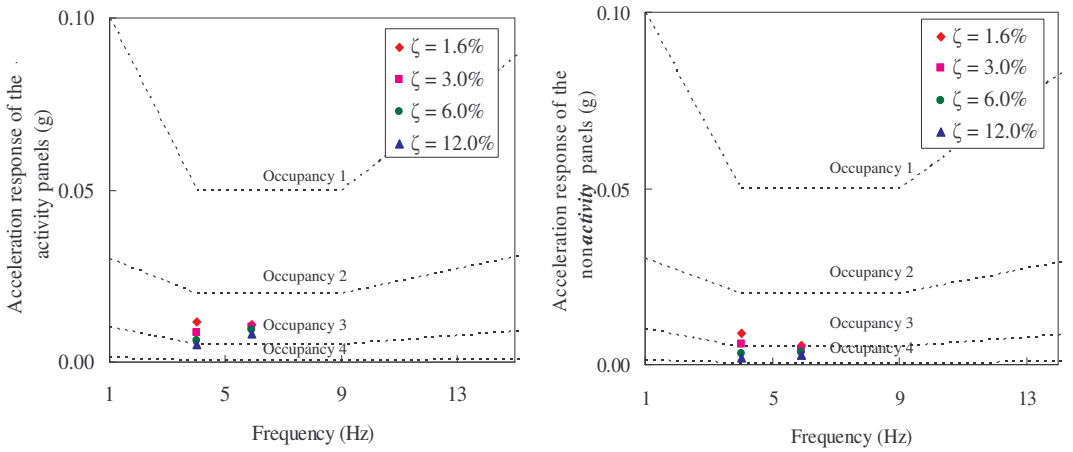

Figure 8-15: Acceleration response due to low impact aerobics event in PL1-1: with VE damper for Q=0.4 kPa

It can be seen that the low impact aerobics can be performed without any discomfort to occupants in the "activity panels" at any of the damping levels. Thus, there has not been a change in the "activity panels" compared to the structure without VE dampers. In the "non-activity panels", occupancy 2 can be fit-out any damping level, while occupancy 3 can be fit-out at 3.0% or higher damping. The fit-out of

occupancy 3 at 3.0% or higher damping was an improvement, since the model without VE dampers needed 6.0% or higher damping. The reductions in acceleration responses due the presence of VE damper varied from 38.8% under 1.6% damping to 5.7% under 12.0% damping in the "activity panels" and 38.4% under 1.6% damping to 13.4% under 12.0% damping in the "non-activity panels.

8.8.5 Results summary and discussion - PL1-1 with VE damper

Overall the presence of VE dampers resulted in reduction of both, deflection and acceleration responses, which improved the behaviour of the structure under PL1-1. Similar to the previous cases without VE dampers, described in Chapter 6, PL1-1 with VE dampers excited fundamental mode, third mode and sometimes the second mode. The reduction of both responses in deflection and acceleration was governed by the structural damping present in the system and how energetic the activity was. Lesser damping gave higher reductions in both, parameters of deflection and acceleration.

The VE dampers lowered the operating structural damping levels which complied with the serviceability deflection criteria. Table 8-4 presents a comparison of these damping levels with those of the structure without VE dampers. The improved activity cases are depicted in shaded cells of Table 8-4 and are as follows:

- The high jumping activity earlier operating at 12.0% or higher damping in the "activity panels" performed at a lower damping level of more than 6.0%. In the case of "non-activity panels", in the model without VE dampers the operating damping levels were lowered from 3.0% to 1.6%.
- Normal jumping activity earlier operating at 6.0% or higher damping in the "activity panels" performed at lower damping levels of more than 3.0%. The "non-activity panels" in the model without VE dampers improved to a lower damping level from 3.0% to 1.6%.

The other activities already complied with the serviceability deflection criteria for the structure without VE dampers and thus these was no change in the cases with VE dampers. This illustrates that the floor structure with VE dampers needs lower operating damping levels to comply with the serviceability deflection criteria. These

are easier to obtain by the non-structural components, equipment and other objects present in the floor system. However, this did not guarantee compliance with the acceleration criteria, which needed to be looked at as this would determine the main cut-off for the occupancy fit-out in the floor system.

Table 8-4: Comparison of operating conditions in PL1-1 with and without VE dampers

	Without VE dampers		With VE dampers	
Dance-type activity in activity panel (AP)	Activity panel (AP)	Non-activity panel (NAP)	Activity panel (AP)	Non-activity panel (NAP)
High impact jumping	$\zeta > 12.0\%$	$\zeta > 3.0\%$	$\zeta > 6.0\%$	$\zeta > 1.6\%$
Normal jumping	$\zeta > 6.0\%$	$\zeta > 3.0\%$	$\zeta > 3.0\%$	$\zeta > 1.6\%$
Rhythmic exercise / high impact aerobics	$\zeta > 1.6\%$	$\zeta > 1.6\%$	$\zeta > 1.6\%$	$\zeta > 1.6\%$
Low impact jumping	$\zeta > 1.6\%$	$\zeta > 1.6\%$	$\zeta > 1.6\%$	$\zeta > 1.6\%$

Similarly with respect to DAFs, the VE dampers reduced the acceleration response for each activity, as illustrated in the previous sections, enabling new occupancy fit-outs. Table 8-5 summaries and compares the possible fit-out of the floor system with and without VE damper. The improved activity cases are depicted in shaded cells in Table 8-5 and are as follows:

- The "non-activity panels" can now be used for occupancy 2 at 6.0% damping during normal jumping event in "activity panels". Previously for occupancy 2 in "non activity panels" without VE dampers at least 12.0% of damping was needed.
- Rhythmic exercise / high impact aerobics can now be performed in "activity panels" at damping levels as low as 1.6%. Without VE dampers rhythmic exercise / high impact aerobics in "activity panels" yielded results beyond acceptance limits in all damping levels and thus caused human discomfort.
- The "non-activity panels" can now be used for occupancy 2 at 1.6% damping during rhythmic exercise / high impact aerobics event in "activity panels". Without VE dampers the "non-activity panels" needed at least 6.0% damping for occupancy 2.

- The “non-activity panels can now be used for occupancy 3 at 3.0% damping during low impact aerobics in the “activity panels”. Without VE dampers “non-activity panels” could not be used for occupancy 3 at any of the damping levels.

After employing the VE dampers all the dance-type human activities other than high impact jumping in “activity panels” yielded lower operating damping levels that complied with the acceleration criteria, in both “activity panels” and “non-activity panels”. These reduced damping levels are easily achievable in the structure by partitions, non-structural elements and other objects. However, in the case of high impact jumping activity in “activity panels”, reduced occupant density is proposed as an alternative solution. The human-density of 0.2 kPa, which already resulted in good improvement in structures without VE dampers, can thus be used.

PL1-1, after employing VE dampers, gave maximum reductions of both DAF acceleration responses at frequency of 2 Hz. These reductions varied with damping level and contact ratios in a human dance-type activity. These reductions were calculated and presented in Figure 8-16 and Figure 8-17 for DAFs and accelerations respectively. These figures also depict the average reductions at each damping level.

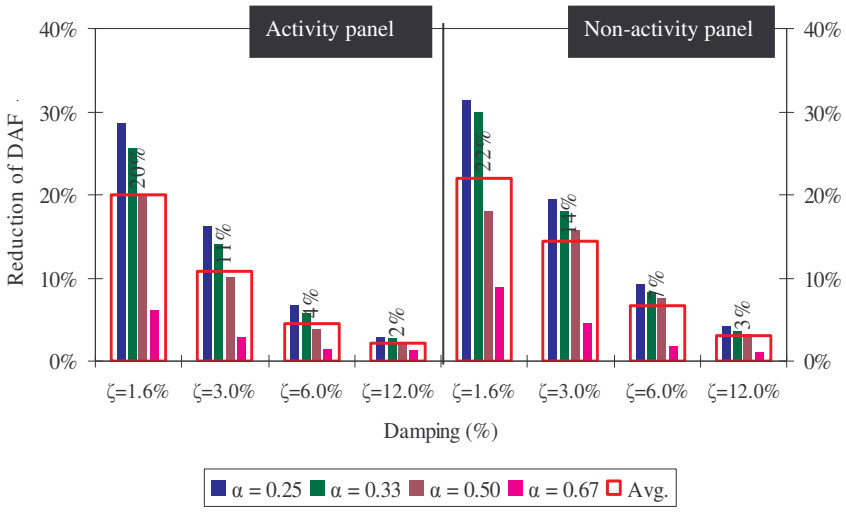

Figure 8-16: Percentage reduction in DAF responses due to VE damper in PL1-1

Table 8-5: Summary and comparison of occupancy fit-out for PL1-1 with and without VE damper

Occupancy description - without VE damper			
Dance-type activity in activity panel (AP)	Activity panel (AP)	Non-activity panel (NAP)	
High Impact Jumping	Occupancy 0	Occupancy 2 $\zeta > 12.0\%$	
Normal Jumping	Occupancy 1 $\zeta > 6.0\%$	Occupancy 2 $\zeta > 12.0\%$	
Rhythmic exercise / high impact aerobics	Occupancy 1 $\zeta > 3.0\%$	Occupancy 2 $\zeta > 3.0\%$	Occupancy 3 $\zeta > 12.0\%$
Low impact jumping	Occupancy 1 $\zeta > 1.6\%$	Occupancy 2 $\zeta > 1.6\%$	Occupancy 3 $\zeta > 6.0\%$

Occupancy description - with VE damper			
Dance-type activity in activity panel (AP)	Activity panel (AP)	Non-activity panel (NAP)	
High Impact Jumping	Occupancy 0	Occupancy 2 $\zeta > 12.0\%$	
Normal Jumping	Occupancy 1 $\zeta > 6.0\%$	Occupancy 2 $\zeta > 6.0\%$	
Rhythmic exercise / high impact aerobics	Occupancy 1 $\zeta > 1.6\%$	Occupancy 2 $\zeta > 1.6\%$	Occupancy 3 $\zeta > 12.0\%$
Low impact jumping	Occupancy 1 $\zeta > 1.6\%$	Occupancy 2 $\zeta > 1.6\%$	Occupancy 3 $\zeta > 3.0\%$

Occupancy 0	Uncomfortable
Occupancy 1	Rhythmic activities / aerobics / dance - type loads
Occupancy 2	Shopping malls (centres) / dining and dancing / weightlifting / stores / manufacturing / warehouse / walkaways / stairs
Occupancy 3	Office / residencies / hotels / multi - family apartments / school rooms / libraries
Occupancy 4	Hospitals / laboratories / critical working areas (e.g. operating theatres, precision laboratories)

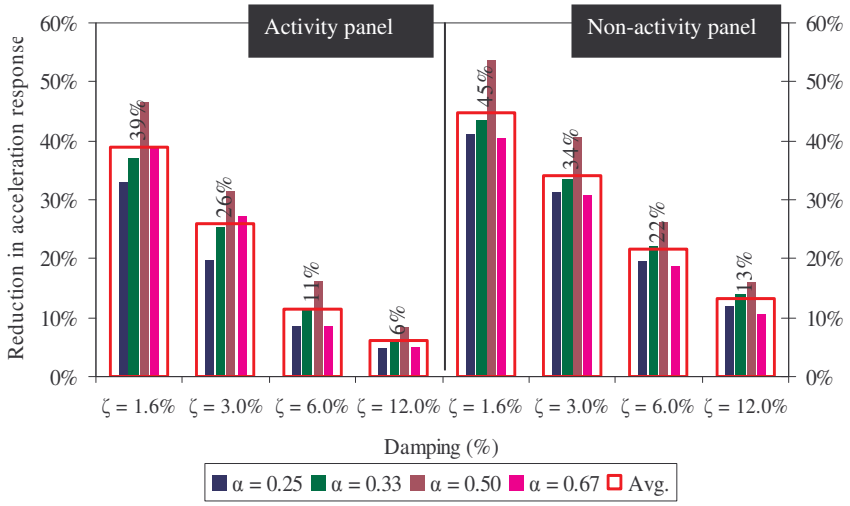

Figure 8-17: Percentage reduction in acceleration response due to VE damper in PL1-1

Reductions of DAFs were observed with the increase of contact ratio. This implies that higher energetic dance-type activity which has lower contact ratio have given higher reductions in DAFs in contrast to the lower energetic dance-type activity which as higher contact ratio. In the other hand, the reduction in acceleration responses due to the VE damper maintained almost equal levels of the four contact ratios investigated. Thus, it can be stated that increase in contact ratio in lesser energetic events such as low impact aerobics where $\alpha = 0.67$ did not considerably reduce the acceleration response.

It was also observed that the structural damping present in the system made a significant impact on the overall reduction in responses in both, acceleration and displacement. Thus, floor systems with higher structural damping, fitted with VE damper may not give large reductions in both accelerations and displacements when compared with those with lower structural damping.

8.6 Dynamic analysis: pattern loading 2 (PL2-1)

This section gives a comprehensive description of the improvement in dynamic behaviour of the floor structure after employing VE dampers for each dance-type activity under PL2-1. PL2-1 considered two-panels subjected to dance-type activity. The human-occupant density performing the activity of 0.4 kPa was used for this analysis. Due to the presence of VE dampers, the DAF limits were increased to 2.04

and 2.54 for the "activity panels" and "non-activity panels" respectively. The responses were obtained for the four dance-type events under the four damping levels and their compliance with the serviceability deflection limits and acceleration limits was evaluated. The acceleration limits used and their occupancies are presented in Section 6.7.

8.6.1 High jumping event – PL2-1 with VE damper

The high impact jumping under PL2-1 gave the variation of DAFs presented in Figure 8-18.

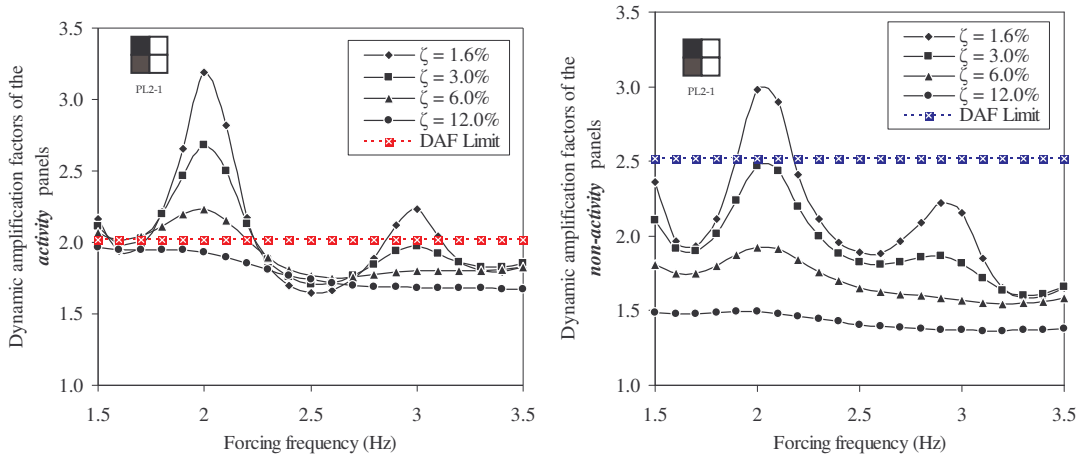

Figure 8-18: DAFs for high impact jumping event in PL2-1 with VE damper for Q=0.4 kPa

The maximum DAF responses observed were 3.19 and 2.98 in the "activity panels" and "non-activity panels" respectively. These DAF responses gave reduction that varied from 31.4% under 1.6% damping to 3.4% under 12.0% damping in "activity panels" and 37% under 1.6% damping to 6.5% under 12.0% damping in "non-activity panels". However, 12.0% damping in "activity panels" and 3.0% or higher damping in the "non-activity panels" gave the responses within the DAF limits. The 3.0% damping in "non-activity panels" using VE damper was an improvement from previous performance of 6.0% without VE dampers.

The peak responses were observed at activity frequencies of 2 Hz and 2.9 Hz, exciting the first and the second mode of vibration. These are plotted in the perceptibility scales and presented in Figure 8-19.

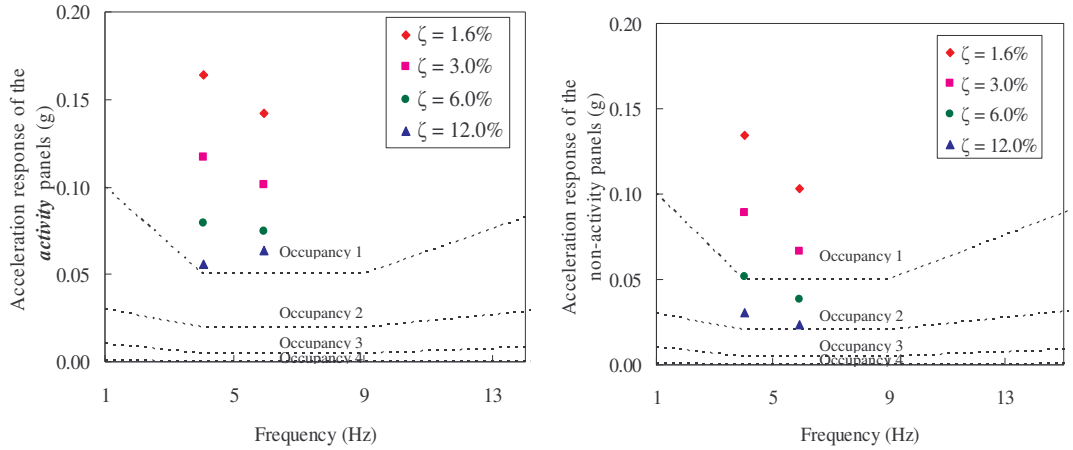

Figure 8-19: Acceleration response due to high impact jumping event in PL2-1 with VE damper for Q=0.4 kPa

It was observed that at all damping levels the "activity panels" did not give acceleration responses that complied with occupancy 1 and consequently may cause to discomfort to the occupants. Therefore, the VE damper although giving reductions of 35% under 1.6% damping to 5.6% under 12.0% damping in "activity panels" did not assist in bringing the acceleration response to human comfort levels in the "activity panels". Similarly in the "non-activity panels", though it gave reductions of 41% under 1.6% damping to 13% under 12.0% damping if did not fit-out to any of the occupancies. Due to these facts, the VE dampers did not provide sufficient reductions to fit-out suitable occupancies at any of the damping levels. This may have been due to the onerous-ness of the high-jumping event. Under these circumstances, in order to comply with the acceleration limits, reduced occupant density posing the high-jumping activity was proposed.

8.6.2 Normal jumping activity – PL2-1 with VE damper

The variation of DAF responses with activity frequency for normal-jumping activity under PL2-1 is presented in Figure 8-20.

The normal jumping event in PL2-1 with VE damper resulted in DAF responses that were lower than those for situations without VE dampers. Infact, reductions in DAF of 29% under 1.6% damping to 3.2% under 12.0% damping in the "activity panels" and 37% under 1.6% to 6.0% under 12.0% damping in the "non-activity panels" were observed. However, it was observed that the "activity panels" with 6.0% or

higher damping and "non-activity panels" with 3.0% or higher damping performed within the desired limiting values. This was an improvement since the structure without the VE dampers performed within the limits only under 12.0% or higher damping in the "activity panels" and 6.0% or higher damping in the "non-activity panels".

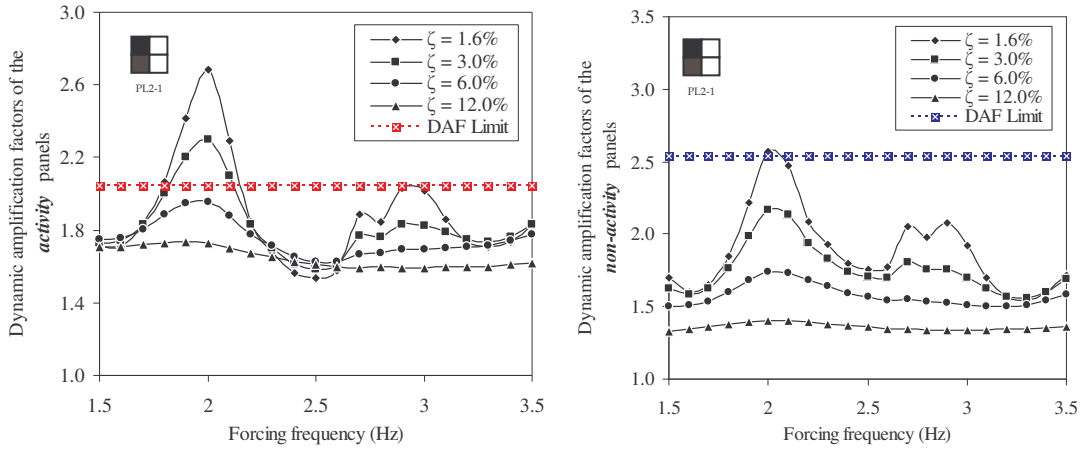

Figure 8-20: DAFs due to normal jumping event in PL2-1 with VE damper for Q=0.4 kPa

The maximum acceleration responses were given at activity frequencies of 2 Hz and 2.9 Hz. Due the presence of the VE damper a reduction in acceleration responses varied from 38% under 1.6% damping to 7% under 12.0% damping in the "activity panels" and 44% under 1.6% damping to 14.5% under 12.0% damping in the "non-activity panels". The acceleration responses observed at activity frequencies of 2 Hz and 2.9 Hz were plotted in the perceptibility scales in Figure 8-21.

It was observed that these reductions did not contribute significantly enough to bring the acceleration response to the acceptable limits at any of the damping levels. Thus, the possible fit-outs under normal jumping activity that comply with the acceleration criteria are the occupancy 1 at 12.0% or higher damping in the "activity panels". Occupancy 2 at 12.0% or higher damping in the "non-activity panels" remains unchanged compared with the occupancies without VE dampers.

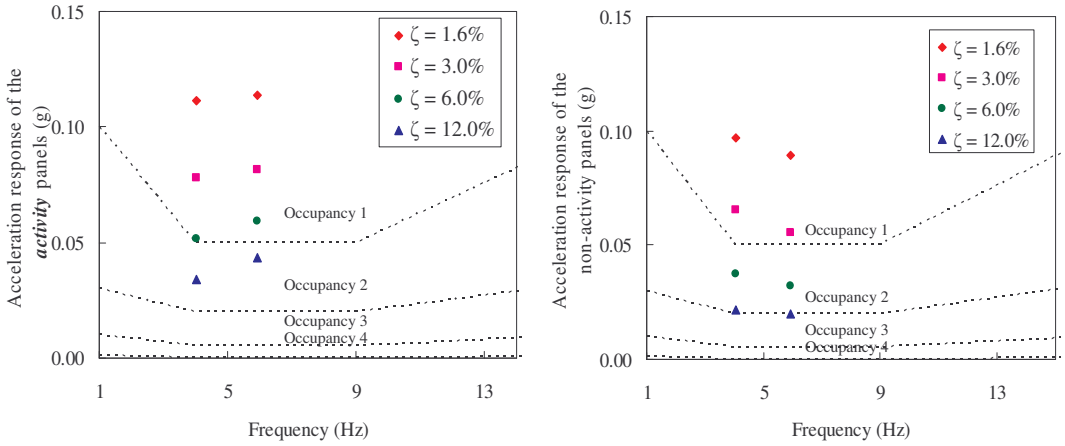

Figure 8-21: Acceleration response due to normal jumping event in PL2-1: with VE damper for Q=0.4 kPa

8.6.3 Rhythmic exercise / high impact aerobics – PL2-1 with VE damper

The variation of DAFs with activity frequencies observed for the rhythmic exercise / high impact aerobics under PL2-1 is presented in Figure 8-22.

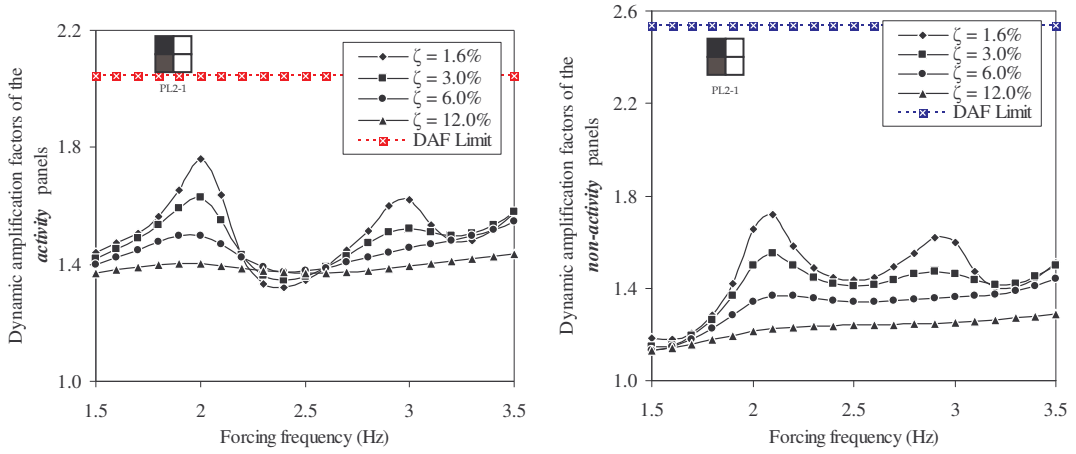

Figure 8-22: DAFs due to Rhythmic exercise / high impact aerobics event in PL2-1 with VE damper for Q=0.4 kPa

It was observed that DAFs responses under this event were within the limits in both "activity panels" and "non-activity panels". In the structure without the VE dampers, responses in the "activity panels" exceeded the limits at 1.6% damping. As a consequence of employing the VE dampers, the responses were within the limits

even at 1.6% damping. Reductions of DAFs of 24% under 1.6% damping to 2.4% under 12.0% damping in the "activity panels" and 31% under 1.6% damping to 4% under 12.0% damping in the "non-activity panels" were observed.

The occupancy fit-out was determined by referring to the maximum acceleration responses observed at 2 Hz and 2.9 Hz and Figure 8-23 presents their plots in perceptibility scales.

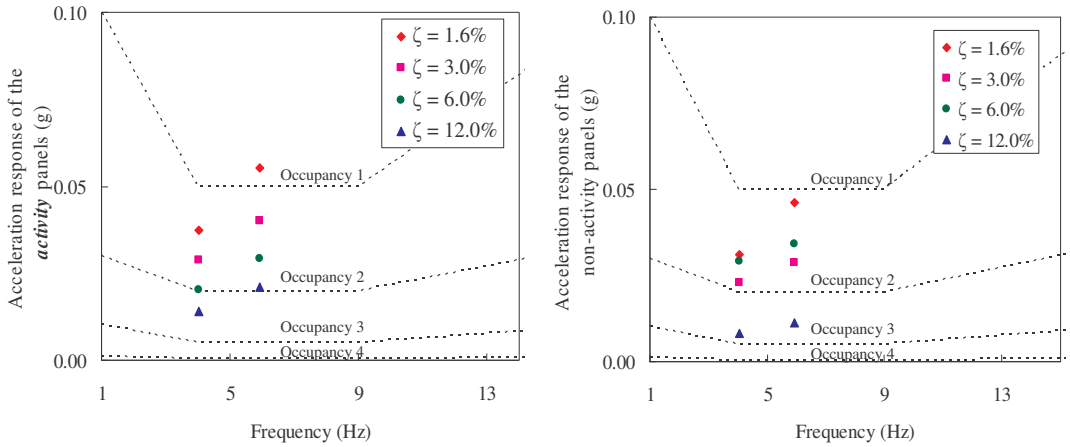

Figure 8-23: Acceleration response due to rhythmic exercise / high impact aerobics event in PL2-1 with VE damper for Q=0.4 kPa

The employment of the VE dampers decreased the acceleration response occurring due to rhythmic exercise / high impact aerobics. Infact 48% under 1.6% damping to 9.5% under 12.0% damping in the "activity panels" and 54% under 1.6% damping to 17% under 12.0% damping in the "non-activity panels" were observed. However, these reductions did not make a significant change in the occupancy fit-out compared to that of the structure without VE dampers. The "activity panels" were seen to accommodate occupancy 1 at 3.0% or higher damping while "non-activity panels" were observed to accommodate occupancy 2 at 12.0% or higher damping, which remained unchanged for the structure with VE dampers.

8.6.4 Low impact aerobics – PL2-1 with VE damper

The responses for low impact aerobics under PL2-1, without the damper did not exceed the DAF limits. Thus, the structure using the VE damper gave DAF responses within limits, as depicted in Figure 8-24.

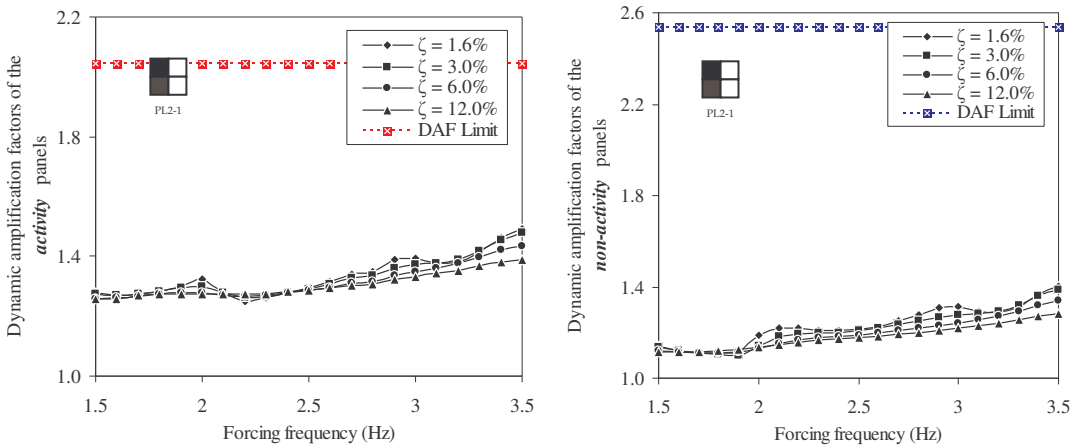

Figure 8-24: DAFs for low impact aerobics event in PL2-1 with VE damper for Q = 0.4 kPa

Consequent reductions in DAFs varying from 8% under 1.6% damping to 1% under 12.0% damping in the "activity panels" and 15% under 1.6% damping to 1% under 12.0% damping in the "non-activity panels" were observed due to the presence of VE dampers. The occupancy fit-out was determined by observing the acceleration response under the low impact aerobics activity in PL2-1. Figure 8-25 presents the acceleration response plotted in perceptibility scales.

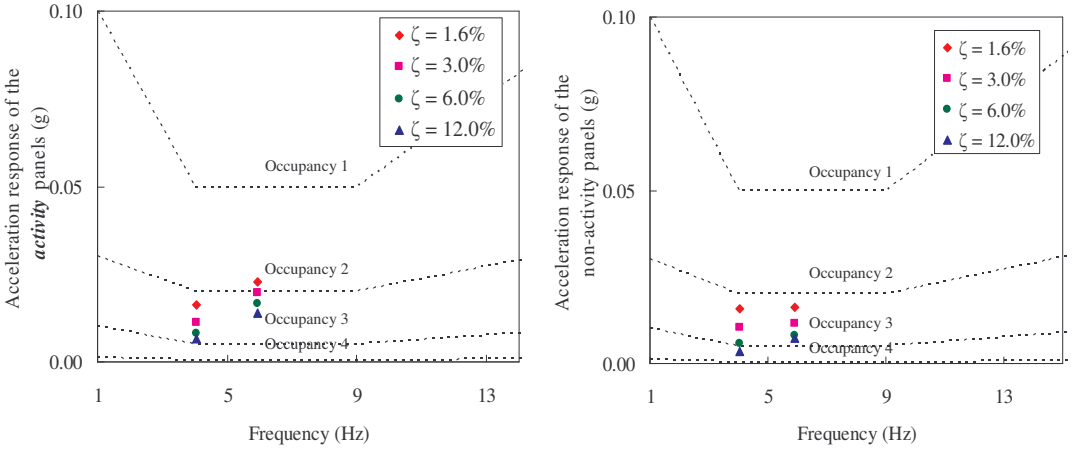

Figure 8-25: Acceleration response for low impact aerobics event in PL2-1 with VE damper for Q=0.4 kPa

The acceleration response for the low impact aerobics under PL2-1 was reduced due to the employment of the VE damper. The percentage reductions in acceleration responses were ranged from 39% under 1.6% damping to 6% under 12.0% damping in the "activity panels" and 38% under 1.6% damping to 13.4% under 12.0%

damping in the “non-activity panels”. These reductions did not cause any change to the occupancy operating conditions in the “activity panels” and thus the same occupancy at that used for the floor system without VE dampers remains. However, an improvement in the “non-activity panels” was noticeable. This is to fit-out occupancy 2 in the “non-activity panels” at 1.6% damping, whereas without VE dampers 3.0% or higher damping was needed for the same occupancy.

8.6.5 Results summary and discussion - PL2-1 with VE damper

Similarly to PL1-1, the presence of VE dampers resulted improved performance of structure that complied the serviceability deflection criteria under PL2-1 loading. Table 8-6 presents and compares the improvements with respect to serviceability deflection criteria. The shaded cells denote the improved performance cases or damping levels, compared with the floor system without VE dampers.

These improvements were:

- When performing high impact jumping in “activity panels”, the permissible damping levels in the “non-activity panels” have improved from 6.0% to 3.0% after employing the VE damper.
- The normal jumping activity earlier operating at damping more than 2.0% in the “activity panels” with the use of VE dampers can be performed at damping levels more than 6.0%. With VE dampers the “non-activity panels” operating damping levels were lowered from 6.0% to 3.0%.
- Rhythmic exercise / high impact aerobics in “activity panels” by using VE dampers can be performed at damping levels as low as 1.6%.

The low impact aerobics in “activity panels” in the structure without VE dampers already complied with the serviceability deflection criteria and thus gave no change in the cases with VE dampers. In summary, the floor structure which uses VE dampers needs lower operating damping levels, which are easier to achieve by the use of non-structural components, equipment and other objects present in the floor system. However, these compliances do not reflect the human comfortability level which needed to be looked at since it would determine the main cut off for the occupancy fit-out of the floor system.

Table 8-6: Comparison of operating conditions in PL2-1 with and without VE dampers

	Without VE dampers		With VE dampers	
Dance-type activity in activity panel (AP)	Activity panel (AP)	Non-activity panel (NAP)	Activity panel (AP)	Non-activity panel (NAP)
High Impact Jumping	$\zeta > 12.0\%$	$\zeta > 6.0\%$	$\zeta > 12.0\%$	$\zeta > 3.0\%$
Normal Jumping	$\zeta > 12.0\%$	$\zeta > 6.0\%$	$\zeta > 6.0\%$	$\zeta > 3.0\%$
Rhythmic exercise / high impact aerobics	$\zeta > 3.0\%$	$\zeta > 1.6\%$	$\zeta > 1.6\%$	$\zeta > 1.6\%$
Low impact jumping	$\zeta > 1.6\%$	$\zeta > 1.6\%$	$\zeta > 1.6\%$	$\zeta > 1.6\%$

Table 8-6 compares the occupancy fit-out for PL2-1 floor structure with VE dampers with that of the structure without VE dampers. The shaded cells denoted the improvement.

Table 8-7: Summary and comparison of occupancy fit-out for PL2-1 with and without VE damper

	Occupancy description - without VE damper	
Dance-type activity in activity panel (AP)	Activity panel (AP)	Non-activity panel (NAP)
High Impact Jumping	Occupancy 0	Occupancy 0
Normal Jumping	Occupancy 1 $\zeta > 12.0\%$	Occupancy 2 $\zeta > 12.0\%$
Rhythmic exercise / high impact aerobics	Occupancy 1 $\zeta > 3.0\%$	Occupancy 2 $\zeta > 6.0\%$
Low impact jumping	Occupancy 1 $\zeta > 1.6\%$	Occupancy 2 $\zeta > 3.0\%$

	Occupancy description - with VE damper	
Dance-type activity in activity panel (AP)	Activity panel (AP)	Non-activity panel (NAP)
High Impact Jumping	Occupancy 0	Occupancy 0
Normal Jumping	Occupancy 1 $\zeta > 12.0\%$	Occupancy 2 $\zeta > 12.0\%$
Rhythmic exercise / high impact aerobics	Occupancy 1 $\zeta > 3.0\%$	Occupancy 2 $\zeta > 6.0\%$
Low impact jumping	Occupancy 1 $\zeta > 1.6\%$	Occupancy 2 $\zeta > 1.6\%$

Occupancy 0	Uncomfortable
Occupancy 1	Rhythmic activities / aerobics / dance- type loads
Occupancy 2	Shopping malls (centres) / dining and dancing / weightlifting / stores / manufacturing / warehouse / walkaways / stairs
Occupancy 3	Office / residencies / hotels / multi - family apartments / school rooms / libraries
Occupancy 4	Hospitals / laboratories / critical working areas (e.g. operating theatres, precision laboratories)

The reductions in acceleration responses after employing VE dampers obtained under PL2-1 did not make any significant improvement in human occupancy fit-out. The only improvement that complied with the acceleration criteria was in the following instance:

- The “non-activity panels” used for occupancy 2 at 1.6% damping for low impact events in the “activity panels”. Without the VE dampers occupancy 2 was not possible at any of the damping levels in the rage of 1.6% - 12.0%.

In summary, the floor model fitted with VE dampers under PL2-1 gave reductions in both deflections and accelerations. Figure 8-26 and Figure 8-27 summarise the maximum percentage reductions for DAF and acceleration response for various dance-type events and damping levels. The percentage reductions were averaged and are also shown in these figures.

Figure 8-26 and Figure 8-27 show that the structural damping plays a major role in achieving the overall reduction in response under PL2-1. Higher damping in floors gave smaller reduction in both responses of DAFs and accelerations. Less energetic dance-type activities of high contact ratio caused lower reduction in DAF responses. This implies that the contact ratio or in other terms the type of event, had influenced the DAFs, which were reduced with lesser energetic events. In contrast, the reduction in acceleration responses due to the VE damper maintained almost equal levels for the four contact ratios. Thus, it can be stated that the change in the type of event did not effect considerably in the reduction in the acceleration response. The same was also observed under PL1-1

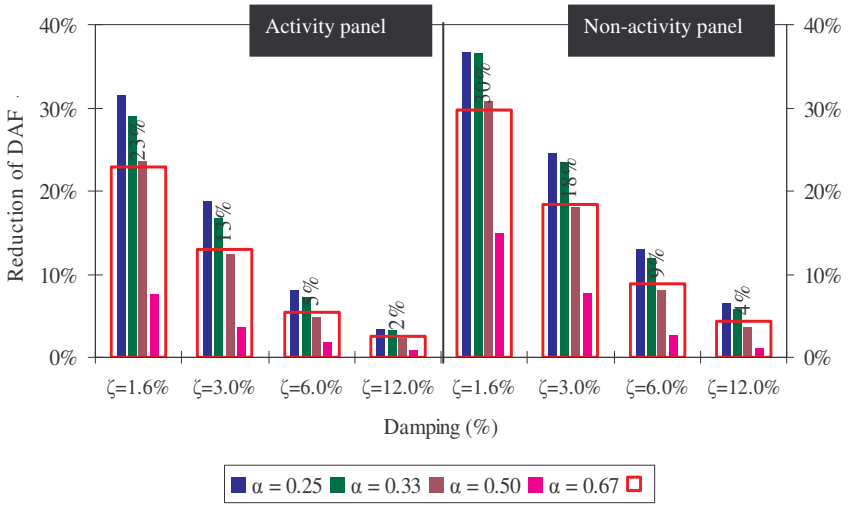

Figure 8-26: Percentage reduction in DAF responses due to VE damper in PL2-1

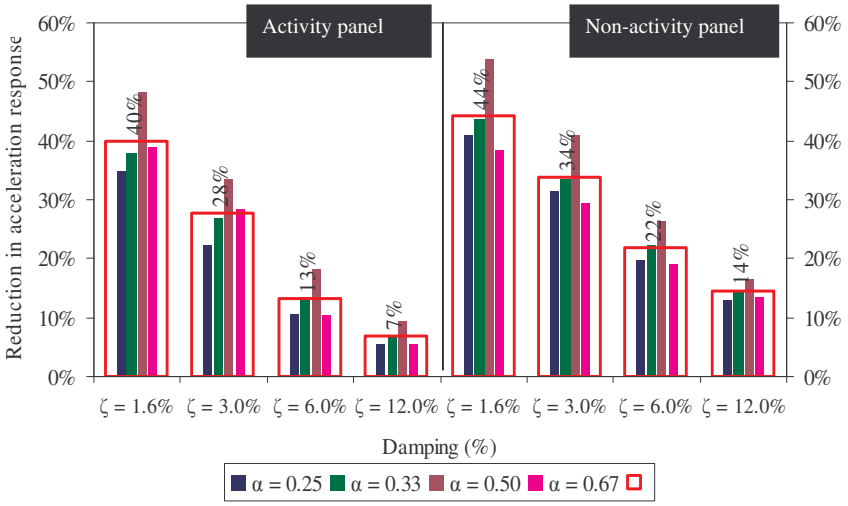

Figure 8-27: Percentage reduction in acceleration response due to VE damper in PL2-1

8.7 Summary

This chapter investigated the responses of a steel-deck composite floor system fitted with VE dampers subjected to different human-induced dance-type loads under two pattern loading cases PL1-1 and PL2-1. The FE models developed were modified with VE dampers and VE dampers properties were established to achieve the objectives. Two VE damper location configurations were tested and the one with the highest reduction was employed in an analytical investigation. The analytical study included simulations of different human-induced activities performed in different

locations, exciting varied modes of vibration. Furthermore, the influence of different human induced dance-type activities, classified by contact ratios and structural damping levels were studied. Reductions in both, displacement and acceleration responses, were calculated. The presented reductions helped to identify the satisfactory performance combinations after employing the VE dampers for both serviceability deflection and acceleration criteria.

Overall the use of VE dampers resulted in reduced dynamic responses in both pattern loading cases. Infact the average reductions in DAF response of 21.5 % under 1.6% damping to 2 % under 12.0% damping in “activity panels” and 26 % under 1.6% damping to 3.5 % under 12.0% damping in the “non-activity panels” were observed. In addition, the acceleration responses gave reductions of 39.5 % under 1.6% to 6.5 % under 12.0% damping in “activity panels” and 44.5 % under 1.6% damping to 13.5 % under 12.0% damping in the “non-activity panels”.

It was observed that the structural damping present in the system significantly influenced an overall reduction in responses in both acceleration and displacement. Consequently floor systems with higher structural damping, fitted with VE dampers when compared with those with lower structural damping gave smaller reductions in both acceleration and displacement. Thus, higher the structural damping in floors, lower the effects of VE dampers.

The differences in contact ratio of human activity did not considerably change the reductions in acceleration response. On the other hand, contact ratios effected the displacement response where lower contact ratios resulted in higher reductions and higher contact ratios resulted in lower reductions.

Chapter 9 - Conclusions and recommendations

9.1 Contribution from this research

Steel-deck composite floors are slender and prone to excessive vibrations under human-activity. These vibrations are large enough to cause vibration problems and discomfort to the occupants. This research project treated the floor vibration characteristics of such slender floor structures under "dance-type" human induced loading at different levels of structural damping. The research information was used to provide a comprehensive assessment of vibration response of these floors and to evaluate their compliance against the criteria for serviceability and comfort. This information in turn has allowed to establish suitable occupancies for these slender composite floor structures. Use of VE dampers to mitigate excessive vibration has also been carried out.

The main findings of this research study revealed that:

- Composite floor systems under human-induced dynamic actions cause excitations of higher modes of vibration in contrast to the common belief of excitation of only the fundamental mode, particularly in multiple panel configurations.
- Vibrations in composite floors can cause dynamic deflections and accelerations which exceed the allowable limits of serviceability and comfort.
- These excessive vibrations can be managed by:
    - Carefully selecting the location for the activity, if that is possible.
    - Changing the type of activity.
    - Using appropriate structural damping.
    - Restricting human densities performing the activity.
- Research information can be used to fit-out the occupancies in composite floor structures that will not cause discomfort to the occupants in both activity and non-activity panels.

Note: The “activity panels” are referred to the panels where the dance-type activity is being performed, while the “non-activity panels” are referred to the adjacent panels in the same floor level, which fit-out other occupancies.

- The VE dampers can be effectively used to mitigate vibration problems in composite floor systems, which can achieve up to 21.5% reduction in deflection response and up to 39.5% reduction in acceleration response. The performance of the VE damper depends on type of activity or contact ratio and level of structural damping. The amount of control increased with decrease in contact ratio and structural damping.

9.2 Discussion and summary

In order to investigate the vibration response of composite floors a popular type of steel-deck composite floor system in Australia was chosen and subjected to various human-induced dance-type events. This type of floor system is constructed with longer spans and reduced sections than the conventional reinforced concrete floors, consequently it is slender, causing vibration problems under service loads. The methodology used to address this problem is based on computer simulations supported by limited experimental tests. The experimental results are used to calibrate and validate FE models as well as to obtain dynamic properties of steel-deck composite floors, while computer simulations are used to achieve the aims and the objectives of this research.

The material presented in this thesis first treats single panel and then multiple panel behaviour, under human-induced loads. The former is important in residential apartments and townhouses which have patio and verandas, where it can be subjected to various in-house human-induced dynamic loads. The latter, on the other hand is important in modern building systems that occupy multiple occupancy floor fit-outs that accommodate office, commercial floors together with leisure activity halls. These occupancies in floors generate pattern loading, termed synchronous multiple panel loading, which happens when some floor panels are used for aerobics and gymnasium activities subjected to lively human-induced activity, while the adjacent floor panels serve for office, commercial or residential occupancy.

A special focus was directed towards assessing the dynamic response under pattern loading in multiple panel floor systems. A range of operating conditions was considered. These operating conditions included, structural damping, human-induced dance-type activities, which were differentiated by contact ratios, human-density performing the activity, activity frequency and location of the activity being performed (in terms of pattern loads). The deflection and acceleration responses were used to assess the floor panels against serviceability defection limits, for structural control and acceleration limits and for human comfort control. Accordingly, these deflection and acceleration responses were used to nominate suitable occupancies that can be used as a design guidance to render the human discomfort complaints. Finally, in order to mitigate excessive vibrations, the use of VE dampers in floor systems was investigated. The properties of VE dampers were established and responses of the floor structure were assessed after employing the VE dampers.

9.2.1 Laboratory experiments and model development

At the initial stages of this research laboratory experiments were carried out to generate data for calibration and validation of FE models. It also aimed to obtain DAFs in a laboratory controlled environment as well as the damping of the investigated floor system. Six test panels, three without top reinforcement and three with top reinforcement each of size 3.2 m in span, 1.8 m in width and 0.1 m thick had undergone static tests, forced vibration tests and heel drop tests. The forced vibration tests revealed increased responses compared to static responses. The heel drop tests resulted in damping of 1.75% and 1.98% for the panels without and with top reinforcement respectively. These damping values are very low and thus contribute to higher responses under dynamic loads.

The results from static tests were used to calibrate the single panel FE models, while the heel-drop test results using natural frequencies were used to validate the FE models. The calibrated and validated single panel FE models were then used to develop a series of single panel FE models of various sizes giving different natural frequencies. The procedure and models used are described in Chapter 4. The natural frequencies of single panel FE models varied from 7 Hz to 9.5 Hz. At the same time, multiple panel floor models were developed, responses of which resulted in lower natural frequencies. These multiple panel FE models consisted of four panel model

and nine panel model, which gave fundamental frequencies of 4 Hz and 4.2 Hz respectively, making them more sensitive to vibration due to human-induced loads.

9.2.2 Single panel vibration

Seven different single panel models giving fundamental frequencies from 7 Hz to 9.5 Hz were investigated. The sizes of the panels were selected to give a range of spans, starting from 3.2 m to 7.2 m and thicknesses of 100 mm to 250 mm. Human-induced event described by aerobics / jumping activity was simulated based on the research by Ginty, Derwent et al. (2001) on each of the models. The simulated activity frequency ranged from 2.2 Hz to 2.8 Hz at damping levels of 1.6%, 3.0%, 6.0% and 12.0%. Herein, an occupant density of 0.4 kPa (assuming 1.75 m^2 per person), which is common in aerobic / jumping activity in a group, was used for the analysis. The respective steady state DAFs and acceleration responses were observed and compared with the serviceability state limits of deflection, for structural control and acceleration and for human perceptibility.

It was found that the single panel floors responded in their fundamental mode. This fundamental mode was excited by the third harmonic, $f_o/f_1 = 0.33$ of the activity frequency. The DAFs observed under these circumstances were below the limits of serviceability and thus did not cause serviceability deflection problems. Nevertheless, to obtain reasonable approximations that occur during human excitation, the variations of DAFs with respect to the frequency ratio f_o/f_1 and damping levels were observed and used to obtain relationships. These relationships are presented below and the derivation of these formulae is presented in Section 5.4.3 of Chapter 5.

$$DAF = \left(A - B\frac{f_0}{f_1} \right)^2 + C, \qquad \textbf{Equation 9-1}$$

where f_o is the activity frequency and f_1 is the fundamental natural frequency.

The constants A, B and C were derived for two cases:

when $f_o/f_1 < 0.33$ → $A = 2.73$, $B = 11.34$, $C = 1.29$,

when $f_o/f_1 > 0.33$ → $A = 8.70$, $B = 24.18$, $C = 2.02$.

DAFs predicted by the above formula when compared with those obtained from FEA gave a standard deviation of 0.025842 and COV of 2.6%, both of which were within the acceptable limits. This Equation 9-1 can be used to obtain DAFs at known activity frequency f_0 and fundamental frequency f_1. The fundamental frequency can be obtained by either FEA or using the approach of Wyatt et al. (1989), for details refer to Section 5.2.3.

DAFs are also a function of damping ζ and are formed in the following Equation 9-2:

$$DAF = \frac{2}{\zeta^{0.11}}. \qquad \textbf{Equation 9-2}$$

DAFs predicted from this formula, when compared with the FEA results gave a standard deviation of 0.018013 and COV 1.8%. This Equation 9-2 can be used to obtain DAFs at known structural damping of the floor system.

Limitations: The above developed formulae are for single panels vibrating in their fundamental mode of vibration, which resulted from the third harmonic of the activity frequency and for models with fundamental frequency in the range of 7 Hz – 9.5 Hz. An occupant density of 0.4 kPa posing aerobics/jumping activity was used for all the analysis with activity frequencies in the range of 2.2 Hz – 2.8 Hz.

To determine the levels of human discomfort the acceleration responses observed for aerobics / jumping activity were compared with a limit of 0.05g (Murray, Allen et al. 1997). All the acceleration responses observed for single panel modal vibration did not exceed this limit, underlying that they had not caused discomfort problems to the occupants. Furthermore, the comparison of acceleration response with the current design equitation (refer to Equation 2-10 in Chapter 2) for human comfort yielded reasonable agreement with FEA results as detailed in Section 5.4.4. Equation 2-10 is thus proposed to be used to obtain acceleration responses for single panel steel-deck composite floor systems.

9.2.3 Multiple panel vibration

Two multiple panel floor models, one with four panels and the other with nine panels, constituted the investigation of multiple panel vibrations. These two models

were subjected to various pattern loading cases, which caused multi-modal vibration. Thus the floor system vibrated not only in its fundamental mode of vibration, but also in higher modes of vibration depending upon the location of the human activity. Table 9-1 summaries the pattern loading cases and the excited mode shapes and natural frequencies.

Table 9-1: Pattern loading cases, excited modes and frequencies

Excitation mode	Pattern loading case	Frequency
First	PL1-1	4.0 Hz
	PL2-1	4.0 Hz
	PL2-2	4.3 Hz
Second	PL4-1	5.4 Hz
	PL2-2	4.8 Hz
Third	PL3-1	5.9 Hz

These modes were excited by either second or third harmonic of human-activity frequency, demonstrating the importance of obtaining not only the fundamental natural frequencies, but also the higher natural frequencies along with their respective mode shapes. These mode shapes provide clues to determining the areas where the dance-type loads should or should not be permitted. Preferably, it's advisable to fit-out occupancies to avoid excitation of such mode shapes. However, this can be impractical as the operating conditions may vary from place to place. Consequently, this research considered different operating conditions, such as damping levels, type of activity, activity frequency and occupant densities and their responses were obtained. These responses were compared with serviceability state limits of deflection for structural control and acceleration limits, for human conformability. The results revealed mixed operating conditions in "activity panels" and "non-activity panels" for different modes of vibration. Table 9-3 summaries suggested occupancy fit-outs and their operating conditions. These occupancy fit-outs can be used as design guidance or retrofitting tool to mitigate floor vibration problems.

In the second phase of this research study, the maximum DAFs and accelerations observed for different pattern loading cases were formulated in equations. The development of these equations is presented in Section 6.12 of Chapter 6. These equations were aimed to estimate DAFs and accelerations *a,* at known damping levels ζ, type of activity α, the desired location of response, activity panel or non-activity panel and were used for different pattern loads. These equations are presented below.

$$DAF = Ae^{-N\alpha}, \qquad \textbf{Equation 9-3}$$

where $A = k_1\zeta^{k_2}$ and $N = k_3\zeta^{k_4}$.

$$a = A'e^{-N'\alpha}, \qquad \textbf{Equation 9-4}$$

where $A' = k_1'\zeta^{k_2'}$ and N' = Constant.

The coefficients k_1, k_2, k_3, k_4, k_1', k_2' and N' were proposed by this research as listed in Table 9-2.

Table 9-2: Proposed coefficient for multi-modal vibrations

	Activity panel(s)						
	k_1	k_2	k_3	k_4	k_1'	k_2'	N'
PL1	9.03	-0.61	3.09	-0.46	0.83	-0.7	4.97
PL2	12.97	-0.71	3.51	-0.45	1.16	-0.75	4.97
PL3	4.06	-0.32	1.98	-0.37	0.85	-0.6	4.97
PL4	4.02	-0.35	1.89	-0.45	0.79	-0.54	4.97
	Non-activity panel(s)						
PL1	7.57	-0.7	3.28	-0.7	0.8	-0.93	5.33
PL2	14.23	-0.81	4.11	-0.6	1.42	-0.93	5.33
PL3	3.01	-0.38	1.76	-0.72	0.69	-1.03	4.78
PL4	3.25	-0.39	1.5	-0.44	0.75	-1.16	4.84

Table 9-3: Summary of occupancy fit-outs

Dance-type activity in AP	Human density in AP	First mode		Second mode		Third mode	
		AP	NAP	AP	NAP	AP	NAP
High impact jumping	0.4 kPa	Occupancy 0	Occupancy 0	Occupancy 1 $\zeta > 12.0\%$	Occupancy 2 $\zeta > 12.0\%$	Occupancy 1 $\zeta > 12.0\%$	Occupancy 2 $\zeta > 12.0\%$
	0.2 kPa	Occupancy 1 $\zeta > 6.0\%$	Occupancy 2 $\zeta > 12.0\%$	Occupancy 1 $\zeta > 6.0\%$	Occupancy 2 $\zeta > 6.0\%$	Occupancy 1 $\zeta > 6.0\%$	Occupancy 2 $\zeta > 6.0\%$
Normal jumping	0.4 kPa	Occupancy 1 $\zeta > 12.0\%$	Occupancy 2 $\zeta > 12.0\%$	Occupancy 1 $\zeta > 6.0\%$	Occupancy 2 $\zeta > 6.0\%$	Occupancy 1 $\zeta > 12.0\%$	Occupancy 2 $\zeta > 12.0\%$
	0.2 kPa	Occupancy 1 $\zeta > 6.0\%$	Occupancy 2 $\zeta > 12.0\%$	Occupancy 1 $\zeta > 3.0\%$	Occupancy 2 $\zeta > 6.0\%$	Occupancy 1 $\zeta > 1.6\%$	Occupancy 2 $\zeta > 6.0\%$
Rhythmic exercise / high impact aerobics	0.4 kPa	Occupancy 1 $\zeta > 3.0\%$	Occupancy 2 $\zeta > 6.0\%$	Occupancy 1 $\zeta > 3.0\%$	Occupancy 2 $\zeta > 3.0\%$ Occupancy 3 $\zeta > 12.0\%$	Occupancy 1 $\zeta > 3.0\%$	Occupancy 2 $\zeta > 6.0\%$ Occupancy 3 $\zeta > 12.0\%$
Low impact jumping	0.4 kPa	Occupancy 1 $\zeta > 1.6\%$	Occupancy 2 $\zeta > 3.0\%$	Occupancy 1 $\zeta > 1.6\%$	Occupancy 2 $\zeta > 1.6\%$ Occupancy 3 $\zeta > 3.0\%$	Occupancy 1 $\zeta > 1.6\%$	Occupancy 2 $\zeta > 1.6\%$ Occupancy 3 $\zeta > 6.0\%$

Occupancy 0	Uncomfortable
Occupancy 1	Rhythmic activities / aerobics / dance- type loads
Occupancy 2	Shopping malls (centres) / weightlifting / stores / manufacturing / warehouse / walkaways / stairs
Occupancy 3	Office / residencies / hotels / multi - family apartments / school rooms / libraries
Occupancy 4	Hospitals / laboratories / critical working areas (e.g. operating theatres, precision laboratories)

AP - Activity panel

NAP - Non-activity panel

Depending upon the pattern loading, the coefficients can be chosen from Table 9-2 to obtain an estimate of the DAFs and accelerations *a*. The DAFs obtained by Equation 9-3 multiplied by the static deflection can be used to determine the likely deflections that could occur under the circumstances used. The acceleration derived by Equation 9-4 gives an estimate of the acceleration response, which can be used to determine the human perceptibility.

Limitations: The equations were developed considering a human-density of 0.4 kPa, which was determined as the maximum density at which an event can be performed without causing problems to the performers and thus the predicted results are at the maximum. PL1 refers to a single panel loaded and vibrating in the first mode, PL2 refers to two panels loaded, vibrating in the first mode, PL3 refers to an excitation of third mode and PL4 refers to vibration in the second mode.

9.2.4 Mitigating floor vibrations using VE dampers

The main objective of this segment of investigation concentrated on using VE dampers to mitigate floor vibrations and to obtain VE damper properties. It also assesses the reductions in deflection and acceleration responses and their variations with damping, type of activity (contact ratio) and location of activity (pattern loading) after using VE dampers. The four-panel floor model with attached VE dampers was developed to achieve these objectives. Two VE damper location configurations were used and the one with the highest reduction was employed in an analytical investigation. This location configuration was presented in Section 8.3.2 of Chapter 8.

The VE dampers were modelled using spring and dashpot elements. The dashpot damping parameter of 1×10^4 Ns/m and the stiffness of spring of 1×10^3 N/m gave the maximum reductions in both deflections and accelerations and were thus used for the analytical investigation. The analytical study included simulation using human-induced activities on different pattern loads exciting various modes of vibration. Two pattern loading cases PL1-1 and PL2-1 were used for this investigation. Different human induced activities, as classified by contact ratios at different structural damping levels, constituted the analytical study. The improved performances

considering both, serviceability deflection and human discomfort criteria under the two pattern loading cases, were identified as a consequence of VE dampers. These were presented in Chapter 8, in Table 8.5 and 8.7 for PL1-1 and PL2-1 respectively.

The reductions in both displacement and acceleration responses were calculated. They resulted in similar percentages in both pattern loading cases and were found to be varying with structural damping and contact ratio. The DAFs were averaged and gave reductions of 21.5 % under 1.6% damping to 2 % under 12.0% damping in "activity panels" and 26 % under 1.6% damping to 3.5 % under 12.0% damping in the "non-activity panels". The acceleration responses gave reductions of 39.5 % under 1.6% damping to 6.5 % under 12.0% damping in "activity panels" and 44.5 % under 1.6% damping to 13.5 % under 12.0% damping in the "non-activity panels".

It was observed that the structural damping present in the system has significantly influenced an overall reduction in responses. The floor systems with higher structural damping fitted with VE dampers did not give large acceleration and displacement reductions, when compared with those with lower damping. Thus, higher the structural damping in floors, lower the effects of VE dampers. The contact ratio of the human-activity or type of activity did bare a considerable effect on reduction of acceleration response. In contrast, it effected the displacement response with lower contact ratios to give higher reductions and with higher contact ratios to give lower reductions.

9.3 Conclusion

Single and multiple panel steel-deck composite floor systems subjected to human-induced loads were investigated under varied operating conditions and their responses were assessed for structural control and human perceptibility. Each of these systems performed in a different manner and their performance varied considerably under different operating conditions.

This research has shown that the single panel behaviour is primarily based on excitation of fundamental mode, while multiple panel behaviour causes the excitation of not only the fundamental mode but also the higher modes of vibrations. The single panels responded within the serviceability state limits for both deflection and

accelerations and thus did not raise a vibration issue. In contrast, multiple panel floors responded in either way of exceeding or not exceeding the serviceability limits of deflection and acceleration, depending upon the operating conditions, such as damping, activity frequency, activity type, human density and location of activity.

This research has shown that it is possible to mitigate the excessive vibrations by carefully laying out the floor for different occupancies. This is an important consideration from a pre-construction prospective as well as post-construction prospective, if the vibration complaints are to be reduced. Such occupancies were illustrated in this thesis along with appropriate damping levels, human densities performing the activity, type of activity and the location of activity.

The findings of this research can be used as design guidance for structural engineers, in a likelihood of an environment causing vibration problems. The research presented in this thesis also demonstrated that the VE dampers can be used effectively to mitigate floor vibration problems. In conclusion, the research information presented in this thesis can be used in design and retrofitting of slender steel-deck composite floor structures making them acceptable.

9.4 Recommendations for future work

The following are suggestions for further research in this area:

- A similar contribution to the knowledge in responses of pattern loading of slender floor structures used for parking is needed. For example, when parking areas are being filled and emptied pattern loads are initiated that may cause the floor structure to vibrate.
- More work is needed to improve the relationships developed for determining the DAFs and acceleration responses. These relationship improvements may include dynamic properties such as higher mode frequencies.
- Use of VE devices in mitigating the human-induced vibration is a new concept tried in this research. The use of VE dampers with given properties needs to be further investigated in real prototype slender floor structures. The use of other types of dampers such as TMDs, hybrid dampers can also be another area for research.

- The use of semi-active damping systems to mitigate floor vibration problems is another area to be investigated.

References

Abacus Analysis User's Manual (2003). **Volume II**.

Abbas, H. and Kelly J.M. (1993). A methodology for design of visco-elastic damper in earthquake-resistant structures. Technical report UCB / EERC - 93 / 09. Berkeley, Earthquake Engineering Research Centre, University of California.

Allen, D. E. (1990a). "Building Vibrations from Human Activities." Concrete International : Design and Construction **12**(6): 66-73.

Allen, D. E. (1990b). "Floor vibration from aerobics." Canadian Journal of Civil Engineering **17**: 771-779.

Allen, D. E. and T. M. Murray (1993). Vibration of composite floors. Structural Engineering in Natural Hazards Mitigation, California, American Society of Civil Engineers.

Allen, D. E., D. M. Onysko, et al. (1999). ATC Design Guide 1: Minimising floor vibration. Applied Technology Council. California**:** 1-64.

Allen, D. E. and G. Pernica (1998). Control of floor vibration. IRC Construction Technology Update.

AS 1012.8.1 Standards Australia (2000). Methods of Testing Concrete. Method 8.1: Method for making and curing concrete - Compression and Indirect Tensile Test Specimens.

AS 1012.9 Standards Australia (1999). "Methods of Testing Concrete. Method 9: Determination of the Compressive Strength of Concrete Specimens."

AS 1391 Standards Australia (1991). Methods for tensile testing of metals.

AS 3600 Standards Australia (2001). Concrete Structures. Sydney, Australia, Standards Australia.

Bachmann, H. (1988). "Case studies of structures with man-induced vibrations." Journal of Structural Engineering **118**(3): 631-646.

Bachmann, H. and W. Ammann (1987). Vibrations in Structures induced by Man and Mechanics, IABSE - AIPC - IVBH (Switzerland).

Bachmann, H., W. Ammann, et al. (1995). Vibration problems in structures. Germany, Birkhauser Verlag Basel.

Bachmann, H., A. J. Pretlove, et al. (1995). Vibration induced by people. Vibration Problems in Structures: Practical Guidelines. B. H. Berlin, Birkhauser.

Baglin, W., K. Cox, et al. (2005a). Comparison of floor vibration data with theoretical predictions. Developments in mechanics of structures and materials, Perth, Australia, A.A. Balkema Publishers.

Baglin, W., K. Cox, et al. (2005b). Full Scale measurements of floor vibrations in multi story buildings under construction. Developments in mechanics of structures and materials, Perth, Australia, A.A. Balkema Publishers.

Benidickson, Y. V. (1993). Dealing with excessive floor vibrations, Institute for Research in Construction, Canada.

Blakeborough, A. and M. S. Williams (2003). "Measurement of floor vibrations using a heel drop test." Proceedings of the Institution of Civil Engineers: Structures and Buildings **154**(SB4): 367-371.

BlueScope Lysaght Burswood International Resort. http://www.bluescopesteel.com.au/au/index.cfm/objectID.F93A0890-8057-11D4-98AF00508BA5461F/pgNum.2. Perth, Australia,.

BlueScope Steel (2003). Using Bondeck : Design & Construction Guide, Blue Scope Steel Limited.

Brand, B. S. and T. M. Murray (1999). Floor vibrations: ultra long-span joist floors. Structural Engineering in the 21st Century, New Orleans, Louisiana, American Society of Civil Engineers.

British Standard : BS5950 : Part 4 (1994). Structural use of steelwork in building - Part 4: Code of practice for design of composite slabs with profiled steel sheeting, British Standard Institute (BSI).

Brownjohn, J. M. W. (2001). "Energy Dissipation from Vibrating Floor Slabs due to Human-Structure Interaction." Shock and Vibration **8**: 315-323.

BS 6472 (1984). Guide to the Evaluation of human Exposure to Vibration in Buildings (1 Hz to 80 Hz). United Kingdom.

Chen, Y. (1999). "Finite element analysis for walking vibration problems for composite pre-cast building floors using ADINA: modelling, simulation, and comparison." Computers & Structures **72**(1-3): 109-126.

Chien, E. Y. L. and J. Richie, .K., (1984). Design and construction of composite floor systems. Toronto, Canadian Institute of Steel Construction.

Cho, K.-P. (1998). Passive visco-elastic damping systems for buildings. Civil Engineering Department. Colorado, Colorado State University**:** 203.

Clough, R. W. and J. Penzien (1993). Dynamics of structures. New York, McGraw-Hill, Inc.

Commentary A (1995). Supplement to the national building code of Canada; commentary on serviceability criteria for deflections and vibrations. Ottawa, National Research Council of Canada.

da Silva, J. G. S., P. C. G. da S Vellasco, et al. (2003). "An evaluation of the dynamical performance of composite slabs." Computers & Structures **81**: 1905-1913.

Dallard, P., T. Fitzpatrick, et al. (2001a). "The Millennium Bridge, London: Problems and Solutions." The Structural Engineer **79**(8): 15-17.

Dallard, P., T. Fitzpatrick, et al. (2001b). "The London Millennium Footbridge." The Structural Engineer **79**(22): 17-36.

Davison, J. B. (2003). Composite Floors. Composite Construction. D. A. Nethercot. London, Spon Press.

Dougill, J. W., A. Blakeborough, et al. (2001). Dynamic performance requirements for permanent grandstands subject to crowd action: interim guidance on assessment and design, Institution of Structural Engineers, UK.

Ebrahimpour, A. and R. L. Sack (1988). Crowd induced dynamic loads. Proceedings of the Symposium / Workshop on Serviceability of Buildings (movements, Deformations, Vibrations), Ottawa, Canada.

Ebrahimpour, A. and R. L. Sack (1989). "Modelling dynamic occupant loads." Journal of Structural Engineering **115**(6): 1476-1496.

Ebrahimpour, A. and R. L. Sack (2005). "A review of vibration serviceability criteria for floor structures." Computers and Structures **83**: 2488-2494.

El-Dardiry, E. and T. Ji (2005). "Modelling of the dynamic behaviour of profiled composite floors." Engineering structures **28**: 567-579.

El-Dardiry, E., E. Wahyuni, et al. (2002). "Improving FE models of a long-span flat concrete floor using natural frequency measurements." Computers & Structures **80**: 2145-2156.

Ellingwood, A. and Tallin A. (1984). "Structural serviceability: Floor vibrations." Journal of Structural Engineering **110**(1): 401-418.

Ellis, B. and T. Ji (1994). "Floor vibration induced by dance-type loads: verification." The Structural Engineer **72**(3): 45-50.

Ellis, B. and J. D. Littler (2004). "Response of cantilever grandstands to crowd loads: Part 2: load estimation." Structures and Buildings **157**(SB5): 297-307.

Ellis, B. R. (2000). "On the response of long-span floors to walking loads generated by individuals and crowds." The Structural Engineer **78**(10): 17-25.

Ellis, B. R. (2001a). Dynamic monitoring. Monitoring and Assessment of Structures. G. S. T. Armer. New York, Spon Press**:** 8-31.

Ellis, B. R. (2001b). "Serviceability evaluation of floor vibrations induced by walking loads." The Structural Engineer **79**(21): 30-36.

Elnimeiri, M. and H. Iyengar (1989). Composite floor vibrations: predicted and measured. Steel Structures, San Francisco, CA, USA, American Society of Civil Engineers.

Eriksson, P. E. (1994). Vibration of low frequency floors. Goteborg, Sweden, Chalmers University of Technology.

Eriksson, P. E. (1996). Dynamic service actions for floor systems. Building and International Community of Structural Engineers, Chicago, ASCE.

Fielders Australia Pty. Ltd. Fielders king-floor composite steel formwork system: floor vibration discussion fact file 0.1. Brisbane, Australia - www.fielders.com.au.

Galambos, F. W. and M. V. Barton (1970). "Ground loading from footsteps." Journal of Acoustic Society of America **48**(5): 1288-1292.

Ginty, D., J. M. Derwent, et al. (2001). "The frequency ranges of dance-type loads." The Structural Engineer **79**(6): 27-31.

Gordon, L. (2005). "Isolating unwanted vibration." American Mechanist **149**(5): 40-50.

Hanagan, L. M. (2003). Floor vibration serviceability: tips and tools for negotiating a successful design. Modern Steel Construction.

Hanagan, L. M. and T. Kim (2001). Development of a simplified design criterion for walking vibration. Structures 2001: A Structural Engineering Odyssey.

Hanagan, L. M. and T. M. Murray (1997). "Active Control Approach for Reducing Floor Vibrations." Journal of Structural Engineering **123**(11): 1497-1505.

Hanagan, L. M., C. Rottmann, et al. (1996a). Control of Floor Vibrations. Building an International Community of Structural Engineers, Chicago, USA,, ASCE, New York.

Hanagan, L. M., C. Rottmann, et al. (1996b). Control of floor vibrations. Building an International Community of Structural Engineers, Chicago, ASCE.

Harper, F. C. (1962). "The mechanics of walking." Research Applied in Industry **5**(1): 33-38.

Hewitt, C. M. and T. M. Murray (2004b). "Talking a fresh look at the damping criteria you've been using to design offices can help you to eliminate floor vibration issues from the very start." Modern Steel Construction: 21-23.

Hewlett Packard Inc. (1992). User and service guide - HP 54600 - Series Oscilloscopes. USA.

Hibbitt Karlsson & Sorensen Inc. (2001). Getting Started with ABAQUS/Standard Version 6.2. U.S.A.

Hicks, S. (2004). "Vibration characteristics of steel-concrete composite floor systems." Prog. Struct. Engineering Materials **4**: 21-38.

Hunadidi, O. (2000). "Traffic Vibrations in Buildings." Institute for Research in Construction : Construction Technology Update No. 39.

Hunaidi, O. (2000). Traffic vibrations in buildings. Construction technology update no. - 39. Ottawa, National Research Council of Canada.

Hyde, H. and H. R. Lintern (1929). "The vibrations of roads and structures." Proceedings of ICE **227**: 187-242.

ISO 10137 (1992). Bases for design of structures - Serviceability of buildings against vibration. Genève, Switzerland, International Organization for Standardization.

Japan Society of Civil Engineers (1996). Impact of Hanshin/Awaji earthquake on seismic design and seismic strengthening of highway bridges, Hyogo ken Nanbu Earthquake Committee of Earthquake Engineering.

Ji, T. (2003). "Understanding the interactions between people and structures." The Structural Engineer **81**(4): 12-13.

Ji, T. and B. R. Ellis (1994). "Floor vibration: floor vibration by dance type loads: theory." The Structural Engineer **72**(3): 37-44.

Keel, C. J. and P. Mahmoodi (1986). Design of viscoelastic dampers for Columbia centre building. Building motion in wind. Isuymov and Tschanz. ASCE, New York**:** 66-88.

Kullaa, J. and A. Talja (1999). Vibration Performance Test for Light-Weight Steel-Joist Floors. Fourth International Conference on Steel and Aluminium

Structures: Light-weight Steel and Aluminium Structures, Espoo, Finland, Elsevier Science Ltd.

Lichtenstein, H. A. (2004). All Shock Up. Modern Steel Construction - American Institute of Steel Construction**:** 45-49.

Luger, K. (2006). Metal Deck : What design engineers should know. Modern Steel Construction**:** 58-59.

Mackriell, L. E., K. C. S. Kwok, et al. (1997). "Critical mode control of a wind-loaded tall building using an active tuned mass damper." Engineering Structures **19**(10).

Maguire, J. R. and T. A. Wyatt (1999). Dynamics - an introduction for civil and structural engineers, Thomas Telford Publishing**:** 80.

Mahrenholtz, O. and H. Bachmann (1995). Appendix C: Damping. Vibration Problems in Structures : Practical Guidelines. Berlin, Germany, Birkhauser Verlag**:** 157-168.

Marko, J., D. P. Thambiratnam, et al. (2004). "Influence of damping systems on building structures subject to seismic effects." Engineering structures **26**: 1939-1956.

Maurenbrecher, P. M. (1997). Induced vibrations from buildings: from people to earthquakes. Delft, Delft University of Technology, Faculty of Applied Earth Sciences**:** 1-1.

McGrath, P. and D. Foote (1981). What happened at the Hyatt? Newsweek. Kansas City , USA**:** 26.

Mullett, D. L. (1998). Composite floor systems. Oxford, Blackwell Science Ltd.,.

Murray, T. M. (1989). Floor vibrations - tips for designers. Steel Structures, San Francisco, CA, USA, American Society of Civil Engineers.

Murray, T. M. (1990a). Acceptability criterion for occupant-induced floor vibrations, Australian Institute of Steel Construction**:** 1-9.

Murray , T. M. (1990b). Floor Vibration in Buildings - State-of-the-art Summary. Floor Vibration in Buildings - Design Methods, Australian Institute of Steel Construction.

Murray, T. M. (2000a). "Floor vibrations: tips for designers of office buildings." Structure: 26-30.

Murray, T. M., D. E. Allen, et al. (1997). Steel design guide series 11: floor vibration due to human activity. Chicago, USA, American Institute of Steel Construction, Inc.

Murray, T. M. and J. N. Howard (1998). "Serviceability: lively floors - North American and British Design Methods." Journal of Constructional Steel Research **46**(1-3).

Naeim, F. (1991). Design practice to prevent floor vibrations. Steel Tips. S. S. E. Council.

Ngo, T., E. Gad, et al. (2006). Vibration of long span concrete floors. Concrete in Australia.

Osborne, K. P. and B. R. Ellis (1990). "Vibration design and testing of a long-span lightweight floor." The Structural Engineer **68**(15): 181-186.

Paskalov, A. and S. Reese (2003). "Deterministic and probabilistic floor response spectra." Soil Dynamics and Earthquake Engineering **23**: 605-618.

Pavic, A. and P. Reynolds (1999). "Experimental assessment of vibration serviceability of existing office floors under human-induced excitation." Experimental Techniques: 41-45.

Pavic, A. and P. Reynolds (2002). "Vibration serviceability of long-span concrete building floors: Part 1: review of background approach." The Shock and Vibration Digest **34**(3): 191-211.

Ribakov, Y. and A. M. Reinhorm (2003). "Design of Amplified Structural Damping Using Optimal Considerations." ASCE Journal of Structural Engineering **129**(10): 1422-1427.

Rogers, D. (2000). Two more 'wobbly' stands. Construction news.

Sachse, R. (2002). "Modelling effects of human occupants on modal properties of slender structures." The Structural Engineer **80**(5): 2.

Sachse, R., A. Pavic, et al. (2003). "Human-Structure Dynamic Interaction in Civil Engineering Dynamics - A Literature Review." The Shock and Vibration Digest **32**(1): 3-18.

Setareh, M., J. K. Ritchey, et al. (2006). "Pendulum tuned mass dampers for floor vibration control." Journal of performance of constructed facilities **20**(1): 64-73.

Shen, K. L., T. T. Soong, et al. (1995). "Seismic behaviour of reinforced concrete frame with added viscoelastic dampers." Engineering structures **17**(5): 372-380.

Sim, J. (2006). Human-structure interaction in cantilever grandstands. Oxford, University of Oxford.

Sim, J., A. Blakeborough, et al. (2006). "Modelling effects of passive crows on grandstand vibration." Structures and Buildings **159**: 261-272.

Smith, J. W. (2002). Human-induced vibration. Dynamic Loading and Design of Structures. K. AJ. New York, Spon Press**:** 285-306.

Steffens, R. J. (1965). Some aspects of structural vibration. Proceedings of the British National Selection of the International Association for Earthquake Engineering Symposium. London, UK**:** 1-30.

Storey, B. D. Computing Fourier series and power spectrum with MATLAB.

Tektronix Inc. (1991). CFG 280 11 MHz Function generator - Instruction manual. Oregon, USA.

Ungar, E. E. and R. W. White (1979). "Footfall-induced vibrations of floors supporting sensitive equipment." Sound and Vibration: 10-13.

Wajon, S. (1996). Aerobics Class. Picture Australia, State Library of New South Wales.

Webster, A. C. and R. Vaicaitis (2003). "Application of tuned mass dampers to control vibrations of composite floor systems." Engineering Journal / American Institute of Steel Construction: 116-124.

Wheeler, J. E. (1982). "Prediction and control of pedestrian induced vibration in footbridges." Journal of the Structural Division **108**(ST9): 2045-2065.

Widjaya, B. R. (1997). Analysis and design of steel-deck concrete composite floors. Civil Engineering. Virginia, US, Virginia Polytechnic Institute and Sate University**:** 96.

Willford, M. (2001). "An Investigation into crowd-Induced vertical dynamic loads using Available Measurements." The Structural Engineer **79**(12): 21-25.

Williams, M. S. and P. Waldron (1994). "Evaluation of methods for predicting occupant-induced vibrations in concrete floors." The Structural Engineer **72**(20): 334-340.

Wright, H. D., H. R. Evans, et al. (1987). "The use of profiled steel sheeting in floor construction." Journal of Constructional Steel Research **7**: 279-295.

Wyatt, T. A. (1985). "Floor vibrations by rhythmic vertical jumping." Engineering Structures **7**: 208-210.

Wyatt. T.A. (1989). Design Guide on the Vibration of Floors, Steel Construction Institute. Berkshire. UK., Construction Industry Research and Information Association. London UK.

Xia, H., N. Zhang, et al. (2005). "Experimental study of train-induced vibration s of environments and buildings." Journal of Sound and Vibration **250**: 1017-1029.

Yazdanniyaz, A., A. Carison, et al. (2003). Design of Vibration Sensitive Laboratory Floors: Vibration Criteria and Prediction Methods compared with Measured Vibrations. Building Integration Solutions, Austin, Texas, American Society of Civil Engineers.

Zivanovic, S., A. Pavic, et al. (2005). "Vibration serviceability of footbridges under human-induced excitation: a literature review." Journal of Sound and Vibration **279**(1-2): 1-74.